Det Kgl. Danske Videnskabernes Selskab.
Mathematisk-fysiske Meddelelser. **XIV**, 1.

EIN SATZ ÜBER STABILE BEWEGUNGEN IN DER EBENE

VON

H. BOHR UND W. FENCHEL

KØBENHAVN
LEVIN & MUNKSGAARD
EJNAR MUNKSGAARD
1936

Printed in Denmark.
Bianco Lunos Bogtrykkeri A/S.

1. Es bezeichne $x = (x_1, x_2, \ldots, x_n)$ einen Punkt des n-dimensionalen Raumes E_n. Ist $x(t)$ für $-\infty < t < \infty$ stetig von t abhängig, so sprechen wir von einer Bewegung in E_n. Eine Bewegung heisst nach LIAPOUNOFF stabil oder kurz stark stabil, wenn es zu jedem $\varepsilon > 0$ ein $\delta = \delta(\varepsilon) > 0$ derart gibt, dass aus

$$\varrho[x(\tau'), x(\tau'')] \leqq \delta$$

die Ungleichung

$$\varrho[x(\tau' + t), x(\tau'' + t)] \leqq \varepsilon$$

für alle t $(-\infty < t < \infty)$ folgt. Hierbei bedeutet $\varrho[x, y]$ den euklidischen Abstand der Punkte x und y. A. MARKOFF hat nun gezeigt, dass jede stark stabile, beschränkte Bewegung fastperiodisch ist[1]. Im folgenden soll u. a. bewiesen werden, dass jede stark stabile, beschränkte Bewegung in der Ebene E_2 sogar periodisch ist.

2. Dies gilt, wie der unten angegebene Beweis lehrt, auch schon unter sehr viel schwächeren Voraussetzungen, nämlich falls die betrachtete Bewegung nur nach POISSON positiv stabil ist. Das soll folgendes heissen:

[1] A. MARKOFF: Stabilität im Liapounoffschen Sinne und Fastperiodizität [Math. Zeitschr. **36**, 708—738 (1933)], insbes. § 3. In der obigen Formulierung ist der Satz von H. BOHR in der Note »Stabilitet og Næstenperiodicitet« [Matematisk Tidsskr. B **1933**, 21—25] ausgesprochen worden.

a) Zu jedem $l > 0$, jedem $\varepsilon > 0$ und jedem τ_0 soll es ein $\delta = \delta(l, \varepsilon, \tau_0) > 0$ derart geben, dass aus

$$\varrho[x(\tau_0),\ x(\tau)] \leqq \delta \tag{1}$$

die Ungleichung

$$\varrho[x(\tau_0 + t),\ x(\tau + t)] \leqq \varepsilon \tag{2}$$

für $-l \leqq t \leqq l$ folgt.

b) Ferner soll es ein t_0 und eine Folge $t_1, t_2, \ldots \to \infty$ geben, so dass die Punktfolge $x(t_\nu)$ für $\nu \to \infty$ gegen $x(t_0)$ konvergiert.

Unsere Behauptung lautet dann: Jede nach Poisson positiv stabile Bewegung in der Ebene ist periodisch.

Dass dies tatsächlich die obige Behauptung enthält, folgt einfach daraus, dass jede beschränkte, stark stabile Bewegung die Eigenschaften a) und b) besitzt. Für a) ist dies klar, und b) kann man z. B. daraus entnehmen, dass die Bewegung nach Markoff fastperiodisch ist.

3. Wenn die rechten Seiten des Differentialgleichungssystems

$$\frac{dx_1}{dt} = f_1(x_1, x_2), \quad \frac{dx_2}{dt} = f_2(x_1, x_2) \tag{3}$$

in einem Gebiet Γ der x_1, x_2-Ebene stetig sind und in der Umgebung eines jeden Punktes von Γ einer Lipschitz-Bedingung genügen, so besitzt jede Lösung $x(t) = [x_1(t), x_2(t)]$ von (3), die für $-\infty < t < \infty$ in Γ verläuft, von selbst die Eigenschaft a), wie man aus der stetigen Abhängigkeit der Lösungen von den Anfangswerten entnimmt. In diesem Spezialfall besagt der genannte Satz: Ist $x(t)$ eine für $-\infty < t < \infty$ in Γ verlaufende Lösung von (3) und existiert eine Folge

$t_1, t_2, \ldots \to \infty$ derart, dass die Punkte $x(t_\nu)$ gegen einen Punkt $x(t_0)$ der Integralkurve konvergieren, so ist $x(t)$ periodisch, also die Integralkurve geschlossen. Dies ist schon von BENDIXSON[1] gezeigt worden.

4. Zum Beweis unseres Satzes genügt es zu zeigen, dass die von $x(t)$ beschriebene Kurve wenigstens einen Doppelpunkt hat. Ist nämlich für zwei verschiedene Werte τ_0 und τ von t

$$x(\tau_0) = x(\tau),$$

so ist (1) für jedes $\delta > 0$, folglich auch (2) für jedes $\varepsilon > 0$ und jedes $l > 0$ erfüllt. Also ist in der Tat

$$x(\tau_0 + t) = x(\tau + t)$$

für alle t. Die Existenz eines Doppelpunktes der Kurve $x(t)$ ergibt sich nun unter noch schwächeren Voraussetzungen: Wir werden a) nur für ein festes, willkürliches l und ein festes τ_0, nämlich $\tau_0 = t_0$ gebrauchen und zeigen, dass der Teil $t \geq t_0 - l$ der Kurve einen Doppelpunkt besitzt. Periodizität der Bewegung lässt sich dann natürlich nicht mehr behaupten. Nach Einführung eines neuen Parameters, für den $t_0 = 0$ und $l = 1$ wird und den wir wieder mit t bezeichnen, können wir also unsere endgültige Behauptung folgendermassen formulieren:

[1] I. BENDIXSON: Sur les courbes définies par des équations différentielles [Acta math. **24**, 1—88 (1901)], insbes. S. 11—12. Vgl. auch L. BIEBERBACH: Theorie der Differentialgleichungen, 3. Aufl. Berlin: J. Springer, 1930, S. 82—83.

Dass der BENDIXSONsche Beweis erheblich einfacher als der folgende ist, beruht darauf, dass bei Selbstapproximation einer Integralkurve von (3) zugleich die Richtungen approximiert werden, worüber hier nichts vorausgesetzt wird.

Satz: Der Punkt $x(t)$ der Ebene sei für $t \geqq -1$ stetig von t abhängig, und es seien die folgenden Bedingungen erfüllt:

A) Es gebe zu jedem $\varepsilon > 0$ ein $\delta = \delta(\varepsilon) > 0$ derart, dass aus

$$\varrho[x(0), x(\tau)] \leqq \delta \qquad (\tau > 0) \tag{4}$$

die Ungleichung

$$\varrho[x(t), x(\tau + t)] \leqq \varepsilon \tag{5}$$

für $-1 \leqq t \leqq 1$ folgt.

B) Ferner existiere eine Folge $t_1, t_2, \ldots \to \infty$ derart, dass $x(t_\nu)$ für $\nu \to \infty$ gegen $x(0)$ konvergiert.

Dann besitzt die von $x(t)$ beschriebene Bahnkurve wenigstens einen Doppelpunkt.

5. Wir bemerken zunächst, dass Voraussetzungen und Behauptung dieses Satzes — übrigens auch der beiden in 1. und 2. formulierten Sätze — gegenüber topologischen Abbildungen der Ebene auf sich invariant sind.

Wir nehmen nun an, dass die Behauptung falsch, dass also die Bahnkurve $x(t)$ doppelpunktfrei ist. Um uns einfacher ausdrücken zu können, wollen wir durch eine topologische Abbildung der Ebene auf sich den Kurvenbogen $x(t), -1 \leqq t \leqq 1$, in eine Strecke der Länge 2 überführen, und zwar so, dass der Parameter t die Länge auf dieser Strecke wird[1]. Alsdann sind unsere Voraussetzungen [viel-

[1] Dass dies möglich ist, kann man etwa so einsehen: Man ergänze den Bogen $x(t), -1 \leqq t \leqq 1$, und eine beliebige Strecke der Länge 2 zu je einer einfach geschlossenen Kurve und bilde diese geschlossenen Kurven topologisch so auf einander ab, dass dem Punkt $x(t), -1 \leqq t \leqq 1$, derjenige Punkt der Strecke entspricht, der von ihrem einen Endpunkt den Abstand $t + 1$ hat. Diese Abbildung der Kurven lässt sich zu einer topologischen Abbildung der ganzen Ebene auf sich erweitern. (Vgl. B. v. Kerékjártó: Vorlesungen über Topologie. Berlin: J. Springer 1923, S. 69.)

leicht mit anderem $\delta(\varepsilon)$] auch für die neue Bewegung erfüllt, und ihre Bahnkurve ist nach unserer (zu widerlegenden) Annahme ebenfalls doppelpunktfrei. Mit anderen Worten: Wir können ohne Beschränkung der Allgemeinheit zu den obigen Voraussetzungen hinzufügen, dass das Stück $-1 \leqq t \leqq 1$ der Bahnkurve eine Strecke der Länge 2 ist und mit der Geschwindigkeit 1 durchlaufen wird.

In der Voraussetzung A) wählen wir $\varepsilon = \frac{1}{4}$ und legen um den Punkt $x(0)$ die abgeschlossene Kreisscheibe K_0 vom Radius $\operatorname{Min}\left(\frac{1}{4}, \delta\left(\frac{1}{4}\right)\right)$ und um $x(-1)$ und $x(1)$ die abgeschlossenen Kreisscheiben K_{-1} und K_1 vom Radius $\frac{1}{4}$. Ist nun τ irgend ein Wert > 1, für den der Punkt $x(\tau)$ zu K_0 gehört, so dass also (4) besteht, so folgt (5), d. h.

$$\varrho[x(t),\ x(\tau+t)] \leqq \tfrac{1}{4} \quad \text{für } -1 \leqq t \leqq 1. \tag{6}$$

Hieraus schliesst man: $x(\tau-1)$ liegt in K_{-1} und $x(\tau+1)$ in K_1. Ferner, dass der Bogen $x(\tau-\frac{1}{2})$, $x(\tau+\frac{1}{2})$ weder mit K_{-1} noch mit K_1 Punkte gemein hat, und schliesslich, dass der Bogen $x(\tau-1)$, $x(\tau+\frac{1}{2})$ zu K_1 und der Bogen $x(\tau-\frac{1}{2})$, $x(\tau+1)$ zu K_{-1} punktfremd sind. Etwas weniger präzis können wir dies so ausdrücken: Jedesmal, wenn der Punkt $x(t)$ nach K_0 gelangt, kommt er notwendig von K_{-1} ohne K_1 zu treffen, und geht nach K_1, ohne K_{-1} zu treffen.

Es bezeichne nun τ' den kleinsten Wert > 1, für welchen $x(\tau')$ zu K_0 gehört. Ein solcher existiert auf Grund der Voraussetzung B). Dann liegt $x(\tau'+1)$ in K_1 und $x(\tau'-1)$ in K_{-1}. Wir verbinden $x(\tau')$ mit $x(0)$ geradlinig. Es sei $x(\tau)$ der $x(0)$ nächste Schnittpunkt dieser Strecke mit dem Kurvenbogen $x(\tau'-1)$, $x(\tau'+1)$ (vgl. Abb. 1). Dann ist

$$\tau' \leqq \tau < \tau'+1, \tag{7}$$

da die Strecke in K_0 liegt und $x(\tau')$ der erste auf $x(1)$

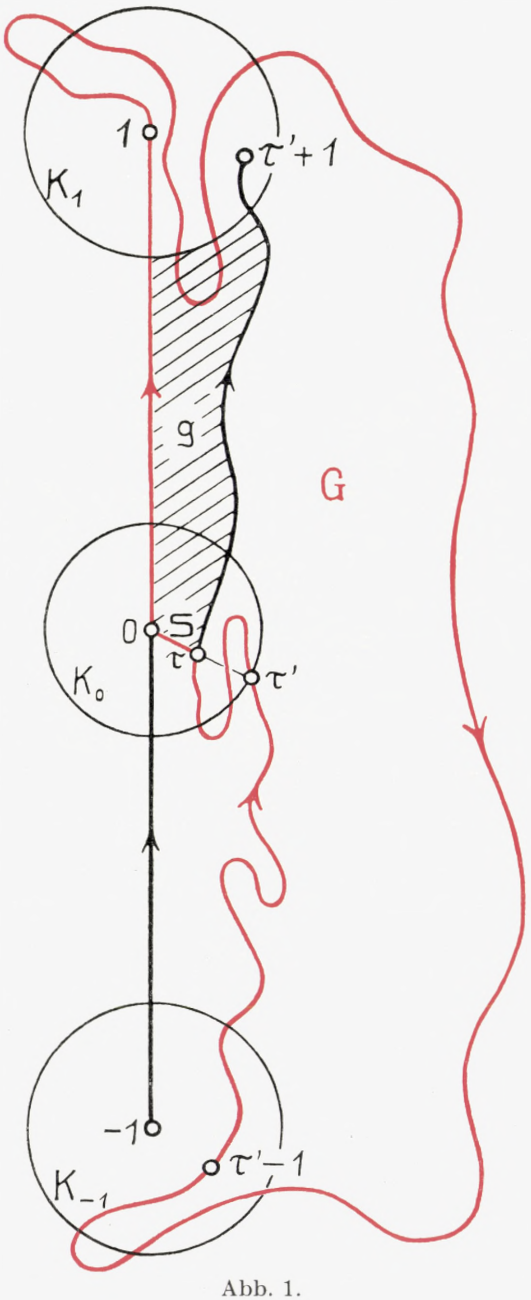

Abb. 1.

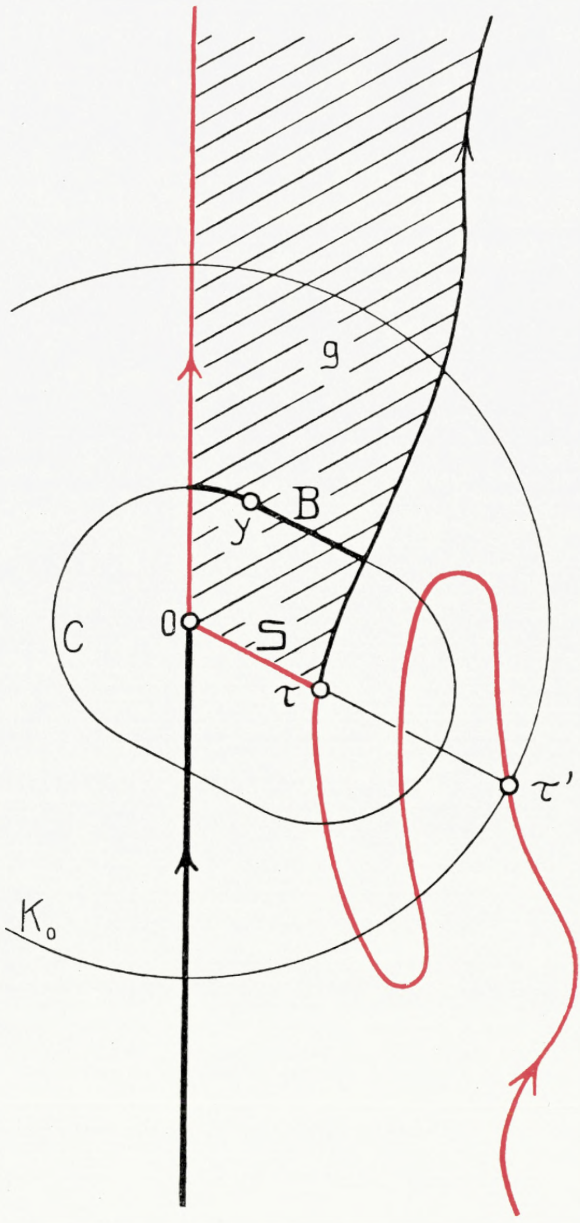

Abb. 2.

folgende Bahnpunkt in K_0 ist. Das Stück der (ja als doppelpunktfrei angenommenen) Bahnkurve von $x(0)$ bis $x(\tau)$ bildet zusammen mit der Strecke $x(\tau)$, $x(0)$, die wir kurz mit S bezeichnen, eine einfach geschlossene Kurve. Dadurch werden in der Ebene zwei Gebiete bestimmt. Der Bogen $x(\tau)$, $x(\tau'+1)$ hat mit dieser geschlossenen Kurve wegen der Konstruktion von $x(\tau)$ und der Doppelpunktfreiheit der Bahnkurve nur den Punkt $x(\tau)$ gemein, verläuft also vollständig in einem der beiden Gebiete. Dieses Gebiet heisse G (in Abb. 1 ist der Rand von G rot gezeichnet). Unser Ziel ist zu zeigen, dass die Bahnkurve in ihrem weiteren Verlauf das Gebiet G nicht verlassen kann und dass andererseits der Punkt $x(-1)$ nicht zu G gehört. Dadurch werden wir nämlich auf einen Widerspruch geführt; denn nach der Voraussetzung B) muss die Bahn dem Punkt $x(0)$ und daher nach A) auch dem Punkt $x(-1)$ beliebig nahe kommen.

Die beiden Stücke der Bahnkurve, die in den Punkten $x(0)$ und $x(\tau)$ beginnen, bis zu ihren ersten Schnittpunkten mit dem Kreis K_1 bilden zusammen mit einem beliebigen der beiden durch diese Schnittpunkte bestimmten Bögen von K_1 und mit der Strecke S eine weitere einfach geschlossene Kurve. Deren Inneres bezeichnen wir mit g (in Abb. 1 schraffiert). Diese ganze Kurve, und daher auch ihr Inneres g, liegt in einer Entfernung $\leqq \frac{1}{4}$ von dem geradlinigen Teil $x(0)$, $x(1)$ der Bahn. Dies gilt nämlich für die Strecke S, da sie zu K_0 gehört, für den Bogen des Kreises K_1, da er den Radius $\frac{1}{4}$ hat, und für den Bogen $x(\tau)$, $x(\tau'+1)$ wegen (6) und (7). Daraus folgt, dass der Teil $x(-1)$, $x(0)$ der Bahn, der mit dem Rand von g nur den Punkt $x(0)$ gemein hat, ganz ausserhalb g liegt. Dasselbe gilt auch für den Bogen $x(\tau'-1)$, $x(\tau)$; denn nach Konstruktion von $x(\tau)$ hat er mit dem Rand von g nur den Punkt $x(\tau)$ gemein,

und der Punkt $x(\tau'-1)$ kann nicht zu g gehören, da er in K_{-1} liegt.

Da $x(\tau')$ der erste auf $x(1)$ folgende Punkt der Bahn ist, der zu K_0 gehört, hat der Bogen $x(1)$, $x(\tau'-1)$ von K_0, also auch von der in K_0 enthaltenen Strecke S einen positiven Minimalabstand. Wir betrachten nun einen beliebigen in g gelegenen Punkt y, dessen Abstand von S kleiner als dieser Minimalabstand und auch kleiner als $\frac{1}{4}$ ist. Es soll zunächst gezeigt werden, dass y auch zu G gehört, woraus dann sofort folgt, dass g und G auf derselben Seite der zu den Begrenzungen beider Gebiete gehörigen Strecke S liegen. Um dies einzusehen, lege man durch y die Kurve C konstanten Abstandes von S, bestehend aus zwei parallelen Geradenstücken und zwei Halbkreisen (Abb. 2), und betrachte den grössten den Punkt y enthaltenden Teilbogen B dieser Kurve, der bis auf die Endpunkte in g liegt. Dieser Bogen kann nicht aus der ganzen Kurve C bestehen, d. h. er hat zwei verschiedene Endpunkte; denn C hat von $x(0)$ einen Maximalabstand $\leqq \frac{1}{2}$, und die in den Endpunkten von S endigenden Bögen $x(-1)$, $x(0)$ und $x(\tau'-1)$, $x(\tau)$, die nach dem früher Festgestellten nicht zu g gehören, werden daher von C geschnitten, da sie im Kreis K_{-1} beginnen, dessen Abstand von $x(0)$ grösser als $\frac{1}{2}$ ist. B hat also zwei verschiedene Endpunkte. Von diesen kann höchstens einer auf $x(0)$, $x(1)$ liegen; denn dieser geradlinige Teil der Bahn hat nur einen Schnittpunkt mit C. Mit K_1 hat C keinen Schnittpunkt. Folglich liegt wenigstens ein Endpunkt von B auf $x(\tau)$, $x(\tau'+1)$. Dieser Bogen liegt aber nach Definition von G innerhalb G. Daraus folgt nun, dass der ganze Bogen B und damit auch der Punkt y in G liegt. B ist nämlich [abgesehen von höchstens einem Endpunkt auf $x(0)$, $x(1)$] zum Rand von G punktfremd; denn der

Bogen $x(1)$, $x(\tau'-1)$ hat einen grösseren Abstand von S als die Kurve C, und der Bogen $x(\tau'-1)$, $x(\tau)$ verläuft ausserhalb g. Damit ist in der Tat gezeigt, dass die Gebiete g und G auf derselben Seite ihrer gemeinsamen Begrenzung S liegen.

Daraus folgt zunächst, dass der Bogen $x(-1)$, $x(0)$, insbesondere also der Punkt $x(-1)$, wie behauptet, ausserhalb G liegt; sonst müsste nämlich $x(-1)$, $x(0)$ auch Punkte von g enthalten, was nicht der Fall ist.

Andererseits ergibt sich nun die Behauptung, dass die Bahn $x(t)$ das Gebiet G für $t \geqq \tau'+1$ nicht mehr verlassen kann. G könnte nämlich nur durch die in K_0 gelegene Strecke S verlassen werden. Nun kann die Kurve nach K_0 nur gelangen, wenn sie von K_{-1} herkommt, ohne K_1 zu treffen. Dies ist jedoch unmöglich, da K_{-1} ausserhalb g liegt und die Kurve von G aus nur durch K_1 in g eindringen kann. Damit ist der Beweis zuende geführt.

---

6. Bei einer fastperiodischen Bewegung $x(t)$ ist offenbar die Voraussetzung b) von 2. erfüllt. Aus dem dort ausgesprochenen Satz ergibt sich also, dass eine ebene fastperiodische Bewegung, die der Voraussetzung a) genügt, notwendig periodisch ist. Es liegt hier die Frage nahe, ob man ohne die Voraussetzung a) noch behaupten kann, dass die Bahnkurve einer fastperiodischen Bewegung stets einen Doppelpunkt besitzt. Dass dies nicht der Fall ist, zeigt ein Beispiel einer doppelpunktfreien fastperiodischen Bewegung in der Ebene, das uns von B. Jessen mitgeteilt worden ist und das wir im folgenden mit seiner Erlaubnis wiedergeben.

Den Ausgangspunkt für die Konstruktion bildet der

folgende Hilfssatz: Es sei $x_a(t)$ eine periodische Bewegung der Periode $4a$, die in der Halbperiode $-a \leqq t \leqq a$ ein doppelpunktfreies offenes Polygon monoton durchläuft und in der zweiten Halbperiode auf demselben Wege derart zurückkehrt, dass

$$x_a(t) = x_a(2a - t) \tag{8}$$

für $a \leqq t \leqq 3a$, also wegen der Periodizität für alle t gilt. Dann gibt es zu jedem $\varepsilon > 0$ eine Bewegung $x_{3a}(t)$ der Periode $12a$ mit den folgenden Eigenschaften:

I. In der Halbperiode $-3a \leqq t \leqq 3a$ durchläuft $x_{3a}(t)$ monoton ein offenes doppelpunktfreies Polygon.

II. Es ist

$$x_{3a}(t) = x_{3a}(6a - t) \tag{9}$$

für $3a \leqq t \leqq 9a$, also für alle t.

III. Für $-a \leqq t \leqq a$ stimmen die Bewegungen $x_a(t)$ und $x_{3a}(t)$ überein:

$$x_a(t) = x_{3a}(t) \quad \text{für} \quad -a \leqq t \leqq a. \tag{10}$$

IV. Für alle t gilt

$$\varrho[x_a(t),\ x_{3a}(t)] \leqq \varepsilon. \tag{11}$$

Um dies zu beweisen, braucht man $x_{3a}(t)$ nur für die Halbperiode $-3a \leqq t \leqq 3a$ so zu konstruieren, dass die Bedingungen I, III und IV in diesem Intervall erfüllt sind, und es dann für die zweite Halbperiode durch (9) zu definieren. Alsdann ist nämlich (11) von selbst für alle t erfüllt; denn aus (8) und der Periodizität von $x_a(t)$ folgt auch für $x_a(t)$

$$x_a(t) = x_a(6a - t).$$

Um $x_{3a}(t)$ für $-3a \leqq t \leqq 3a$ zu konstruieren, setze man an die Endpunkte $-a$ und a des von $x_a(t)$ beschriebenen Polygons je ein weiteres offenes Polygon $-3a$, $-a$ bzw. a, $3a$ derart an, dass insgesamt ein offenes doppelpunktfreies Polygon $-3a$, $-a$, a, $3a$ entsteht und dass die beiden zugefügten Polygone in genügender (durch ε bestimmter)

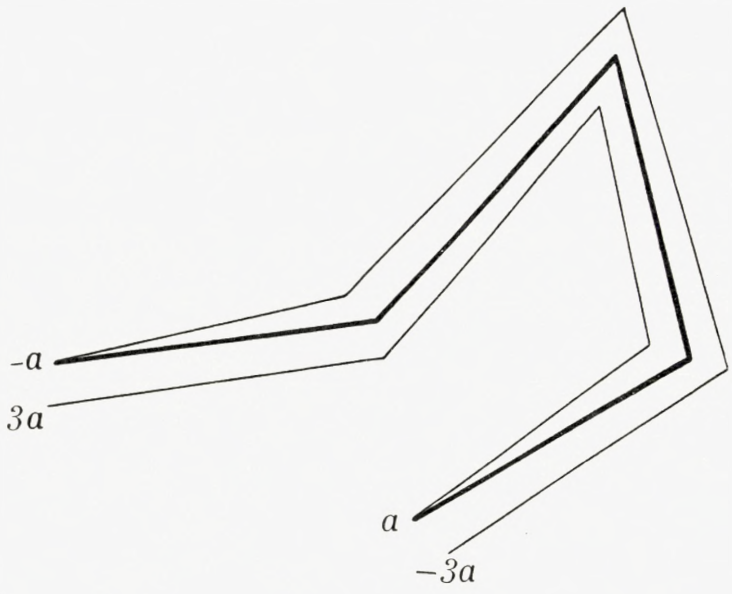

Abb. 3.

Nähe des ursprünglichen verlaufen (Abb. 3). Dann ist es, wie nicht näher ausgeführt zu werden braucht, möglich, das Polygon $-3a$, $3a$ von $x_{3a}(t)$ im Intervall $-3a \leqq t \leqq 3a$ so durchlaufen zu lassen, dass die Bedingungen (10) und (11) erfüllt sind.

Man gehe nun von einer beliebigen Bewegung $x_1(t)$ der Periode 4 aus, die den im Hilfssatz genannten Voraussetzungen für $a = 1$ genügt, und konstruiere auf Grund des Hilfssatzes zu $\varepsilon = \frac{1}{2}$ eine Bewegung $x_3(t)$ der Periode 12, von dieser ausgehend eine Bewegung $x_{3^2}(t)$ zu $\varepsilon = \dfrac{1}{2^2}$ und so fort,

wenn $x_{3n}(t)$ bereits definiert ist, eine Bewegung $x_{3n+1}(t)$ zu $\varepsilon = \frac{1}{2^{n+1}}$. Die so entstehende Folge periodischer Bewegungen ist gleichmässig konvergent; denn es ist ja nach (11)

$$\varrho\,[x_{3n}(t),\ x_{3n+1}(t)] \leqq \frac{1}{2^{n+1}}.$$

Die Grenzbewegung $x(t)$ ist also stetig und grenzperiodisch. Wegen (10) stimmt sie in einem beliebigen Intervall $-3^k \leqq t \leqq 3^k$ mit $x_{3n}(t)$ für $n > k$ überein, und da $x_{3n}(t)$ in $-3^n \leqq t \leqq 3^n$ doppelpunktfrei ist, gilt dasselbe von der Grenzbewegung $x(t)$.

Forelagt paa Mødet den 21. Februar 1936.
Færdig fra Trykkeriet den 24. Juni 1936.

Det Kgl. Danske Videnskabernes Selskab.
Mathematisk-fysiske Meddelelser. **XIV**, 2.

KLEINERE BEITRÄGE ZUR THEORIE DER FASTPERIODISCHEN FUNKTIONEN VI

VON

HARALD BOHR

KØBENHAVN
LEVIN & MUNKSGAARD
EJNAR MUNKSGAARD
1936

Printed in Denmark.
Bianco Lunos Bogtrykkeri A/S.

Der Picardsche Satz.

Die vorliegende Note behandelt eine Frage aus der Theorie der analytischen fastperiodischen Funktionen $f(s)$ einer komplexen Veränderlichen $s = \sigma + it$. Die allgemeine Theorie dieser Funktionen sowie ihrer Dirichletentwicklungen $\sum A_n e^{\lambda_n s}$ wurde in der Abhandlung »Zur Theorie der fastperiodischen Funktionen III« (Acta Mathematica Bd. 47) entwickelt.

Ich erinnere an die Definition: Eine im Streifen $(-\infty \leqq)$ $\alpha < \sigma < \beta$ $(\leqq +\infty)$ analytische Funktion $f(s)$ heisst fastperiodisch in $\alpha < \sigma < \beta$ oder kürzer »fastperiodisch in (α, β)«, falls es zu jedem ε eine relativ dichte Menge von Verschiebungszahlen, d. h. reellen Zahlen τ gibt, welche für alle s des genannten Streifens der Ungleichung $|f(s + i\tau) - f(s)| \leqq \varepsilon$ genügen.

Ferner wurde eine in $\alpha < \sigma < \beta$ reguläre Funktion »fastperiodisch in $[\alpha, \beta]$« bzw. »fastperiodisch in $[\alpha, \beta)$« genannt, falls sie in jedem beiderseits beschnittenen Streifen $(\alpha <)$ $\alpha_1 < \sigma < \beta_1 (< \beta)$ bzw. in jedem einseitig beschnittenen Streifen $(\alpha <)$ $\alpha_1 < \sigma < \beta$ fastperiodisch ist.

Für eine in einer rechten Halbebene $[\alpha, \infty]$ fastperiodische Funktion

$$f(s) \sim \sum A_n e^{\lambda_n s}$$

habe ich in der genannten Abhandlung betreffs ihres Verhaltens im »Punkt $\sigma = \infty$« die folgenden Tatsachen dargetan,

die ein klassisches Resultat über reinperiodische Funktionen auf fastperiodische Funktionen verallgemeinern.

Es bestehen für das Verhalten der Funktion $f(s)$ für $\sigma \to \infty$ genau drei Möglichkeiten, die als der reguläre, der polare und der wesentlich singuläre Fall zu bezeichnen sind.

I. Die Funktion $f(s)$ strebt für $\sigma \to \infty$ gleichmässig in t einem endlichen Grenzwerte Γ zu, und es ist in diesem Fall $f(s)$ nicht nur in $[\alpha, \infty]$, sondern sogar in $[\alpha, \infty)$ fastperiodisch. Dieser »reguläre Fall« tritt dann und nur dann ein, wenn die Dirichletexponenten der Funktion alle ≤ 0 sind, und der genannte Grenzwert Γ ist gerade das konstante Glied der Dirichletentwicklung von $f(s)$ (d. h. natürlich der Wert Null, falls alle Exponenten negativ sind). Was das nähere Verhalten von $f(s)$ für $\sigma \to \infty$ betrifft, so sind hier zwei Unterfälle zu unterscheiden:

I^a. Falls unter den negativen Exponenten λ_n kein absolut kleinster vorkommt, nimmt die Funktion $f(s)$ in jeder rechten Halbebene $\sigma > \sigma_0$ den Grenzwert Γ an.

I^b. Falls es dagegen unter den negativen Exponenten λ_n einen absolut kleinsten gibt, wird bei hinreichend grossem σ_0 der Grenzwert Γ in der Halbebene $\sigma > \sigma_0$ nirgends angenommen.

II. Der absolute Betrag von $f(s)$ strebt für $\sigma \to \infty$ gegen Unendlich und zwar gleichmässig in t. Dieser »polare Fall« tritt dann und nur dann ein, wenn es positive Exponenten λ_n gibt und unter ihnen einen grössten, etwa λ_N. Genauer gilt, dass die Funktion $f(s)$ sich asymptotisch wie das Glied $A_N e^{\lambda_N s}$ verhält, d. h. es gilt gleichmässig in t die Limesgleichung $\lim_{\sigma \to \infty} f(s)\, e^{-\lambda_N s} = A_N$.

III. Die Funktion $f(s)$ nimmt in jeder Halbebene $\sigma > \sigma_0$ Werte an, die in der ganzen komplexen Ebene überall dicht liegen. Dieser »wesentlich singuläre Fall« tritt dann und nur dann ein, wenn es positive Exponenten λ_n gibt, unter ihnen aber keinen grössten. Wie im Fall I sind auch hier zwei Unterfälle zu unterscheiden:

III^a. Falls die Menge der positiven Exponenten λ_n beschränkt ist (ohne dass aber ihre obere Grenze selbst zur Exponentenmenge gehört), so nimmt die Funktion $f(s)$ in jeder Halbebene $\sigma > \sigma_0$ jeden Wert ohne irgendwelche Ausnahme an.

III^b. Falls dagegen die Menge der positiven Exponenten nicht nach oben beschränkt ist, kann (wie schon der Spezialfall der reinperiodischen Funktionen lehrt) natürlich nicht allgemein behauptet werden, dass $f(s)$ sämtliche Werte annimmt. Wohl aber gilt als Verallgemeinerung des klassischen PICARDschen Satzes, dass $f(s)$ in jeder Halbebene $\sigma > \sigma_0$ sämtliche Werte mit höchstens einer einzigen Ausnahme annimmt.

Die zum Beweise der verschiedenen oben angeführten Tatsachen verwendeten allgemeinen funktionentheoretischen Hilfsmittel waren alle relativ einfacher Art bis auf diejenigen, welche zur Begründung der unter III^b genannten Verallgemeinerung des PICARDschen Satzes herangezogen wurden. Die einfache und sinnreiche Methode, durch welche LINDELÖF für den klassischen Fall lauter ganzzahliger Exponenten den Beweis des PICARDschen Satzes durch Verwendung eines fundamentalen Satzes von SCHOTTKY erbringen konnte, liess sich nämlich nicht auf den Fall der fastperiodischen Funktionen übertragen, und der Verf. sah

sich daher genötigt, um den Picardschen Satz für beliebige fastperiodische Funktionen zu beweisen, einen recht tiefliegenden Satz »geometrischer« Art heranzuziehen, welcher von Iversen durch das Studium der inversen Funktion einer analytischen Funktion gefunden war. Neuerdings ist es aber dem Verfasser gelungen, eine Variante des Lindelöfschen Beweises des klassischen Picardschen Satzes zu finden, welche im Gegensatz zu dem ursprünglichen Lindelöfschen Beweise auf den fastperiodischen Fall übertragbar ist. Dadurch ergibt sich ein neuer Beweis des Picardschen Satzes für fastperiodische Funktionen, welcher wesentlich einfacher ist als der in der anfangs zitierten Arbeit gegebene. Diesen neuen Beweis mitzuteilen ist der Zweck der vorliegenden Note.

Die genannte Variante des Lindelöfschen Beweises — sowie eine daraus folgende allgemein-funktionentheoretische (d.h. von der Theorie der fastperiodischen Funktionen unabhängige) Verallgemeinerung des Picardschen Satzes — habe ich in einer Note »Zum Picardschen Satz« in der Herrn Gravé gewidmeten Festschrift auseinandergesetzt. Sie basiert auf dem folgenden funktionentheoretischen Lemma, welches unter Benutzung einer einfachen konformen Abbildung aus einer bekannten von Landau herrührenden Verschärfung des oben erwähnten Schottkyschen Satzes abgeleitet werden kann.

Lemma: Es seien a und b $(\neq a)$ zwei komplexe Zahlen und k eine positive Grösse. Dann gibt es eine positive Konstante $K = K(a, b, k)$ mit der folgenden Eigenschaft: Jede in der Halbebene $\sigma > 0$ reguläre und von a und b verschiedene Funktion $f(s)$, welche auf der Geraden $\sigma = 1$ die Ungleichung

$$|f(s)| < k$$

befriedigt, genügt in der ganzen Halbebene $\sigma > 1$ der Ungleichung

$$|f(s)| < e^{K\sigma}.$$

Aus diesem Lemma, für dessen Beweis ich auf die letztzitierte Arbeit verweise, folgt der PICARDsche Satz für fastperiodische Funktionen — den wir nochmals explizite als »Satz« formulieren — in wenigen Worten.

Satz. Es sei $f(s)$ in der Halbebene $\sigma > \alpha$ regulär und in $[\alpha, \infty]$ fastperiodisch, und es besitze die Dirichletentwicklung $\sum A_n e^{\Lambda_n s}$ von $f(s)$ beliebig grosse positive Exponenten Λ_n. Dann nimmt die Funktion $f(s)$ in jeder Halbebene $\sigma > \sigma_0$ alle Werte mit höchstens einer einzigen Ausnahme an.

Beweis: Wir nehmen den Satz als falsch an, d.h. dass es ein $\sigma_0 > \alpha$ sowie zwei Werte a und $b\,(\neq a)$ derart gäbe, dass $f(s) \neq a$ und $\neq b$ für $\sigma > \sigma_0$. Ohne Beschränkung der Allgemeinheit darf $\sigma_0 = 0$ angenommen werden; sonst ersetze man nur $f(s)$ durch $f(s + \sigma_0)$. Auf der Geraden $\sigma = 1$ ist $f(s)$ beschränkt, etwa $|f(s)| < k$, einfach weil die Funktion $F(t) = f(1 + it)$ eine fastperiodische Funktion der reellen Veränderlichen t ist. Zu den Werten a, b und k bestimmen wir eine positive Konstante K im Sinne des obigen Lemmas. Dann würde in der ganzen Halbebene $\sigma > 1$ die Ungleichung

$$|f(s)| < e^{K\sigma}$$

gelten. Nunmehr wählen wir in der Dirichletentwicklung von $f(s)$ ein Glied $A_N e^{\Lambda_N s}$, dessen Exponent Λ_N grösser als diese Konstante K ist. Für jedes $\sigma > 0$ gilt

$$M_t\{f(\sigma+it)\,e^{-i\Lambda_N t}\} = \lim_{T\to\infty}\frac{1}{2T}\int_{-T}^{+T} f(\sigma+it)\,e^{-i\Lambda_N t}\,dt = A_N\,e^{\Lambda_N\sigma},$$

und es ist also a fortiori

$$\underset{-\infty<t<\infty}{\text{Obere Grenze}}\,|f(\sigma+it)| \geqq |A_N|\,e^{\Lambda_N\sigma}.$$

Diese für alle $\sigma > 0$ gültige Ungleichung steht aber (wegen $\Lambda_N > K$) in offenbarem Widerspruch zu der obigen, unter der zu widerlegenden Annahme $f(s) \neq a, b$ für $\sigma > 1$ abgeleiteten Ungleichung

$$|f(\sigma+it)| < e^{K\sigma},$$

womit der Satz dargetan ist.

Forelagt paa Mødet den 1. Maj 1936.
Færdig fra Trykkeriet den 15. Juni 1936.

Det Kgl. Danske Videnskabernes Selskab.
Mathematisk-fysiske Meddelelser. **XIV**, 3.

STUDIES ON HALOGEN-CYANIDES II.

THE DISTRIBUTION OF IODINE CYANIDE AND CYANOGEN BROMIDE BETWEEN BENZENE AND WATER, AND BETWEEN BENZENE AND SOME AQUEOUS SALT SOLUTIONS. THE SYNTHESIS AND THE MOLECULAR WEIGHT OF IODINE CYANIDE

BY

MAX MØLLER

KØBENHAVN
LEVIN & MUNKSGAARD
EJNAR MUNKSGAARD
1936

Printed in Denmark.
Bianco Lunos Bogtrykkeri A/S.

1. Introduction.

In an investigation of the equilibrium:

$$ICN + I^- + H^+ \rightleftarrows I_2 + HCN,$$

KOVACH[1] attempted to calculate the equilibrium constant. But the value which was obtained from the conductivity measurements and the potentiometric estimations cannot be correct, such as it was realized already by KOVACH, since the value of the iodine-iodide ion potential, calculated by means of the equilibrium constant, is not in agreement with the accepted value.

This disagreement may be due to, either that the activity of iodine cyanide is strongly effected by salts in general, or that iodine cyanide reacts with iodide ions and cyanide ions to form complex compounds, or to both of these effects.

The following research was started to investigate the salting out effect on iodine cyanide and cyanogen bromide, and to investigate if these substances actually are able to unite with halogen ions to form complex ions, similar to the tri-iodide ion, I_3^-.

When this investigation was in progress YOST & STONE[2] published a paper dealing with the complexformation of iodine cyanide with iodide and cyanide ions.

[1] Z. phys. Chem. **80** (1912) 107.

[2] Jour. Amer. Chem. Soc. **55** (1933) 1889.

From the distribution of iodine cyanide between carbon tetrachloride and aqueous solutions of potassium iodide and potassium cyanide, these authors have estimated two quantities, which should be the complexity constants of the ions $ICNI^-$ and $ICNCN^-$. In the calculation they have assumed, that the activity of the iodine cyanide, for the same concentration of iodine cyanide, is the same in water and in an aqueous salt solution. This, however, is not permissible, since a considerable salting out effect is observed, such as it will be seen in the following. If the authors had used sodium iodide and sodium cyanide, in place of the potassium salts, the computed complexity constants would have been different, but equally wrong.

In the following investigation of the distribution of iodine cyanide and cyanogen bromide between benzene and aqueous salt solutions the effect of iodide ions has not been dealt with, as it appeared to require special precautions. Even a minute quantity of carbon dioxide in the solutions produces a formation of free iodine, which changes the distribution ratio (estimated by thiosulphate titrations) considerably. In solutions of potassium cyanide the hydroxyl ions produce a slow hydrolysis of iodine cyanide and a rapid hydrolysis of cyanogen bromide, probably accompanied by other reactions, and the cyanide solutions, therefore, have not been dealt with in this paper.

2. The Synthesis of Cyanogen Bromide and Iodine Cyanide.

The cyanogen bromide was prepared as mentioned in a previous paper[1] and was perfectly pure.

[1] Det Kgl. Danske Vid. Selskab. Math.-fys. Medd. XII, 17 (1934).

According to SERULLAS[1] and SEUBERT & POLLARD[2] iodine cyanide may be prepared from mercuric cyanide and iodine, either by sublimation of the stoechiometric mixture, or by adding the iodine in the form of an ethereal solution to the mercuric cyanide, evaporate to dryness, and extract the iodine cyanide, which is formed, by means of ether[3].

None of these methods, however, are practical for the production of larger quantities of iodine cyanide, and it is difficult to obtain a perfect separation from free iodine and the mercuric salts.

Another method, therefore, was applied, similar to SCHOLL's cyanogen bromide synthesis, and a similar method has been employed by YOST & STONE (l. c.).

21.1 grams of pure sodium cyanide (98—99 %) were dissolved in 80 ccs. of water in a bottle with a wide neck. The solution was placed in ice and stirred by means of a glass rod fitted to an electric stirrer. To the ice-cold solution 100 grams of iodine were added in small portions (2—3 grams at the time), and the next portion first added when the previous had reacted. When all the iodine is added, the solution, which still contains a slight excess of cyanide ions, is extracted trice with ether in a separatory funnel. The first time with 90 ccs., then with 70 ccs. and finally with about 50 ccs. of ether.

The ethereal solution is now evaporated at ordinary temperature in a hood with good ventilation, until all ether has disappeared. The crystalline mass is dissolved in alcohol, just enough to effect a complete dissolution. After a filtra-

[1] Ann. Chim. Phys. (2) **27** (1824) 188.
[2] B. **23** (1890) 1062.
[3] Linnemann: Lieb. Ann. **120** (1861) 36.

tion water is added to the alcoholic solution, until a slight precipitation occurs, which does not disappear on stirring. After 24 hours the major part of the iodine cyanide has crystallized out. It is filtered by suction, washed with water, and dried over calcium chloride (which has been treated with carbon dioxide to remove any alkaline components). The yield is about 45 to 47 grams of a slightly brownish substance (theory 60.3 grams).

To effect a further purification the iodine cyanide is sublimed. This has been done in two ways. The first method is to place the brownish iodine cyanide in the bottom of an ordinary filter pump suction flask, cover it with a piece of filter paper, and in the neck of the flask fix a wide test tube filled with carbon dioxide snow and ether. On evacuation of the flask the iodine cyanide sublimes and deposites on the test tube in needleshaped crystals. The sublimation may also be effected by placing the impure iodine cyanide in the bottom of a wide glass tubing, cover it with a piece of filter paper, close the tube with a rubber stopper fitted with a glass stopcock, evacuate and place the tube on the top of a radiator for heating the room.

The products obtained by these sublimations are perfectly pure, i. e. they give the theoretical quantity of iodine on addition to a solution of potassium iodide acidifyed with acetic acid.

For instance 0.9212 gram of iodine cyanide was dissolved with water in a measuring flask, and the volume made up to 500.2 ccs. The solution thus is 0.01204 molar. 10.01 ccs. of this solution were added to a solution of 2 grams of potassium iodide in 25 ccs. of 5 % acetic acid, and the liberated iodine titrated with a 0.01017 N. solution of sodium thiosulphate. In 6 estimations the consumption of iodine

was: 23.72, 23.71, 23.69, 23.71, 23.69, 23.69 ccs., or on the average 23.70 ccs. From this result the molarity of the iodine cyanide solution is calculated to 0.01204, which is in complete agreement with the result above.

3. The Analytical Estimation of Cyanogen Bromide and Iodine Cyanide.

Cyanogen bromide and iodine cyanide have in the following been estimated, as already mentioned, by an iodometric titration with thiosulphate. It should only be mentioned that special precautions are necessary when 0.01 N. solutions of sodium thiosulphate are standardized, such as it has been stated in a previous paper.[1]

4. The Molecular Weight of Iodine Cyanide in Aqueous Solutions and in Benzene.

To be certain that no polymerization occurs in benzene solutions of iodine cyanide, the molecular weight was determined by the freezing point method. The applied benzene was of a pure brand for molecular weight estimations. It was dried over metallic sodium and distilled. After this it had the correct freezing point.

In a series of estimations it was found, within an experimental error of about 2—3 %, that the molecular weight of iodine cyanide is the same in benzene and aqueous solutions and equal to the theoretical value.

The molecular weight of cyanogen bromide has been investigated in a previous paper[2] and has the theoretical value both in water and benzene.

[1] Max Møller: Z. analyt. Chem. **99** (1934) 353.
[2] l. c.

5. The Distribution of Iodine Cyanide and Cyanogen Bromide between Water and Benzene at 25°. The Estimation of d_0.

The experiments were made by weighing out a certain quantity of the halogen cyanide in a small phial with glass stopper, dissolving the content in water saturated with benzene at 25° and making the solution up to the desired volume. This solution was then titrated by the usual iodometric method. Then a certain volume of the halogen cyanide solution (50 or 100 ccs.) was taken out by means of a pipette and runned to the equal volume of benzene (saturated with water at 25°) in a glass stoppered bottle. After securing the stopper with a rubber cap, the bottle was rotated in a water thermostate at $25° \pm 0.02°$. The equilibrium is attained in less than half an hour. Samples of the benzene solution and the aqueous solution were pipetted into solutions of potassiun iodide in 5% acetic acid and titrated with an 0.01 N. solution of sodium thiosulphate.

The results of the distribution experiments for iodine cyanide between water and benzene are given in the table I. Here the column ICN, H_2O is the molar concentration of iodine cyanide in the aqueous layer and the column ICN, C_6H_6 the molar concentration in the benzene layer. d is the distribution ratio, i. e. the ratio of the iodine cyanide concentration in the benzene layer to the concentration in the aqueous layer.

It may be seen from the table, that the value of d is the same for the three lowest iodine cyanide concentrations. We may accept, therefore, for the distribution ratio at infinite dilution, d_0, the value:

$$d_0 = 1.421.$$

Assuming that the activity of the iodine cyanide in the benzene solution is equal to the concentration for the entire range of concentrations in the table, the activity coefficient of the iodine cyanide in the aqueous solution is given by:

$$f = \frac{d}{d_0}.$$

The values of f together with the value of log f are given in the table.

Table I.

The distribution of iodine cyanide between water and benzene at 25°.

ICN, H_2O Molarity	ICN, C_6H_6 Molarity	d	f	log f
0.0005411	0.0007690	1.421		
0.001077	0.001532	1.422	1.000	0.0000
0.002163	0.003075	1.421		
0.003217	0.004578	1.423	1.002	0.0009
0.003235	0.004607	1.424		
0.004759	0.006781	1.425	1.003	0.0013
0.006423	0.009177	1.429	1.006	0.0026
0.009644	0.01383	1.434	1.009	0.0039
0.01278	0.01841	1.441	1.014	0.0060
0.01600	0.02310	1.444	1.016	0.0069

Table II.

The distribution of iodine cyanide between water and carbon tetrachloride at 25°. Yost & Stone's experiments recalculated with $d_0 = 0.1755$.

ICN, H_2O Molarity	ICN, CCl_4 Molarity	log f Y. & S.	log f recalculated
0.02480	0.004460	0.0066	0.0105
0.02596	0.004673	0.0071	0.0110
0.03312	0.006007	0.0104	0.0143
0.05144	0.009441	0.0154	0.0193
0.06697	0.01239	0.0190	0.0229
0.07173	0.01330	0.0199	0.0238
0.07960	0.01482	0.0218	0.0257

In fig. 1 the curve (ICN) gives the values of log f plotted against the iodine cyanide concentration in the aqueous layer.

Yost & Stone (l. c.) have estimated the distribution of iodine cyanide between water and carbon tetrachloride for iodine cyanide concentrations higher than the here applied,

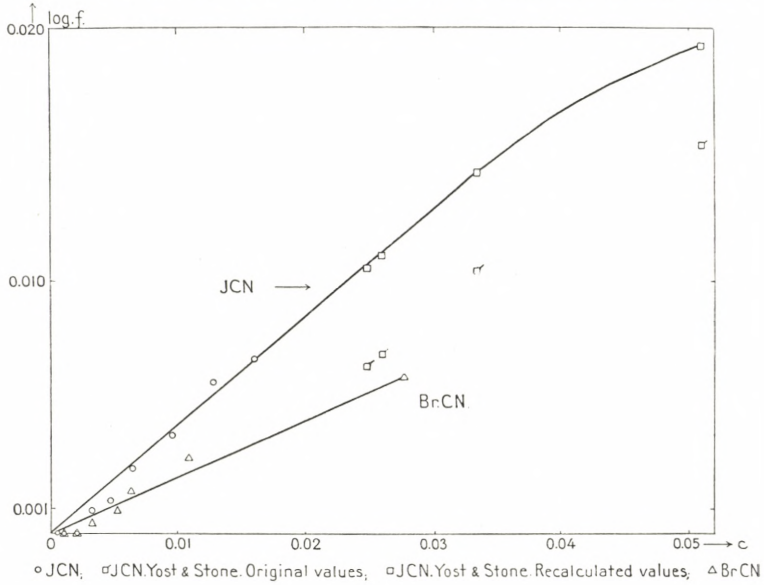

Fig. 1.

and have by a graphic method extrapolated to the value of d_0, the distribution ratio at infinitive dilution. If the activity coefficient of the iodine cyanide in the aqueous solution is calculated from Yost & Stone's experiments and their value for d_0 (table II column log f, Y & S), the results do not fit in with the experiments in table I. However, it appears that the curve for Yost & Stone's values of log f, plotted against the iodine cyanide concentration, is not directed toward the zeropoint at infinitive dilution. When the distribution ratios are plotted against the concen-

trations of iodine cyanide in the aqueous layer, it appears, that in the extrapolation to the value of $d_0 = 0.1771$, these authors have omitted the two lowest concentrations. When these are taken into consideration the value obtained is $d_0 = 0.1755$. When the activity coefficient is calculated by means of this value (table II, log f recalculated), the results fit in nicely with the experiments in table I (see fig. 1).

Table III.

The distribution of cyanogen bromide between water and benzene at 25°.

BrCN, H_2O Molarity	BrCN, C_6H_6 Molarity	d	f	log f
0.001040	0.003646	3.506	1.000	0.0000
0.002091	0.007331	3.506		
0.003119	0.01094	3.508	1.001	0.0004
0.003187	0.01117	3.505		
0.005207	0.01829	3.512	1.002	0.0009
0.006340	0.02232	3.520	1.004	0.0017
0.01089	0.03845	3.530	1.007	0.0030
0.02773	0.07065	3.548	1.012	0.0052

The distribution ratio of cyanogen bromide between water and benzene are given in table III. Here BrCN, H_2O and BrCN, C_6H_6 are the cyanogen bromide concentrations in the aqueous layer and the benzene layer respectively, when the distribution equilibrium is attained. The value of the distribution ratio at infinitive dilution is found to $d_0 = 3.506$. By means of this value the activity coefficient of cyanogen bromide in the aqueous solution has been calculated (f and log f in the table), and in fig. 1 the values of log f have been plotted against the cyanogen bromide concentrations (curve BrCN).

It may be observed that the two curves in fig. 1 are of a similar shape, but that the "self-salting-out effect" is less for cyanogen bromide than for iodine cyanide.

6. The Distribution of Iodine Cyanide and Cyanogen Bromide between Benzene and Aqueous Salt Solutions.

These experiments were made in a manner similar to the distribution of the halogen cyanides between water and benzene. The solutions of the salts, potassium chloride, sodium chloride, potassium bromide, sodium bromide, potassium nitrate, sodium nitrate, sodium perchlorate and sodium sulphate, were made by weighing out the dry, anhydrous salts and dissolve to a definite volume with water.

After addition of a measured volume of a halogen cyanide solution of a known concentration to a measured volume of the salt solution (all the aqueous solutions were made from water saturated with benzene at 25°), an equal volume of benzene (saturated with water) was added, and the mixture rotated in a thermostate at $25° \pm 0.02°$. When the equilibrium had been attained, samples of the two layers were drawn by means of pipettes, runned into acidified solutions of potassium iodide and the liberated iodine titrated with a 0.01 N. solution of sodium thiosulphate. From the results of the two titrations the distribution coefficient (d in the following tables III to XVII) was calculated. By means of this value and the distribution coefficient d'_0 (obtained from table I or III) for the halogen cyanide distribution between pure water and benzene, when the benzene layer has the same halogen cyanide concentration as the benzene layer in the distribution experiment in question, the quantity f, the "apparent activity coefficient", has been calculated. This is defined by the equation:

$$f = \frac{d}{d'_0}.$$

The values of f are given in the tables, and in the graphs, figs. 2 and 4, the values of log f have been plotted against the normal salt concentration.

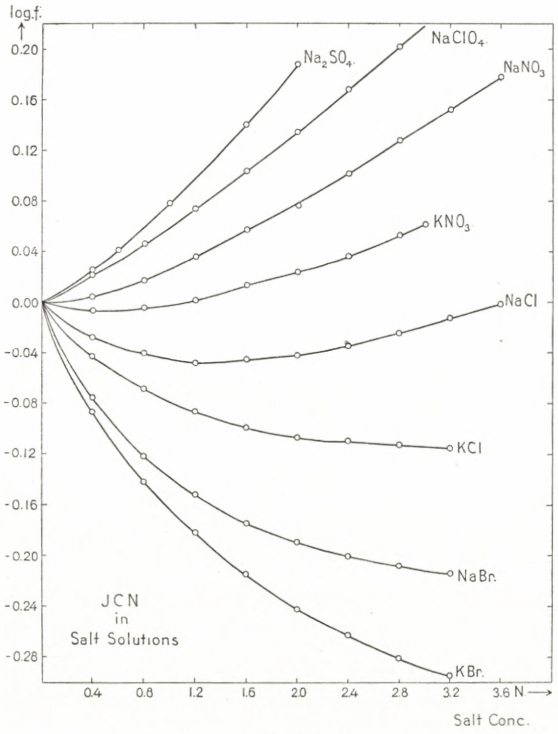

Fig. 2.

Further a quantity k has been calculated, defined by the equation:

$$\log f = k \cdot c,$$

where f is the apparent activity coefficient of the halogen cyanide in the salt solution of the normal concentration c. The values of k are given in the tables, and in the graphs, figs. 3 and 5, k has been plotted against the normal salt concentration.

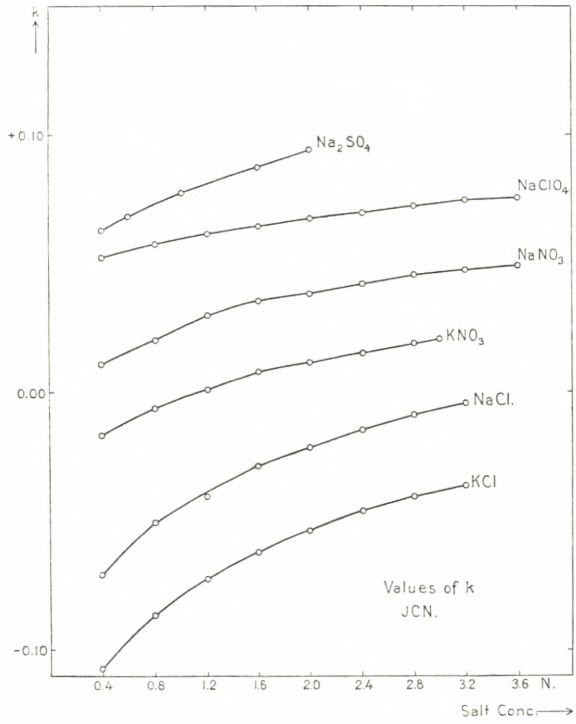

Fig. 3a.

Table IV.

The distribution of ICN between benzene and aqueous solutions of KCl at 25°.

KCl conc. Normality	ICN, Salt, aq. Molarity	ICN, C_6H_6 Molarity	d	f	log f	k
		$d'_0 = 1.424$				
0.4000	0.003581	0.004617	1.289	0.9055	— 0.0432	— 0.1080
0.8000	0.003703	0.004493	1.213	0.8520	— 0.0696	— 0.0870
1.200	0.003786	0.004410	1.165	0.8180	— 0.0872	— 0.0727
1.600	0.003846	0.004350	1.131	0.7944	— 0.1000	— 0.0625
2.000	0.003883	0.004313	1.111	0.7802	— 0.1078	— 0.0539
2.400	0.003896	0.004301	1.104	0.7754	— 0.1105	— 0.0460
2.800	0.003908	0.004287	1.097	0.7704	— 0.1133	— 0.0405
3.200	0.003922	0.004275	1.090	0.7654	— 0.1161	— 0.0363

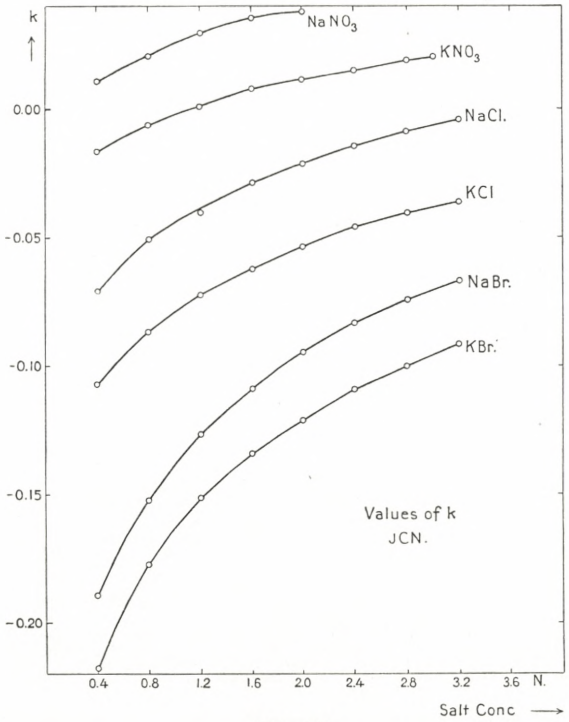

Fig. 3 b.

Table V.

The distribution of ICN between benzene and aqueous solutions of NaCl at 25°.

NaCl conc. Normality	ICN, Salt, aq. Molarity	ICN, C_6H_6 Molarity	d	f	log f	k
		$d'_0 =$	1.424			
0.4000	0.004385	0.005845	1.333	0.9375	— 0.0280	— 0.0710
0.8000	0.004493	0.005823	1.296	0.9110	— 0.0405	— 0.0506
1.200	0.004480	0.005703	1.273	0.8948	— 0.0483	— 0.0403
1.600	0.004517	0.005785	1.281	0.9008	— 0.0454	— 0.0284
2.000	0.004484	0.005789	1.291	0.9068	— 0.0425	— 0.0213
2.400	0.004418	0.005795	1.312	0.9226	— 0.0350	— 0.0146
2.800	0.004360	0.005855	1.343	0.9442	— 0.0249	— 0.00888
3.200	0.004321	0.005967	1.381	0.9707	— 0.0129	— 0.00403

Table VI.

The distribution of ICN between benzene and aqueous solutions of KBr at 25°.

KBr conc. Normality	ICN, Salt, aq. Molarity	ICN, C_6H_6 Molarity	d	f	log f	k
		$d'_0 =$	1.425			
0.4000	0.005332	0.006208	1.164	0.8180	— 0.0872	— 0.2180
0.8000	0.005689	0.005843	1.027	0.7208	— 0.1422	— 0.1778
1.200	0.005963	0.005577	0.9357	0.6577	— 0.1820	— 0.1517
1.600	0.006175	0.005354	0.8670	0.6084	— 0.2158	— 0.1344
2.000	0.006353	0.005176	0.8146	0.5717	— 0.2428	— 0.1214
2.400	0.006484	0.005045	0.7779	0.5459	— 0.2629	— 0.1095
2.800	0.006743	0.005029	0.7459	0.5234	— 0.2812	— 0.1004
3.200	0.006700	0.004840	0.7225	0.5077	— 0.2944	— 0.0920

Table VII.

The distribution of ICN between benzene and aqueous solutions of NaBr at 25°.

NaBr conc. Normality	ICN, Salt, aq. Molarity	ICN, C_6H_6 Molarity	d	f	log f	k
		$d'_0 =$	1.424			
0.4000	0.004765	0.005694	1.195	0.8392	— 0.0761	— 0.1902
0.8000	0.005038	0.005410	1.074	0.7541	— 0.1225	— 0.1531
1.200	0.005224	0.005235	1.002	0.7037	— 0.1526	— 0.1271
1.600	0.005345	0.005088	0.9520	0.6685	— 0.1749	— 0.1093
2.000	0.005435	0.004998	0.9196	0.6460	— 0.1899	— 0.09495
2.400	0.005480	0.004913	0.8966	0.6300	— 0.2009	— 0.08370
2.800	0.004586	0.004830	0.8802	0.6182	— 0.2089	— 0.0746
3.200	0.005541	0.004816	0.8690	0.6103	— 0.2145	— 0.0670

Table VIII.

The distribution of ICN between benzene and aqueous solutions of $NaClO_4$ at 25°.

$NaClO_4$ conc. Normality	ICN, Salt, aq. Molarity	ICN, C_6H_6 Molarity	d	f	log f	k
		$d'_0 = 1.424$				
0.4000	0.004006	0.005987	1.494	1.049	0.0209	0.0523
0.8000	0.003871	0.006127	1.583	1.112	0.0460	0.0575
1.200	0.003708	0.006253	1.686	1.184	0.0734	0.0615
1.600	0.003568	0.006448	1.807	1.269	0.1035	0.0647
2.000	0.003397	0.006607	1.945	1.366	0.1354	0.0677
2.400	0.003233	0.006778	2.097	1.472	0.1680	0.0700
2.800	0.003068	0.006971	2.272	1.596	0.2029	0.0725
3.200	0.002906	0.007185	2.472	1.736	0.2396	0.0749
3.600	0.002730	0.007293	2.671	1.876	0.2732	0.0759

Table IX.

The distribution of ICN between benzene and aqueous solutions of KNO_3 at 25°. Conc. of ICN in benzene layer before distribution 0.009914 molar.

KNO_3 conc. Normality	ICN, Salt, aq. Molarity	ICN, C_6H_6 Molarity	d	f	log f	k
		$d'_0 = 1.424$				
0.4000	0.004127	0.005787	1.402	0.9845	−0.0068	−0.0170
0.8000	0.004118	0.005796	1.408	0.9888	−0.0049	−0.0061
1.200	0.004085	0.005829	1.427	1.002	0.0009	0.0008
1.600	0.004021	0.005893	1.466	1.030	0.0126	0.0079
2.000	0.003964	0.005950	1.502	1.055	0.0232	0.01160
2.400	0.003894	0.006020	1.547	1.087	0.0360	0.01500
2.800	0.003802	0.006112	1.608	1.129	0.0528	0.01886
3.000	0.003737	0.006134	1.642	1.153	0.0619	0.02063

Table X.

The distribution of ICN between benzene and aqueous solutions of $NaNO_3$ at 25°. Conc. of ICN in benzene layer before distribution 0.009964 molar.

$NaNO_3$ conc. Normality	ICN, Salt, aq. Molarity	ICN, C_6H_6 Molarity	d	f	log f	k
		$d'_0 =$	1.424			
0.4000	0.004089	0.005875	1.437	1.0093	0.0040	0.0110
0.8000	0.004022	0.005942	1.478	1.038	0.0162	0.0203
1.200	0.003915	0.006049	1.546	1.086	0.0357	0.0298
1.600	0.003797	0.006167	1.624	1.141	0.0571	0.0357
2.000	0.003697	0.006267	1.696	1.191	0.0759	0.0380
2.400	0.003563	0.006401	1.797	1.262	0.1010	0.0421
2.800	0.003424	0.006540	1.911	1.342	0.1278	0.0456
3.200	0.003303	0.006661	2.017	1.417	0.1513	0.0472
3.600	0.003171	0.006793	2.143	1.506	0.1778	0.0493

Table XI.

The distribution of ICN between benzene and aqueous solutions of Na_2SO_4 at 25°.

Na_2SO_4 conc. Normality (2 · Molarity)	ICN, Salt, aq. Molarity	ICN, C_6H_6 Molarity	d	f	log f	k
		$d'_0 =$	1.422			
0.4000	0.002551	0.003842	1.506	1.059	0.0249	0.0623
0.6000	0.002498	0.003901	1.562	1.099	0.0408	0.0680
1.000	0.002366	0.004020	1.700	1.195	0.0775	0.0775
1.600	0.002161	0.004241	1.962	1.380	0.1398	0.0874
2.000	0.002008	0.004401	2.192	1.541	0.1879	0.0940

Table XII.

The distribution of BrCN between benzene and aqueous solutions of KCl at 25°.

KCL conc. Normality	BrCN, Salt, aq. Molarity	BrCN, C_6H_6 Molarity	d	f	log f	k
		$d'_0 =$	3.505			
0.4000	0.003157	0.01126	3.565	1.017	0.0073	0.0182
0.8000	0.003097	0.01132	3.653	1.042	0.0180	0.0225
1.200	0.003035	0.01139	3.752	1.070	0.0295	0.0246
1.600	0.002964	0.01145	3.863	1.102	0.0422	0.0264
2.000	0.002892	0.01154	4.022	1.147	0.0597	0.0299
2.400	0.002787	0.01162	4.171	1.190	0.0755	0.0315
2.800	0.002710	0.01171	4.322	1.233	0.0910	0.0325
3.200	0.002632	0.01179	4.476	1.277	0.1062	0.0332

Table XIII.

The distribution of BrCN between benzene and aqueous solutions of NaCl at 25°.

NaCl conc. Normality	BrCN, Salt, aq. Molarity	BrCN, C_6H_6 Molarity	d	f	log f	k
		$d'_0 =$	3.510			
0.4000	0.004639	0.01700	3.663	1.044	0.0186	0.0465
8.0000	0.004479	0.01718	3.835	1.093	0.0385	0.0481
1.200	0.004239	0.01714	4.043	1.152	0.0614	0.0512
1.600	0.004055	0.01734	4.276	1.218	0.0857	0.0536
2.000	0.003854	0.01749	4.538	1.293	0.1116	0.0558
2.400	0.003654	0.01755	4.812	1.371	0.1370	0.0571
2.800	0.003472	0.01764	5.081	1.448	0.1607	0.0574
3.200	0.003302	0.01775	5.376	1.532	0.1852	0.0578
3.600	0.003154	0.01788	5.665	1.614	0.2079	0.0578

Table XIV.

The distribution of BrCN between benzene and aqueous solutions of KBr at 25°.

KBr conc. Normality	BrCN, Salt, aq. Molarity	BrCN, C_6H_6 Molarity	d	f	log f	k
		$d'_0 = 3.505$				
0.4000	0.003231	0.01118	3.460	0.9872	— 0.0056	— 0.0140
0.8000	0.003243	0.01115	3.436	0.9804	— 0.0086	— 0.0108
1.200	0.003247	0.01116	3.438	0.9808	— 0.0084	— 0.0070
1.600	0.003238	0.01115	3.444	0.9826	— 0.0076	— 0.0047
2.000	0.003219	0.01119	3.477	0.9920	— 0.0035	— 0.0018
2.400	0.003184	0.01123	3.527	1.006	0.0027	0.0011
2.800	0.003156	0.01126	3.566	1.017	0.0075	0.0026
3.200	0.003120	0.01129	3.618	1.032	0.0138	0·0043

Table XV.

The distribution of BrCN between benzene and aqueous solutions of NaBr at 25°.

NaBr conc. Normality	BrCN, Salt, aq. Molarity	BrCN, C_6H_6 Molarity	d	f	log f	k
		$d'_0 = 3.505$				
0.4000	0.003133	0.01109	3.538	1.009	0.0041	0.0102
0.8000	0.003085	0.01109	3.596	1.026	0.0111	0.0139
1.200	0.003020	0.01112	3.680	1.050	0.0211	0.0176
1.600	0.002955	0.01118	3.782	1.079	0.0330	0.0206
2.000	0.002885	0.01117	3.870	1.104	0.0430	0.0215
2.400	0.002793	0.01115	3.990	1.139	0.0563	0.0234
2.800	0.002712	0.01120	4.126	1.177	0.0709	0.0253
3.200	0.002625	0.01119	4.260	1.215	0.0847	0.0265

Table XVI.

The distribution of BrCN between benzene and aqueous solutions of $NaClO_4$ at 25°.

$NaClO_4$ conc. Normality	BrCN, Salt, aq. Molarity	BrCN, C_6H_6 Molarity	d	f	log f	k
		$d'_0 =$	3.506			
0.4000	0.001979	0.007101	3.589	1.023	0.0102	0.0255
0.8000	0.001925	0.007099	3.688	1.052	0.0220	0.0275
1.200	0.001867	0.007094	3.799	1.084	0.0349	0.0291
1.600	0.001817	0.007158	3.939	1.123	0.0506	0.0316
2.000	0.001737	0.007233	4.164	1.188	0.0747	0.0374
2.400	0.001686	0.007306	4.334	1.236	0.0921	0.0384
2.800	0.001626	0.007406	4.556	1.300	0.1138	0.0406
3.200	0.001571	0.007470	4.755	1.356	0.1324	0.0414
3.600	0.001507	0.007480	4.963	1.416	0.1510	0.0419

Table XVII.

The distribution of BrCN between benzene and aqueous solutions of KNO_3 at 25°.

KNO_3 conc. Normality	BrCN, Salt, aq. Molarity	BrCN, C_6H_6 Molarity	d	f	log f	k
		$d'_0 =$	3.506			
0.4000	0.002334	0.008236	3.529	1.0063	0.0027	0.0067
0.8000	0.002316	0.008254	3.563	1.016	0.0069	0.0086
1.200	0.002294	0.008276	3.609	1.0295	0.0126	0.0105
1.600	0.002250	0.008320	3.698	1.055	0.0232	0.0145
2.000	0 002201	0.008369	3.803	1.085	0.0354	0.0177
2.400	0.002150	0.008420	3.915	1.117	0.0480	0.0200
2.800	0.002103	0.008467	4.027	1.149	0.0602	0.0215
3.000	0.002071	0.008499	4.095	1.168	0.0674	0.0225

Table XVIII.

The distribution of BrCN between benzene and aqueous solutions of $NaNO_3$ at 25°.

$NaNO_3$ conc. Normality	BrCN, Salt, aq. Molarity	BrCN, C_6H_6 Molarity	d	f	log f	k
		$d'_0 = 3.507$				
0.4000	0.002300	0.008298	3.609	1.0295	0.0126	0.0315
0.8000	0.002240	0.008358	3.733	1.065	0.0273	0.0341
1.200	0.002174	0.008425	3.874	1.105	0.0432	0.0360
1.600	0.002104	0.008494	4.039	1.152	0.0614	0.0384
2.000	0.002010	0.008588	4.275	1.219	0.0861	0.0431
2.400	0.001937	0.008661	4.472	1.275	0.1056	0.0440
2.800	0.001866	0.008732	4.687	1.337	0.1261	0.0450
3.200	0.001790	0.008808	4.929	1.406	0.1479	0.0462
3.600	0.001718	0.008880	5.176	1.476	0.1692	0.0470

Table XIX.

The distribution of BrCN between benzene and aqueous solutions of Na_2SO_4 at 25°.

Na_2SO_4 conc. Normality	BrCN, Salt, aq. Molarity	BrCN, C_6H_6 Molarity	d	f	log f	k
		$d'_0 = 3.506$				
0.4000	0.002506	0.009894	3.947	1.126	0.0515	0.1287
0.6000	0.002398	0.01005	4.190	1.195	0.0774	0.1290
1.000	0.002155	0.01023	4.748	1.354	0.1317	0.1317
1.600	0.001821	0.01052	5.774	1.647	0.2167	0.1354
2.000	0.001629	0.01069	6.560	1.871	0.2721	0.1365

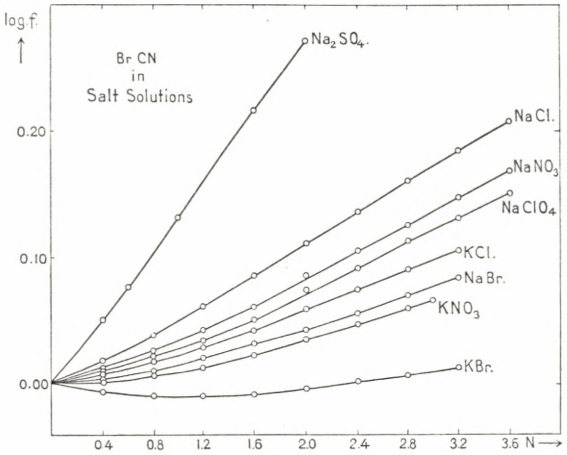
log f.
Br CN
in
Salt Solutions
Na_2SO_4
NaCl.
$NaNO_3$
$NaClO_4$
KCl.
NaBr.
KNO_3
KBr.
0.20
0.10
0.00
0.4
0.8
1.2
1.6
2.0
2.4
2.8
3.2
3.6 N
Salt Conc.

Fig. 4.

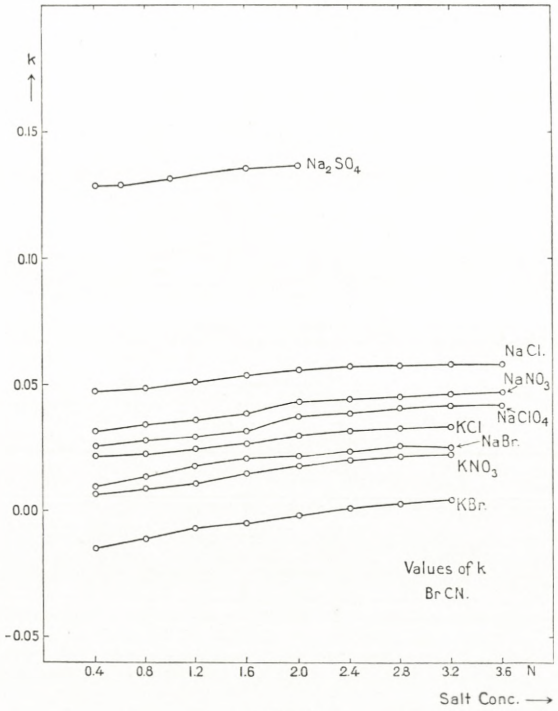
k
0.15
0.10
0.05
0.00
-0.05
Na_2SO_4
NaCl.
$NaNO_3$
$NaClO_4$
KCl.
NaBr.
KNO_3
KBr.
Values of k
Br CN.
0.4
0.8
1.2
1.6
2.0
2.4
2.8
3.2
3.6 N
Salt Conc.

Fig. 5.

7. Discussion of the Distribution Experiments.

a. Introduction.

Observing the plots of log f against the salt concentration (figs. 2 and 4) one is struck immediately by the difference in the appearance of the curves for iodine cyanide and cyanogen bromide. While the iodine cyanide curves are wide apart and show a curvature in the entire range of salt solutions investigated, the cyanogen bromide curves are much closer together, and from a salt concentration of about 1.2 or 1.6 N. the curves are straight lines (excepting the curves for NaBr and KBr).

It may also be observed that the sodium chloride and the sodium nitrate curves of cyanogen bromide are placed above the sodium perchlorate curve, while the opposite is the case for iodine cyanide. Further, for cyanogen bromide the sodium chloride curve is above the sodium nitrate curve and the potassium chloride curve above the potassium nitrate curve, while the opposite is the case for iodine cyanide. Similar differences may be observed also in other cases.

Still more striking is the difference in the appearance of the curves which have been obtained by plotting the values of k against the salt concentrations (figs. 3a, 3b and 5).

The iodine cyanide curves are wide apart and, in the majority of cases, have a strong curvature. The curves of two salts with a common anion are parallel and the distance between the curves for a sodium salt and a potassium salt is almost the same in all cases independent of the anion. But the curves of such salts which have a common cation are not parallel.

In the case of cyanogen bromide all of the k-curves are practically parallel (with the exception of the curves for the bromides which differ slightly) and at higher salt concentrations almost straight lines.

Among the k-curves of iodine cyanide the only one of the same shape as the k-curves of cyanogen bromide is the sodium perchlorate curve. The perchlorate ion, however, is a perfectly "saturated" ion, which has no or at least only a very minute tendency to form complex ions. The shape of the sodium perchlorate k-curve of cyanogen bromide, therefore, must be due entirely to the "salting out effect" of the sodium and the perchlorate ions and not to complex formation. Since the other k-curves for cyanogen bromide have the same shape (the curves for the bromides differ slightly), it may be concluded that cyanogen bromide does not form complex ions with the sulphate, the nitrate and the chloride ion. Since the curves for sodium and potassium bromide differ, if only slightly, from the other, it is likely that this is due to a complex formation. This, however, must be very slight.

As the sodium perchlorate-k-curve of iodine cyanide is practically of the same shape as the k-curves of cyanogen bromide, it may further be concluded that iodine cyanide does not form complex ions with the perchlorate ion. That the other iodine cyanide-k-curves have a different appearence must be due to a complex formation with the anions of the salts. From the shape and the relative position of the curves one might expect that iodine cyanide forms complex ions more readily with bromide ions than with cloride ions, and more readily with these than with nitrate and sulphate ions.

b. Salting out Effect and Complex Formation.

The value of the salting out effect of a certain salt solution with a certain non-electrolyte cannot, in general, be predicted with any degree of certainty[1].

It is impossible, therefore, to apply directly any universal formula for the salting out coefficient, similar to the formula for the activity coefficient of an ion in a dilute solution of an electrolyte, when the salting out effect has to be separated from the effect due to a complex formation.

The quantity f, the "apparent activity coefficient", in the previous tables includes simultaneously the change in the activity due to the salting out effect and the change in the concentration of the free halogen cyanide due to the complex formation.

Let it be assumed, however, that the distribution ratio, entirely due to the salting out effect, is d′, defined by the equation:

$$d' = \frac{J_b}{J_f}, \qquad (1)$$

where J_b is the concentration of the halogen cyanide in the benzene layer, and J_f is the concentration of free, not complex bound halogen cyanide in a certain salt solution of a certain concentration. The actual salting out coefficient is then defined by the equation:

$$f' = \frac{d'}{d'_0}, \qquad (2)$$

where d'_0 is the distribution ratio of the halogen cyanide between benzene and water as previously discussed.

[1] See for instance Randall & Fairbanks Faily: Chem. Rev. **4** (1927) 285; Åkerlof: J. Amer. Chem. Soc. **51** (1929) 984.

When the equation for the complex formation is:

$$J + X^- \rightleftarrows JX^-,$$

where J is the halogen cyanide and X^- a certain monovalent ion, the equilibrium constant K_{JX^-} is obtained from the equation:

$$K_{JX^-} = \frac{a_{JX^-}}{a_J \cdot a_{X^-}}, \tag{3}$$

where a_{JX^-}, a_J and a_{X^-} are the activities of the substances in question.

If the total concentration of the halogen cyanide in the salt solution, after the distribution equilibrium has been attained between this and the benzene layer, is J_w, we have that:

$$J_w = J_f + J_c, \tag{4}$$

where J_f is the concentration of the free halogen cyanide and J_c the concentration of the complex bound halogen cyanide.

If the total halogen cyanide concentration in the aqueous salt solution, before the distribution between a certain volume of the salt solution and the same volume of benzene, is J_0, we may write:

$$J_0 = J_w + J_b. \tag{5}$$

The apparent distribution ratio of the halogen cyanide between an aqueous salt solution containing the ion X^- and benzene is then:

$$d_x = \frac{J_b}{J_w}. \tag{6}$$

This gives

$$J_0 = J_w (1 + d_x) \text{ or } J_w = \frac{J_0}{1 + d_x}, \tag{7}$$

and

$$J_b = J_0 - J_w = \frac{J_0 \cdot d_x}{1 + d_x}. \tag{8}$$

The actual distribution ratio, however, is:

$$d'_x = \frac{J_b}{J_f},$$

which gives:

$$J_f = \frac{J_b}{d'_x} = \frac{J_0 \cdot d_x}{(1 + d_x)\, d'_x}. \tag{9}$$

Introducing these values in (4) we get:

$$J_c = \frac{J_0 (d'_x - d_x)}{(1 + d_x)\, d'_x}. \tag{10}$$

Introducing these values of the concentrations in the equation for the equilibrium constant we have:

$$K_x = \frac{J_c \alpha_c}{J_f \alpha_f [X^-]\, \alpha_x}. \tag{11}$$

Here α_c is the activity coefficient of the complex ion JX^-, $[X^-]$ the concentration and α_x the activity of the X^- ions, and finally α_f the activity coefficient of the free halogen cyanide.

As the halogen cyanide concentration in the previous experiments is very small compared to the salt concentration, the concentration of the free X^- ions may be put equal to the total salt concentration c. Further, according to previous considerations, we have that $\alpha_f = f'_x$, and the equation for the complexity constant may be written, therefore:

$$\frac{\alpha_x}{\alpha_c} \cdot K_x = \frac{J_c}{J_f \cdot f'_x \cdot c}, \qquad (12)$$

or, by introducing the values J_c and J_f from (9) and (10),

$$\frac{\alpha_x}{\alpha_c} \cdot K_x = \frac{d'_x - d_x}{d_x \cdot f'_x \cdot c}. \qquad (13)$$

On division by d'_0 in nominator and denominator this equation is transformed to:

$$\frac{\alpha_x}{\alpha_c} \cdot K_x = \frac{1}{c} \cdot \left(\frac{1}{f_x} - \frac{1}{f'_x} \right). \qquad (14)$$

Here α_c is unknown, while α_x may be obtained from the measurements of other authors and f'_x has not yet been estimated.

c. The estimation of f'_x, the actual salting out coefficient of iodine cyanide in salt solutions.

As previously discussed it may be concluded that cyanogen bromide does not form complex compounds with any other of the investigated anions than with the bromide ion, and here the complex formation, judged from the shape of the k-curve, must be very slight, so slight that it may be considered negligible in the following investigation. In the case of cyanogen bromide the values of f_x, which have been found in the experiments and are given in the tables XII to XIX (f in the tables), must be the actual salting out coefficients.

Iodine cyanide, on the other hand, as judged from the position of the apparent activity curves in comparison with the corresponding cyanogen bromide curves and from

the shape of the k-curves, forms complex ions, to different extent, with the bromide, the chloride and the nitrate ions, but not with the perchlorate ion. The k-curves for iodine cyanide and cyanogen bromide in sodium perchlorate solutions are parallel.

In table XX the value $\Delta = k_{ICN,\ NaClO_4} - k_{BrCN,\ NaClO_4}$ at different salt concentrations has been calculated, and it may be observed that it is fairly constant within the experimental error, as an error in the estimation of f of about 0.2 per cent. may cause deviations from the average value of Δ, which are very closely equal to the deviations observed in table XX.

Table XX.

$NaClO_4$ conc. Normality	k ICN, $NaClO_4$	k BrCN, $NaClO_4$	Δ
0.400	0.0523	0.0255	0.0268
0.800	0.0575	0.0275	0.0300
1.200	0.0615	0.0291	0.0324
1.600	0.0647	0.0316	0.0331
2.000	0.0677	0.0374	0.0303
2.400	0.0700	0.0384	0.0316
2.800	0.0725	0.0406	0.0319
3.200	0.0749	0.0414	0.0335
3.600	0.0759	0.0419	0.0340
		Mean...	0.0315

It has now been assumed, since cyanogen bromide and iodine cyanide are closely related and differ in structure probably only by a displacement of a pair of shared electrons, that the actual salting out effect on iodine cyanide by a sodium salt of a monovalent ion X^- may be expressed by the same equation, i. e.

$$\Delta = k'_{ICN,\ NaX} - k_{BrCN,\ NaX}$$

or:

$$k'_{ICN,\ NaX} = k_{BrCN,\ NaX} + \Delta.$$

Here $k'_{ICN,\ NaX}$ is the k-value which corresponds to the actual salting out coefficient, $f'_{ICN,\ NaX}$, of iodine cyanide in solutions of the salt NaX, and these two naturally are connected by the equation:

$$\log f'_{ICN,\ NaX} = c \cdot k'_{ICN,\ NaX} ,$$

where c as usual is the concentration of the salt, NaX, in the solution. The values of $k_{BrCN,\ NaX}$ are the k-values in the tables XIII, XV and XVIII.

By means of the value of Δ obtained in the table XX the values of the logarithm of the actual salting out coefficient of iodine cyanide, log f', in solutions of sodium bromide, sodium chloride and sodium nitrate have been calculated in the table XI, XII and XIII respectively.

By introducing these computed values of f' and the previously estimated values of f (the apparent activity coefficient) in the equation (14), the values of the quantity $\frac{\alpha_x}{\alpha_c} \cdot K_x$ have been calculated for the various salts at various salt concentrations and are given in the tables and in the graph fig. 6.

Table XXI.

Estimation of the complexity constant of the complex ion $ICNBr^-$.

$\Delta = 0.0315$.

NaBr conc.	k BrCN, NaBr	k' ICN, NaBr	log f' ICN, NaBr	log f ICN, NaBr	$\frac{\alpha_{Br}}{\alpha_c} \cdot K_{Br}$	α_{Br}	α_c
0.0000	Extrapolated graphically				0.650		
0.4000	0.0102	0.0417	0.0167	— 0.0761	0.575	0.71	0.81
0.8000	0.0139	0.0454	0.0363	— 0.1225	0.508	0.69	0.88
1.200	0.0176	0.0491	0.0589	—.0.1526	0.457	0.69	1.01
1.600	0.0206	0.0521	0.0834	— 0.1749	0.419	0.69	1.10
2.000	0.0215	0.0530	0.1060	— 0.1899	0.382	0.73	1.24
2.400	0.0234	0.0549	0.1318	— 0.2009	0.354	0.76	1.39
2.800	0.0253	0.0568	0.1590	— 0.2089	0.330	0.80	1.58
3.200	0.0265	0.0580	0.1856	— 0.2145	0.308	0.85	1.79

Table XXII.

Estimation of the complexity constant of the complex ion $ICNCl^-$.

$\Delta = 0.0315$.

NaCl conc.	k BrCN, NaCl	k′ ICN, NaCl	log f′ ICN, NaCl	log f ICN, NaCl	$\frac{\alpha_{Cl}}{\alpha_c} \cdot K_{Cl}$	α_{Cl}	α_c
0.0000	Extrapolated graphically				0.39		
0.4000	0.0465	0.0780	0.0312	— 0.0280	0.339	0.70	0.81
0.8000	0.0481	0.0796	0.0637	— 0.0405	0.293	0.67	0.89
1.200	0.0512	0.0827	0.0992	— 0.0483	0.264	0.66	0.98
1.600	0.0536	0.0851	0.1362	— 0.0454	0.238	0.67	1.10
2.000	0.0558	0.0873	0.1746	— 0.0425	0.221	0.67	1.18
2.400	0.0571	0.0886	0.2126	— 0.0350	0.206	0.69	1.22
2.800	0.0574	0.0889	0.2489	— 0.0249	0.194	0.71	1.43
3.200	0.0578	0.0893	0.2858	— 0.0129	0.182	0.73	1.56

Table XXIII.

Estimation of the complexity constant of the complex ion $ICNNO_3^-$.

$\Delta = 0.0315$.

$NaNO_3$ conc.	k BrCN, $NaNO_3$	k′ ICN, $NaNO_3$	log f′ ICN, $NaNO_3$	log f ICN, $NaNO_3$	$\frac{\alpha_{NO_3}}{\alpha_c} \cdot K_{NO_3}$	α_{NO_3}	α_c
0.0000	Extrapolated graphically				0.14		
0.4000	0.0315	0.0630	0.0252	0.0040	0.118	0.64	0.76
0.8000	0.0341	0.0656	0.0525	0.0162	0.0965	0.57	0.83
1.2000	0.0360	0.0675	0.0810	0.0357	0.0759	0.53	0.98
1.600	0.0384	0.0699	0.1118	0.0571	0.0647	0.50	1.08
2.000	0.0431	0.0746	0.1492	0.0759	0.0651	0.47	..
2.400	0.0440	0.0755	0.1812	0.1010	0.0557	0.45	1.13
2.800	0.0450	0.0765	0.2142	0.1278	0.0479	0.43	1.26
3.200	0.0462	0.0777	0.2486	0.1513	0.0443	0.41	1.30

As it may be observed, the value of this quantity is not constant, but decreases with increasing salt concentration. By a graphical extrapolation (see fig. 6), however, it is possible to obtain the approximate value at the salt concentration zero. When the salt concentration approaches

zero the values of α_x and α_c both approach unity, and thus the value obtained in the extrapolations is the approximate value of K_x.

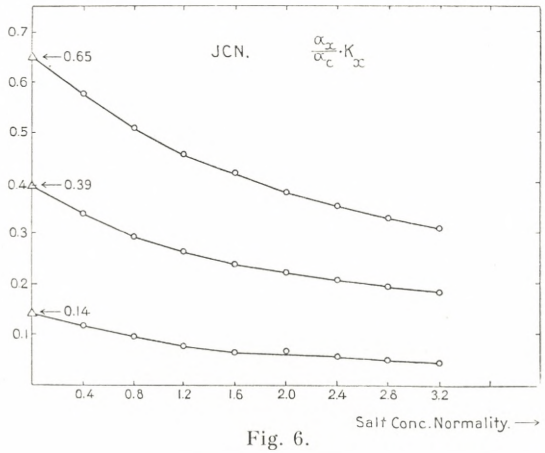

Fig. 6.

In this manner the complexity constants have been estimated as follows:

$$\frac{[ICNBr^-]}{[ICN] \cdot [Br^-]} = 0.65 \qquad A = -255 \text{ cal.}$$

$$\frac{[ICNCl^-]}{[ICN] \cdot [Cl^-]} = 0.39 \qquad A = -557 \text{ cal.}$$

$$\frac{[ICNNO_3^-]}{[ICN] \cdot [NO_3^-]} = 0.14 \qquad A = -1163 \text{ cal.}$$

The brackets here indicate the activities of the substances within the brackets.

By means of the equation:

$$A = RT \ln K_x$$

the affinity, A, of the complex formation at 25° may be calculated and is given above.

The values of α_{Br}, α_{Cl} and α_{NO_3} in the tables XXI, XXII and XXIII respectively have been taken from the tables of activity coefficients in Landolt Börnsteins tables (II Erg. Bd. 1931). By means of these, the value of K_x obtained in the extrapolation, and the values of $\frac{\alpha_x}{\alpha_c} \cdot K_x$, the values of α_c have been calculated and are given in the tables XXI to XIII.

The increase in the value of the complex-ion activity coefficients with increasing salt concentration is unusual but not improbable high.

d). Reflections on the structure of cyanogen bromide and iodine cyanide.

From an investigation of the Raman spectrum of cyanogen chloride[1] the conclusion has been drawn that this molecule is Cl–C≡N, and that, similar to hydrogen cyanide, H–C≡N, it probably is linear[2].

Since the three substances cyanogen chloride, cyanogen bromide and iodine cyanide show the same type of absorption spectre[3], it may be concluded that all three substances have the general structure X–C≡N (X is a halogen atom), and that their molecules are linear.

Cyanogen bromide and iodine cyanide in aqueous solutions (and in several other solvents) are non-electrolytes[4], and even if they may behave abnormally in certain solvents, this is probably due to a chemical reaction with the solvent molecules[5]. The bromine and the iodine in cyanogen

[1] West & Farnsworth: Jour. Chem. Phys. **1** (1933) 402.

[2] Badger & Binder: Phys. Rev. **37** (1931) 800.

[3] Badger & Sho-Chow Wo: Jour. Amer. Chem. Soc. **53** (1933) 2572.

[4] Max Møller: Det Kgl. Danske Vid. Selskabs Math.-fysiske Medd. XII, 17. Walden: Z. phys. Chem. **43** (1903) 401.

[5] Audrieth & Birr: Jour. Amer. Chem. Soc. **55** (1933) 672.

bromide and iodine cyanide respectively, therefore, are bound to the carbon atom of the cyanide group with a homopolar bond.

However, in the alkaline hydrolysis of cyanogen bromide and iodine cyanide (and in several other reactions[1]) a great difference in their behaviour is observed. With silver hydroxide, for instance, cyanogen bromide gives silver bromide and silver cyanate, while iodine cyanide gives silver iodide, silver iodate and silver cyanide. This seems to indicate that these halogen cyanides form polar molecules, and while bromine in the cyanogen bromide seems to be the electronegative part of the molecule, iodine in cyanogen iodide seems to be the electropositive part.

As far as it can be seen this, however, may meen nothing more than the pair of shared electrons in cyanogen bromide is pulled fairly close to the bromine atom, while in iodine cyanide they are pulled close to the cyanide group, (or that in cyanogen bromide the probability of their occurance is greater close to the bromine atom than to the cyanide group, and naturally the opposite for iodine cyanide.) The greater ability of iodine cyanide to form complex ions with cations may be due just to this displacement of the electronic bond.

Since the actual salting out coefficient is greater for iodine cyanide than for cyanogen bromide, it might be expected that the dipole momentum of iodine cyanide is smaller than the dipole momentum of cyanogen bromide, but this will be taken up for an experimental investigation in a following paper.

[1] See for instance CHATTAWAY & WADMORE: Jour. Chem. Soc. **81** (1902) 197.

8. Summary.

The molecular weight of iodine cyanide has been determined in water and benzene.

The distribution between water and benzene of iodine cyanide and cyanogen bromide has been investigated and the activities in very dilute aqueous solutions estimated.

The distribution of iodine cyanide and cyanogen bromide between benzene and aqueous solutions of the bromides, the chlorides, the nitrates, the sulphates and the perchlorates (of sodium only) of sodium and potassium has been investigated.

In the case of cyanogen bromide these experiments permit a direct calculation of the salting out effect, as cyanogen bromide does not form complex ions with any of the anions mentioned above, probably with the exception of the bromide ion. But here the complex formation is exceedingly slight and may be disregarded in this connection.

In the case of iodine cyanide the salting out effect is complicated by a simultaneous complex formation, to a different extent, with the bromide, the chloride, the sulphate and the nitrate ion. But no complex formation is observed with the perchlorate ion. By application of this fact, and by means of the salting out effect on cyanogen bromide it has been possible to separate, at least with a certain approximation, the effect due to the complex formation of iodine cyanide with the anion in question and the salting out effect.

The following complexity constants have been estimated:

$$\frac{[ICNBr^-]}{[ICN]\cdot[Br^-]} = 0.65; \quad \frac{[ICNCl^-]}{[ICN]\cdot[Cl^-]} = 0.39; \quad \frac{[ICNNO_3^-]}{[ICN]\cdot[NO_3^-]} = 0.14.$$

Here the brackets indicate the activity of the substances.

Finally the structure of the cyanogen bromide and the iodine cyanide molecules has been discussed.

A part of this work has been made in the Jones Chemical Laboratory of Chicago University, and it is a dear duty to express my thanks to the Head of the Department, Professor, Dr. J. STIEGLITZ, for his interest and the readiness with which all I needed was placed to my disposal.

The other part of this work has been made in the Department of Chemistry for Chemical Engineers of the Royal Polytechnic Institute, Copenhagen. I wish to thank the Head of the Department Professor, Dr. J. A. CHRISTIANSEN for his kind interest.

The author is also much indebted to the Carlsberg Foundation for a grant, which made it possible to continue the investigation.

May 1935.

Færdig fra Trykkeriet den 8. Oktober 1936.

Det Kgl. Danske Videnskabernes Selskab.
Mathematisk-fysiske Meddelelser. **XIV**, 4.

ÜBER DIE WERTEVERTEILUNG DER CHARAKTERE ABELSCHER GRUPPEN

VON

SVEND B. E. BUNDGAARD

KØBENHAVN
LEVIN & MUNKSGAARD
EJNAR MUNKSGAARD
1936

Printed in Denmark.
Bianco Lunos Bogtrykkeri A/S.

Den Inhalt dieser Arbeit bilden gewisse Verallgemeinerungen klassischer Sätze von KRONECKER [3] über diophantische Approximationen und hieran anschliessender Sätze von H. WEYL [5] über Gleichverteilung[1].

Zunächst sollen einige zu benutzende Hilfsmittel kurz besprochen werden.

$\mathfrak{G}$ bezeichne überall im folgenden eine willkürliche (abstrakte) abelsche Gruppe. Das Gruppenprodukt der Elemente $a \varepsilon \mathfrak{G}$ und $b \varepsilon \mathfrak{G}$ wird wie gewöhnlich mit ab bezeichnet; 1 sei das Einselement der Gruppe.

Ich erinnere an den Begriff des Mittelwertes einer in $\mathfrak{G}$ definierten, komplexwertigen, in v. NEUMANNschem Sinne [4] fastperiodischen (f. p.) Funktion $f(t)$: Es existiert eine und nur eine komplexe Zahl, die gleichmässig approximiert werden kann durch Summen der Form

$$\alpha_1 f(a_1 t) + \alpha_2 f(a_2 t) + \ldots + \alpha_n f(a_n t),$$

wo die a_i feste Elemente von $\mathfrak{G}$, die α_i reelle positive Zahlen mit der Summe $\alpha_1 + \alpha_2 + \ldots + \alpha_n = 1$ sind und t die Gruppe $\mathfrak{G}$ durchläuft. Diese Zahl wird mit $M\{f\}$ oder ausführlicher mit $\underset{t}{M}\{f(t)\}$ bezeichnet und der Mittelwert von f genannt.

[1] Die eingeklammerten Zahlen beziehen sich auf das Literaturverzeichnis.

Für das Funktional $M\{f\}$ gilt:

1°. $M\{1\} = 1$.
2°. $M\{f+g\} = M\{f\} + M\{g\}$.
3°. $M\{\alpha f\} = \alpha M\{f\}$, wo α eine komplexe Zahl ist.
4°. Wenn $f(t)$ nur reelle nichtnegative Werte annimmt, dann ist $M\{f\} \geqq 0$, und in dieser Ungleichung gilt das Gleichheitszeichen nur, wenn $f(t) \equiv 0$.
5°. $\underset{t}{M}\{f(at)\} = \underset{t}{M}\{f(t)\}$, wo a ein willkürliches Gruppenelement ist.

Eine nicht identisch verschwindende, in $\mathfrak{G}$ definierte komplexwertige Funktion $\varphi(t)$, die der Funktionalgleichung

$$\varphi(t_1 t_2) = \varphi(t_1)\,\varphi(t_2)$$

genügt, heisst ein Charakter der Gruppe. $\varphi(t) \equiv 1$ heisst der Hauptcharakter. Im folgenden werden nur beschränkte Charaktere $\varphi, \psi, \ldots$ betrachtet. Diese spielen in der v. Neumannschen Theorie der in $\mathfrak{G}$ f. p. Funktionen eine Rolle, die der Rolle der reinen Schwingungen $e^{2\pi i \lambda t}$ (der stetigen, beschränkten Charaktere der additiven Gruppe der reellen Zahlen) in der Bohrschen Theorie der f. p. Funktionen entspricht, und haben ähnliche Eigenschaften, nämlich:

1°. $\varphi(1) = 1$.
2°. $|\varphi(t)| = 1$ und $\varphi(t^{-1}) = \overline{\varphi(t)}$ für alle $t \varepsilon \mathfrak{G}$.
3°. Das Produkt von endlich vielen beschränkten Charakteren ist ein beschränkter Charakter.
4°. Jeder beschränkte Charakter ist f. p.
5°. Für jeden vom Hauptcharakter verschiedenen, beschränkten Charakter $\varphi(t)$ ist $M\{\varphi\} = 0$.

Weiter sei bemerkt: Ist

$$P(t) = c_1 \varphi_1(t) + c_2 \varphi_2(t) + \ldots + c_s \varphi_s(t),$$

wo $c_1, c_2, \ldots, c_s$ willkürliche komplexe Zahlen, und φ_1, $\varphi_2, \ldots, \varphi_s$ untereinander verschiedene beschränkte Charaktere sind, dann ist

$$c_\sigma = M_t\{P(t)\overline{\varphi_\sigma(t)}\}. \qquad (\sigma = 1, 2, \ldots, s.)$$

Dieses folgt unmittelbar aus 1°—5°.

N beschränkte Charaktere $\varphi_1(t), \varphi_2(t), \ldots, \varphi_N(t)$ heissen unabhängig, wenn eine Relation

$$\{\varphi_1(t)\}^{\nu_1} \cdot \{\varphi_2(t)\}^{\nu_2} \cdot \ldots \cdot \{\varphi_N(t)\}^{\nu_N} \equiv 1$$

mit ganzzahligen $\nu_1, \nu_2, \ldots, \nu_N$ nur stattfindet, sofern $\nu_1 = \nu_2 = \ldots = \nu_N = 0$.

Für stetige Charaktere

$$\varphi_1(t) = e^{2\pi i \lambda_1 t}, \quad \varphi_2(t) = e^{2\pi i \lambda_2 t}, \ldots, \varphi_N(t) = e^{2\pi i \lambda_N t}$$

in der additiven Gruppe der reellen Zahlen ist Unabhängigkeit gleichbedeutend mit der linearen Unabhängigkeit der N Zahlen $\lambda_1, \lambda_2, \ldots, \lambda_N$.

$\mathfrak{G}$ bezeichne die Produktgruppe $(\mathfrak{G}_1, \mathfrak{G}_2, \ldots, \mathfrak{G}_M)$ der M abelschen Gruppen $\mathfrak{G}_1, \mathfrak{G}_2, \ldots, \mathfrak{G}_M$ und $t = (t_1, t_2, \ldots, t_M)$ ein Gruppenelement von $\mathfrak{G}$. Ist $\varphi_\mu(t_\mu)$ ein beschränkter Charakter von $\mathfrak{G}_\mu$ $(\mu = 1, 2, \ldots, M)$, dann ist die Funktion $\varphi(t) = \varphi_1(t_1) \cdot \varphi_2(t_2) \ldots \varphi_M(t_M)$ ein Charakter von $\mathfrak{G}$. Die Funktion $\varphi(t)$ ist dann und nur dann der Hauptcharakter von $\mathfrak{G}$, wenn $\varphi_\mu(t_\mu)$ für alle μ der Hauptcharakter von $\mathfrak{G}_\mu$ ist.

Die Menge der komplexen Vorzeichen — geometrisch: die Menge der Punkte auf dem Einheitskreis — bildet eine Gruppe C mit der gewöhnlichen Multiplikation als Gruppenoperation. Die Produktgruppe

$$Q_N = (C, C, \ldots, C)$$

von N Einheitskreisen nennt man den N-dimensionalen Torusraum. Ein Punkt z aus Q_N ist also ein N-tupel

$$z = (z_1, z_2, \ldots, z_N) \tag{1}$$

von N komplexen Vorzeichen. Eine Folge $z', z'', \ldots$ von Punkten aus Q_N heisst konvergent, wenn Konvergenz in gewöhnlichem Sinne in jeder der N Koordinaten stattfindet. Die Begriffe: Häufungspunkt einer Punktmenge, abgeschlossene und offene Punktmenge, abgeschlossene Hülle einer Punktmenge, stetige Funktion u. s. v. werden wie gewöhnlich definiert. Speziell sei erwähnt, dass eine Punktmenge E überall dicht in Q_N heisst, wenn Q_N mit der abgeschlossenen Hülle von E identisch ist.

In Q_N gilt der Weierstrasssche Approximationssatz:

Für eine willkürliche in Q_N stetige, komplexwertige Funktion $g(z)$ gibt es zu jedem $\varepsilon > 0$ ein Polynom

$$S(z) = \sum_{\nu_1, \nu_2, \ldots, \nu_N} c_{\nu_1, \nu_2, \ldots, \nu_N} z_1^{\nu_1} z_2^{\nu_2} \ldots z_N^{\nu_N},$$

so dass

$$|g(z) - S(z)| \leq \varepsilon$$

für alle $z \varepsilon Q_N$.

Auf dem Einheitskreis C soll die Bogenlänge mit der Länge der Kreisperipherie als Einheit gemessen werden. $b_1, b_2, \ldots, b_N$ seien N Bogen; die Länge von b_i sei ebenfalls mit b_i bezeichnet. Die Menge der Punkte (1) mit

$z_1 \varepsilon b_1, z_2 \varepsilon b_2, \ldots, z_N \varepsilon b_N$ heisst ein Intervall in Q_N. Das Produkt

$$b_1 \cdot b_2 \cdot \ldots \cdot b_N$$

wird der Inhalt des Intervalles genannt. Speziell ist Q_N ein Intervall, dessen Inhalt gleich 1 ist.

Hiernach können die Begriffe: Riemann-integrierbare Funktion und Jordan-messbare Punktmenge auf gewöhnliche Weise eingeführt werden. Das Integral der in Q_N Riemann-integrierbaren Funktion $f(z)$ bezeichnen wir mit

$$\int_{Q_N} f(z)\, dw_N .$$

Hierzu sei bemerkt: zu einem gegebenen $\varepsilon > 0$ lässt sich ein δ derart bestimmen, dass jede zu einer Intervalleinteilung des Q_N von der »Feinheit« $\leqq \delta$ gehörige Näherungssumme σ der Relation

$$\left| \sigma - \int_{Q_N} f(z)\, dw_N \right| \leqq \varepsilon$$

genügt. Es seien $I_1, I_2, \ldots, I_n$ die Intervalle einer bestimmten Einteilung von der Feinheit $\leqq \delta$; der Inhalt von I_ν sei α_ν, und z_ν sei ein willkürlicher Punkt von I_ν. Dann ist also

$$\left| \sum_{\nu=1}^{n} \alpha_\nu f(z_\nu) - \int_{Q_N} f(z)\, dw_N \right| \leqq \varepsilon .$$

Ist nun u ein willkürlicher Punkt von Q_N, so ist, wie leicht einzusehen, $\sum \alpha_\nu f(z_\nu u)$ eine Näherungssumme, die ebenfalls zu einer (im allgemeinen neuen) Einteilung von der Feinheit $\leqq \delta$ gehört, so dass also die Ungleichung

$$\left| \sum_{\nu=1}^{n} \alpha_\nu f(z_\nu u) - \int_{Q_N} f(z)\, dw_N \right| \leqq \varepsilon$$

für jedes $u \varepsilon Q_N$ gilt.

I. Approximationssätze.

§ 1. Es seien $\lambda_1, \lambda_2, \ldots, \lambda_N$ reelle, linear unabhängige Zahlen; wir betrachten die Punktmenge

$$(\lambda_1 t + \gamma_1, \lambda_2 t + \gamma_2, \ldots, \lambda_N t + \gamma_N)$$

im N-dimensionalen Zahlenraum R_N, wo t die Menge aller reellen Zahlen und $(\gamma_1, \gamma_2, \ldots, \gamma_N)$ die Menge aller Punkte in R_N mit ganzzahligen Koordinaten durchlaufen. Ein bekannter Satz von KRONECKER besagt, dass diese Punktmenge überall dicht in R_N liegt, oder anders ausgedrückt: Die Menge der Punkte

$$\zeta(t) = (e^{2\pi i \lambda_1 t}, e^{2\pi i \lambda_2 t}, \ldots, e^{2\pi i \lambda_N t})$$

liegt in Q_N überall dicht.

Es zeigt sich nun, dass dieser Satz seine Gültigkeit behält, wenn die beschränkten, unabhängigen, stetigen Charaktere $e^{2\pi i \lambda_1 t}, e^{2\pi i \lambda_2 t}, \ldots, e^{2\pi i \lambda_N t}$ der additiven Gruppe der reellen Zahlen durch N unabhängige Charaktere von $\mathfrak{G}$ ersetzt werden. Es gilt nämlich der

Satz 1. *Sind $\varphi_1(t), \varphi_2(t), \ldots, \varphi_N(t)$ unabhängige beschränkte Charaktere in $\mathfrak{G}$, dann liegt die Menge der Punkte*

$$\zeta(t) = (\varphi_1(t), \varphi_2(t), \ldots, \varphi_N(t))$$

überall dicht in Q_N.

Wir betrachten ferner die Menge E der Punkte

$$(\lambda_1 t+\gamma_1, \lambda_2 t+\gamma_2, \ldots, \lambda_N t+\gamma_N)$$

in R_N, wo $\lambda_1, \lambda_2, \ldots, \lambda_N$ nun willkürliche, also nicht mehr als linear unabhängig vorausgesetzte, feste reelle Zahlen sind; t ist eine freie reelle Variable, und $(\gamma_1, \gamma_2, \ldots, \gamma_N)$ durchläuft die Menge aller »ganzen« N-tupel. Ein allgemeinerer Satz von KRONECKER besagt: Die abgeschlossene Hülle von E ist identisch mit der Menge derjenigen Punkte $(a_1, a_2, \ldots, a_N)$, für welche

$$g_1 a_1 + g_2 a_2 + \ldots + g_N a_N$$

für alle ganzzahligen N-tupeln $(g_1, g_2, \ldots, g_N)$ mit

$$g_1 \lambda_1 + g_2 \lambda_2 + \ldots + g_N \lambda_N = 0$$

eine ganze Zahl ist.

Dieser Satz lässt sich auch so formulieren: Die abgeschlossene Hülle der Menge der Punkte

$$\zeta(t) = (e^{2\pi i \lambda_1 t}, e^{2\pi i \lambda_2 t}, \ldots, e^{2\pi i \lambda_N t})$$

in Q_N, wo $\lambda_1, \lambda_2, \ldots, \lambda_N$ willkürliche reelle Zahlen sind und t eine freie reelle Variable ist, ist identisch mit der Menge der Punkte

$$z = (z_1, z_2, \ldots, z_N),$$

für welche

$$z_1^{g_1} \cdot z_2^{g_2} \cdot \ldots \cdot z_N^{g_N} = 1$$

bei allen N-tupeln $(g_1, g_2, \ldots, g_N)$ von ganzen Zahlen mit

$$\left\{e^{2\pi i \lambda_1 t}\right\}^{g_1} \cdot \left\{e^{2\pi i \lambda_2 t}\right\}^{g_2} \cdot \ldots \cdot \left\{e^{2\pi i \lambda_N t}\right\}^{g_N} \equiv 1.$$

Auch dieser Satz bleibt richtig, wenn $e^{2\pi i\lambda_1 t}, e^{2\pi i\lambda_2 t}, \ldots,$ $e^{2\pi i\lambda_N t}$ durch N willkürliche beschränkte Charaktere von $\mathfrak{G}$ ersetzt werden:

Satz 2. Es seien $\varphi_1(t), \varphi_2(t), \ldots, \varphi_N(t)$ beschränkte Charaktere in $\mathfrak{G}$. Dann ist die abgeschlossene Hülle der Punktmenge

$$\zeta(t) = \big(\varphi_1(t), \varphi_2(t), \ldots, \varphi_N(t)\big)$$

in Q_N identisch mit der Menge der Punkte

$$z = (z_1, z_2, \ldots, z_N),$$

für welche

$$z_1^{g_1} \cdot z_2^{g_2} \cdot \ldots \cdot z_N^{g_N} = 1$$

für jedes ganzzahlige N-tupel $(g_1, g_2, \ldots, g_N)$ mit

$$\{\varphi_1(t)\}^{g_1} \cdot \{\varphi_2(t)\}^{g_2} \cdot \ldots \cdot \{\varphi_N(t)\}^{g_N} = 1$$

gilt.

Ausserdem erwähne ich einen noch allgemeineren Kroneckerschen Satz: Von den N Linearformen

$$L_\nu = \lambda_{\nu 1} t_1 + \lambda_{\nu 2} t_2 + \ldots + \lambda_{\nu M} t_M \quad (\nu = 1, 2, \ldots, N),$$

wo die λ willkürliche feste reelle Zahlen und $t_1, t_2, \ldots,$ t_M freie reelle Variable sind, ausgehend, bilden wir die Menge E der Punkte

$$\big(L_1 + \gamma_1, L_2 + \gamma_2, \ldots, L_N + \gamma_N\big),$$

wo $(\gamma_1, \gamma_2, \ldots, \gamma_N)$ die Menge aller ganzen N-tupel durchläuft. Die abgeschlossene Hülle von E ist dann identisch mit der Menge derjenigen Punkte $(a_1, a_2, \ldots, a_N)$, für welche die Zahl

$$a_1 g_1 + a_2 g_2 + \ldots + a_N g_N$$

ganz ist für alle ganzzahligen $(g_1, g_2, \ldots, g_N)$ mit der Eigenschaft, dass

$$L_1 g_1 + L_2 g_2 + \ldots + L_N g_N$$

identisch in den M Variabeln $t_1, t_2, \ldots, t_M$ verschwindet.

Mit Hilfe der Exponentialfunktion ausgedrückt lautet dieser Satz: Die abgeschlossene Hülle der Menge der Punkte

$$\zeta(t_1, t_2, \ldots, t_M)$$
$$= \left(e^{2\pi i \lambda_{11} t_1} \cdot \ldots \cdot e^{2\pi i \lambda_{1M} t_M}, \ldots, e^{2\pi i \lambda_{N1} t_1} \cdot \ldots \cdot e^{2\pi i \lambda_{NM} t_M}\right)$$

in Q_N ist identisch mit der Menge derjenigen Punkte

$$z = (z_1, z_2, \ldots, z_N),$$

für welche

$$z_1^{g_1} \cdot z_2^{g_2} \cdot \ldots \cdot z_N^{g_N} = 1$$

gilt für jedes ganzzahlige $(g_1, g_2, \ldots, g_N)$ mit der Eigenschaft, dass die Gleichung

$$\left\{e^{2\pi i \lambda_{11} t_1} \cdot \ldots \cdot e^{2\pi i \lambda_{1M} t_M}\right\}^{g_1} \cdot \ldots \cdot \left\{e^{2\pi i \lambda_{N1} t_1} \cdot \ldots \cdot e^{2\pi i \lambda_{NM} t_M}\right\}^{g_M} = 1$$

identisch in den Variabeln $t_1, t_2, \ldots, t_M$ erfüllt ist.

Auch dieser Satz, der ebenfalls ein Satz über beschränkte Charaktere der additiven Gruppe der reellen Zahlen ist, lässt sich auf abelsche Gruppen verallgemeinern; in dieser Verallgemeinerung wird jede der Variabeln t_μ ihre eigene Gruppe $\mathfrak{G}_\mu$ durchlaufen:

Satz 3. Es seien $\mathfrak{G}_1, \mathfrak{G}_2, \ldots, \mathfrak{G}_M$ abelsche Gruppen und $\varphi_{1\mu}(t_\mu), \varphi_{2\mu}(t_\mu), \ldots, \varphi_{N\mu}(t_\mu)$ N beschränkte Charaktere von $\mathfrak{G}_\mu$ $(\mu = 1, 2, \ldots, M)$. Die abgeschlossene Hülle der Menge der Punkte

$$\zeta(t_1, t_2, \ldots, t_M)$$
$$= (\varphi_{11}(t_1) \cdot \ldots \cdot \varphi_{1M}(t_M), \ldots, \varphi_{N1}(t_1) \cdot \ldots \cdot \varphi_{NM}(t_M))$$

ist identisch mit der Menge der Punkte

$$z = (z_1, z_2, \ldots, z_N),$$

für welche

$$z_1^{g_1} \cdot z_2^{g_2} \cdot \ldots \cdot z_N^{g_N} = 1$$

für jedes ganzzahlige N-tupel $(g_1, g_2, \ldots, g_N)$ mit der Eigenschaft, dass

$$\{\varphi_{11}(t_1) \cdot \ldots \cdot \varphi_{1M}(t_M)\}^{g_1} \cdot \ldots \cdot \{\varphi_{N1}(t_1) \cdot \ldots \cdot \varphi_{NM}(t_M)\}^{g_N} = 1$$

identisch in $t_1, t_2, \ldots, t_M$ gilt.

§ 2. Für die angeführten klassischen Kroneckerschen Sätze sind im Laufe der Zeit viele Beweise, teils von analytischer, teils von geometrischer Natur gegeben worden. Mehrere von ihnen — z. B. einige von H. Bohr und H. Bohr- B. Jessen gegebene analytische Beweise — lassen sich in einfacher Weise zu Beweisen für die entsprechenden Sätze 1—3 verallgemeinern. Beispielsweise will ich im folgenden Paragraphen den Beweis für Satz 1 durch Übertragung eines Bohrschen Beweises [1] führen und in § 4 zeigen, wie eine geometrische Beweismethode von M. Riesz[1] sich zur Herleitung des Satzes 2 verwenden lässt. Zuletzt zeige ich, dass der Satz 3 schon im Satz 2 enthalten ist.

§ 3. Bei den genannten analytischen Beweisen — die ihren Ausgangspunkt in der früher erwähnten Arbeit von

[1] Dieser Beweis wurde von M. Riesz in einem Vortrag in Matematisk Forening in Kopenhagen am 26. Mai 1935 mitgeteilt.

H. WEYL haben — ist die Bildung des Integralmittelwertes $\lim_{T=\infty} \frac{1}{T} \int_0^T$ ein wesentliches Hilfsmittel. Entsprechend beruhen die auf Gruppen übertragenen Beweise auf der Bildung des v. NEUMANNschen Mittelwertes.

Der angekündigte Beweis für den Satz 1 verläuft so: Wir betrachten die in $\mathfrak{G}$ f. p. Funktion

$$F(t) = 1 + z_1 \varphi_1(t) + z_2 \varphi_2(t) + \ldots + z_N \varphi_N(t),$$

wo $\varphi_1, \varphi_2, \ldots, \varphi_N$ die in $\mathfrak{G}$ unabhängigen Charaktere des Satzes 1 sind und $z_1, z_2, \ldots, z_N$ willkürliche komplexe Vorzeichen bezeichnen. Der Satz 1 ist — wie leicht einzusehen — bewiesen, wenn wir gezeigt haben, dass die obere Grenze Γ der Funktion $|F(t)|$ gleich $N+1$ ist; da offenbar $\Gamma \leqq N+1$ ist, ist alles gezeigt, wenn die Gültigkeit der Relation

$$\Gamma \geqq N+1 \tag{2}$$

bewiesen wird.

Wir setzen, indem $x_1, x_2, \ldots, x_N$ Unbestimmte bezeichnen,

$$G(x_1, x_2, \ldots, x_N) = 1 + x_1 + x_2 + \ldots + x_N,$$

und

$$\{G(x_1, x_2, \ldots, x_N)\}^p = \sum_{\nu_1, \nu_2, \cdots, \nu_N}{}' \alpha^{(p)}_{\nu_1, \nu_2, \cdots, \nu_N} x_1^{\nu_1} \cdot x_2^{\nu_2} \ldots x_N^{\nu_N}. \tag{3}$$

Dann ist

$$\{F(t)\}^p = \sum_{\nu_1, \cdots, \nu_N}{}' \alpha^{(p)}_{\nu_1, \cdots, \nu_N} \cdot z_1^{\nu_1} \cdot \ldots \cdot z_N^{\nu_N} \cdot \{\varphi_1(t)\}^{\nu_1} \cdot \ldots \cdot \{\varphi_N(t)\}^{\nu_N}.$$

Die Funktionen $\{\varphi_1(t)\}^{\nu_1} \cdot \{\varphi_2(t)\}^{\nu_2} \ldots \{\varphi_N(t)\}^{\nu_N}$ sind als Produkte von beschränkten Charakteren wieder beschränkte

Charaktere, und sie sind paarweise verschieden, da φ_1, φ_2, ..., φ_N unabhängig sind. Daher ist (vergl. Bemerkung auf Seite 5)

$$\alpha^{(p)}_{\nu_1, \nu_2, \cdots, \nu_N} z_1^{\nu_1} \cdot z_2^{\nu_2} \cdot \ldots \cdot z_N^{\nu_N}$$
$$= M_t \left\{ \{F(t)\}^p \{\varphi_1(t^{-1})\}^{\nu_1} \{\varphi_2(t^{-1})\}^{\nu_2} \cdot \ldots \cdot \{\varphi_N(t^{-1})\}^{\nu_N} \right\},$$

woraus folgt, dass

$$\alpha^{(p)}_{\nu_1, \nu_2, \cdots, \nu_N} \leqq M\{F^p\} = F^p.$$

Die Anzahl der Glieder auf der rechten Seite von (3) ist, wie man durch eine grobe Abschätzung sieht, höchstens $(p+1)^N$; also ist

$$\sum_{\nu_1, \nu_2, \cdots, \nu_N}{}' \alpha^{(p)}_{\nu_1, \nu_2, \cdots, \nu_N} \leqq (p+1)^N F^p.$$

Da aber

$$\sum_{\nu_1, \nu_2, \cdots, \nu_N}{}' \alpha^{(p)}_{\nu_1, \nu_2, \cdots, \nu_N} = (N+1)^p$$

ist, gilt für jedes p die Relation

$$F \geqq \frac{N+1}{(p+1)^{\frac{N}{p}}}.$$

Der Grenzübergang $p \to \infty$ zeigt danach die Gültigkeit von (2).

§ 4. Obzwar der eben mitgeteilte Beweis sehr einfach erscheint, muss man doch bedenken, dass die Mittelwertbildung ein entscheidendes Hilfsmittel des Beweises bildet. In dem jetzt zu besprechenden Beweis für Satz 2 wird dieses Hilfsmittel nicht benutzt. Dagegen wird der folgende Satz von M. Riesz über Vektormoduln zur Anwendung kommen:

Es bezeichne V einen Vektormodul in R_N. Die Menge der Vektoren $u = (u_1, u_2, \ldots, u_N)$, für welche das innere Produkt

$$(u, v) = u_1 v_1 + u_2 v_2 + \ldots + u_N v_N$$

für alle zu V gehörigen Vektoren $v = (v_1, v_2, \ldots, v_N)$ ganz ist, ist ein Modul, der mit V^{-1} bezeichnet und der zu V reziproke Modul genannt wird. $\overline{V}$ bezeichne die abgeschlossene Hülle von V. Dann ist

$$(V^{-1})^{-1} = \overline{V}. \tag{4}$$

Mit Hilfe dieses Satzes kann der Beweis folgendermassen geführt werden: Wir verlegen die Betrachtungen von Q_N nach R_N, indem wir für jede der in Satz 2 auftretenden Funktionen $\varphi_\nu(t)$ eine reellwertige Funktion $\lambda_\nu(t)$ durch die Festsetzung:

$$\varphi_\nu(t) = e^{2\pi i \lambda_\nu(t)} \quad 0 \leqq \lambda_\nu(t) < 1 \quad (\nu = 1, 2, \ldots, N)$$

definieren. Dann ist für jedes Paar von Elementen $t_1 \varepsilon \mathfrak{G}$ und $t_2 \varepsilon \mathfrak{G}$

$$\lambda_\nu(t_1 t_2^{-1}) \equiv \lambda_\nu(t_1) - \lambda_\nu(t_2) \pmod 1 \quad (\nu = 1, 2, \ldots, N).$$

Hieraus folgt, dass die Menge der Vektoren

$$v(t, \gamma) = \big(\lambda_1(t) + \gamma_1,\ \lambda_2(t) + \gamma_2,\ \ldots,\ \lambda_N(t) + \gamma_N\big),$$

wo t die Gruppe $\mathfrak{G}$, und $\gamma = (\gamma_1, \gamma_2, \ldots, \gamma_N)$ die Menge der »ganzen« Vektoren von R_N durchlaufen, ein Modul V ist. Der Satz 2 lässt sich hiernach so formulieren: Der Modul $\overline{V}$ ist identisch mit der Menge derjenigen Vektoren $(a_1, a_2, \ldots, a_N)$, für welche

$$g_1 a_1 + g_2 a_2 + \ldots + g_N a_N$$

eine ganze Zahl ist, sobald $(g_1, g_2, \ldots, g_N)$ ein »ganzer« Vektor ist mit der Eigenschaft, dass

$$g_1\lambda_1(t)+g_2\lambda_2(t)+\ldots.+g_N\lambda_N(t)$$

für alle $t\varepsilon\mathfrak{G}$ ganz ausfällt. $\overline{V}$ ist aber zufolge der Relation (4) mit $(V^{-1})^{-1}$ identisch. V^{-1} besteht aus den Vektoren $g=(g_1, g_2, \ldots., g_N)$, für welche das innere Produkt

$$(g, v(t,\gamma))$$
$$=g_1\lambda_1(t)+g_2\lambda_2(t)+\ldots+g_N\lambda_N(t)+g_1\gamma_1+g_2\gamma_2+\ldots+g_N\gamma_N$$

für alle $t\varepsilon\mathfrak{G}$ und alle ganzen Vektoren γ eine ganze Zahl ist. Notwendig hierfür ist aber, dass $g_1, g_2, \ldots., g_N$ ganze Zahlen sind, denn für $t=1$ und dasjenige γ für welches $\gamma_\nu=1$ und alle übrigen Koordinaten gleich Null sind, ist $(g, v)=g_\nu$. Der Modul V^{-1} ist also identisch mit der Menge derjenigen Vektoren $(g_1, g_2, \ldots., g_N)$ mit ganzen Koordinaten, für welche die Zahl

$$g_1\lambda_1(t)+g_2\lambda_2(t)+\ldots.+g_N\lambda_N(t)$$

für alle $t\varepsilon\mathfrak{G}$ ganz ist. $(V^{-1})^{-1}$ besteht also aus allen Vektoren $(a_1, a_2, \ldots., a_N)$, für welche die Zahl

$$g_1a_1+g_2a_2+\ldots.+g_Na_N$$

ganz ist, sobald

$$g_1\lambda_1(t)+g_2\lambda_2(t)+\ldots.+g_N\lambda_N(t)$$

für jedes $t\varepsilon\mathfrak{G}$ ganz ist. Hiermit haben wir den Satz 2 bewiesen.

§ 5. Endlich soll gezeigt werden, dass der Satz 3 schon im Satz 2 enthalten ist. Es bezeichne $t=(t_1, t_2, \ldots., t_M)$ ein Gruppenelement der Produktgruppe $\mathfrak{G}=(\mathfrak{G}_1, \mathfrak{G}_2, \ldots., \mathfrak{G}_M)$ der im Satz 3 genannten abelschen Gruppen $\mathfrak{G}_1, \mathfrak{G}_2, \ldots., \mathfrak{G}_M$. Die Funktion

$$\varphi_\nu(t) = \varphi_{\nu_1}(t_1) \cdot \varphi_{\nu_2}(t_2) \cdot \ldots \cdot \varphi_{\nu M}(t_M) \qquad (\nu = 1, 2, \ldots N)$$

ist dann (vergl. Bemerkung auf Seite 5) ein Charakter in $\mathfrak{G}$ und Satz 3 die wörtliche Wiederholung des Satzes 2.

II. Verteilungssätze.

§ 6. Wir betrachten wieder die Funktion

$$\zeta(t) = \left(e^{2\pi i \lambda_1 t},\ e^{2\pi i \lambda_2 t},\ \ldots,\ e^{2\pi i \lambda_N t}\right),$$

deren Definitionsbereich die reelle t-Achse ist, und deren Werte Q_N angehören. Der erste in I erwähnte Kroneckersche Satz besagt, dass die Wertmenge von $\zeta(t)$ überall dicht in Q_N verteilt ist, wenn die Zahlen $\lambda_1, \lambda_2, \ldots, \lambda_N$ linear unabhängig sind. Dieses Resultat ist von H. Weyl [5] folgendermassen verschärft worden:

Satz A: $\zeta(t)$ ist in Q_N gleichverteilt.

Die genaue Bedeutung des Wortes »gleichverteilt« wird weiter unten angeführt.

Die genannte Verschärfung wird erst durch Einführung eines Masses für Punktmengen auf der reellen Achse ermöglicht. Es bezeichne E eine solche Menge und $h(t)$ ihre charakteristische Funktion, d. h. die Funktion, die in den Punkten von E gleich 1 und sonst gleich 0 ist. E heisst relativ messbar, wenn der Grenzwert

$$\mu(E) = \lim_{T=\infty} \frac{1}{T} \int_x^{x+T} h(t)\, dt$$

gleichmässig in x existiert, sowohl wenn das Integral als das obere wie als das untere Darbouxsche Integral gedeu-

tet wird. Der Menge E wird der relative Inhalt $\mu(E)$ zugeschrieben.

Es bezeichne hiernach $z(t) = (z_1(t), z_2(t), \ldots, z_N(t))$ eine auf der t-Achse definierte Funktion, deren Werte Q_N angehören. $z(t)$ heisst in Q_N gleichverteilt, wenn folgendes gilt: Für jedes Intervall I in Q_N ist die Menge E_I der t-Werte, für welche $z(t)$ dem Intervall I angehört, relativ messbar und

$$\mu(E_I) = \text{Inhalt von } I.$$

(Ersetzt man in dieser Definition »Intervall I« durch »Jordan-messbare Menge I«, bekommt man wiederum einen Gleichverteilungsbegriff; dieser ist nur scheinbar vom hier genannten verschieden).

Der Beweis des Satzes A kann bekanntlich [5] mittels des folgenden Weylschen Kriteriums geführt werden: Notwendig und hinreichend dafür, dass $z(t) = (z_1(t), z_2(t), \ldots, z_N(t))$ gleichverteilt ist, ist dass die Relation

$$\lim_{T=\infty} \frac{1}{T} \int_x^{x+T} \{z_1(t)\}^{\nu_1} \cdot \{z_2(t)\}^{\nu_2} \ldots \{z_N(t)\}^{\nu_N} dt = 0,$$

wo $(\nu_1, \nu_2, \ldots, \nu_N) \neq (0, 0, \ldots, 0)$, gleichmässig in x gilt sowohl wenn das Integral als oberes wie als unteres Darbouxsches Integral verstanden wird. Bei Herleitung dieses Kriteriums ist der (auf Seite 6 formulierte) Weierstrasssche Approximationssatz ein wesentliches Hilfsmittel.

Dass der Satz A in der Tat eine Verschärfung des Kroneckerschen Satzes ist, ist klar; denn wenn eine Funktion $z(t)$ gleichverteilt ist, dann liegt ihre Wertmenge in Q_N überall dicht.

§ 7. H. Bohr und R. Courant [2] haben einen vom Weylschen wesentlich verschiedenen Beweis für den Satz A

gegeben. WEYL benutzt, wie schon bemerkt, den WEIERSTRASSschen Approximationssatz. Dass die Wertemenge von $\zeta(t)$ in Q_N überall dicht liegt, wird bei ihm gleichzeitig bewiesen. Das Überalldichtliegen von $\zeta(t)$ ist dagegen der Ausgangspunkt des BOHR-COURANTschen Beweises, der insofern einfacher erscheint, als er ausser dem KRONECKERschen Satz nur solche Eigenschaften des relativen Inhaltes $\mu(E)$ benutzt, welche schon in der Definition des Inhaltes als Integralmittelwert ausgesprochen sind.

In den folgenden Paragraphen wollen wir zeigen, wie sich der Satz A zu einem Satz über unabhängige Charaktere in $\mathfrak{G}$ — dem Hauptsatz dieses Abschnittes — verallgemeinern lässt. In § 8 definieren wir einen Massbegriff für Teilmengen in $\mathfrak{G}$; dieser soll den oben definierten Inhalt $\mu(E)$ ersetzen. Hieran anschliessend wird dann die Gleichverteilung einer in $\mathfrak{G}$ definierten Funktion $z(t)$ definiert, und nach dem Vorbild von WEYL einige Kriterien für die Gleichverteilung angeführt. Für den Hauptsatz, der in § 10 formuliert wird, gebe ich zwei Beweise. Der erste (in § 11) ist eine Übertragung des WEYLschen Beweises für Satz A. Im zweiten werden wie im erwähnten BOHR-COURANTschen Beweis für Satz A ausser dem Satz 1 nur unmittelbare Konsequenzen der Definition des Masses benutzt.

§ 8. Es sei $f(x)$ eine in $a \leqq x \leqq b$ beschränkte reellwertige Funktion; $\alpha(x)$ bzw. $\beta(x)$ durchlaufe die Menge der in $a \leqq x \leqq b$ stetigen, reellwertigen Funktionen, für welche $\alpha(x) \leqq f(x)$ bzw. $f(x) \leqq \beta(x)$. Die DARBOUXschen Integrale $\overline{\int_a^b} f(x)\,dx$ und $\underline{\int_a^b} f(x)\,dx$ haben dann, wie unmittelbar zu sehen, die Werte

$$\overline{\int_a^b} f(x)\,dx = \text{Untere Grenze aller } \int_a^b \beta(x)\,dx$$

$$\underline{\int_a^b} f(x)\,dx = \text{Obere Grenze aller } \int_a^b \alpha(x)\,dx.$$

Mit dieser Bemerkung als Ausgangspunkt werden wir die v. Neumannsche Mittelwertbildung folgendermassen verallgemeinern:

Für eine in $\mathfrak{G}$ definierte, beschränkte, reellwertige Funktion $f(t)$ setzen wir

$$\overline{M}\{f\} = \text{Untere Grenze aller } M\{\beta\}$$

$$\text{bzw. } \underline{M}\{f\} = \text{Obere Grenze aller } M\{\alpha\},$$

wo $\beta(t)$ bzw. $\alpha(t)$ die Menge der reellwertigen in $\mathfrak{G}$ f. p. Funktionen, für welche $f(t) \leqq \beta(t)$ bzw. $\alpha(t) \leqq f(t)$, durchläuft.

Aus trivialen Gründen ist dann $\underline{M}\{f\} \leqq \overline{M}\{f\}$.

Definition: Die Menge der in $\mathfrak{G}$ definierten beschränkten Funktionen $f(t) = u(t) + iv(t)$, für welche $\underline{M}\{u\} = \overline{M}\{u\}$ und $\underline{M}\{v\} = \overline{M}\{v\}$, bezeichnen wir mit $\mathfrak{R}$. Einer der Klasse $\mathfrak{R}$ angehörigen Funktion f soll der Mittelwert $M\{f\} = \underline{M}\{u\} + i\underline{M}\{v\} = \overline{M}\{u\} + i\overline{M}\{v\}$ zugeordnet werden.

Man sieht unmittelbar, dass jede f. p. Funktion $\mathfrak{R}$ angehört.

Die Klasse $\mathfrak{R}$ hat folgende Eigenschaften:

1°. Aus $f \varepsilon \mathfrak{R}$ und $g \varepsilon \mathfrak{R}$ folgt $(f+g) \varepsilon \mathfrak{R}$ und $M\{f+g\} = M\{f\} + M\{g\}$.

2°. Aus $f \varepsilon \mathfrak{R}$ folgt $(kf) \varepsilon \mathfrak{R}$ und $M\{kf\} = kM\{f\}$, wo k eine willkürliche komplexe Zahl ist.

3°. Aus $f \varepsilon \mathfrak{R}$ und $g \varepsilon \mathfrak{R}$ folgt $(f \cdot g) \varepsilon \mathfrak{R}$.

4°. $f_1(t), f_2(t), \ldots, f_n(t), \ldots$ sei eine in $\mathfrak{G}$ gleichmässig konvergente Folge von Funktionen, die $\mathfrak{R}$ angehören; dann gehört auch die Grenzfunktion $f(t)$ der Klasse $\mathfrak{R}$ an und $M\{f_n\} \to M\{f\}$.

5°. $f_1, f_2, \ldots, f_N$ seien Funktionen, die $\mathfrak{R}$ angehören, $g(x_1, x_2, \ldots, x_N)$ eine Funktion der N komplexen Variabeln $x_1, x_2, \ldots, x_N$, die in einem abgeschlossenen Intervall, welches $(f_1(t), \ldots, f_N(t))$ für jedes $t \varepsilon \mathfrak{G}$ enthält, stetig ist. Dann gehört $F(t) = g(f_1(t), f_2(t), \ldots, f_N(t))$ der Klasse $\mathfrak{R}$ an.

Um die in den angeführten Eigenschaften 1°—5° hervortretende Analogie zwischen $\mathfrak{R}$ und der Klasse der Riemann-integrierbaren Funktionen weiter zu beleuchten, sei noch bemerkt:

6°. Zu jeder der Klasse $\mathfrak{R}$ angehörigen Funktion f gibt es eine und nur eine komplexe Zahl, die durch Summen der Form

$$\alpha_1 f(a_1 t) + \alpha_2 f(a_2 t) + \ldots + \alpha_n f(a_n t),$$

wo α_i eine reelle positive Zahl und $\sum_{i=1}^{n} \alpha_i = 1$ ist, gleichmässig approximiert werden kann, und diese Zahl ist $M\{f\}$.

7°. Eine reelle Funktion $f(t)$ gehört dann und nur dann $\mathfrak{R}$ an, wenn

$$\text{Obere Grenze aller } M\{\gamma\} = \text{Untere Grenze aller } M\{\delta\},$$

wo $\gamma(t)$ bzw. $\delta(t)$ die Menge aller $\mathfrak{R}$ angehörigen Funktionen durchläuft, für welche $\gamma(t) \leqq f(t)$ bzw. $f(t) \leqq \delta(t)$ ist.

Analog der Definition der auf einem Intervall Jordanmessbaren Mengen wird nun die Messbarkeit von Teilmengen von $\mathfrak{G}$ definiert.

Definition. E sei eine Teilmenge von $\mathfrak{G}$ mit der charakteristischen Funktion $H(t)$. Wir wollen E messbar nennen, wenn $H \varepsilon \mathfrak{N}$. Die nicht negative Zahl $M\{H\}$ nennen wir den Inhalt (oder ausführlicher: den relativen Inhalt) von E, und wir bezeichnen diesen mit $m(E)$.

Für das System der in $\mathfrak{G}$ messbaren Mengen gilt:

Sind E_1 und E_2 messbare Mengen, dann sind $E_1 + E_2$ und $E_1 \cdot E_2$ messbar, und es ist $m(E_1 + E_2) + m(E_1 \cdot E_2) = m(E_1) + m(E_2)$.

Die Beweise für die oben angeführten Tatsachen liegen auf der Hand; daher führe ich sie hier nicht aus.

Bezüglich des Spezialfalles, wo $\mathfrak{G}$ die additive Gruppe der reellen Zahlen ist, bemerken wir folgendes:

Es sei E eine Menge auf der reellen Achse und $H(t)$ ihre charakteristische Funktion; $H(t)$ habe die folgende Eigenschaft: Zu jedem $\varepsilon > 0$ gibt es zwei stetige, reellwertige, f. p. Funktionen $\alpha(t)$ und $\beta(t)$ mit $\alpha(t) \leqq H(t) \leqq \beta(t)$ und $M\{\beta\} - M\{\alpha\} \leqq \varepsilon$. Dann ist E sowohl in dem in § 6, wie auch in dem soeben auseinandergesetzten Sinne messbar, und es ist

$$\mu(E) = m(E).$$

Für eine stetige f. p. Funktion auf der reellen Achse stimmt nämlich der v. Neumannsche Mittelwert mit dem Integralmittelwert überein.

§ 9. Da wir jetzt ein Mass für Teilmengen in $\mathfrak{G}$ zur Verfügung haben, können wir wie oben die Gleichverteilung einer in $\mathfrak{G}$ definierten Funktion $z(t)$, deren Werte Q_N angehören, definieren:

$z(t)$ soll gleichverteilt heissen, wenn für jedes

Interval I in Q_N die Menge E_I derjenigen Elemente $t \varepsilon \mathfrak{G}$, für welche $z(t)$ dem Intervall I angehört, messbar ist und

$$m(E_I) = \text{Inhalt von } I.$$

Für die Gleichverteilung gelten die folgenden Kriterien:

Hilfssatz 1. Notwendig und hinreichend für die Gleichverteilung von $z(t)$ ist, dass für eine willkürliche in Q_N Riemann-integrierbare Funktion $f(z)$ die Funktion $f(z(t))$ der Klasse $\mathfrak{R}$ angehört und dass

$$\int_{Q_N} f(z)\, dw_N = M_t\{f(z(t))\} \tag{5}$$

ist.

Beim Beweis können wir ohne Beschränkung der Allgemeinheit voraussetzen, dass f reellwertig ist.

Dass die genannte Bedingung hinreichend ist, ist klar. Dass sie notwendig ist, können wir folgendermassen zeigen: $z(t)$ sei in Q_N gleichverteilt; also gilt sicher die Relation (5), wenn $f(z)$ die charakteristische Funktion eines willkürlichen Intervalles von Q_N bezeichnet; also auch wenn $f(z)$ eine willkürliche in Q_N intervallweise konstante Funktion ist. Es bezeichne jetzt $f(z)$ eine willkürliche (reellwertige) Riemann-integrierbare Funktion in Q_N; dann gibt es zu jedem $\varepsilon > 0$ zwei intervallweise konstante, reellwertige Funktionen $h_1(z)$ und $h_2(z)$, für welche

$$h_1(z) \leqq f(z) \leqq h_2(z)$$

und

$$\int_{Q_N} h_2(z)\, dw_N - \int_{Q_N} h_1(z)\, dw_N \leqq \varepsilon.$$

Die Funktionen $h_1(z(t))$ und $h_2(z(t))$ gehören der Klasse $\mathfrak{R}$ an und genügen den Relationen

$$h_1(z(t)) \leqq f(z(t)) \leqq h_2(z(t))$$

und

$$\int_{Q_N} h_1(z)\, dw_N = \underset{t}{M}\{h_1(z(t))\} \text{ und } \int_{Q_N} h_2(z(t)) = \underset{t}{M}\{h_2(z(t))\}.$$

Also ist

$$\underset{t}{M}\{h_2(z(t))\} - \underset{t}{M}\{h_1(z(t))\} \leq \varepsilon,$$

woraus die Richtigkeit des Hilfssatzes 1 folgt.

Ersetzt man in der Definition der Gleichverteilung »Intervall I« durch »Jordan-messbare Menge I«, so erhält man wiederum einen Gleichverteilungsbegriff. Der eben besprochene Hilfssatz zeigt, dass die zwei Begriffe identisch sind.

Hilfssatz 2. Notwendig und hinreichend für die Gleichverteilung von $z(t)$ ist, dass für jede in Q_N stetige Funktion $g(z)$ die Funktion $g(z(t))$ der Klasse $\mathfrak{R}$ angehört und dass

$$\int_{Q_N} g(z)\, dw_N = \underset{t}{M}\{g(z(t))\}. \tag{6}$$

Beweis: Wie oben können wir ohne Beschränkung der Allgemeinheit annehmen, dass $g(z)$ reellwertig ist. — Dass die Bedingung notwendig ist, ist eine unmittelbare Folge des Hilfssatzes 1. Dass sie hinreichend ist, können wir folgendermassen einsehen: $z(t)$ sei eine in $\mathfrak{G}$ definierte Funktion, welche der Relation (6) für alle stetigen $g(z)$ genügt, und $f(z)$ eine willkürliche in Q_N intervallweise konstante Funktion; dass $z(t)$ gleichverteilt ist, beweisen wir, indem wir die Gültigkeit der Relation (5) wie folgt nachweisen: zu jedem $\varepsilon > 0$ gibt es zwei stetige Funktionen $g_1(z)$ und $g_2(z)$ so, dass

$$g_1(z) \leqq f(z) \leqq g_2(z)$$

und

$$\int_{Q_N} g_2(z)\, dw_N - \int_{Q_N} g_1(z)\, dw_N \leqq \varepsilon.$$

Die Funktionen $g_1(z(t))$ und $g_2(z(t))$ gehören der Klasse $\mathfrak{R}$ an, und wegen (6) gilt

$$\int_{Q_1} g_1(z)\, dw_N = M_t\{g_1(z(t))\} \text{ und } \int_{Q_N} g_2(z)\, dw_N = M_t\{g_2(z(t))\}.$$

Hieraus schliesst man, dass $f(z)$ der Klasse $\mathfrak{R}$ angehört, und dass die Relation (5) gilt.

Hilfssatz 3. Notwendig und hinreichend für die Gleichverteilung der Funktion $z(t) = (z_1(t), z_2(t), \ldots, z_N(t))$ ist, dass für jedes ganze N-tupel $(\nu_1, \nu_2, \ldots, \nu_N) \neq (0, 0, \ldots, 0)$ die Funktion $\{z_1(t)\}^{\nu_1} \cdot \{z_2(t)\}^{\nu_2} \cdot \ldots \cdot \{z_N(t)\}^{\nu_N}$ der Klasse $\mathfrak{R}$ angehört, und dass

$$(7) \qquad M_t\{\{z_1(t)\}^{\nu_1} \cdot \{z_2(t)\}^{\nu_2} \cdot \ldots \cdot \{z_N(t)\}^{\nu_N}\} = 0.$$

Beweis: Dass die Bedingung notwendig ist, ist im Hilfssatz 2 enthalten, da die Funktion $z_1^{\nu_1} z_2^{\nu_2} \ldots z_N^{\nu_N}$ eine in Q_N stetige Funktion ist. Auch beim Beweis dafür, dass die Bedingung hinreichend ist, wollen wir den Hilfssatz 2 benutzen. Es sei $g(z)$ eine willkürliche in Q_N stetige Funktion; dann gibt es zufolge des Weierstrassschen Approximationssatzes (vergl. Seite 6) eine Folge von Polynomen $S_1(z), S_2(z), \ldots$, die gleichmässig gegen $g(z)$ konvergiert. Nehmen wir an, dass $z(t)$ der Bedingung des Satzes genügt; dann gehört jede der Funktionen der Folge

$$(8) \qquad S_1(z(t)),\ S_2(z(t)),\ \ldots.$$

zu der Klasse $\mathfrak{R}$, und wegen (7) ist

$$\int_{Q_N} S_r(z)\, dw_N = M_t\{S_r(z(t))\} \qquad r = 1, 2, \ldots .$$

Die Folge (8) konvergiert natürlich gleichmässig gegen $g(z(t))$; also gehört $g(z(t))$ zu $\mathfrak{R}$, und wir haben

$$\int_{Q_N} g(z)\, dw_N = \lim \int_{Q_N} S_r(z)\, dw_N = \lim M_t\{S_r(z(t))\} = M_t\{g(z(t))\}.$$

Also ist nach dem Hilfssatz 2 die Funktion $z(t)$ gleichverteilt.

§ 10. Nach diesen Vorbereitungen sind wir nun im Stande, den Hauptsatz zu formulieren und zu beweisen; der Hauptsatz lautet:

Satz 4. *$\varphi_1(t), \varphi_2(t), \ldots, \varphi_N(t)$ seien in $\mathfrak{G}$ beschränkte unabhängige Charaktere. Dann ist die Funktion $\zeta(t) = (\varphi_1(t), \varphi_2(t), \ldots, \varphi_N(t))$ in Q_N gleichverteilt.*

Bevor wir in den zwei folgenden Paragraphen den Satz beweisen, bemerken wir:

Wenn eine in $\mathfrak{G}$ definierte Funktion $z(t)$ gleichverteilt ist, dann liegt natürlich ihre Wertemenge in Q_N überall dicht; also enthält der Hauptsatz den Satz 1.

$\varphi_1(t), \varphi_2(t), \ldots, \varphi_N(t)$ seien stetige beschränkte Charaktere der additiven Gruppe der reellen Zahlen, I ein Intervall in Q_N mit der charakteristischen Funktion $h(z)$ und E_I die Menge derjenigen Zahlen t, für welche $\zeta(t) = (\varphi_1(t), \varphi_2(t), \ldots, \varphi_N(t))$ dem Intervall I angehört. Es gibt zu jedem $\varepsilon > 0$ zwei stetige reellwertige Funktionen $h_1(z)$ und $h_2(z)$ mit $h_1(z) \leq h(z) \leq h_2(z)$ und $\int_{Q_N} h_2(z)\, dw_N - \int_{Q_N} h_1(z)\, dw_N \leq \varepsilon$. Wir setzen $H(t) = h(\zeta(t))$, $H_1(t) = h_1(\zeta(t))$

und $H_2(t) = h_2(\zeta(t))$; $H(t)$ ist die charakteristische Funktion von E_I, und $H_1(t)$ und $H_2(t)$ sind stetige f. p. Funktionen, für welche $H_1(t) \leqq H(t) \leqq H_2(t)$; nach Satz 4 und Satz 2 ist $M(H_1) = \int_{Q_N} h_1(z)\, dw_N$ und $M(H_2) = \int_{Q_N} h_2(z)\, dw_N$, also $M\{H_2\} - M\{H_1\} \leqq \varepsilon$. Zufolge der Bemerkung auf Seite 22 ist also $\mu(E_I) = m(E_I)$. Hiermit ist gezeigt, dass der Satz 4 in der Tat eine Verallgemeinerung des Satzes A ist.

§ 11. Unter Benutzung des Hilfssatzes 3 kann der Satz 4 in wenigen Worten bewiesen werden. Sind nämlich φ_1, φ_2, ..., φ_N unabhängige Charaktere in $\mathfrak{G}$, dann ist die Funktion

$$\{\varphi_1(t)\}^{\nu_1} \cdot \{\varphi_2(t)\}^{\nu_2} \cdot \ldots \cdot \{\varphi_N(t)\}^{\nu_N}$$

für jedes ganzzahlige N-tupel $(\nu_1, \nu_2, \ldots, \nu_N) \neq (0, 0, \ldots, 0)$ ein vom Hauptcharakter verschiedener Charakter. Also ist

$$M_t\{\{\varphi_1(t)\}^{\nu_1} \cdot \{\varphi_2(t)\}^{\nu_2} \cdot \ldots \cdot \{\varphi_N(t)\}^{\nu_N}\} = 0;$$

also ist $\zeta(t) = (\varphi_1(t), \varphi_2(t), \ldots, \varphi_N(t))$ gleichverteilt.

§ 12. Der zweite der in § 7 angekündigten Beweise hat Hilfssatz 2 zum Ausgangspunkt. Wir führen ihn dadurch, dass wir zeigen:

Hilfssatz 4. Bezeichnet $g(z)$ eine willkürliche in Q_N stetige Funktion, dann gilt für die in $\mathfrak{G}$ f. p. Funktion $G(t) = g(\zeta(t))$ die Relation

$$\int_{Q_N} g(z)\, dw_N = M_t\{G(t)\}.$$

Dieser Satz ist bewiesen, wenn nachgewiesen wird, dass zu einem willkürlichen $\varepsilon > 0$ endlich viele Elemente

$a_1, a_2, \ldots, a_n$ in $\mathfrak{G}$ und ebenso viele positive Zahlen $\alpha_1, \alpha_2, \ldots, \alpha_n$ mit $\alpha_1 + \alpha_2 + \ldots + \alpha_n = 1$ existieren, für welche

$$\left| \int_{Q_N} g(z)\, dw_N - \sum_{i=1}^{n} \alpha_i G(a_i t) \right| \leqq \varepsilon$$

für alle $t \in \mathfrak{G}$.

Da $g(z)$ stetig ist, gibt es ein $\delta > 0$ so, dass alle Näherungssummen σ, die zu Intervalleinteilungen des Q_N von einer Feinheit $\leqq \delta$ gehören, der Ungleichung

$$\left| \sigma - \int_{Q_N} g(z)\, dw_N \right| \leqq \varepsilon$$

genügen[1]. $I_1, I_2, \ldots, I_n$ bezeichnen die Intervalle einer bestimmten Einteilung der Feinheit $\leqq \delta$; da $\varphi_1, \varphi_2, \ldots, \varphi_N$ unabhängige Charaktere sind, gibt es zufolge des Satzes 1 ein Element $a_i \in \mathfrak{G}$ $(i = 1, 2, \ldots, n)$ so, dass $z_i = \zeta(a_i)$ dem Intervalle I_i angehört. Bezeichnet α_i den Inhalt von I_i, so ist $\alpha_1 + \alpha_2 + \ldots + \alpha_n = 1$ und

$$\sum_{i=1}^{n} \alpha_i g(z_i) = \sum_{i=1}^{n} \alpha_i G(a_i)$$

eine zu einer Einteilung der Feinheit $\leqq \delta$ gehörige Näherungssumme; für jedes u in Q_N ist $\sum_{i=1}^{n} \alpha_i g(z_i u)$ ebenfalls eine solche; speziell gilt dies für die Summe

$$\sum_{i=1}^{n} \alpha_i g\left(z_i \zeta(t)\right) = \sum_{i=1}^{n} \alpha_i g\left(\zeta(a_i t)\right) = \sum_{i=1}^{n} \alpha_i G(a_i t).$$

Also ist

[1] Für das folgende beachte man die Bemerkung auf den Seiten 7—8.

$$\left| \int_{Q_N} g(z)\, dw_N - \sum_{i=1}^{n} \alpha_i\, G(a_i t) \right| \leqq \varepsilon$$

für alle $t \varepsilon \mathfrak{G}$.

Die in dieser Arbeit bewiesenen Sätze wurden teilweise von Prof. H. Bohr und Prof. B. Jessen als Vermutungen ausgesprochen; auch wurden Ansätze für die im ersten Teil geführten Beweise von ihnen angedeutet. — Ich danke den beiden Herren für ihre freundliche Anregung, die mich veranlasst hat, mich mit diesen Fragen zu beschäftigen, und für das freundliche Interesse, das sie dem Vorwärtsschreiten meiner Arbeit bezeugt haben.

LITERATURVERZEICHNIS

[1]. H. Bohr: Again the Kronecker Theorem. Journal of the London Math. Soc. Vol. 9.

[2]. H. Bohr und R. Courant: Neue Anwendungen der Theorie der Diophantischen Approximationen auf die Riemannsche Zetafunktion. Journal für reine und angewandte Matematik 1914. Bd. 144.

[3]. L. Kronecker: Näherungsweise ganzzahlige Auflösung linearer Gleichungen. Werke Bd. III, S. 47—109.

[4]. J. v. Neumann: Almost periodic functions in a group I. Transactions of the american mathematical society 1934, Vol. 36.

[5]. H. Weyl: Über die Gleichverteilung von Zahlen mod. Eins. Mathematische Annalen 1916 Bd. 77.

Færdig fra Trykkeriet den 26. August 1936.

Det Kgl. Danske Videnskabernes Selskab.
Mathematisk-fysiske Meddelelser. **XIV**, 5.

THE ACTION OF NEUTRONS ON THE RARE EARTH ELEMENTS

BY

G. HEVESY AND HILDE LEVI

KØBENHAVN
LEVIN & MUNKSGAARD
EJNAR MUNKSGAARD
1936

Printed in Denmark.
Bianco Lunos Bogtrykkeri A/S.

The action of neutrons on the rare earth elements can be followed up in two ways: by investigating the radioactivity induced in these elements under neutron bombardment, and by observing their absorbing power for a beam of slow neutrons. In this paper both these lines of attack will be discussed for the rare earth group and for yttrium and scandium.

Artificial radioactivity of the rare earth elements.

The artificial radioactivity of some of the rare earth elements was investigated by AMALDI, D'AGOSTINO, FERMI, PONTECORRO, RASETTI and SEGRE (1); others were investigated by ourselves (2), by SUGDEN (3), by MARSH and SUGDEN (4), by MCLENNAN and RANN (5), and by E. RONA (6). The neutrons used were produced by the action on beryllium of the α-rays from radium emanation and were in many cases slowed down by inserting layers of paraffin 10—20 cm thick in the path of neutrons; a GEIGER-MÜLLER counter was used to measure the activities obtained.

Scandium.

A sample of scandium oxide prepared by Prof. STERBA-BÖHM and kindly presented to us by Prof. HÖNIGSCHMID, who used the preparation in determining the atomic weight of scandium, was activated for a few days using an emanation-beryllium source of 200—300 MC. The oxide was then

dissolved in dilute hydrochloric acid and 100—150 mg sodium chloride and the same amount of calcium oxide were added. The filtrate obtained after precipitation with carbonate-free ammonia was treated with oxalic acid and the calcium oxalate formed was removed. The sodium chloride which had been added was recovered, after the removal of the ammonium chloride content of the last filtrate, by evaporation and ignition. The activities of the three fractions, namely scandium oxide, sodium chloride, and calcium oxalate, were then determined. The two first mentioned preparations were found to be active, the activity of the scandium oxide decaying very slowly and that of the sodium chloride fraction having a half-life of 16 hours. The activities are due to the formation of ${}^{46}_{21}\mathrm{Sc}$ and ${}^{42}_{19}\mathrm{K}$ respectively; the reactions leading to these products are

$$ {}^{45}_{21}\mathrm{Sc} + {}^{1}_{0}\mathrm{n} = {}^{46}_{21}\mathrm{Sc} $$

and

$$ {}^{45}_{21}\mathrm{Sc} + {}^{1}_{0}\mathrm{n} = {}^{42}_{19}\mathrm{K} + {}^{4}_{2}\alpha . $$

The mass numbers occuring in these equations follow from the fact that scandium has only one stable isotope, ${}^{45}\mathrm{Sc}$. The calcium oxalate investigated was inactive; we are thus unable to find any evidence for the reaction ${}^{45}_{21}\mathrm{Sc} + {}^{1}_{0}\mathrm{n} = {}^{45}_{20}\mathrm{Ca} + {}^{1}_{1}\mathrm{H}$ which possibly takes place also. The activity which cannot be separated from scandium is presumably due to ${}^{46}_{21}\mathrm{Sc}$; most of this activity decays with a period of about two months but a small part does not decay appreciably within a year or two. We are still engaged in following up this long living activity by using a preparation of very great purity most kindly given us by Prof. Sterba-Böhm. In dealing with long periods, which are difficult to measure directly, some idea of the half-life can be ob-

tained by comparing the absorbing power of the element in question with that of another element of known period, as discussed on page 15.

While $^{42}_{19}$K emits hard β-rays having a half value thickness of 0.19 g/cm^2 Al, $^{46}_{21}$Sc emits soft β-rays with a half value thickness of 0.01 g/cm^2 Al; these are the softest β-rays yet observed from any artificial radio-element as is to be expected in view of the long period of $^{46}_{21}$Sc.

Yttrium.

We investigated (2) samples of yttrium oxide kindly given us by the late Baron Auer v. Welsbach, by Prof. Prandtl, and by Prof. Rolla. The two first named preparations were used some time ago by Hönigschmid to determine the atomic weight of yttrium and investigated by one of us on that occasion by X-ray spectroscopy. While the investigation of Baron Auer's preparation revealed the presence of some dysprosium, that of Prandtl was found to be of the highest purity. The great purity of this preparation and of that of Rolla was also shown by their behaviour under neutron bombardment: No initial decay with the period of dysprosium (2.5 h.) could be observed, the sole period being one of 70 h., which we found to be the period of decay of yttrium. Auer's preparation decayed initially with a half-life of 2.5 h., which was obviously that of dysprosium; but afterwards it showed a 70 h. period like the other preparations. The molecular volumes of corresponding compounds of yttrium and dysprosium are only very slightly different*, so these elements

* The volumes of the octahydrosulfates differ by less than 0,8 % (G. v. Hevesy, Zs. anorg. Chem. 147, 217; 150, 68, 1925) and the ionic radii by about the same amount (V. M. Goldschmidt, Ullrich and Barth, Oslo. Acad. Proc. Nr. 5, 1925).

are unusually closely related chemically and their separation is attended with very great difficulties. Figure 1 shows the decay of a pure preparation and of one containing some dysprosium.

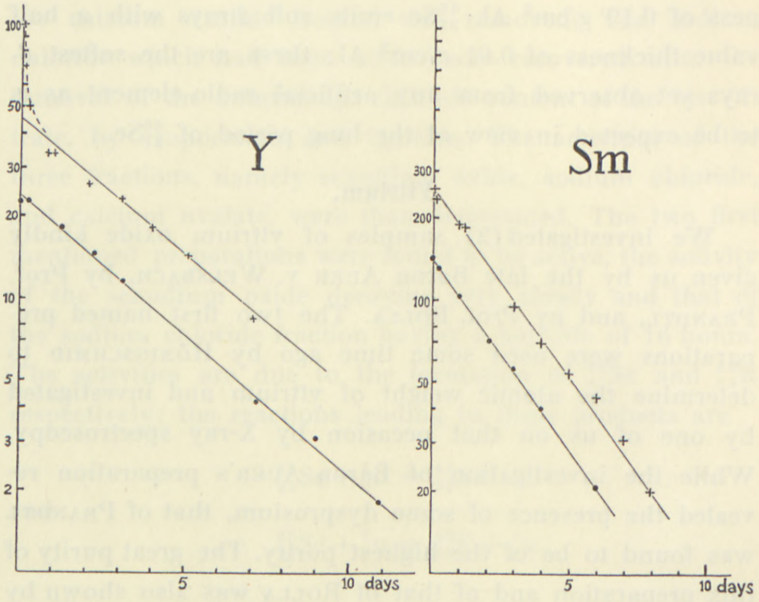

Fig. 1.
a) Decay Curve of a Pure and an Impure Yttrium Preparation.
b) Samarium Decay Curves (the two days' period only; the weak period of 40 min is not visible).

Since yttrium has only one stable isotope, ^{89}Y, the artificial radioactivity obtained from it is due to the formation $^{90}_{39}Y$. We find the intensity of the yttrium activity to be 0.005 times as large as that of dysprosium, both preparations having been activated until saturation was obtained in a paraffin block of $30 \times 30 \times 25$ cm edge; the neutron source was placed on the top of the preparation which was covered by a thin shield of paper. The β-rays emitted by yttrium are absorbed to half of their initial value by 0.6 mm Al.

Lanthanum.

MARSH and SUGDEN (4) find 1,9 days as the half-life of lanthanum, and for the intensity of the β-rays emitted, a value amounting to 35 % of that observed for the activity of praseodymium. As we find a value of 22 for the ratio of the radiation intensities of dysprosium and praseodymium, the lanthanum activity works out at 2.0 % of that of dysprosium. As lanthanum has but one stable isotope, ^{139}La, the activity obtained is due to the formation of $^{140}_{57}$La. FERMI's coefficient α, indicating the increase in activity when the bombarding neutrons are slowed down by a thick layer of paraffin or other hydrogen-containing substances instead of being allowed to impinge directly from the beryllium source on to the substance to be activated, was found to be 12.

Cerium.

No activity was observed after bombardment of cerium for several days with a neutron source of few hundred millicurie.

Praseodymium.

AMALDI, FERMI, and others (1) found the artificial radioactivity of praseodymium to decay with a 19 h. period, the same value being found later by other experimenters (4), (5). Although only one stable isotope of praseodymium is known, ^{141}Pr, the above mentioned investigators found a second period of decay (5 min.) which in contrast to the first period is not hydrogen-sensitive. One possible explanation of the observation that there are two periods is that one of the activities is not due to the usual building up of higher isotope as the result of a nuclear capture but is for example due to the formation of an isotope of element

57 after emission of an α-particle; such an effect has not, however, been observed (7) for elements heavier than zinc. An alternative explanation is that a second stable isotope of praseodymium exists, not yet revealed by the mass spectrograph, and that it has a large absorbing power for slow neutrons. A stable praseodymium isotope present at a concentration of less than 0.1 % and having a smaller absorbing power than the gadolinium isotope responsible for the great absorbing power of this element (cp. page 20), would sufficiently account for the effect observed. Finally we must envisage the possibility of an isotope decaying with more than one period. The β-rays emitted by praseodymium decaying with a period of 19 h. have a half-value thickness of 0.02 cm Al.

Neodymium.

Fermi and his collaborators (1) found that activated neodymium decays with a period of 1 h.; we find (2) that this activity is 2500 times as small as that of dysprosium. Marsh and Sugden (4) found no activity, while according to McLennan and Rann (5) the half life is 35 min. Neodymium having the stable isotopes 142, 143, 144, 145, and 146, the activity observed must be due to the formation and decay of $^{147}_{60}$Nd.

Samarium.

The artificial radioactivity of samarium decays, as was found by Fermi (1), and later by us, with a period of 40 min. We find (2) the intensity of the activity to be 0.6 % of that of dysprosium. Samarium has furthermore, as was first noticed by Marsh and Sugden (4), a much longer period as well. We determined the period of this isotope to be 2 d., as can be seen from figure 1 and found its intensity to be $\frac{1}{50}$ of that of dysprosium, i. e. 2.0 on our re-

lative scale. Samarium having the stable isotopes 144, 147, 148, 149, 150, 152, and 154, it is not possible to determine the mass number of the active samarium isotopes with certainty; in view of the existence of the stable isotopes of europium 151 and 153 the active samarium isotopes have possibly the mass-numbers 151 and 153.

Europium.

A very intense activity was obtained by SUGDEN (3) on bombarding europium with slow neutrons. It decayed with a period of 9.2 h. The intensity of the europium radiation was found by us (2) to be 80 % of the dysprosium radiation emitted by the same amount of dysprosium, both preparations being activated until saturation was reached. Care was taken, too, that the neutron beam was weakened only to a small extent by the activation process, i. e. very thin layers were activated. As is discussed on page 17, europium absorbs slow neutrons to an appreciably larger extent than is to be expected from the activity of the radioactive europium isotope formed. Europium has two stable isotopes 151 and 153 and the activity is possibly due to the formation of ^{154}Eu. The europium : dysprosium activity ratio is found to be smaller for thick layers than for thin layers.

The value 40 was found for the hydrogen-effect, α. The half-value thickness (2) of the β-rays emitted is 0.02 cm Al, and it was concluded from absorption measurements that energies up to $2.0 \cdot 10^6$ eV occur.* In addition, γ-rays have been detected which are little absorbed by 4 mm. lead.

* R. NAIDU and R. E. SIDAY (Proc. Roy. Soc. A. 48, 332, 36) by using a cloud chamber determined recently the energies of the β-ray spectra and found that the maximum energy lies at $1.3 \cdot 10^6$ eV, while the upper limit of the spectrum is $2.6 \cdot 10^6$ eV.

Gadolinium.

Fermi and others (1) found gadolinium to decay with a period of 8 h. after neutron bombardment, McLennan and Rann (5) found a half-life of 6.4 h. and twice the intensity found for neodymium. The combination of the last mentioned figure with our intensity data leads to an intensity value which is 250 times as small as that observed for dysprosium. Marsh and Sugden (4) could not find any activity.

Terbium.

The activity of terbium (3) decays with a period of 3.9 h. As this element has only one stable isotope, $^{159}_{65}$Tb, the activity observed is due to the formation and decay of $^{160}_{65}$Tb. The intensity of the radiation (2) observed is 2.5 per cent of that of dysprosium.

Dysprosium.

The activity of dysprosium (2), (4) decays with a period of 2.5 h. and is the strongest yet observed in the domain of artificial radioactivity. We have therefore chosen it (2) as a standard of comparison for the activities of the rare earth elements: we denote the intensity of dysprosium arbitrarily by 100. It is of interest to remark that the 2.3 min. activity of silver, which is considered a very strong activity, is 12 times as weak as the activity of an equal amount of dysprosium. The hydrogen effect (α) was found to be 100, the half-value thickness of the β-rays emitted was 0.025 cm Al; and the upper limit of the continuous β-spectrum concluded from absorption measurements with aluminium had an energy of $1.4 \cdot 10^6$ eV (2).* Dysprosium

* R. Naidu and R. E. Siday loc. cit. found that the maximum energy lies at $0.75 \cdot 10^6$ eV, while $1.8 \cdot 10^6$ eV is the upper limit.

is one of the commoner rare earth elements of the yttria group and as it is very strongly active, samples of rare earth elements denoted as "erbia", "holmia", "yttria", etc. often decay with the period of dysprosium.

Holmium.

We found (2) the activity of holmium to decay with a period of 35 h., while E. Rona (6) recently found the value of 33 h. The half-life of 2.6 h. measured by Marsh and Sugden (4) and later by McLennan and Rann (5) is due to the presence of dysprosium in their preparations; some of our impure preparations, too, showed an initial decay with the period of dysprosium. The samples of holmia investigated were given us by the late Baron Auer. Holmium has one stable isotope, 165; the activity observed is therefore due to the decay of $^{166}_{67}$Ho, the intensity of the activity observed being 20 per cent of that of dysprosium. The hydrogen-effect (α) is much smaller (2) than that of dysprosium; the half value thickness is 0.04 g/cm^2 Al; and the upper limit of the β-ray spectrum has an energy of $1.6 \cdot 10^6$ eV.

Erbium.

Erbium has a very weak activity of similar intensity to the 40 min. samarium radiation, decaying with a 7 min. period according to Marsh and Sugden (4), and with a 4.5 min. according to McLennan and Rann (5). A second period (2) was found by us to be 12 h.; the period of 2.5 h. ascertained by Sugden (3) using a commercial preparation was due to the presence of dysprosium, and that found by Marsh and Sugden (4), 1.6 d., to the presence of holmium in the sample investigated. Recently Rona (6) has given the value of 13 h. for the longer period.

The intensity (2) of the longer period of erbium is 0.35 per cent of that of dysprosium, and the half value thickness of the β-rays emitted is 0.03 cm Al. Erbium has the stable isotopes 166, 167, 168, and 170, so the active isotopes must have the mass numbers 169 and 171. Which of these has the shorter life cannot be stated with certainty, but possibly it is $^{171}_{68}$Er that decays with a period of 7 min. The possibility has also to be envisaged that both periods are due to the same isotope.

Thulium.

This element shows an activity having a long life as first stated by Rona (6) who finds that the β-rays emitted are half absorbed by 0.015 cm Al. E. Neuninger and E. Rona* found recently a period of 4 ($\pm$ 1/2) months. After bombarding 100 mg TmO_2 kindly lent us by Prof. Jantsch with about 100 MC for 23 days we obtained 60 kicks per minute, while 100 mg of dysprosium activated to saturation with the same source gave about 4000 kicks per minute. The activity of this preparation decayed with a period of about 3.5 months; a thulium preparation activated to saturation would therefore exhibit an activity about 1/10 of that of dysprosium.

Ytterbium.

The activity of ytterbium (2), (3) decays with a period of 3.5 h. As ytterbium has the isotopes 171, 172, 173, 174, and 176, it cannot be decided whether the activity is due to the formation and decay of $^{175}_{70}$Yb or of $^{177}_{70}$Yb; in view of the existence of $^{175}_{71}$Lu the former is more probable. The ytterbium radiation (2) is somewhat weaker than that of erbium, and amounts to 0.3 per cent of that of dysprosium. The half value thickness of the β-rays emitted is 0.04 cm Al.

* E. Neuninger and E. Rona, Wien. Anz. **73**, 159, 1936.

Lutecium.

Lutecium (cassiopeium) exhibits an activity of fairly long life (2), namely one decaying with a period of 6—7 d., and having an intensity of 1.4 per cent of that of dyspro-

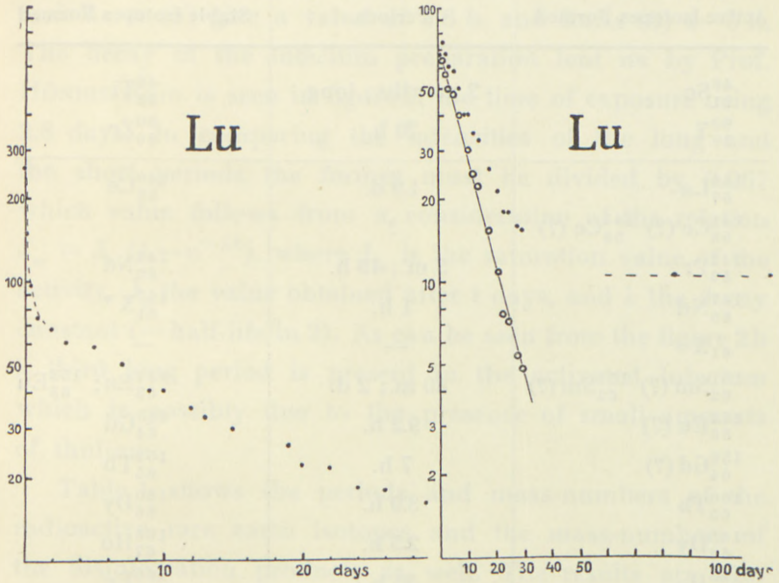

Fig. 2. Lutecium Decay Curve.
a) showing the short period and the beginning of the 7 days' period.
b) showing the measured points for the 7 days' period and the curve obtained after subtracting the residual activity.

sium; there is a second activity of somewhat less intensity decaying with a period (2) of 4 h.; lutecium (cassiopeium) and ytterbium being very closely related elements, and lutecium being usually contaminated with ytterbium, we considered it possible that the 4 h. period observed might be due to the presence of ytterbium in the sample investigated. A very pure lutecium (cassiopeium) preparation, however, prepared by Auer and kindly lent us by Prof. Hönigschmid, also showed the 4 h. period. Furthermore the intensity

Table 1.

Formation of Rare Earth Isotopes under Neutron Bombardment.

Active Isotopes Formed	Periods	Stable Isotopes Formed
$^{46}_{21}Sc$	2 months; long	$^{46}_{22}Ti$
$^{90}_{39}Y$	70 h.	$^{90}_{40}Zr$
$^{140}_{57}La$	1.9 d.	$^{140}_{58}Ce$
$^{141}_{58}Ce$ (?) $^{143}_{58}Ce$ (?)	?	
$^{142}_{59}Pr$	5 m.; 19 h.	$^{142}_{60}Nd$
$^{147}_{60}Nd$	1 h.	$^{147}_{61}X$ *
$_{61}X$	—	—
$^{151}_{62}Sm$ (?) $^{153}_{62}Sm$ (?)	40 m.; 2 d.	$^{151}_{63}Eu$; $^{153}_{63}Eu$
$^{154}_{63}Eu$ (?)	9.2 h.	$^{155}_{64}Gd$
$^{159}_{64}Gd$ (?)	7 h.	$^{159}_{65}Tb$
$^{160}_{65}Tb$	3.9 h.	$^{160}_{66}Dy$
$^{165}_{66}Dy$	2.5 h.	$^{165}_{67}Ho$
$^{166}_{67}Ho$	35 h.	$^{166}_{68}Er$
$^{169}_{68}Er$ $^{171}_{68}Er$ (?)	7 m.; 12 h.	$^{169}_{69}Tm$ $^{171}_{69}Tm$
$^{170}_{69}Tm$	long	$^{170}_{70}Yb$
$^{175}_{70}Yb$ (?)	3.5 h.	$^{175}_{71}Lu$
$^{176}_{71}Lu$	4 h.; 6-7 d.	$^{176}_{72}Hf$

of this radiation was stronger than that emitted by a pure ytterbium preparation activated by a neutron source of the same strength. So we must conclude that both the periods observed are due to lutecium. As only one stable lutecium isotope, 175, is known, the existence of two periods of decay possibly indicates that there is a second stable lutecium isotope present in small amounts, but

* X denotes element 61.

having a high absorbing power for slow neutrons. The long period of decay has not been observed by any experimenter besides us, presumably because the times of exposure have been too short. For the shorter period McLennan and Rann (5) give a value of 3.6 h. and Rona (6) 4—5 h. The decay of the lutecium preparation lent us by Prof. Hönigschmid is seen in figure 2, the time of exposure being 2.8 days. In comparing the intensities of the long and the short periods the former must be divided by 0.267 which value follows from a consideration of the relation $J_\infty = J_t\ (1 - e^{-\lambda t})$, where J_∞ is the saturation value of the activity, J_t the value obtained after t days, and λ the decay constant (= half-life/ln 2). As can be seen from the figure 2b a third long period is present in the activated lutecium which is possibly due to the presence of small amounts of thulium.

Table 1 shows the periods and mass-numbers of the radioactive rare earth isotopes and the mass-numbers of the disintegration products as well. The results are also recorded in the diagrams at the end of this paper. The relative intensities of the activities will be found in table 6 on page 22.

Absorption of slow neutrons by rare earth elements.

Determination of the period of decay from absorption data.

When faced with the problem of determining the period of very slowly decaying radioactive isotopes having half lives of several months or years, decay measurements become very tedious. In such a case we can obtain information about the decay constant required by comparing the absorption of slow neutrons in the rare earth element in question with that in another rare earth element of known

period. A knowledge of this ratio and of the activities obtained for both elements after a known time of exposure allows us to calculate the unknown period of decay provided we can assume that all the neutrons absorbed are captured by the nuclei of the absorbing element and that mainly thermal neutrons are involved in both cases. In the oxides investigated, only the nuclei of the rare earth element absorb, for oxygen nuclei capture only a small number of neutrons. Let us consider, for example, the case of scandium. Denote by R_1 the observed absorption ratio for equal numbers of scandium and dysprosium atoms, and by R_2 the ratio of the activities obtained after an exposure of N days; then the half-life of scandium is $\frac{N \cdot R_1 \cdot 0.69}{R_2}$ days. We compared the activity of 66 mg of scandium and 100 mg of dysprosium and found after an activation of 24 days an activity ratio of 0.92×10^{-2}. During this activation time, full saturation of the dysprosium activity was obtained, while the scandium was far from being saturated. For equal numbers of scandium and dysprosium atoms we found an intensity ratio of 0.40×10^{-2}.

To compare the absorbing powers of scandium and dysprosium we inserted in the path of the neutron beam, which had been slowed down in the usual way by a block of paraffin, first a layer of scandia (590 mg/cm^2 Sc) and then a layer of dysprosia (340 mg/cm^2 Dy) and measured the activation of a rhodium foil, first in the absence and then in the presence of the absorbing layer. The amounts of the absorbing material necessary to reduce the activity of rhodium in each case to 90 % of its initial value were calculated to be 300 mg/cm^2 Sc and 43 mg/cm^2 Dy. A more satisfactory way to proceed in comparing the absorbing powers would have been to have used a dysprosium in-

dicator to measure the absorption in dysprosium and a scandium indicator to measure the absorption in scandium, but the small activation of scandium after a few days' exposure to neutrons rendered this infeasible. We have, however, applied the last mentioned method to compare the absorption of neutrons in dysprosium, europium, and holmium, as discussed in the next section. The comparison of the absorbing powers of equal numbers of atoms of dysprosium and scandium led to the result that the former absorbed 25 times as strongly as the latter. It follows from this result and from the comparison of the activities of the two elements, that the half-life of $^{46}_{21}$Sc is two months. A similar value was obtained by decay measurements.

Strongly absorbing rare earth isotopes forming stable products.

The unusually strong activities of some rare earth nuclei are to be ascribed to the existence of strong nuclear resonance levels in the nuclei in question, these levels corresponding to energies of slow neutrons abundant in the neutron beam passing through them, and also to the fact that the isotope formed by the capture process is not a stable one already known but an active one hitherto unknown. It is a matter of experience that a mass number cannot be occupied both by a stable and an active isotope of the same element, so that should the mass number 166 be occupied by a stable dysprosium isotope the high capturing power for slow neutrons shown by $^{165}_{65}$Dy would not lead to an active but to a stable dysprosium isotope. The appearance of a strong activity shows that at least one isotope of this element captures neutrons strongly, but high absorption does not necessarily imply strong activity because nuclei yielding

stable isotopes can also be very strong absorbers of neutrons. To obtain information about the existence of strongly capturing rare earth nuclei not leading to the formation of radioactive products, we compared the activities of dysprosium, europium, and holmium with their absorbing powers for the same neutron beam as was used to activate them. The results of these measurements, in which the absorbing element itself was used as indicator, are seen in table 2.

Table 2.

Absorption of Slow Neutrons in Rare Earth Elements.

(Amount necessary to reduce the activity of the indicator by ten per cent).

Element	Indicator	mg/cm^2
Europium	Europium	13
Dysprosium	Dysprosium	40
Holmium	Holmium	120

While the activity of europium is slightly smaller than that of dysprosium its absorbing power is more than twice as big; europium thus absorbs slow neutrons to an appreciably larger extent than is to be expected from the activity of the radioactive europium isotope formed. To explain this discrepancy we have to assume that besides the 9 h. period a second period, long and therefore not observed, is present, or alternatively that the second stable europium isotope too captures neutrons strongly, and gives rise to a stable isotope not revealed by the mass spectrograph, or alternatively to an active one of long life.

Samarium also shows an absorption much stronger than

is to be expected from the activity of the two known radioactive samarium isotopes. Of the numerous isotopes of samarium not leading to the formation of active isotopes at least one must therefore have a strong resonance level for slow neutrons. In view of the fairly weak activity of samarium the absorption measurements could not be carried out by using a samarium indicator, so rhodium was used for that purpose. The results of these measurements and also of absorption measurements with other rare earths using rhodium as indicator are shown in table 3.

Table 3.

Absorption of Slow Neutrons in Rare Earth Elements.

(Amount necessary to reduce the activity of the indicator by ten per cent).

Element	Indicator	mg/cm^2
Europium	Rhodium	16
Dysprosium	Rhodium	43
Holmium	Rhodium	160
Gadolinium	Rhodium	2
Samarium	Rhodium	12
Yttrium	Rhodium	500
Scandium	Rhodium	300
Cadmium	Rhodium	18

It is well known that the activity obtained by the action of slow neutrons is not a trustworthy measure of the intensity of the neutron beam, because the neutron absorbing powers of different elements are very specific and depend very much on the neutron velocities. The ambiguity arising from this fact can, however, be avoided by using the same

element as indicator and absorber in absorption experiments. Should that not be feasible, as would happen if, for example, the absorbing substance did not show any or had only a very slight activity — this is the case with gadolinium — it is advisable to adopt the following procedure. The maximum absorption obtained in a thick layer of gadolinium is measured using, say, rhodium as indicator; then the thick layer is replaced by a few milligrams of material and the absorbing power measured again. The first mentioned measurement gives the result that no more than 67 % absorption can be obtained for the neutron beam in question through a thick layer of gadolinium, while the last mentioned measurement shows that 2 mg of gadolinium are necessary to reduce the intensity of the neutron beam by 10 %. To arrive at a figure giving the amount of gadolinium necessary to reduce the intensity of neutrons of such velocities as are actually absorbed in gadolinium we must multiply 2 mg by 0.67 and thus obtain a value of 1.3 mg. The corresponding figures for a few elements are given in table 4 and 5. Of all the rare earth elements gadolinium — as can be seen from the table — has the highest absorbing power; it is indeed, as has already been shown by Dunning, Pegram, Fink, and Mitchell (8), the strongest known absorber of slow neutrons. In view of the very strong absorbing power of gadolinium great care must be taken in interpreting the results of absorption measurements on rare earth preparations which might contain traces of gadolinium. The presence of less then $^1/_2$ per cent of gadolinium in erbium, for example, would suffice to explain the whole absorption shown by erbium. As europium is often contaminated with gadolinium we used various preparations of europium to compare the absorption in euro-

pium and dysprosium. One of the preparations was kindly given us by Prof. PRANDTL and was entirely free of gadoli-

Table 4.

Percentage of Initial Intensity of the Neutron Beam Present after the Passage of a "Thick" Layer.

Element	mg/cm²	Intensities
Samarium	580	28 %
Gadolinium	120	33 %
Dysprosium	610	40 %
Cadmium	390	43 %

Table 5.

Absorption of Slow Neutrons in Rare Earth Elements.

(Amount necessary to reduce the activity of the indicator by ten per cent of that observed after passage of the neutrons through a "thick" layer).

Element	Indicator	mg/cm²
Samarium	Rhodium	10
Gadolinium	Rhodium	1.6
Dysprosium	Rhodium	30
Cadmium	Rhodium	12

nium; it gave a value only slightly lower than the other specimens investigated.

The high values found by different observers for the absorbing power of yttrium are clearly due to the presence of impurities in the preparations used. According to AMALDI

and his colleagues (1) the absorbing power of yttrium is 70 per cent of that of cadmium, and Dunning, Pegram, Fink, and Mitchell (8) give 30 per cent; whereas using very pure preparations as described on page 5 we find that yttrium is a very poor absorber, its absorbing power being only 4 per cent of that of cadmium and 0.3 per cent of that of gadolinium, if the absorption of equal numbers of atoms of the different elements are compared. In table 6 are given the relative intensities of the activities produced in the rare earth elements by neutrons that have been slowed down by large amounts of paraffin wax. We are still investigating the intensities obtained under the action of fast and semi-fast neutrons and the possible existence of resonance levels.

Table 6.

The Relative Activities of the Rare Earth Elements.

Element Bombarded	Relative Intensity	Element Bombarded	Relative Intensity
Yttrium	0.5	Terbium	2.5
Lanthanum	2	Dysprosium	100
Cerium	—	Holmium	20
Praseodymium	4.5	Erbium	0.35
Neodymium	0.04	Thulium	12
Samarium	0.6; 2.0	Ytterbium	0.25
Europium	80	Lutecium	1.4; 1
Gadolinium	very low		

Comparison between the effect of neutrons on rare earth elements and other elements.

As is shown in this paper numerous radioactive isotopes of the elements of the rare earth group are formed under the action of neutrons, a result which was to be expected

from the known existence of a large number of stable isotopes of these elements. Thus the reactions of neutrons with the rare earth elements show the same typical features as their reactions with elements of lower and higher atomic number. The most remarkable feature is perhaps the comparatively frequent occurrence of pronounced resonance phenomena, which phenomena are much commoner among the rare earth elements than in any other part of the periodic system. This fact may also be considered as a simple consequence of BOHR's theoretical considerations (9) on neutron capture, since it would be expected that the distribution of resonance levels would be an especially close one in this region. In fact the product of the number of nuclear particles multiplied by the binding energy of a neutron in the nucleus reaches a maximum in the domain of the rare earth nuclei on account of the circumstance that the binding energy for higher particle numbers decreases considerably until — for the natural radioactive bodies — it has fallen to about half its maximum value. The more frequent occurrence of resonance capture in processes leading to the formation of stable isotopes, than in those giving radioactive isotopes is also in conformity with general experience and is easily explained by the theoretical considerations mentioned above (10), since the distribution of levels will be much closer in the former case on account of the fact that the binding energy is considerably larger in processes of this kind than in those leading to the production of unstable isotopes.

To give a comprehensive picture of the present experimental material we have included, at the end of this paper, a number of tables showing all known stable and radioactive isotopes.

The use of neutrons in analytical chemistry.

The usual chemical methods of analysis fail, as is well known, for most of the rare earth elements and have to be replaced by spectroscopic, X-ray, and magnetic methods. The latter methods can now be supplemented by the application of neutrons to analytical problems by making use both of the artificial radioactivity and of the great absorbing power of some of the rare earth elements for slow neutrons.

Qualitative analysis with the aid of artificial radioactivity is based on the determination of periods of decay. All rare earth elements with the exception of cerium and thulium have half lives varying from a few minutes to a few days, so they can all be measured conveniently. The period of decay of 2.5 h., for example, is completely characteristic of dysprosium and is an unambiguous indication of its presence in the sample investigated; as little as 0.1 mg can be determined without difficulty. We used the method of artificial radioactivity to determine the dysprosium content of yttrium preparations. The procedure was the following: we mixed 0.1 %, 1 % etc. of dysprosium with neodymium oxide, the latter being chosen because it is one of the cheapest rare earth elements, and determined the intensity obtained. The yttrium sample to be investigated was then activated under exactly the same conditions, and a comparison of the dysprosium activities obtained gave 1 % as the dysprosium content of the yttrium sample. In carrying out such intensity comparisons, it is of importance to activate very thin layers of the sample, for if a thick layer containing, for example, gadolinium or other strongly absorbing substances is bombarded, the deeper layers

of the sample will hardly acquire any activity because most of the neutrons will be absorbed by the upper layers.

Another very beautiful analytical method is based on the very different absorbing powers of the different rare earth elements. A sample, 5 mg of which spread over 1 cm^2 absorbed a quarter of the slow neutrons falling on it, could be identified at once as gadolinium, no other element having so high an absorbing power.

Unlike the method of artificial radioactivity, the absorption method is limited in its application by the fact that the absorption measure is the sum of the absorptions of the different elements present in the sample. This limitation is, however, largely due to the fact that our knowledge of the absorption of neutrons and still more our devices for producing neutrons of different energies are only in an embryonic state. The absorbing powers of different nuclei depend to a high degree on the energy of the neutrons in question and the future development of our knowledge of neutron absorption will presumably make it possible to apply absorption methods of neutron analysis of great simplicity and reliability. This method of analysis, as also that based on periods of decay, gives a direct means of identification of the nuclei involved; this distinguishes them from all other analytical methods, chemical, spectroscopic, X-ray, and magnetic, which are based on the investigation of the electronic properties of the atom in question.

Effect of neutrons on minerals containing rare earth elements.

Many of the rare earth minerals, because they are products of residual magmatic crystallisation, contain rare earth elements, thorium, and uranium, along with beryl-

lium and other light elements. The last mentioned element is far the most effective neutron source under bombardment with α-particles or with the γ-rays emitted by uranium, thorium, and their disintegration products; the nuclei of other elements, such as lithium, boron, magnesium, aluminium etc. are much less effective.* In minerals containing large amounts of strongly capturing rare earth elements the neutrons produced in the mineral or in its surroundings are absorbed to a large extent in the element in question. The mineral gadolinite, for example, contains about 50 % of rare earths, of which according to Goldschmidt and Thomassen** up to about 15 % is gadolina; this mineral often contains, too, other light elements including considerable amounts of beryllium, about 0.3 % of thorium, and some uranium as well. 1 g of thorium and its disintegration products produces up to 10^8 neutrons per year or in all 10^{16} neutrons since the formation of the minerals. If these neutrons are all absorbed in 1 kg of the mineral in question and are absorbed primarily by the gadolinium content, 10^{16} gadolinium atoms will be formed having an atomic weight one unit higher than before the absorption. As 1 kg gadolinite contains about 10^{22} of gadolinium atoms the equivalent weight of gadolinium will increase during that long span of time by but one unit in the fourth decimal place.

While this result is only a very rough estimate it suffices to demonstrate that some of the rare earth elements which primarily form higher stable isotopes by capturing neutrons, increase in equivalent weight as time proceeds.

* We compared the activities obtained when dysprosia was bombarded with neutrons of a beryllium-radon and a magnesium-radon source in the presence of large amounts of paraffin wax and the figures obtained were as 100 : 1.

** V. M. Goldschmidt and L. Thomassen, Oslo, Vidskap Selskapets Skrifter I, Nr. 5, S. 44 (1924).

Dysprosium on the other hand forms holmium, holmium forms erbium etc.; the process in such cases leads to an increase in the amounts of rare earths of higher atomic number and to a corresponding decrease in the amounts of those of lower atomic number. Such behaviour is not confined to the rare earth elements; during their presence in the earth's crust many elements heavier than zinc will undergo increases, though small ones, of their equivalent weights or of their abundance relative to the lighter elements. The behaviour first named is shown primarily by even and the latter by odd elements, because elements having an odd atomic number have always only a few isotopes so that the consecutive mass numbers are not filled by stable isotopes and the formation of radioactive isotopes through neutron addition is possible. In the case of several even elements like cadmium, tin, gadolinium, osmium, mercury, lead etc., a long series of consecutive mass numbers are filled by stable isotopes so that the capture of neutrons leads chiefly to the formation of higher stable isotopes. It is therefore even elements that undergo an increase of their equivalent weights with time while the relative abundance of the elements of odd atomic number shifts towards the heavier elements.

Below zinc conditions are very different: the result of neutron action in minerals leads here to a large extent to the formation of elements of lower atomic number and only to a smaller extent to the formation of heavier isotopes or heavier elements. For example, bombardment of aluminium leads to the formation of a stable magnesium isotope and to a minor extent to a stable sodium isotope; the branching ratio between these two processes depends greatly on the energy of the neutrons.

Summary.

The artificial radioactivity of the rare earth elements including scandium and yttrium was investigated. The periods of decay of numerous radioactive isotopes produced lie between 5 min. and a few years. The biggest and smallest saturation intensities of the radiation emitted by these isotopes are in the ratio 10 000 : 1. The half-value thickness in aluminium of the β-radiation emitted was measured in several cases, and, in a few cases, the maximum energy of the continuous β-ray spectrum and Fermi's constant α as well.

The absorption of slow neutrons in rare earth elements was measured with a view to discovering the presence of strongly absorbing nuclei not giving rise to active isotopes.

The application of artificial radioactivity to analytical chemistry is discussed.

It is shown that the combination weight of the rare earth elements occurring in minerals in which a continual production of neutrons takes place has undergone a slight change during geological time.

We would like to express our best thanks to Professor Niels Bohr for the very kind interest he has taken in this work, to Professor Prandtl, Rolla, and Sterba-Böhm for lending us some of the preparations used.

(Institute of Theoretical Physics, University of Copenhagen.)

Diagrams of Stable and Radioactive Isotopes.

The abundant stable isotopes are in plain circles, the rare ones ($< 5\,\%$) in black circles. The rest are radioactive and their periods are given. In the last diagram between thulium and uranium the naturally occuring radioactive isotopes are placed along with their periods in circles.

The ordinates are the differences between the mass number and twice the atomic number.

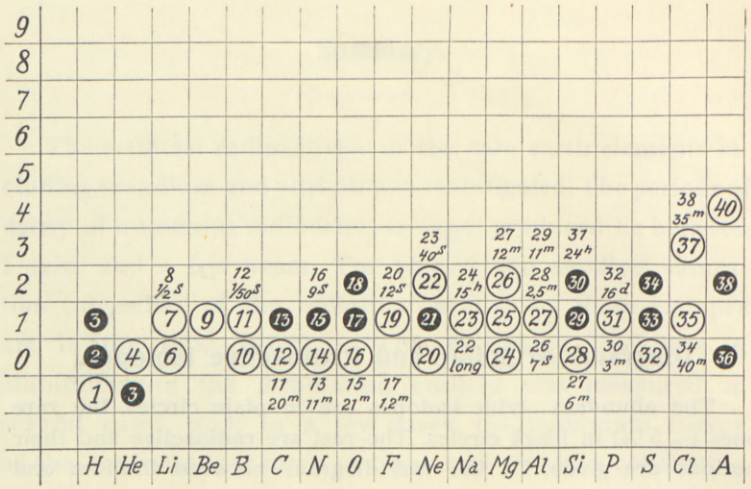

Diagram a.

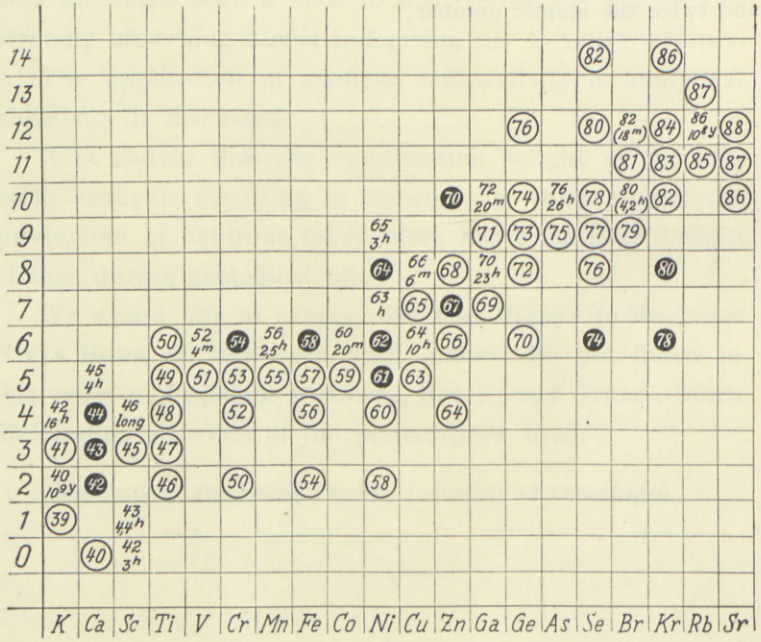

Diagram b.

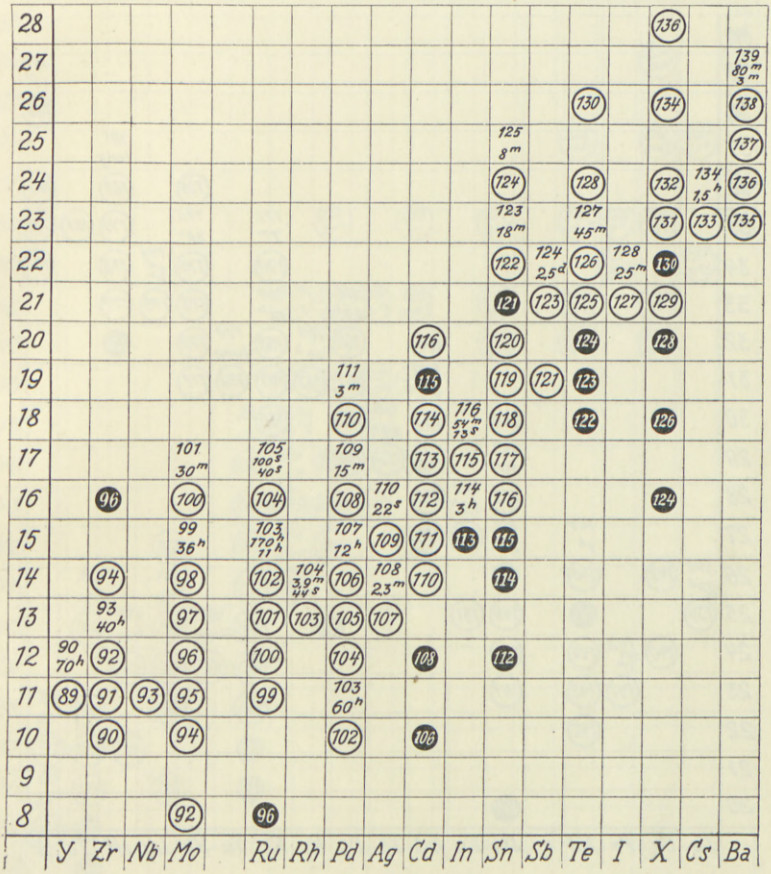
28
27
26
25
24
23
22
21
20
19
18
17
16
15
14
13
12
11
10
9
8
Y
Zr
Nb
Mo
Ru
Rh
Pd
Ag
Cd
In
Sn
Sb
Te
I
X
Cs
Ba

Diagram c.

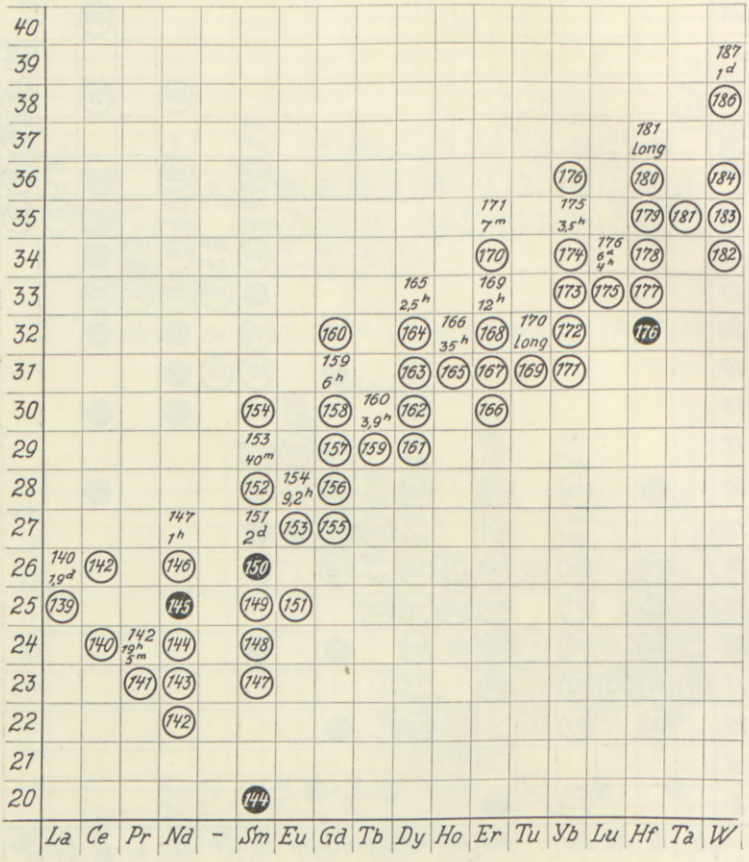
40
39
38
37
36
35
34
33
32
31
30
29
28
27
26
25
24
23
22
21
20
La
Ce
Pr
Nd
–
Sm
Eu
Gd
Tb
Dy
Ho
Er
Tu
Yb
Lu
Hf
Ta
W
140 3,9d
147 1h
151 2d
153 40m
154 9,2h
159 6h
160 3,9h
165 2,5h
166 35h
169 12h
170 long
171 7m
175 3,5h
176 6d 4h
181 long
187 1d
139
140
142
141
142 19h 3m
143
144
145
146
147
148
149
150
151
152
153
154
155
156
157
158
159
160
161
162
163
164
165
166
167
168
169
170
171
172
173
174
175
176
177
178
179
180
181
182
183
184
186
144

Diagram d.

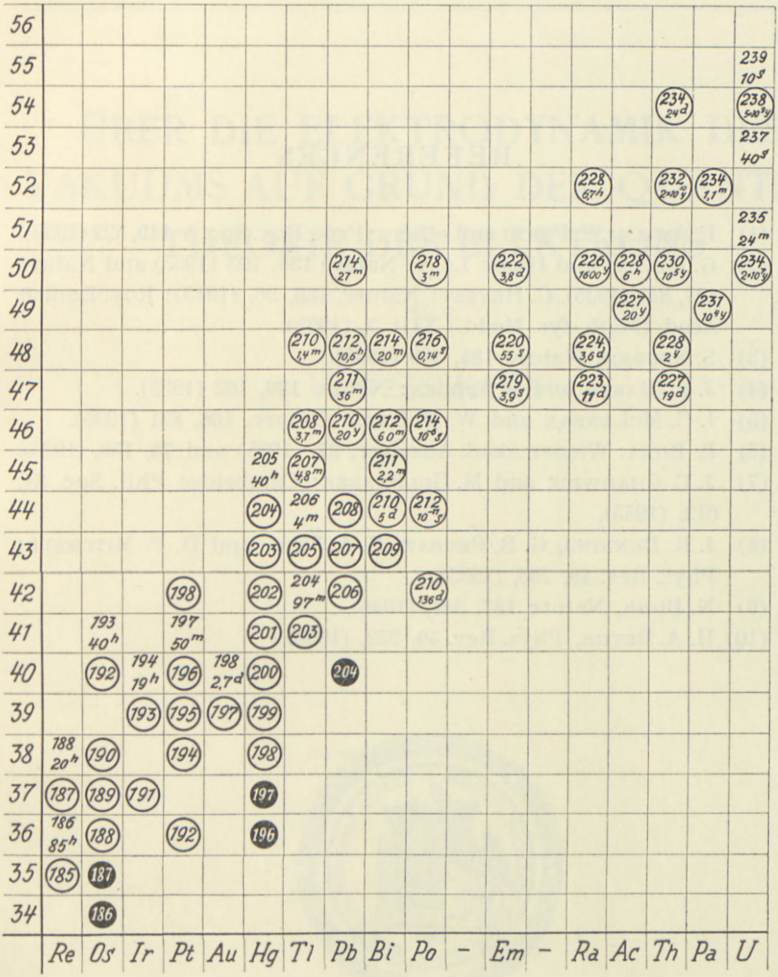
56
55
54
53
52
51
50
49
48
47
46
45
44
43
42
41
40
39
38
37
36
35
34
Re
Os
Ir
Pt
Au
Hg
Tl
Pb
Bi
Po
–
Em
–
Ra
Ac
Th
Pa
U
239 10⁵
234 24d
238 5·10⁹y
237 40⁵
228 67h
232 2·10⁹y
234 1,1m
235 24m
214 27m
218 3m
222 3,8d
226 1600y
228 6h
230 10⁵y
234 2·10⁵y
227 20y
231 10⁴y
210 1,4m
212 10,6h
214 20m
216 0,14s
220 55s
224 3,6d
228 2y
211 36m
219 3,9s
223 11d
227 19d
208 3,7m
210 20y
212 60m
214 10⁻⁴s
205 40h
207 4,8m
211 2,2m
204
206 4m
208
210 5d
212 10⁻⁶s
203
205
207
209
202
204 97m
206
210 136d
198
201
203
193 40h
197 50m
192
194 19h
196
198 2,7d
200
204
193
195
197
199
188 20h
190
194
198
187
189
191
197
186 85h
188
192
196
185
187
186

Diagram e.

REFERENCES

(1) E. Amaldi, E. Fermi and others: Proc. Roy. Soc. A. **149**, 522 (1935).
(2) G. Hevesy and Hilde Levi: Nature **136**, 103 (1935) and Nature **137**, 849 (1935). G. Hevesy: Nature, **135**, 96, (1935); Roy. Danish Acad. (Math.-fys. Medd.) XIII, 3, (1935).
(3) S. Sugden: Nature **135**, 469 (1935).
(4) J. K. Marsh and S. Sugden: Nature **136**, 102 (1935).
(5) I. C. McLennan and W. H. Rann: Nature, **136**, 831 (1935).
(6) E. Rona: Wiener Akad. Anzeiger, **27**, (1935) and **73**, 159, (1936).
(7) J. C. Chadwick and M. Goldhaber: Cambridge Phil. Soc. **31**, 612, (1935).
(8) J. R. Dunning, G. B. Pegram, G. A. Fink, and D. P. Mitchell: Phys. Rev. **48**, 265, (1935).
(9) N. Bohr, Nature **137**, 344, (1936).
(10) H. A. Bethe, Phys. Rev. **50**, 332, (1936).

Færdig fra Trykkeriet den 29. Oktober 1936.

Det Kgl. Danske Videnskabernes Selskab.
Mathematisk-fysiske Meddelelser. **XIV**, 6.

ÜBER DIE ELEKTRODYNAMIK DES VAKUUMS AUF GRUND DER QUANTEN-THEORIE DES ELEKTRONS

VON

V. WEISSKOPF

KØBENHAVN
LEVIN & MUNKSGAARD
EJNAR MUNKSGAARD
1936

Printed in Denmark.
Bianco Lunos Bogtrykkeri A/S.

This paper deals with the modifications introduced into the electrodynamics of the vacuum by Dirac's theory of the positron. The behaviour of the vacuum can be described unambigously by assuming the existence of an infinite number of electrons occupying the negative energy states, provided that certain well defined effects of these electrons are omitted, but only those to which it is obvious that no physical meaning can be ascribed.

The results are identical with these of Heisenberg's and Dirac's mathematical method of obtaining finite expressions in positron theory. A simple method is given of calculating the polarisability of the vacuum for slowly varying fields.

Eines der wichtigsten Ergebnisse in der neueren Entwicklung der Elektronentheorie ist die Möglichkeit, elektromagnetische Feldenergie in Materie zu verwandeln. Ein Lichtquant z. B. kann bei Vorhandensein von andern elektromagnetischen Feldern im leeren Raum absorbiert und in Materie verwandelt werden, wobei ein Paar von Elektronen mit entgegengesetzter Ladung entsteht.

Die Erhaltung der Energie erfordert, falls das Feld, in welchem die Absorption vor sich geht, statisch ist, dass das absorbierte Lichtquant die ganze zur Erzeugung des Elektronenpaares notwendige Energie aufbringt. Die Frequenz derselben muss somit der Beziehung $h\nu = 2mc^2 + \varepsilon_1 + \varepsilon_2$ genügen, wobei mc^2 die Ruhenergie eines Elektrons und ε_1 und ε_2 die übrige Energie der beiden Elektronen ist. Diesen Fall haben wir z. B. bei der Erzeugung eines Elektronenpaares durch ein γ-Quant im Coulombfeld eines Atomkerns vor uns.

Die Absorption kann auch in Feldern stattfinden, die von andern Lichtquanten stammen, wobei die letzteren zur Energie des Elektronenpaares beitragen können, sodass in diesem Falle die Energie $2mc^2 + \varepsilon_1 + \varepsilon_2$ der beiden Elektronen gleich der Summe aller bei diesem Prozess absorbierten Lichtquanten sein muss.

Das Phänomen der Absorption von Licht im Vakuum

stellt eine wesentliche Abweichung von der Maxwell'schen Elektrodynamik dar. Das Vakuum sollte nämlich unabhängig von den dort herrschenden Feldern für eine Lichtwelle frei durchdringlich sein, da sich verschiedene Felder nach den Maxwell'schen Gleichungen infolge der Linearität derselben unabhängig überlagern können.

Es ist bereits ohne näheres Eingehen auf die spezielle Theorie verständlich, dass auch in solchen Feldern, die nicht die nötige Energie besitzen, um ein Elektronenpaar zu erzeugen, Abweichungen von der Maxwell'schen Elektrodynamik auftreten müssen: wenn hochfrequentes Licht in elektromagnetischen Feldern absorbiert werden kann, so wird man für Lichtstrahlen, deren Frequenz zur Paarerzeugung nicht ausreicht, eine Streuung oder Ablenkung erwarten, analog zur Streuung des Lichts an einem Atom, dessen kleinste Absorptionsfrequenz grösser als die des Lichts ist. Das Licht wird sich also beim Durchgang durch elektromagnetische Felder so verhalten, als ob das Vakuum unter der Einwirkung der Felder eine von der Einheit verschiedene Dielektrizitätskonstante erhalten würde.

Um diese Erscheinungen darstellen zu können, muss die Theorie dem leeren Raum gewisse Eigenschaften zuschreiben, die die erwähnten Abweichungen von der Maxwell'schen Elektrodynamik hervorrufen. Tatsächlich führt die relativistische Wellengleichung des Elektrons auch zu derartigen Folgerungen, wenn man die aus der Dirac'schen Wellengleichung folgenden Zustände mit negativer kinetischer Energie zur Beschreibung des Vakuums heranzieht.

Die Grundannahme der Dirac'schen Theorie des Positrons besteht darin, dass das physikalische Verhalten des Vakuums im gewissen Sinne beschrieben werden kann durch das Verhalten einer unendlichen Menge von Elektronen, — die

Vakuumelektronen — die sich in den Zuständen negativer kinetischer Energie befinden und sämtliche dieser Zustände besetzt halten. Die Übereinstimmung kann selbstverständlich nicht vollkommen sein, da die Vakuumelektronen eine unendliche Ladungs- und Stromdichte besitzen, die sicher keine physikalische Bedeutung haben darf. Es zeigt sich aber, dass z. B. die Paarerzeugung (und ihr Umkehrprozess) gut wiedergegeben wird als ein Sprung eines Vakuumelektrons in einen Zustand positiver Energie unter dem Einfluss elektromagnetischer Felder, wodurch es als ein reales Elektron in Erscheinung tritt, während das Vakuum um ein negatives Elektron ärmer geworden ist, was sich durch das Auftreten eines positiven Elektrons äussern muss. Die von diesem Bilde ausgehende Berechnung der Paarerzeugung und -Vernichtung zeigt eine gute Übereinstimmung mit der Erfahrung.

Die Berechnung der meisten andern Effekte, die aus der Positronentheorie folgen, stossen immer auf das Problem, in welchem Ausmass das Verhalten der Vakuumelektronen tatsächlich als das des Vakuums anzusehen ist. Dieses Problem wird noch durch den Umstand erschwert, dass Ladungs-, Strom- und Energiedichte der Vakuumelektronen unendlich sind, sodass es sich meistens darum handelt, von einer unendlichen Summe in eindeutiger Weise einen endlichen Teil abzutrennen und diesem Realität zuzuschreiben. Die Lösung dieses Problems wurde von Dirac und Heisenberg dadurch durchgeführt, dass sie eine widerspruchsfreie Methode angaben, den physikalisch bedeutungsvollen Teil der Wirkungen der Vakuumelektronen zu bestimmen. Es wird im folgenden gezeigt, dass diese Bestimmung weitgehend frei von jeder Willkür ist, da sie in konsequenter Weise nur folgende Eigenschaften der Vakumelektronen als physikalisch bedeutungslos annimmt:

(I)
1) Die Energie der Vakuumelektronen im feldfreien Raum.
2) Die Ladungs- und Stromdichte der Vakuumelektronen im feldfreien Raum.
3) Eine räumlich und zeitlich konstante feldunabhängige elektrische und magnetische Polarisierbarkeit des Vakuums.

Diese Grössen[1] beziehen sich nur auf das feldfreie Vakuum, und es darf als selbstverständlich angesehen werden, dass diese keine physikalische Bedeutung haben können. Alle drei Grössen erweisen sich nach Summierung der Beiträge aller Vakuumselektronen als divergierende Summen. Es sei noch hinzugefügt, dass eine konstante Polarisierbarkeit in keiner Weise feststellbar wäre, sondern nur sämtliche Ladungs- und Feldstärkenwerte mit einem konstanten Faktor multiplizieren würde.

Wir werden im nächsten Abschnitt auf Grund dieser Annahmen die physikalischen Eigenschaften des Vakuums bei Anwesenheit von Feldern berechnen, die zeitlich und räumlich langsam veränderlich sind. Wir verstehen darunter solche Felder F, die sich auf Strecken der Länge $\frac{h}{mc}$ und in Zeiten der Länge $\frac{h}{mc^2}$ nur wenig verändern[2] und somit den Bedingungen

$$(1) \qquad \frac{h}{mc}|\operatorname{grad} F| \ll |F|, \quad \frac{h}{mc^2}\left|\frac{\partial F}{\partial t}\right| \ll |F|$$

genügen. Bei Anwesenheit solcher Felder werden im allgemeinen keine Paare erzeugt, da die auftretenden Lichtquanten zu geringe Energie haben. Die Extremfälle, in denen die Strahlungsdichte so hoch ist, um das Zusammenwirken

[1] Die Annahmen, 1.) oder 2.) oder 3.) als bedeutungslos anzusehen, werden im folgenden mit I_1, I_2 bzw. I_3 zitiert.

[2] h ist die durch 2π geteilte Planck'sche Konstante.

von sehr vielen Quanten zu gestatten, oder in denen elektrostatische Felder mit Potentialdifferenzen von über $2mc^2$ vorhanden sind (in diesem Falle würden auf Grund des KLEIN'schen Paradoxons Paare entstehen) wollen wir von der Betrachtung ausschliessen. Unter diesen Umständen lassen sich die elektromagnetischen Eigenschaften des Vakuums durch eine feldabhängige elektrische und magnetische Polarisierbarkeit des leeren Raums darstellen, die z. B. zu einer Lichtbrechung in elektrischen Feldern oder zu einer Streuung von Licht an Licht führt. Der Dielektrizitäts- und Permeabilitätstensor des Vakuums hat dann für schwächere Feldstärken näherungsweise folgende Form: ($\vec{E}$, $\vec{H}$, $\vec{D}$, $\vec{B}$ sind die vier elektromagnetischen Feldgrössen[1].)

$$D_i = \sum_k \varepsilon_{ik} E_k, \quad H_i = \sum_k \mu_{ik} B_k$$

$$(2)\quad \varepsilon_{ik} = \delta_{ik} + \frac{e^4 h}{45\pi m^4 c^7}\left[2(E^2 - B^2)\,\delta_{ik} + 7 B_i B_k\right]$$

$$\mu_{ik} = \delta_{ik} + \frac{e^4 h}{45\pi m^4 c^7}\left[2(E^2 - B^2)\,\delta_{ik} - 7 E_i E_k\right].$$

$$\delta_{ik} = \begin{cases} 1, & i = k \\ 0, & i \neq k \end{cases}$$

Die Berechnung dieser Erscheinungen wurde von EULER u. KOCKEL[2] und von HEISENBERG u. EULER[3] bereits durchgeführt. Im nächsten Abschnitt sollen jedoch bedeutend einfachere Methoden angewendet werden. Ausserdem sollen die Eigenschaften des Vakuums auf Grund der skalaren relativistischen Wellengleichung des Elektrons von KLEIN u. GORDON berechnet werden. Diese Wellengleichung liefert nach PAULI u. WEISSKOPF[4] die Existenz positiver und negativer Partikel, und ihre Erzeugung und Vernichtung durch elektro-

[1] Es werden im folgenden nur dort Pfeile über Vektorgrössen gesetzt, wo Verwechslungen möglich sind.

[2] H. EULER u. B. KOCKEL, Naturwiss. **23**, 246, 1935; H. EULER, Ann. d. Phys. V. **26**, 398.

[3] W. HEISENBERG u. H. EULER, ZS. f. Phys. **38**, 714, 1936.

[4] W. PAULI u. V. WEISSKOPF, Helv. Phys. Acta. **7**, 710, 1934.

magnetische Felder ohne jede besondere Zusatzannahme. Jedoch besitzen diese Partikel keinen Spin und befolgen die Bosestatistik, weshalb diese Theorie nicht auf die realen Elektonen anwandbar ist. Es ist jedoch bemerkenswert, dass auch diese Theorie auf Eigenschaften des Vakuums führt, denen keine physikalische Bedeutung zukommen kann. So erhält man z. B. ebenfalls eine unendliche räumlich und zeitlich konstante feldunabhängige Polarisierbarkeit des Vakuums. Nach Weglassung der entsprechenden Glieder gelangt man zu ähnlichen Resultaten, wie die der Positronentheorie Dirac's. Die physikalischen Eigenschaften des Vakuums rühren in dieser Theorie von der »Nullpunktsenergie« der Materie her, die auch bei nichtvorhandenen Teilchen von den äusseren Feldstärken abhängt und somit ein Zusatzglied zu der reinen Maxwell'schen Feldenergie liefert.

Im 3. Abschnitt behandeln wir die Folgerungen aus der Dirac'schen Positronentheorie für den Fall allgemeiner äusserer Felder und wir zeigen, dass man auf Grund der genannten drei Annahmen über die Wirkungen der Vakuumelektronen stets zu endlichen und eindeutigen Resultaten kommt. Die Heisenberg'schen Subtraktionsvorschriften erweisen sich als identisch mit diesen drei Annahmen und erscheinen somit bedeutend weniger willkürlich als es in der Literatur bisher angenommen wurde.

Alle folgende Rechnungen berücksichtigen nicht explizit die gegenseitigen Wechselwirkungen der Vakuumelektronen sondern betrachten ausschliesslich jedes einzelne Vakuumelektron allein unter der Einwirkung eines vorhandenen Feldes. Bei diesem Verfahren sind aber die gegenseitigen Einwirkungen nicht vollkommen vernachlässigt, da man das äussere Feld gar nicht von dem Feld trennen kann, das von den Vakuumselektronen selbst erzeugt ist, sodass das in die Rech-

nung eingehende Feld die Wirkungen der andern Vakuumelektronen zum Teil implizit enthält. Dieses Vorgehen ist analog zur HARTREE'schen Berechnung der Elektronenbahnen eines Atoms in dem Feld, das von den Elektronen selbst verändert wird. Zur expliziten Berechnung der Wechselwirkungen müsste man die Quantenelektrodynamik anwenden, d. h. die Quantelung der Wellenfelder vornehmen. Dies führt bekanntlich auch bereits ohne die Annahme unendlich vieler Vakuumselektronen zu Divergenzen und soll im folgenden nicht näher berührt werden.

II.

In diesem Abschnitt soll die Elektrodynamik des Vakuums für Felder behandelt werden, die den Bedingungen (1) genügen. Die Feldgleichungen sind durch die Angabe der Energiedichte U als Funktion der Feldstärken festgelegt. Wir bestimmen diese aus der Energiedichte $\tilde{U}$ der Vakuumelektronen, die für das Verhalten des Vakuums massgebend sein sollen.

Es ist vorteilhaft, auf die Lagrangefunktion L des elektromagnetischen Feldes zurückzugreifen, da diese durch die Forderung der relativistischen Invarianz schon weitgehend festgelegt ist. Zwischen der Lagrangefunktion L und der Energiedichte U bestehen folgende Beziehungen:

$$U = \sum_i E_i \frac{\partial L}{\partial E_i} - L. \tag{3}$$

In der MAXWELL'schen Elektrodynamik gilt:

$$L = \frac{1}{8\pi}(E^2 - B^2), \quad U = \frac{1}{8\pi}(E^2 + B^2).$$

Die Zusätze zu dieser Lagrangefunktion müssen ebenso wie diese selbst relativistische Invarianten sein. Solange wir uns

nur auf langsam veränderliche Felder beschränken, (Bedingung (1)), werden diese Zusätze nur von den Werten der Feldstärken abhängen und nicht von deren Ableitungen. Sie können daher nur Funktionen der Invarianten $(E^2 - B^2)$ und $(EB)^2$ sein. Entwickeln wir die Zusätze nach Potenzen der Feldstärken bis zur 6. Ordnung, so erhalten wir:

$$L = \frac{1}{8\pi}(E^2 - B^2) + L'$$
$$L' = \alpha (E^2 - B^2)^2 + \beta (EB)^2 + \\ + \xi (E^2 - B^2)^3 + \zeta (E^2 - B^2)(EB)^2 + \cdots$$

und daher nach (3)

$$(4) \quad \begin{cases} U = \frac{1}{8\pi}(E^2 + B^2) + U' \\ U' = \alpha (E^2 - B^2)(3E^2 + B^2) + \beta (EB)^2 + \\ \quad + \xi (E^2 - B^2)^2 (5E^2 + B^2) + \zeta (EB)^2 (3E^2 - B^2) + \cdots \end{cases}$$

Der Zusatz zur Energiedichte ist somit durch die Invarianzeigenschaften weitgehend festgelegt; es wird also im folgenden nur notwendig sein die vorkommenden Konstanten $\alpha, \beta, \xi, \zeta, \ldots$ zu bestimmen. Diesen Ansätzen liegt schon die spezielle Annahme zugrunde, dass U' keine Glieder 2. Ordnung in den Feldstärken enthält, sondern nur höhere. Dies ist gleichbedeutend damit, dass das Vakuum keine von den Feldern unabhängige Polarisierbarkeit besitzt.

Die Rechnungen von Euler u. Kockel und von Heisenberg u. Euler liefern für die vier Konstanten die Werte:

$$\alpha = \frac{1}{360\pi^2}\frac{e^4 h}{m^4 c^7}, \quad \beta = 7\alpha, \quad \xi = \frac{1}{630\pi^2}\frac{e^6 h^3}{m^8 c^{13}}, \quad \zeta = \frac{13}{2}\xi.$$

Die in (2) angegebenen Dielektrizitäts- und Permeabilitätstensoren ergeben sich aus den Beziehungen:

$$D_i = 4\pi \frac{\partial L}{\partial E_i}, \quad H_i = -4\pi \frac{\partial L}{\partial B_i}.$$

Wir werden im folgenden diese Resultate auf eine wesentlich einfachere Weise herleiten.

Der Zusatz U' zur MAXWELL'schen Energiedichte des Vakuums soll durch den Zusatz $\tilde{U}'$ bestimmt sein, den die Vakuumelektronen beitragen. Die Energiedichte bei Anwesenheit von Elektronen in den Zuständen $\psi_1, \psi_2 \ldots \psi_i \ldots$ ist gegeben durch

$$U = \frac{1}{8\pi}(E^2 + B^2) + \tilde{U}'$$

$$\tilde{U}' = \sum_i \left\{ \psi_i^*, \left[\left(\vec{\alpha}, \frac{hc}{i} \operatorname{grad} + e\vec{A} \right) + \beta mc^2 \right] \psi_i \right\}$$

wobei $\vec{\alpha}, \beta$ die DIRAC'schen Matrizen und $\vec{A}$ das vektorielle Potential ist. Der Zusatz $\tilde{U}'$ zur MAXWELL'schen Dichte ist somit nicht gleich der ganzen materiellen Energiedichte U_{mat}

$$U_{\text{mat}} = ih \sum_i \left\{ \psi_i^*, \frac{\partial}{\partial t} \psi_i \right\} \tag{5}$$

sondern

$$\tilde{U}' = U_{\text{mat}} - \sum_i \{ \psi_i^*, eV\psi_i \} \tag{6}$$

wobei V das skalare Potential ist. Man kann $\tilde{U}'$ als die kinetische Energiedichte bezeichnen. Die gesamte materielle Energiedichte U_{mat} lässt sich, wie wir sehen werden, leicht berechnen; der zweite Term von (6) — die potentielle Energiedichte — ergibt sich aus U_{mat} in folgender Weise: Wenn

* Zwei Eigenfunktionen ψ und φ in geschwungenen Klammern: $\{\psi, \varphi\}$ bedeutet hier und im folgenden das innere Produkt der beiden Spinozen ψ u. φ: $\{\psi, \varphi\} = \sum_k \psi^k \varphi^k$, wobei k der Spinindex ist.

man sich das skalare Potential proportional zu dem konstanten Faktor λ denkt, so gilt:[1]

$$\lambda \int \sum_i \{\psi_i^*, eV\psi_i\} d\tau = \lambda \frac{\partial}{\partial \lambda} \int U_{\text{mat}} d\tau \tag{7}$$

wobei die Integrationen sich über den ganzen Raum erstrecken. Im Grenzfall konstanter Felder, den wir hier wegen der Bedingungen (1) betrachten wollen, können wir die Feldstärke E selbst als den konstanten Faktor λ ansehen, und können ausserdem die Beziehung (7) auch auf die Energiedichten übertragen. Wir erhalten dann für die kinetische Energiedichte

$$\tilde{U}' = U_{\text{mat}} - E \frac{\partial U_{\text{mat}}}{\partial E}. \tag{7a}$$

Vergleicht man dies mit (3) so sieht man, dass zwischen der materiellen und der kinetischen Energiedichte dieselbe Beziehung besteht, wie zwischen $-L$ und U. U_{mat} kann also hier dem durch die Vakuumelektronen hervorgerufenen Zusatz zur Lagrangefunktion gleichgesetzt werden:

$$U_{\text{mat}} = -\tilde{L}'. \tag{8}$$

Da die Form von U' weitgehend durch die relativistischen Invarianzforderungen festgelegt ist, so genügt es, U' für ein

[1] Der Beweis läuft folgendermassen: Wenn der Energieoperator H von einem Parameter λ abhängig ist, so ändert sich das Diagonalelement H_{ii} des Energieoperators bei einer infinitisemalen adiabatischen Änderung $d\lambda$ von λ um:

$$dH_{ii} = \left(\frac{\partial H}{\partial \lambda}\right)_{ii} d\lambda.$$

Wenn wir nun setzen:

$$H = H_0 + \lambda eV$$

so gilt dann:

$$\lambda (eV)_{ii} = \lambda \frac{\partial H_{ii}}{\partial \lambda}.$$

spezielles Feld zu bestimmen. Wir wählen ein homogenes magnetisches Feld $B = (B_x, 0, 0)$ und ein dazu paralleles räumlich periodisches elektrostatisches Feld, dessen Potential durch

$$V = V_0 e^{\frac{igx}{h}} + V_0^* e^{\frac{-igx}{h}} \tag{9}$$

gegeben ist. Wir vergleichen dann dieses Resultat mit dem allgemeinen Form (4) und werden daraus die Koeffizienten dieser Form bestimmen.

Heisenberg u. Euler wählen im Gegensatz hierzu ein konstantes elektrisches Feld, wodurch Schwierigkeiten infolge des Klein'schen Paradoxons entstehen: Jedes noch so schwache homogene elektrische Feld erzeugt Elektronenpaare, wenn es sich über den ganzen Raum erstreckt. Die Elektronenbesetzung der Energiezustände ist dann nicht exakt stationär. In der vorliegenden Rechnung kann durch die Periodizität vermieden werden, dass Potentialdifferenzen über $2mc^2$ vorkommen, sodass keine Paarerzeugungen stattfinden.

Die materielle Energiedichte ist bei voller Besetzung aller negativen Energiezustände gegeben durch

$$U_{\text{mat}} = \sum_i W_i \{\psi_i^*, \psi_i\} \tag{10}$$

W_i ist die zur Eigenfunktion ψ_i gehörige Energie, summiert wird über alle negative Zustände. Die Summe ist selbstverständlich unendlich. Welcher endliche Teil dieser Summe von physikalischer Bedeutung ist, wird sich eindeutig aus dem expliziten Ausdruck für U_{mat} ergeben.

Die ψ_i befolgen die Wellengleichung:

$$\left\{\frac{ih}{c}\frac{\partial}{\partial t} - \frac{eV}{c} + \alpha_x ih\frac{\partial}{\partial x} + K\right\}\psi = 0 \tag{11}$$

$$(12) \qquad K = \alpha_y ih\frac{\partial}{\partial y} + \alpha_z\left[ih\frac{\partial}{\partial z} - \frac{e}{c}|B|y\right] - \beta mc.$$

Wir folgen vorläufig der Rechnung Heisenbergs u. Eulers l. c., wobei wir nur unwesentliche Änderungen in der Bedeutung der Variabeln anbringen.

Als Lösung setzen wir an:

$$(13) \qquad \psi_i = \frac{1}{\sqrt{2\pi h}} e^{\frac{i}{h}(p_z z - W_i t)} \cdot u(y)\, X(x).$$

Der Operator K ergibt, zweimal auf ψ angewendet:

$$K^2\psi = \left[-h^2\frac{\partial^2}{\partial y^2} - i\alpha_y\alpha_z\frac{eh}{c}|B| + \left(p_z + \frac{e}{c}|B|y\right)^2 + m^2c^2\right]\psi.$$

Wir setzen nun

$$\eta = \left(y + \frac{2p_z h}{b}\right)\sqrt{\frac{b}{2h^2}}, \quad b = \frac{2eh}{c}|B|.$$

b ist das Mass des Magnetfeldes. Durch Einführung von η erreichen wir, dass K^2 die Form einer Oszillator-Hamiltonfunktion erhält. Wir setzen daher

$$u(y) = \tilde{H}_n(\eta)\left(\frac{b}{2h^2}\right)^{1/4}$$

wobei $\tilde{H}_n(\eta)$ die n-te auf 1 normierte Oszillator-Eigenfunktion ist. Dann gilt $\int |u(y)|^2 dy = 1$ und

$$(14) \qquad K^2\psi = \left\{m^2c^2 + b\left(n + \frac{1-\sigma_x}{2}\right)\right\}\psi, \quad \sigma_x = i\alpha_y\alpha_z.$$

Es lässt sich nun eine Darstellung der 4-komponentigen ψ wählen, in der σ_x diagonal ist:

$$\sigma_x = \begin{pmatrix} 1 & 0 & 0 & 0 \\ 0 & 1 & 0 & 0 \\ 0 & 0 & -1 & 0 \\ 0 & 0 & 0 & -1 \end{pmatrix}.$$

Den ersten beiden Komponenten von ψ entspricht dann ein positiver, den beiden andern ein negativer Spin in der x-Richtung. Bei dieser Wahl zerfällt die Wellengleichung (11) in zwei getrennte Gleichungssysteme für die beiden Komponentenpaare mit gleichem Spin, sodass wir zwei Wellengleichungen mit zweireihigen Matrizen gewinnen. Der Operator K lässt sich dann in der Form $K = \gamma |K|$ schreiben, wobei γ eine zweireihige Matrix ist, die die Bedingung $\gamma^2 = 1$ erfüllt und $|K|$ die gewöhnliche Zahl

$$|K| = \sqrt{m^2 c^2 + b\left(n + \frac{1-\sigma_x}{2}\right)}$$

bedeutet, die vom Wert σ_x des Spins abhängt. Ebenso ist die in der Wellengleichung auftretende Matrix α_x zweireihig und ist mit γ antikommunativ: $\alpha_x \gamma + \gamma \alpha_x = 0$, da α_x nach (12) auch mit K antikommutativ ist. Die beiden Wellengleichungen lassen sich dann in der Form

$$\left\{\frac{ih}{c}\frac{\partial}{\partial t} + \alpha_x ih\frac{\partial}{\partial x} - \frac{e}{c}V + \gamma|K|\right\}\psi = 0 \tag{16}$$

schreiben, wobei α_x und γ zweireihige Matrizen sind, die sich nur auf ein Komponentenpaar gleichen Spins beziehen. Der Unterschied in der Wellengleichung für die beiden Spinrichtungen liegt nur in dem verschiedenen Wert von $|K|$. Nachdem die Abhängigkeit von ψ von den Variabeln y and z durch (13) bereits festgelegt wurde, stellt (16) eine Wellengleichung für die Funktion $X(x)$ allein dar. Bisher ist der

Rechnungsgang im wesentlichen identisch mit dem Heisenbergs und Eulers.

Nun behandeln wir vorerst den Fall $V = 0$. Die Eigenwerte und die normierten Eigenfunktionen für (16) lauten

$$(17) \qquad X_n^{(\pm)}(p_x) = a^{(\pm)}(p_x)\frac{1}{\sqrt{2\pi h}} e^{\frac{ip_x x}{h}} \cdot e^{\frac{iW_n^{\pm}(p_x)}{h}t}$$

$$(18) \quad W_n^{\pm}(p_x) = \pm c\sqrt{p_x^2 + |K|^2} = \pm c\sqrt{p_x^2 + m^2c^2 + b\left(n + \frac{1-\sigma_x}{2}\right)}.$$

Der obere Index (+) oder (−) unterscheidet die Zustände positiver und negativer Energie. $a^{\pm}(p)$ ist ein normierter 2-komponentiger »Spinor«. Die Gleichung (16) und ihre Lösungen (17), (18) stellen ein eindimensionales Analogon zu Dirac'gleichung dar, in dem $\gamma|K|\psi$ statt des Massengliedes $\beta mc \cdot \psi$ steht. Zu einem Impuls p_x gehören ein positiver und ein negativer Energiewert. (Die beiden andern Energiewerte liefert die Wellengleichung mit entgegengesetztem Spin).

Setzen wir nun diese Grössen in die Energiedichte (10) ein, so erhalten wir

$$U_{\text{mat}} = \sum_{\sigma=-1}^{+1}\sum_{n=0}^{\infty}\iint \frac{dp_x\,dp_z}{2\pi h} W_n^{-}(p_x)\,|\tilde{H}(\eta)|^2\left(\frac{b}{2h^2}\right)^{\frac{1}{2}}|X_n^{(-)}(p_x)|^2.$$

Die Integration über p_z liefert infolge $dp_z = \sqrt{\frac{b}{2}}\,d\eta$ und $|X_n^{(-)}(p)|^2 = \frac{1}{2\pi h}$

$$(19) \qquad U_{\text{mat}} = \frac{b}{8\pi^2 h^3}\sum_{\sigma=-1}^{+1}\sum_{n=0}^{\infty}\int_{+\infty}^{-\infty} dp\; W_n^{-}(p).$$

Von hier ab schreiben wir p statt p_x.

Um die Summation durchzuführen, bilden wir

$$\sum_{\sigma=-1}^{+1}\sum_{n=0}^{\infty}{}' W_n^- = W_0^- + 2\sum_{n=1}^{\infty}{}' W_n^- .$$

Wir verwenden nun die EULER'sche Summenformel für eine Funktion $F(x)$:

$$\frac{1}{2}F(a) + \sum_{r=1}^{N}{}' F(a+rb) - \frac{1}{2}F(a+Nb) =$$

$$= \frac{1}{b}\left[\int_a^{a+Nb} F(x)\,dx - \sum_{m=1}^{\infty}{}' (-)^m \frac{B_m}{(2m)!} b^{2m} \left\{F^{(2m-1)}(a+Nb) - F^{(2m-1)}(a)\right\}\right]$$

B_m ist die m-te BERNOULLI'sche Zahl. $F^{(m)}(x)$ ist die m-te Ableitung von $F(x)$. Wenn wir dies auf (19) anwenden, erhalten wir:

$$U_{\text{mat}} = \frac{1}{4\pi^2 h^3}\int dp \left[\int_0^{\infty} F(x)\,dx + \sum_{m=1}^{\infty}{}' b^{2m} \frac{B_m}{(2m)!} (-)^m F^{(2m-1)}(0)\right] \tag{20}$$

$$F(x) = -c\sqrt{p^2 + m^2c^2 + x}.$$

In dem Spezialfall eines reinen Magnetfeldes, kann man nach (7 a) U_{mat} und $\tilde{U}'$ gleich setzen. Dieser Ausdruck stellt bereits die Energiedichte dar, in einer Entwicklung nach Potenzen der magnetischen Feldstärke b. Nun ist es sehr leicht, jenen Teil des Beitrages $\tilde{U}'$ der Vakuumelektronen zu bestimmen, der für das wirkliche Vakuum massgebend sein soll: Das von b unabhängige Glied stellt die Energiedichte des feldfreien Vakuums dar und ist ein divergentes Integral; da die Energiedichte für das feldfreie Vakuum verschwinden muss, kann dieser Ausdruck keine reale Bedeutung haben. Weiter müssen die (übrigens auch divergierenden) Glieder mit b^2 weggelassen werden, da die Energiedichte keine

Glieder zweiter Ordnung in den Feldstärken besitzen soll. Das Weglassen dieser Glieder ist durch die Annahme begründet, dass die Polarisierbarkeit des Vakuums mit verschwindenden Feldern gegen Null strebt. Es sei hervorgehoben, dass die hier vorgenommenen Subtraktionen ausschliesslich auf triviale Annahmen über das feldlose Vakuum beruhen.

So erhalten wir für den Zusatz zur MAXWELL'schen Energiedichte:

$$(21)\quad U' = -\frac{c}{4\pi^2 h^3}\sum_{m=2}^{\infty}\frac{B_m(-)^m}{(2m)!}b^{2m}\frac{1.3\ldots(4m-5)}{2^{2m-1}}\int_{-\infty}^{+\infty}\frac{dp}{(p^2+m^2c^2)^{\frac{4m-3}{2}}}.$$

Diese Potenzreihe lässt sich leicht durch die Potenzreihenentwicklung des hyperbolischen Ctg darstellen. Man erhält:

$$U' = \frac{1}{8\pi^2}m^2c^2\left(\frac{mc}{h}\right)^3\int_0^{\infty}\frac{d\eta}{\eta^3}e^{-\eta}\left\{\eta\mathfrak{B}\operatorname{Ctg}\eta\mathfrak{B}-1-\frac{\eta^2}{3}\mathfrak{B}^2\right\}$$

wobei $\mathfrak{B}$ die magnetische Feldstärke gemessen in Einheiten der kritischen Feldstärke $\frac{m^2c^3}{eh}$ ist:

$$\mathfrak{B} = \frac{eh}{m^2c^3}B.$$

Das erste und zweite Glied der Entwicklung liefert:

$$U' - = \frac{1}{360\pi^2}\frac{e^4h}{m^4c^7}B^4 + \frac{1}{630\pi^2}\frac{e^6h^3}{m^8c^{13}}B^6 + \cdots$$

Wenn wir dies mit jenen Gliedern von (4) vergleichen, die das Magnetfeld in 4. und 6. Potenz enthalten, bekommen wir:

$$\alpha = \frac{1}{360\pi^2}\frac{e^4h}{m^4c^7},\quad \beta = \frac{1}{630\pi^2}\frac{e^6h^3}{m^8c^{13}}.$$

Es werde nun das elektrische Feld mitberücksichtigt. Zu diesem Zweck lösen wir die Wellengleichung (16) für $X(x)$ mit der BORN'schen Näherungsmethode. Wir erwarten, dass die vom Potential V abhängigen Teile von U_{mat} in der zweiten, zu V^2 proportionalen Näherung erscheinen. Wenn wir U_{mat} nach Potenzen von V entwickeln: $U_{\text{mat}} = U_{\text{mat}}^{(0)} + U_{\text{mat}}^{(1)} + \cdots$ so erhalten wir nach (10):

$$(22) \quad U_{\text{mat}}^{(2)} = \sum_i W_i^{-(2)} (|\psi_i|^2)^{(0)} + \sum_i W_i^{-(0)} (|\psi_i|^2)^{(2)}.$$

$W_i^{-(k)}, (|\psi_i|^2)^{(k)}$ sind die k-ten Näherungen in der entsprechenden Entwicklung von W_i^- und $|\psi_i|^2$. Man beachte, dass $W_i^{-(1)}$ in dem angegebenen elektrischen Feld verschwindet. Es lässt sich leicht zeigen, dass

$$\int (|\psi|^2)^{(2)} \, dx \, dy \, dz = 0$$

sodass der räumliche Mittelwert von U_{mat} nur durch das erste Glied in (22) gegeben ist:

$$\overline{U_{\text{mat}}^{(2)}} = \sum_i W_i^{-(2)} (|\psi_i|^2)^{(0)}.$$

$(|\psi_i|^2)^{(0)}$ wurde bereits im Falle des reinen Magnetfeldes berechnet und wir erhalten somit ganz analog zu (19)

$$\overline{U_{\text{mat}}^{(2)}} = \frac{b}{8\pi^2 h^3} \sum_{\sigma=-1}^{+1} \sum_{n=0}^{\infty} \int_{-\infty}^{+\infty} dp \, W_n^{-(2)}(p).$$

Der Wert von $W_n^{-(2)}$ lässt sich mit der BORN'schen Näherungsmethode berechnen. Mit den Eigenfunktionen (17) ergibt sich:

$$(23)\quad \begin{cases} W_n^{-(2)}(p) = e^2 |V_0|^2 \left[\dfrac{|\{a^{(+)*}(p+g),\, a^{(-)}(p)\}|^2}{W_n^-(p) - W_n^+(p+g)} + \right. \\ \qquad \left. + \dfrac{|\{a^{(-)*}(p+g),\, a^{(-)}(p)\}|^2}{W_n^-(p) - W_n^-(p+g)} \right] + \\ \qquad + (\text{dasselbe mit } -g). \end{cases}$$

Der zwischen den { }-Klammern stehende Ausdruck stellt ein skalares Produkt zweier zweikomponentiger Spinoren dar. Bei der Integration von (23) über p fallen die zweiten Glieder in den [ ]-Klammern weg, wenn man die Integration der Glieder mit $-g$ mit der Variabeln $p' = p - g$ ausführt:

$$(24)\quad \begin{cases} \int dp\, W_n^{-(2)} = e^2 |V_0|^2 \int dp \dfrac{|\{a^{(+)*}(p+g),\, a^{(-)}(p)\}|^2}{W_n^{(-)}(p) - W_n^{(+)}(p+g)} + \\ \qquad + (\text{dasselbe mit } -g). \end{cases}$$

Dieses Vorgehen ist im allgemeinen keineswegs eindeutig, da die Integration des zweiten Gliedes in den [ ]-Klammern von (23) zu einem divergenten Resultat führt, das aber nach Addition des entsprechenden Gliedes mit $-g$ endlich gemacht werden oder, wie in (24), zum Verschwinden gebracht werden kann, je nachdem in welcher Weise man die Integrationsvariabeln wählt. Diese Willkür berührt aber unsere Rechnung nicht, da wir nach Ausführung der Summation über n nur die zu b^2, b^4, etc. proportionalen Glieder verwenden, in denen auf Grund der Euler'schen Summenformel nur Ableitungen von $W_n^{-(2)}(p)$ nach n auftreten. Wie man sich leicht überzeugen kann, divergieren diese Ableitungen des zweiten Gliedes in den [ ]-Klammern nicht mehr bei der Integration über p, sodass das Resultat dieser Integration unabhängig von der Wahl der Integrationsvariabeln ist.

Es ergibt sich weiter aus (24):

$$\int dp\, W_n^{(2)} = -e^2 |V_0|^2 \frac{g^2}{4} \int dp \frac{|K|^2}{c(p^2+|K|^2)^{\frac{5}{2}}}$$

wobei bereits eine Reihenentwicklung nach Potenzen von g durchgeführt wurde und die Glieder höherer als zweiter Ordnung weggelassen wurden. Dies bedeutet die Vernachlässigung der Ableitungen der Feldstärke auf Grund der Bedingungen (1). Ebenso, wie in der vorigen Rechnung, ist nun $\overline{U_{\text{mat}}^{(2)}}$ durch (20) gegeben, wenn man setzt:

$$F(x) = -e^2 |V_0|^2 \frac{g^2}{4} \frac{m^2c^2+x}{c(p^2+m^2c^2+x)^{\frac{5}{2}}}.$$

Man erhält dann, wenn man zuerst über p integriert:

$$\overline{U_{\text{mat}}^{(2)}} = -\frac{1}{4\pi h^3 c} \frac{g^2}{3} e^2 |V_0|^2 \left[\int_0^\infty \frac{dx}{m^2c^2+x} + \right.$$

$$\left. + \sum_{m=1}^{\infty} b^{2m} \frac{B_m (-)^m}{(2m)!} \left(\frac{d^{2m-1}}{dx^{2m-1}} \frac{1}{m^2c^2+x} \right)_{x=0} \right].$$

Da dieser Ausdruck quadratisch in den elektrischen Feldstärken ist, erhalten wir für die kinetische Energiedichte nach (7a)

$$\overline{\tilde{U}'^{(2)}} = -\overline{U_{\text{mat}}^{(2)}}.$$

Aus den früher diskutierten Gründen können erst die Glieder 4. und höherer Ordnung in den Feldstärken für das Vakuum von physikalischer Bedeutung sein, sodass das divergierende Integral wegzulassen ist. Wir ersetzen nun V_0 durch die elektrische Feldstärke E:

$$\overline{E^2} = 2\frac{g^2}{h^2} |V_0|^2$$

wobei die Querstriche Raummittelungen bedeuten und erhalten für die ersten beiden Glieder:

$$(25)\quad U'^{(2)} = \frac{5}{360\pi^2}\frac{e^4 h}{m^4 c^7} E^2 B^2 - \frac{7}{2}\frac{1}{630\pi^2}\frac{e^6 h^3}{m^8 c^{13}} E^2 B^4 + \cdots$$

für den Grenzfall schwach veränderlichen Felder bei welchem die Raummittelungen weggelassen werden können.

Vergleicht man (25) mit den zu $E^2 B^2$ und $E^2 B^4$ proportionalen Gliedern in (4) so erhält man die Beziehungen

$$\beta - 2\alpha = \frac{5}{360}\frac{e^4 h}{m^4 c^7}, \quad 3\xi - \zeta = \frac{7}{2}\frac{1}{630\pi^2}\frac{e^6 h^3}{m^8 c^{13}},$$

und mit den bereits berechneten Werten von α und β

$$\beta = 7\alpha, \quad \zeta = \frac{13}{2}\xi.$$

Der in der magnetischen Feldstärke exakte Ausdruck für $U'^{(2)}$ ergibt sich zu

$$U'^{(2)} = \frac{1}{8\pi^2} mc^2 \left(\frac{mc}{h}\right)^3 \frac{1}{3} \mathfrak{E}^2 \int_0^\infty \frac{d\eta}{\eta^3} e^{-\eta} \{\eta \mathfrak{B} \operatorname{Ctg} \mathfrak{B} - 1\},$$

wobei $\mathfrak{E} = \dfrac{m^2 c^3}{eh} E$ ist.

Die höheren Näherungen in E lassen sich leicht bis auf einen konstanten Faktor bestimmen. Denken wir die k-te Näherung $W_n^{-(k)}(p)$ der Energie des durch p und n gegebenen Zustandes bestimmt; sie wird auf Grund der Wellengleichung (16) die folgende Gestalt haben:

$$W_n^{-(k)}(p) = g^k e^k |V_0|^k \cdot G(c, h, |K|, p)$$

wobei G eine Funktion ist, in welcher nur die angegebenen Grössen vorkommen. $W^{(k)}$ muss infolge der Eichinvarianz min-

destens k-ter Ordnung in g sein. Die höheren Potenzen von g sind vernachlässigt. Die Energiedichte in k-ter Ordnung wird dann:

$$U_{\text{mat}}^{(k)} = \frac{1}{8\pi h^3 c} g^k e^k |V_0|^k \left[\int_0^\infty dx \int_{-\infty}^{+\infty} G dp + \right.$$
$$\left. + \sum_{m=1}^{\infty} b^{2m} \frac{B_m}{(2m)!} (-)^m \left(\frac{d^{2m-1}}{dx^{2m-1}} \int_{-\infty}^{+\infty} G dp \right)_{x=0} \right]. \tag{26}$$

Das Integral über G muss die Dimension (Energie)$^{-(k-1)}$ (Impuls)$^{-(k-1)}$ haben, und darf nur mehr von den Grössen $c, h, |K|$ abhängen, was nur in der Form möglich ist:

$$\int_{-\infty}^{+\infty} G dp = f_k \frac{1}{c^{k-1} |K|^{2k-2}} = f_k \frac{1}{c^{k-1} (m^2 c^2 + x)^{k-1}}$$

wobei f_k ein Zahlenfaktor ist.

Wenn man dieses in (26) einsetzt, so lässt sich $U_{\text{mat}}^{(k)}$ bis auf den Faktor f_k vollständig angeben.

Die Zahlenfaktoren f_k bestimmen sich aber leicht durch die Überlegung, dass U_{mat} nach (8) eine relalivistische Invariante sein muss. Da deswegen U_{mat} nur von $E^2 - B^2$ und $(EB)^2$ abhängen darf, muss z. B. der Koeffizient von E^k sich von dem Koeffizient von B^k nur durch den Faktor $(-)^{\frac{k}{2}}$ unterscheiden. Der letztere Koeffizient wurde bereits berechnet und ist durch (21) gegeben. Man erhält dann

$$f_{2m} = \binom{2m}{m} \frac{2^{m-1} B^m}{m(2m-1)}$$

und kann damit die Darstellung berechnen, die Heisenberg u. Euler für L' angegeben haben[1]:

[1] In der Frage der Konvergenz dieses Integrals verweisen wir auf die diesbezüglichen Bemerkungen in der Arbeit von Heisenberg u. Euler S. 729.

$$L' = -\frac{i}{8\pi^2} mc^2 \left(\frac{mc}{h}\right)^3 \int_0^\infty \frac{d\eta}{\eta^3} e^{-\eta} \left\{ \eta \mathfrak{B} \operatorname{Ctg} \mathfrak{B} \cdot \eta \mathfrak{E} \operatorname{ctg} \mathfrak{E} - 1 + \frac{\eta^2}{3} (\mathfrak{E}^2 - \mathfrak{B}^2) \right\}$$

$$\mathfrak{E} = \frac{m^2 c^3}{eh} E, \quad \mathfrak{B} = \frac{m^2 c^3}{eh} B.$$

Dieser Ausdruck ist für parallele Felder berechnet. Um ihn auf beliebige Felder zu verallgemeinern, muss man ihn als Funktion der beiden Invarianten $E^2 - B^2$ und $(EB)^2$ schreiben. Dies ist nach Heisenberg und Euler in einfacher Weise mit der Beziehung

$$\operatorname{Ctg} \alpha \operatorname{ctg} \beta = -i \frac{\cos \sqrt{\beta^2 - \alpha^2 + 2i\alpha\beta} + \text{conj}}{\cos \sqrt{\beta^2 - \alpha^2 + 2i\alpha\beta} - \text{conj}}$$

möglich und man erhält

$$L' = \frac{1}{8\pi^2} \frac{e^2}{hc} \int_0^\infty e^{-\eta} \frac{d\eta}{\eta^3} \left\{ i\eta (EB) \frac{\cos \eta \sqrt{\mathfrak{E}^2 - \mathfrak{B}^2 + 2i(\mathfrak{E}\mathfrak{B})} + \text{conj}}{\cos \eta \sqrt{\mathfrak{E}^2 - \mathfrak{B}^2 + 2i(\mathfrak{E}\mathfrak{B})} - \text{conj}} + \right.$$
$$\left. + \frac{m^4 c^6}{e^2 h^2} + \frac{\eta^2}{3} (B^2 - E^2) \right\}.$$

Wegen der Realität des Gesamtausdrucks ist dieser tatsächlich nur von $E^2 - B^2$ und $(EB)^2$ abhängig.

Die Berechnung der Energiedichte und Lagrangefunktion des Vakuums ist in der skalaren Theorie des Positrons mit den gleichen mathematischen Hilfsmitteln durchzuführen. Eine Energiedichte des Vakuums entsteht in dieser Theorie durch die Nullpunktsenergie der Materiewellen. Die Gesamtenergie ist nach Pauli und Weisskopf l. c. (Formel (29)) durch

$$E_{\text{mat}} = \sum_k W_k (N_k^+ + N_k^- + 1)$$

gegeben, wobei W_k die Energie des k-ten Zustandes ist und N_k^+ die Anzahl der Positronen, N_k^- die Anzahl der Elektronen ist, die diesem Zustand angehören. Im leeren Vakuum bleibt die Summe über alle Energien W_k übrig, wobei die Energie W_k des durch den Impuls p und der Quantenzahl n charakterisierten Zustandes in einem Magnetfeld B den Wert hat:

$$W_n^{\text{skal}}(p, B) = c \sqrt{p^2 + m^2 c^2 + b\left(n + \frac{1}{2}\right)}.$$

Die Summation über alle Zustände und Division durch das Gesamtvolumen führt zur Energiedichte, die sich leicht analog zu (19) ergibt:

$$U_{\text{mat}} = \frac{b}{8\pi^2 h^3} \sum_{n=0}^{\infty} \int_{-\infty}^{+\infty} dp \; W_n^{\text{skal}}(p, B).$$

Der einzige Unterschied gegen die frühere Rechnung besteht in dem Wegfallen der Summierung über die beiden Spinrichtungen. Nun verifiziert man leicht die folgende Beziehung zwischen der Energie $W_n^{\text{skal}}(p,B)$ in der skalaren und der Energie $W_n^-(p, B)$ in der DIRAC'schen Elektronentheorie:

$$2\sum_{n=0}^{N} W_n^{\text{skal}}(p, B) = \sum_{\sigma=-1}^{+1} \sum_{n=0}^{N} W_n^-(p, B) - \sum_{\sigma=-1}^{+1} \sum_{n=0}^{2N} W_n^-(p, B/2).$$

Wir können daher die Energiedichte in der skalaren Theorie $\tilde{U}'_{\text{skal}}$ durch die Energiedichte $\tilde{U}'$ der DIRAC'schen Positronentheorie in folgender Weise ausdrücken:

$$2\tilde{U}'_{\text{skal}}(B) = \tilde{U}'(B) - \tilde{U}'(B/2).$$

Man sieht daran, dass auch hier der von den Feldstärken unabhängige und der in ihnen quadratische Anteil unendlich ist. Der letztere liefert also eine unendliche von den Feld-

stärken unabhängige Polarisierbarkeit. Um für das feldlose Vakuum ein brauchbares Resultat zu erhalten, muss man wieder diese beiden Anteile streichen und erhält infolge der Beziehung

$$\operatorname{Ctg}\beta - \operatorname{Ctg}\frac{\beta}{2} = -\frac{1}{\operatorname{Sin}\beta};$$

$$U'_{\text{skal}} = -\frac{1}{16\pi^2} mc^2 \left(\frac{mc}{h}\right)^3 \int_{(0)}^{\infty} \frac{d\eta}{\eta^3} e^{-\eta} \left\{ \eta \mathfrak{B} \frac{1}{\operatorname{Sin}\eta\mathfrak{B}} - 1 + \frac{\eta^2}{6}\mathfrak{B}^2 \right\}.$$

Die Durchführung einer analogen Störungsrechnung im elektrischen Feld führt in gleicher Weise zu einem Zusatz zur Lagrangefunktion des Feldes, der mit dem aus der Dirac'schen Positronentheorie gewonnenen sehr verwandt ist:

$$L'_{\text{skal}} = -\frac{1}{16\pi^2}\frac{e^2}{hc}\int_0^{\infty} \frac{d\eta}{\eta^3} e^{-\eta} \left\{ \frac{2i\eta\,(EB)}{\cos\eta\sqrt{(\mathfrak{E}^2-\mathfrak{B}^2)+2i(\mathfrak{E}\mathfrak{B})}} - \text{conj} + \right.$$
$$\left. + \frac{m^4c^6}{e^2h^2} - \frac{\eta^2}{6}(B^2-E^2) \right\}.$$

Für die in (4) definierten Koeffizienten α, β erhält man daher:

$$\alpha = \frac{7}{16}\,\frac{1}{360\pi^2}\,\frac{e^4h}{m^4c^7}, \quad \beta = \frac{24}{7}\alpha.$$

Es sei hier noch auf folgende Eigenschaft der Lagrangefunktion des Vakuums hingewiesen. Für sehr grosse Feldstärken E oder B haben die höchsten Glieder des Zusatzes L' zur Maxwell'schen Lagrangefunktion in der Dirac'schen Theorie des Positrons die Form

$$L' \sim -\frac{e^2}{24\pi^2 hc} E^2 \lg \mathfrak{E} \quad \text{bzw.} \quad L' \sim \frac{e^2}{24\pi^2 hc} B^2 \lg \mathfrak{B}.$$

Das Verhältnis zwischen diesem Zusatz L' und der Maxwell'schen Lagrangefunktion $L_0 = \frac{1}{8\pi}(E^2 - B^2)$ ist somit

logarithmisch in den Feldstärken für hohe Werte derselben und ist ausserdem mit dem Faktor $\frac{e^2}{hc}$ multipliziert:

$$\frac{L'}{L_0} \sim \frac{e^2}{3\pi hc} \lg \mathfrak{E} \quad \text{bzw.} \frac{L'}{L_0} \sim \frac{e^2}{3\pi hc} \lg \mathfrak{B}.$$

Die Nichtlinearitäten der Feldgleichungen stellen somit auch bei Feldstärken, die wesentlich höher als die kritische Feldstärke $\frac{m^2 c^3}{eh}$ sind, nur kleine Korrektionen dar. Die in der Note von EULER und KOCKEL l. c. und in der Arbeit von EULER l. c. zitierte Verwandschaft der aus der Positronentheorie folgenden Nichtlinearität der Feldgleichungen mit der nichtlinearen Feldtheorie von BORN und INFELD[1] ist daher nur äusserlich. In der letzteren Theorie sind die MAXWELL'schen Gleichungen bei der kritischen Feldstärke $F_0 = \frac{m^2 c^4}{e^3}$ »am Rande des Elektrons« bereits vollkommen abgeändert, wodurch dann die endliche Selbstenergie einer Punktladung erreicht wird. Hier hingegen sind die Abweichungen von den MAXWELL'schen Feldgleichungen für Felder der Grösse F_0 noch sehr klein und wachsen viel zu langsam an, um eine ähnliche Rolle in den Selbstenergieproblem zu spielen. Die Extrapolation der vorliegenden Rechnungen auf die Felder am »Rande des Elektrons« ist allerdings nicht einwandfrei, da dort die Bedingungen (1) nicht erfüllt sind. Es ist jedoch nicht wahrscheinlich, dass eine exaktere Betrachtung in dieser Hinsicht ein wesentlich verschiedenes Resultat liefert.

III.

In diesem Abschnitt soll der Einfluss beliebiger Felder auf das Vakuum behandelt werden. Wir beschränken uns vorerst auf statische Felder. Die stationären Zustände des

[1] M. BORN u. L. INFELD, Proc. Roy. Soc. **143**, 410, 1933.

Elektrons auf Grund der Dirac'schen Wellengleichung und ihre Energieeigenwerte werden sich im allgemeinen in zwei Gruppen einteilen lassen, die bei einer adiabatischen Einschaltung des statischen Feldes aus den positiven bzw. aus den negativen Energieniveaus des freien Elektrons entstanden sind. Dies trifft z. B. im Coulombfeld eines Atomkernes zu und bei allen in der Natur vorkommenden statischen Feldern.

Es sind jedoch auch solche statische Felder angebbar, in denen eine derartige Einteilung versagt, da infolge der Felder Übergänge von negativen zu positiven Zuständen vorkommen. Ein bekanntes Beispiel hierfür ist eine Potentialstufe der Höhe $> 2mc^2$. Diese Ausnahmsfälle sind stationär nicht behandelbar und müssen als ein zeitabhängiges Feld betrachtet werden, das zu einer gegebenen Zeit eingeschaltet wird. Dies ist umsomehr schon deswegen notwendig, da derartige Felder infolge der fortwährende Paarentstehung gar nicht stationär aufrechterhalten werden könnten.

Im Falle dass aber das Eigenwertspektrum sich eindeutig in die beiden Gruppen einteilen lässt, kann man die Energiedichte U und die Strom-Ladungsdichte $\vec{\imath}$, ϱ der Vakuumelektronen nach den Formeln

$$(29)\quad \begin{cases} U = ih \sum_i \left\{ \psi_i^*, \ \frac{\partial}{\partial t} \psi_i \right\} \\ \varrho = e \sum_i \{ \psi_i^*, \ \psi_i \} \\ \vec{\imath} = e \sum_i \{ \psi_i^*, \ \vec{\alpha} \psi_i \} \end{cases}$$

berechnen, wobei über die Zustände zu summieren ist, die den negativen Energiezuständen des freien Elektrons entsprechen. Die angeschriebenen Summen werden divergieren.

Wenn aber die physikalisch bedeutungslosen Teile abgetrennt werden, erhalten wir konvergente Ausdrücke.

Um diese Teile auf Grund der Annahmen (I) festzulegen, entwickeln wir die Summanden der Ausdrücke (29) nach Potenzen der äusseren Feldstärken in der Weise, dass wir uns die letzteren mit einem Faktor λ multipliziert denken und nach Potenzen dieses Faktors entwickeln. Dieses Verfahren ist identisch mit einer successiven Störungsrechnung, die von den freien Elektronen als nullte Näherung ausgeht.

Die Annahmen I_1, I_2 verlangen vor allem das Verschwinden der von λ unabhängigen Glieder, die aus den Beiträgen der vom Felde unabhängigen freien Vakuumelektronen bestehen. Wenn wir vorläufig nur jene freien Vakuumelektronen berücksichtigen, deren Impuls $|p| < P$ ist, so erhalten wir hierfür folgende Beiträge:[1]

$$(30)\quad \begin{cases} U_0 = -\dfrac{1}{4\pi^3 h^3}\displaystyle\int_{|p|<P} d\vec{p}\,\sqrt{p^2+m^2c^2}\,, \\ \varrho_0 = \dfrac{e}{4\pi^3 h^3}\displaystyle\int_{|p|<P} d\vec{p}\,, \\ \vec{i}_0 = \dfrac{e}{4\pi^3 h^3}\displaystyle\int_{|p|<P} d\vec{p}\,\dfrac{c\vec{p}}{\sqrt{p^2+m^2c^2}}\,. \end{cases}$$

Die Beiträge sämtlicher Elektronen — $P \to \infty$ — divergieren natürlich.

Durch das Abtrennen der von λ unabhängigen Glieder ist aber die Annahme I_2 noch nicht vollständig erfüllt. Die Ladungs- und Stromdichte ϱ_0, $\vec{i}_0$ der feldfreien Vakuum-

[1] Es ist nämlich der zum Impuls $\vec{p}$ gehörige Strom: $\dfrac{ec\vec{p}}{\sqrt{p^2+m^2c^2}}$ und die Anzahl der Zustände in Intervall $d\vec{p}$: $\dfrac{d\vec{p}}{4\pi^3 h^3}$.

elektronen äussert sich nämlich auch dadurch, dass sie bei Anwesenheit von Potentialen V, $\vec{A}$ einen Zusatz $\varrho_0 V$ und $(\vec{i}_0 \vec{A})$ zur Energiedichte liefert, der ebenfalls abgetrennt werden muss. Diese Zusätze treten auf, da auch die Energie und der Impuls der von den Feldern noch unbeeinflussten Vakuumelektronen bei Anwesenheit von Potentialen um den Betrag eV bzw. $\frac{e}{c}\vec{A}$ geändert wird.

Die Annahmen I_1 und I_2 sind daher erst vollkommen erfüllt, wenn man die wegzulassende Beiträge (30) folgendermassen modifiziert:

$$(31)\quad \begin{cases} U_0' = -\dfrac{1}{4\pi^3 h^3}\displaystyle\int_{|p|<P} d\vec{p}\left[\sqrt{\left(p+\frac{e}{c}A\right)^2 + m^2c^2} + eV\right] \\ \varrho_0' = \dfrac{e}{4\pi^3 h^3}\displaystyle\int_{|p|<P} d\vec{p} \\ \vec{i}_0' = \dfrac{e}{4\pi^3 h^2}\displaystyle\int_{|p|<P} d\vec{p}\,\dfrac{c\left(\vec{p}+\frac{e}{c}\vec{A}\right)}{\sqrt{\left(p+\frac{e}{c}A\right)^2 + m^2c^2}}, \end{cases}$$

wobei auch wieder nur der von freien Vakuumelektronen mit Impulsen $|p| < P$ herrührenden Teil angeschrieben ist. Nun ist noch die Bedingung I_3 zu erfüllen. Hierzu beachten wir, dass eine konstante feldunabhängige Polarisierbarkeit zu Gliedern in Energiedichte $U(x)$ führt, die proportional zu den Quadrat $E^2(x)$ und $B^2(x)$ der Feldstärken an der Stelle x sind. Ebenso führt sie zu einer Strom- und Ladungsdichte, die zu den ersten Ableitungen der Felder proportional ist, auf Grund der Beziehungen

$$i = \operatorname{rot} M + \frac{dP}{dt}$$
$$\varrho = \operatorname{div} P$$

worin M und P die magnetischen und elektrischen Polarisationen sind, die im Falle einer konstanten Polarisierbarkeit zu den Feldern proportional sind. Um die Annahme I_3 zu erfüllen, müssen daher in der Energiedichte U der Vakuumelektronen die zu E^2 und zu B^2 proportionalen Glieder verschwinden und in der Strom-Ladungsdichte die zu den ersten Ableitungen proportionalen Glieder weggelassen werden. Es ist praktischer, die Form dieser Glieder nicht explizit anzugeben, sondern dieselben im Laufe der Rechnung an ihren Eigenschaften zu erkennen.

Als Erläuterung berechnen wir die Ladungs- und Stromdichte des Vakuums unter dem Einfluss eines elektrischen Potentials

$$V = V_0 e^{\frac{i(\vec{g}\vec{r})}{h}} + V_0^* e^{-\frac{i(\vec{g}\vec{r})}{h}} \tag{32}$$

und eines magnetischen Potentials

$$\vec{A} = \vec{A}_0 e^{\frac{i(\vec{g}\vec{r})}{h}} + \vec{A}_0^* e^{-\frac{i(\vec{g}\vec{r})}{h}}, \quad (\vec{A}_0, \vec{g}) = 0 \tag{33}$$

mit Hilfe der Störungstheorie. Diese Berechnungen sind bereits von HEISENBERG[1] und noch viel allgemeiner von SERBER[2] und PAULI u. ROSE[3] durchgeführt worden und sollen hier nur als Illustration zu unserer physikalischen Interpretation der Substraktionsterme dienen. Die Ladungsdichte ϱ ist bis zur ersten Ordnung gegeben durch $\varrho = \varrho^{(0)} + \varrho^{(1)}$,

$$\varrho^{(1)} = e \sum_i {\sum_k}' \frac{H_{ik}\{\psi_i^*, \psi_k\}}{W_i - W_k} + \text{conj}$$

[1] HEISENBERG, Z. f. Phys. **90**, 209, 1934.
[2] R. SERBER, Phys. Rev. **48**, 49, 1935.
[3] W. PAULI u. M. ROSE, Phys. Rev. **49**, 462, 1936.

wobei die i über die besetzten, die k über die unbesetzten Zustände zu summieren sind, und H_{ik} das Matrixelement der Störungsenergie ist. Setzen wir das Potential (32) als Störung ein, so erhalten wir $(W(p) = c\sqrt{p^2 + m^2 c^2})$

$$\varrho^{(1)} = \frac{e^2 V_0}{8\pi^3 h^3} \cdot \int d\vec{p} \left\{ \frac{W(p)\, W(p+g) - c^2 (p, p+g) - m^2 c^4}{W(p)\, W(p+g) \left[W(p) + W(p+g) \right]} + \right.$$
$$\left. + \begin{pmatrix} \text{dasselbe} \\ \text{mit } -g \end{pmatrix} \right\} e^{\frac{i(\vec{g}\vec{r})}{h}} + \text{conj}.$$

Entwickelt man dies nach Potenzen von $\vec{g}$ so erhält man

$$\varrho^{(1)} = \frac{e^2 V_0}{8\pi^3 h^3} \int d\vec{p}\, \frac{c^2}{W^3(p)}\, e^{\frac{i(\vec{g}\vec{r})}{h}}$$
$$\left\{ \frac{g^2}{2} - \frac{c^2 (pg)^2}{W^2(p)} - \frac{c^2 g^4}{4 W^2(p)} + \frac{11}{8} \frac{c^4 (pg)^2 g^2}{W^4(p)} - \frac{21}{16} \frac{c^6 (pg)^4}{W^6(p)} + \cdots \right\} + \text{conj}.$$

Welcher Teil dieser Ladungsdichte hat nun physikalische Bedeutung? Wegen der Annahme I_2 muss ϱ_0 wegfallen; in $\varrho^{(1)}$ sind die Glieder mit g^2 proportional zur zweiten Ableitung von V und somit zur ersten Ableitung der Feldstärken und müssen wegen I_3 weggelassen werden. Man bemerke, dass auch nur diese Glieder zu Divergenzen führen. Der Rest liefert endliche Integrale und ist nach Heisenberg in der Form

$$(34)\quad \varrho^{(1)} = \frac{1}{240\pi^2} \frac{e^2}{hc} \left(\frac{h}{mc} \right) \triangle \triangle V + \text{höhere Ableitungen von V}$$

zu schreiben. Die exakte Ausrechnung der ersten Näherung wurde von Serber und Pauli u. Rose l. c. geliefert.

Als weiteres Beispiel betrachten wir die Stromdichte $\vec{i}$ in der ersten Näherung des Feldes (33)

$$\vec{i}^{(1)} = e \sum_{ik}' \frac{H_{ik} \{\psi_i^*, \vec{\alpha} \psi_k\}}{W_i - W_k} + \text{conj}$$

Es ergibt sich

$$\vec{i}^{(1)} = -e^2 \frac{\vec{A}_0}{8\pi^3 h^3} \int d\vec{p}\, e^{\frac{i(\vec{gr})}{h}} \left\{ \frac{W(p)\,W(p+g)+E^2(p)+c^2(pg)-2c^2(n,p+g)(n,p)}{W(p+g)\,W(p)\,[W(p+g)+W(p)]} + \right.$$
$$\left. + \begin{pmatrix}\text{dasselbe}\\ \text{mit } -g\end{pmatrix} \right\} + \text{conj}$$

wobei n der Einheitsvektor in der Richtung $\vec{A}$ ist. Dieses ergibt nach g entwickelt:

$$(35)\quad \left\{ \begin{aligned} \vec{i}^{(1)} &= -\frac{e^2\vec{A}}{4\pi^3 h^3} \int d\vec{p}\, \frac{1}{W^3(p)}\, e^{\frac{i(\vec{gr})}{h}} \\ &\left\{ W^2(p) - c^2(np)^2 - \frac{c^2 g^2}{2} + \frac{3}{4}\frac{c^4(pg)^2}{W^2(p)} - \frac{5}{2}\frac{c^6(np)^2(pg)^2}{W^4(p)} + \right. \\ &\left. + \frac{3}{4}\frac{c^4(np)^2 g^2}{W^2(p)} + \text{Glieder 4. u. höherer Ordnung in } g \right\}. \end{aligned} \right.$$

Hier treten auch von g unabhängige, also nicht eichinvariante Glieder auf. Diese sind aber mit den wegzulassenden Beiträgen $\vec{i}_0'$ aus (31) identisch: Entwickelt man nämlich $\vec{i}_0'$ nach $\vec{A}$, so erhält man:

$$\vec{i}_0' = \frac{e}{4\pi^3 h^3} \int d\vec{p} \left\{ \frac{cp}{W(p)} + \frac{e\vec{A}}{W(p)} - \frac{c^2 p\,(e\vec{A}, \vec{p})}{W^3(p)} + \cdots \right\}$$
$$= \vec{i}_0 + e^2 \frac{\vec{A}}{4\pi^3 h^3} \int d\vec{p}\, \frac{1}{W^3(p)} \{ W^2(p) - c^2(np)^2 + \cdots \}.$$

Die Glieder erster Ordnung in $\vec{A}$ stimmen mit den von g unabhängigen Gliedern in (35) überein. Die zu g^2 proportionalen Glieder von (35) werden ebenfalls weggelassen, der Rest ergibt das zu (34) entsprechende konvergierende Resultat:

$$\vec{i}^{(1)} = \frac{1}{240\pi^2}\frac{e^2}{hc}\left(\frac{h}{mc}\right)\triangle\triangle\vec{A} + \text{höhere Ableitungen.}$$

Die beiden Beispiele sollen zeigen, dass bei einer Störungsrechnung die wegzulassenden Beiträge unmittelbar erkenntlich sind und dass die übrigen durch die Annahmen (I) nicht berührten Beiträge der Vakuumelektronen bei der Summierung zu keinen Divergenzen mehr führen. Die angeführten Beispiele beweisen dies zwar nur in erster Näherung. Die Überlegungen lassen sich aber ohne weiteres auf höhere Näherungen ausdehnen.

Die Behandlung zeitabhängiger Felder ist im wesentlichen nicht von dem obigen Verfahren verschieden. Es ist notwendig, die zeitabhängigen Felder von einem Zeitpunkt t_0 an wirken zu lassen, an welchem die Vakuumelektronen in feldfreien Zuständen waren, oder in solchen stationären Zuständen, die sich einwandfrei in besetzte und unbesetzte einteilen lassen. Die zeitliche Veränderung dieser Zustände von diesem Zeitpunkt t_0, an lässt sich dann mit Hilfe einer Störungsrechnung in Potenzen der äusseren Felder darstellen. Die Ausdrücke (31) und die aus der Bedingung (I_3) folgenden Glieder können dann abgetrennt werden, wobei der übrigbleibende Rest nicht mehr zu Divergenzen führt. Die Berechnung der Ladungs- und Stromdichte des Vakuums bei beliebigen zeithängigen Feldern in erster Näherung findet sich bei SERBER l. c. und bei PAULI u. ROSE l. c. Die abzuziehenden Teile werden dort aus der HEISENBERG'schen Arbeit formal entnommen. Sie sind aber mit jenen, die aus den Annahmen I folgen, vollkommen identisch.

Wie äussert sich nun die Entstehung von Paaren durch zeitabhängige Felder? Die Paare kommen bei der Berechnung der Energie-, Strom- und Ladungsdichte nicht unmittelbar zum Ausdruck. Die Paarerzeugung zeigt sich nur in einer

proportional zur Zeit wachsenden Gesamtenergie, die der Energie der entstehenden Elektronen entspricht. Die Ladungs- und Stromdichte ist nicht unmittelbar von der Paarentstehung beeinflusst, da stets positive und negative Elektronen zugleich erzeugt werden, die die Strom-Ladungsdichte erst dadurch beeinflussen, dass die äusseren Felder auf die entstandenen Elektronen je nach der Ladung verschieden einwirken.[1]

Es ist daher praktischer, die Paarentstehung durch äussere Felder direkt zu berechnen als Übergang eines Vakuumelektrons in einen Zustand positiver Energie. Die Entstehungswahrscheinlichkeit des Elektronenpaares ist dann identisch mit der Zunahme der Intensität der betreffenden Eigenfunktion positiver Energie bzw. mit der Abnahme der Intensität der entsprechenden Eigenfunktion negativer Energie infolge des Einwirkens der zeitabhängigen Felder auf die Zustände, die bis zur Zeit t_0 geherrscht haben. Die Berechnung wurde von Bethe u. Heitler[2], Hulme u. Jaeger[3] u. s. w. ausgeführt.

Die Paarvernichtung unter Lichtausstrahlung lässt sich wie jeder anderer spontane Ausstrahlungsprozess nur durch Quantelung der Wellenfelder behandeln, oder durch korrespondenzmässige Umkehrung des Lichtabsorptionsprozesses.

In der bisherigen Darstellung wurden die abzutrennenden Teile der Vakuumelektronen nicht explizit angegeben, sondern nur ihre Form und ihre Abhängigkeit von

[1] Die von Serber berechnete Strom- und Ladungsdichte bei paarerzeugenden Feldern ist daher dem Mitschwingen der Vakuumelektronen zuzuschreiben und ist nicht etwa die »erzeugte Strom-Ladungsdichte«. Die auftretenden Resonanznenner rühren daher, dass dieses Mitschwingen besonders stark ist, wenn die äussere Frequenz sich einer Absorptionsfrequenz des Vakuums nähert.

[2] H. Bethe u. W. Heitler, Proc. Roy. Soc. **146**, 84, 1934.

[3] H. R. Hulme u. J. C. Jaeger, Proc. Roy. Soc.

den äusseren Feldern bestimmt. Um sie explizit darzustellen muss man ein etwas anderes Verfahren wählen, da diese Teile ja divergente Ausdrücke enthalten. Hierzu eignet sich die von Dirac eingeführte Dichtematrix, die dann von Dirac und spezieller von Heisenberg l. c. auf dieses Problem angewendet wurde. Die Dichtematrix R ist durch folgenden Ausdruck gegeben:

$$(x', k' \,|\, R \,|\, x'' k'') = \sum_i \psi_i^* (x', k') \, \psi_i (x'' k'')$$

wobei x' und x'' zwei Raum-Zeitpunkte, k' und k'' zwei Spinindizes bedeuten. Die Summe soll über alle besetzten Zustände erstreckt werden. Aus dieser Matrix kann man dann leicht die Strom- und Ladungsdichte $\vec{i}$, ϱ und der Energie-Impuls-Tensor[1] U_ν^μ bilden auf Grund den Beziehungen

$$\vec{i} = \lim_{x' = x''} e \sum_{k' k''} (\vec{\alpha})_{k' k''} (x' k' \,|\, R \,|\, x'' k'')$$

$$\varrho = \lim_{x' = x''} e \sum_{k'} (x' k' \,|\, R \,|\, x'' k'')$$

$$U_\nu^\mu = \lim_{x' = x''} \frac{1}{2} \left\{ ich \left[\frac{\partial}{\partial x'_\mu} - \frac{\partial}{\partial x''_\mu} \right] - e \left[A^\mu (x') + A^\mu (x'') \right] \right\}$$
$$\sum_{k' k''} (\alpha^\nu)_{k' k''} (x' k' \,|\, R \,|\, x'' k''). \qquad \alpha^4 = \text{Einheitsmatrix}$$

Die Dichte-Matrix hat den Vorteil, dass für $x' \neq x''$ die Summation über die Vakuumelektronen nicht divergieren, sondern einen Ausdruck ergeben der für $x' = x''$ singulär wird.

Man kann nun aus den Annahmen (I) eindeutig angeben, welche Teile der Dichtematrix der Vakuumelektronen für

[1] Der vollständige Energie-Impuls-Tensor besteht aus der Summe von U_ν^μ und dem Maxwell'schen Energie-Impuls-Tensor des Feldes. Die U_4^4-komponente ist daher nicht die gesamte materielle Energiedichte, sondern nur die kinetische.

$x' = x''$ in die wegzulassenden Teile übergehen und gewinnt auf diese Weise eine explizite Darstellung dieser Glieder.

Der physikalisch bedeutungslose Teil der Dichtematrix muss dann aus jenen Gliedern bestehen, die von den Feldstärken unabhängig sind, aus denen, die zu Gliedern in der Stromdichte führen, die zu den Ableitungen der Felder proportional sind und aus denen die zu Gliedern in der Energiedichte führen, die proportional zum Quadrat der Feldstärke sind. Ausserdem muss der abzuziehende Teil der Dichtematrix noch mit dem Faktor

$$u' = \exp\left[\frac{ie}{hc}\int_{x'}^{x''}\left(\sum_{i=1}^{3} A_i dx_i - V dt\right)\right]$$

multipliziert werden, wobei das Integral im Exponenten in gerader Linie vom Punkte x' zu dem Punkt x'' zu erstrecken ist. Dieser Faktor fügt zum abzuziehenden Energie-Impuls-Tensor gerade die Beitrage hinzu, die davon herrühren, dass die noch ungestörten Vakuumelektronen im Feld eine Zusatzenergie eV und einen Zusatzimpuls $\frac{e}{c}\vec{A}$ erhalten, und die infolge der Annahme I_2 mit abgezogen werden sollen.

Da der abzuziehende Teil der Dichtematrix bis auf den Faktor u' höchstens zweiter Ordnung in den Feldstärken ist, lässt er sich durch eine Störungsrechnung aus der Dichtematrix der freien Elektronen gewinnen. Diese im Prinzip einfache, in der Ausführung jedoch sehr komplizierte Rechnung liegt der Bestimmung dieser Matrix von Heisenbreg l. c. zu Grunde. Das Ergebnis lässt sich mathematisch einfacher formulieren, wenn man bei jeder Grösse stets das Mittel bildet aus der Berechnung mit Hilfe der vorliegenden Theorie und aus der Berechnung mit Hilfe einer Theorie in der die Elektronenladung positiv ist, und das negative

Elektron als »Loch« dargestellt wird. Das Resultat ist ja in beiden Fällen dasselbe. Die Dichtematrix R wird dann durch R′ ersetzt:

$$(x'k'|R'|x''k'') = \frac{1}{2}\Big\{\sum_i \psi_i^*(x'k')\,\psi_i(x''k'') - \\ - \sum_k \psi_k^*(x'k')\,\psi_k(x''k'')\Big\},$$

wobei die erste Summe über die besetzten, die zweite Summe über die unbesetzten Zustände zu erstrecken ist.
Der abzuziehende Teil $(x'k'|S|x''k'')$ hat dann die Form

$$(x'k'|S|x''k'') = u'S_0 + \frac{\bar{a}}{|x'-x''|^2} + \bar{b}\lg\frac{|x'-x''|^2}{C}.$$

Hierbei ist S_0 die Matrix R' für verschwindene Potentiale, $\bar{a}$ und $\bar{b}$ sind Funktionen der Feldstärken und ihrer Ableitungen, C ist eine Konstante. Diese Grössen sind bei Heisenberg l. c. und bei Heisenberg u. Euler l. c. explizit angegeben.

Für die Ausführungen spezieller Rechnungen ist es praktischer, nicht auf den expliziten Ausdruck Heisenberg's zurückzugreifen, sondern die wegzulassenden Glieder an ihrer Struktur zu erkennen. Dies ist vor allem deshalb einfacher, da die übrig bleibenden Ausdrücke nicht mehr bei $x' = x''$ singulär werden, sodass man für die Berechnung derselben gar nicht das formale Hilfsmittel der Dichtematrix benötigt. Die Summierungen über alle Vakuumelektronen führen hierbei nicht mehr zu divergenten Ausdrücken. Allerdings eignet sich die explizite Darstellung Heisenberg's gut dazu, die relativistische Invarianz und die Gültigkeit der Erhaltungssätze in dem Verfahren zu zeigen.

Es ist hieraus ersichtlich, dass die hier beschriebene Bestimmung der physikalischen Eigenschaften der Vakuum-

elektronen im wesentlichen keine Willkür enthält, da ausschliesslich nur jene Wirkungen derselben weggelassen werden, die infolge der Grundannahme der Positronentheorie wegfallen müssen: die Energie und die Ladung der von den Feldern ungestörten Vakuumelektronen, und die physikalisch sinnlose feldunabhängige konstante Polarisierbarkeit des Vakuums. Alle physikalisch sinnvollen Wirkungen der Vakuumelektronen werden mitberücksichtigt und führen zu konvergenten Ausdrücken. Man darf daraus wohl den Schluss ziehen, dass die Löchtertheorie des Positrons keine wesentlichen Schwierigkeiten für die Blektronentheorie mit sich geführt hat, solange man sich auf die Behandlung der ungequantelten Wellenfelder beschränkt.

Ich möchte an dieser Stelle den Herren Prof. Bohr, Heisenberg und Rosenfeld meinen herzlichsten Dank für viele Disskussionen aussprechen. Auch bin ich dem Rask-Ørsted-Fond Dank schuldig, der es mir ermöglicht hat, diese Arbeit am Institut for teoretisk Fysik in Kopenhagen auszuführen.

Færdig fra Trykkeriet den 24. November 1936.

Det Kgl. Danske Videnskabernes Selskab.
Mathematisk-fysiske Meddelelser **XIV**, 7.

KLEINERE BEITRÄGE ZUR THEORIE DER FASTPERIODISCHEN FUNKTIONEN

VII—VIII

VON

HARALD BOHR

KØBENHAVN
LEVIN & MUNKSGAARD
EJNAR MUNKSGAARD
1936

Printed in Denmark.
Bianco Lunos Bogtrykkeri A/S.

VII.

Stark stationäre und schwach stationäre Funktionen.

Die Untersuchungen dieser Note sind durch die schöne und wichtige Arbeit von R. CAMERON "Almost periodic properties of bounded solutions of linear differential equations with almost periodic coefficients" (Journal of Mathematics and Physics, Vol. XV (1936) pag. 73—81) angeregt worden. Es sollen hier einige Begriffe, die als wesentliche Hilfsmittel in der CAMERONschen Arbeit benutzt werden (und im Prinzip auf FAVARD zurückgehen), in ihrem gegenseitigen Zusammenhang näher analysiert werden, was vor allem durch die Konstruktion und Erörterung einiger »Gegenbeispiele« geschieht; diese Konstruktion schliesst sich übrigens eng einem interessanten Verfahren an, welches TOEPLITZ in der Abhandlung »Ein Beispiel zur Theorie der fastperiodischen Funktionen« (Mathematische Annalen, Bd. 98 (1927) pag. 281—295) zu anderen Zwecken verwendet hat.

Sämtliche auftretenden Funktionen $f(x)$, $\varphi(x)$, ... sollen komplexwertige Funktionen einer reellen Veränderlichen x sein, von denen wir überall stillschweigend voraussetzen werden, dass sie im ganzen unendlichen Intervalle $-\infty < x < \infty$ definiert und stetig sind. Wir werden oft mit Funktionenfolgen $f_n(x)$ zu tun haben, die in $-\infty < x < \infty$ gegen eine Grenzfunktion $f(x)$ konvergieren. Hierbei wer-

den für uns nur zwei Arten von Konvergenz in Frage kommen, die wir abkürzungsweise als »starke« bzw. »schwache« Konvergenz bezeichnen werden. Die Konvergenz von $f_n(x)$ gegen $f(x)$ soll stark genannt werden, falls sie gleichmässig im ganzen unendlichen Intervalle $-\infty < x < \infty$ gilt, und sie soll schwach heissen, wenn von ihr nur vorausgesetzt wird, dass sie gleichmässig in jedem endlichen Intervall stattfindet. Zunächst wollen wir uns mit starker Konvergenz beschäftigen; es ist bekanntlich diese Art von Konvergenz, welche in der Theorie der fastperiodischen Funktionen die entscheidende Rolle spielt.

1°. Von einer beliebigen (stetigen) Funktion $\varphi(x)$ ausgehend, bilden wir die Funktionenmenge $\{\varphi(x+h)\}$, wo h ein reeller Parameter ist, welcher das Intervall $-\infty < h < \infty$ durchläuft, und erweitern sie im Sinne der starken Konvergenz zur abgeschlossenen Hülle $\boldsymbol{H}\{\varphi(x+h)\}$, welche also aus allen Funktionen $\psi(x)$ besteht, die als Grenzfunktionen von stark konvergierenden Funktionenfolgen $\varphi(x+h_n)$ auftreten können. Jede Funktion $\psi(x)$ dieser Hülle $\boldsymbol{H}\{\varphi(x+h)\}$ werden wir als eine starke Transformierte der Ausgangsfunktion $\varphi(x)$ bezeichnen. Durch die Bildung dieser abgeschlossenen Hüllen wird, wie unmittelbar zu ersehen, eine gewisse Klasseneinteilung aller stetigen Funktionen vorgenommen; denn, falls $\psi(x)$ eine starke Transformierte von $\varphi(x)$ ist, wird umgekehrt $\varphi(x)$ eine starke Transformierte von $\psi(x)$ sein, und falls $\psi(x)$ eine starke Transformierte von $\varphi(x)$ und $\chi(x)$ eine starke Transformierte von $\psi(x)$ ist, wird auch $\chi(x)$ eine starke Transformierte von $\varphi(x)$ sein.

In dem Falle, wo die Ausgangsfunktion $\varphi(x)$ eine fastperiodische Funktion ist, habe ich in einer meiner ersten

Arbeiten über diesen Funktionentypus diese abgeschlossene Hülle $H\{\varphi(x+h)\}$ näher studiert; hier ist auch jede starke Transformierte von $\varphi(x)$ wieder fastperiodisch (übrigens mit denselben Fourierexponenten wie $\varphi(x)$), und wir haben es also hier mit einer Klasseneinteilung innerhalb der Gesamtheit der fastperiodischen Funktionen zu tun.

Ein interessantes Kriterium im Rahmen der obigen Begriffe für die Fastperiodizität einer (wie immer) stetigen Funktion $\varphi(x)$ — welches übrigens für die Ausdehnung der Theorie der fastperiodischen Funktion auf beliebige Gruppen von ausschlaggebender Bedeutung gewesen ist — rührt bekanntlich von BOCHNER her. Es besagt, dass es für die Fastperiodizität einer Funktion $\varphi(x)$ notwendig und hinreichend ist, dass die Funktionenmenge $\{\varphi(x+h)\}$ im Sinne starker Konvergenz kompakt ist, d. h. dass jede Funktionenfolge $\varphi(x+h_n)$ eine Teilfolge $\varphi(x+h_{n'})$ enthält, welche stark gegen eine Grenzfunktion konvergiert. Indem wir eine Funktion $\varphi(x)$ mit dieser starken Kompaktheitseigenschaft eine stark normale Funktion nennen (gewöhnlich wird sie einfach als »normal« bezeichnet) besagt also der BOCHNERsche Satz, *dass die Funktion* $\varphi(x)$ *dann und nur dann fastperiodisch ist, wenn sie stark normal ist.*

Bei verschiedenen Untersuchungen, z. B. bei Problemen über Differentialgleichungen mit fastperiodischen Koeffizienten, ist es nützlich, im Rahmen unserer Begriffsbildungen auch ein Kriterium dafür zur Verfügung zu haben, dass eine Funktion $\varphi(x)$ nicht nur fastperiodisch ist, sondern derart fastperiodisch ist, dass ihre Fourierexponenten alle einem vorgegebenen abzählbaren Zahlenmodul M angehören. Ein solches Kriterium ist dem klassischen Tatbestand der Theorie der fastperiodischen Funktionen leicht zu entnehmen und wird z. B. in

der zitierten Arbeit von Cameron verwendet. Wir werden von einer reellen Zahlenfolge h_n sagen, dass sie an einen vorgegebenen (immer als abzählbar angenommenen) Modul M »angepasst« ist, wenn für jede Zahl μ dieses Moduls M die Kongruenzgrenzbeziehung

$$\lim_{n\to\infty} \mu \cdot h_n = 0 \pmod{2\pi}$$

gilt, und wir werden eine Funktion $\varphi(x)$ stark stationär in bezug auf M nennen, falls für jede an den Modul M angepasste Zahlenfolge h_n die entsprechende Funktionenfolge $\varphi(x+h_n)$ stark gegen $\varphi(x)$ selbst konvergiert. Das erwähnte Kriterium besagt dann einfach: *Damit eine Funktion $\varphi(x)$ fastperiodisch mit lauter Fourierexponenten aus dem Modul M sei, ist notwendig und hinreichend, dass sie stark stationär in bezug auf M ist.*

Da jede starke Transformierte $\psi(x)$ einer fastperiodischen Funktion $\varphi(x)$ wieder fastperiodisch ist und dieselben Exponenten wie $\varphi(x)$ besitzt, folgt z. B. aus dem angegebenen Kriterium sofort, dass jede starke Transformierte einer in bezug auf M stark stationären Funktion wiederum stark stationär in bezug auf M ist. Ferner ist nach diesem Kriterium (in Verbindung mit dem Satz von Bochner) klar, dass eine in bezug auf einen Modul M stark stationäre Funktion $\varphi(x)$ von selbst stark normal sein muss.

2°. Wir gehen nun dazu über, ähnliche Begriffe wie die unter 1° aufgestellten einzuführen, indem wir nur überall starke Konvergenz durch schwache Konvergenz ersetzen. Ausgehend von einer Funktion $\varphi(x)$ bilden wir wiederum die Funktionenmenge $\{\varphi(x+h)\}$ und erweitern sie zur abgeschlossenen Hülle $\boldsymbol{h}\{\varphi(x+h)\}$, diesmal aber im Sinne der schwachen Konvergenz, und wir bezeichnen jede Funktion $\psi(x)$ dieser Hülle $\boldsymbol{h}\{\varphi(x+h)\}$ als eine

schwache Transformierte von $\varphi(x)$. Zur Orientierung sei hervorgehoben, dass diese Bildung — im Gegensatz zu der Bildung $\boldsymbol{H}\{\varphi(x+h)\}$ — nicht zu einer Klasseneinteilung der stetigen Funktion führt; es gilt wohl, wie leicht zu sehen, dass, falls $\psi(x)$ eine schwache Transformierte von $\varphi(x)$ und $\chi(x)$ eine schwache Transformierte von $\psi(x)$ ist, auch $\chi(x)$ eine schwache Transformierte von $\varphi(x)$ ist; dagegen gilt nicht allgemein, dass $\varphi(x)$ eine schwache Transformierte von $\psi(x)$ ist, wenn $\psi(x)$ eine schwache Transformierte von $\varphi(x)$ ist. (Z. B. ist die Funktion $\psi(x) = 0$ für alle x eine schwache Transformierte der Funktion $\varphi(x) = \begin{cases} 0 & \text{für } -\infty < x \leqq 0 \\ \sin x & \text{für } 0 \leqq x < \infty \end{cases}$; dagegen ist $\varphi(x)$ keine schwache Transformierte von $\psi(x)$, da diese letzte, konstante, Funktion natürlich nur sich selbst als schwache Transformierte besitzt.)

Wenn man speziell von einer fastperiodischen Funktion $\varphi(x)$ ausgeht, sind die beiden Hüllen $\boldsymbol{H}\{\varphi(x+h)\}$ und $\boldsymbol{h}\{\varphi(x+h)\}$ mit einander identisch, denn bei einer fastperiodischen Funktion $\varphi(x)$ gilt bekanntlich, dass jede Funktionenfolge $\varphi(x+h_n)$, die schwach gegen eine Grenzfunktion $\psi(x)$ konvergiert, von selbst — wegen der relativen Dichte der Verschiebungszahlen — stark gegen $\psi(x)$ konvergiert.

Eine Funktion $\varphi(x)$ soll schwach normal (bei Cameron semi-normal) heissen, wenn die Funktionenmenge $\{\varphi(x+h)\}$ im Sinne der schwachen Konvergenz kompakt ist, wenn also jede Funktionenfolge $\varphi(x+h_n)$ eine schwach konvergente Teilfolge $\varphi(x+h_{n'})$ enthält. Im Gegensatz zu dem Begriff stark normal, der eine eingreifende und eigenartige Forderung, nämlich die der Fastperiodizität, an die Funktion $\varphi(x)$ stellt, ist die Eigenschaft der schwachen

Normalität an sich keine aufregende, indem sie, wie eine leichte Ueberlegung zeigt, einfach damit gleichwertig ist, dass die Funktion $\varphi(x)$ im ganzen unendlichen Intervall beschränkt und gleichmässig stetig ist. Uebrigens ersehen wir sofort aus dieser letzten Charakterisierung einer schwach normalen Funktion, dass jede schwache Transformierte einer solchen Funktion wiederum schwach normal ist.

Bei dem Studium der Lösungen von linearen Differentialgleichungen, deren Koeffizienten fastperiodisch, d. h. stark normal sind, wird man zwangsläufig nicht nur auf schwach normale Funktionen geführt, sondern auch auf Funktionen $\varphi(x)$, die in bezug auf einen gegebenen Modul M schwach stationär sind, d. h. welche die Eigenschaft besitzen, dass für jede Zahlenfolge h_n, die im obigen Sinne an den Modul M angepasst ist, die entsprechende Funktionenfolge $\varphi(x+h_n)$ schwach gegen die Funktion $\varphi(x)$ selbst konvergiert. Man möchte daher natürlich gern einen Satz zur Verfügung haben, welcher erlaubt, von der schwachen Stationarität einer Funktion $\varphi(x)$ etwa durch Hinzufügung weiterer Forderungen an $\varphi(x)$ auf ihre starke Stationarität zu schliessen, um dadurch nachweisen zu können, dass die Funktionen, auf welche man bei den Differentialgleichungsproblemen gestossen ist, von fastperiodischem Charakter sind. Ein diesbezüglicher Satz ist von Cameron in der anfangs zitierten Arbeit bewiesen und bildet gewissermassen die Grundlage seiner weiteren wichtigen Ueberlegungen. Dieser Satz, welcher sich dadurch auszeichnet, dass sämtliche Voraussetzungen, die über die Funktion $\varphi(x)$ gemacht werden, nur von schwacher Konvergenz handeln, besagt:

Damit eine in bezug auf den Modul M schwach stationäre

Funktion $\varphi(x)$ in bezug auf M stark stationär sei (d. h. also fastperiodisch mit Exponenten aus M), ist notwendig und hinreichend, dass sie schwach normal ist, und dass nicht nur $\varphi(x)$ selbst, sondern auch jede schwache Transformierte von $\varphi(x)$ ebenfalls schwach stationär in bezug auf M ist.

Dass die angegebenen Bedingungen notwendig sind, ist nach dem vorangehenden trivial. Der Inhalt des CAMERONschen Satzes ist, dass sie auch hinreichend sind.

Nun ist aber die schwache Stationarität einer Funktion $\varphi(x)$ in bezug auf einen Modul M eine an sich recht undurchsichtige Eigenschaft, und es entsteht von selbst die Frage, ob nicht vielleicht bei »schwacher« Konvergenz die Sachlage tatsächlich eine ganz analoge ist wie bei »starker« Konvergenz in dem Sinne, dass auch jede in bezug auf einen Modul M schwach stationäre Funktion $\varphi(x)$ von selbst schwach normal ist, und dass jede schwache Transformierte einer solchen Funktion $\varphi(x)$ wiederum schwach stationär in bezug auf M ausfällt. Dies würde bedeuten, dass der CAMERONsche Satz dahin vereinfacht werden könnte, dass jede in bezug auf M schwach stationäre Funktion immer in bezug auf M auch stark stationär wäre. Das dem nicht so ist, soll im Folgenden gezeigt werden, und zwar wollen wir durch die Konstruktion zweier »Gegenbeispiele« nachweisen:

I. *Es gibt eine Funktion $\varphi_1(x)$, die in bezug auf einen Modul M schwach stationär ist, ohne schwach normal zu sein,*

und ferner, was wichtiger ist,

II. *Es gibt eine Funktion $\varphi_2(x)$, die in bezug auf einen Modul M schwach stationär und ausserdem schwach normal ist, die aber eine schwache Transformierte besitzt, welche nicht schwach stationär in bezug auf M ist.*

Vorbemerkung: Wenn wir den Cameronschen Satz heranziehen, ist die Aussage II mit der folgenden Aussage gleichwertig: *Es gibt eine schwach normale und in bezug auf einen Modul M schwach stationäre Funktion $\varphi_2(x)$, welche nicht in bezug auf M stark stationär ist.* Es wird uns bequem sein, II in dieser Form darzutun.

Bevor wir an die Konstruktion der Funktionen $\varphi_1(x)$ und $\varphi_2(x)$ herangehen, müssen wir zunächst einen bestimmten Modul M wählen, den wir unseren Betrachtungen zugrundelegen werden. Am bequemsten wäre es natürlich, den einfachst möglichen Modul zu benutzen, nämlich einen solchen, der aus lauter ganzzahligen Multipla einer einzigen Zahl, etwa der Zahl 2π, besteht. Dieser Modul M_0 ist aber zu einfach, um das Gewünschte leisten zu können; denn wie wir sofort zeigen können, wird jede Funktion $\varphi(x)$, die in bezug auf M_0 schwach stationär ist, notwendigerweise auch stark stationär in bezug auf M_0 sein. In der Tat kommt offenbar jede Folge von lauter ganzen Zahlen unter den an M_0 angepassten Zahlenfolgen h_n vor, speziell also die Folge $h_n = 1$ für alle n, und die Forderung der schwachen Konvergenz der Funktionenfolge $\varphi(x+h_n) = \varphi(x+1)$ gegen $\varphi(x)$ involviert natürlich, dass $\varphi(x+1) = \varphi(x)$ ist für alle x, so dass $\varphi(x)$ eine (stetige) rein periodische Funktion der Periode 1 ist, d. h. in der Sprache der fastperiodischen Funktionen, eine fastperiodische Funktion mit lauter Exponenten aus M_0, also tatsächlich eine in bezug auf M_0 stark stationäre Funktion.

Wir sind also genötigt, bei der Konstruktion unserer Gegenbeispiele einen Modul komplizierterer Art als M_0 zugrundezulegen; wie wir sehen werden, kommen wir aber mit einem relativ sehr einfachen Modul aus, nämlich einem solchen, der aus lauter rationalen Multipla einer einzigen

Zahl besteht, und zwar werden wir den Modul M^* betrachten, welcher aus allen Zahlen der Form $2\pi \cdot r$ besteht, wo r eine rationale Zahl ist, deren Nenner eine Potenz von 2 ist. Machen wir uns zunächst klar, was eigentlich die Forderung besagt, dass eine Funktion $\varphi(x)$ in bezug auf diesen Modul M^* schwach stationär ist. Wir nennen eine Zahlenfolge h_n »pseudoganz«, wenn sie die Bedingung $\lim h_n = 0 \pmod 1$ erfüllt. Da unser Modul M^* speziell die Zahl $\mu = 2\pi$ enthält, ist evident, dass jede an M^* angepasste Zahlenfolge h_n pseudoganz sein muss. Indem wir bei einer pseudoganzen Zahlenfolge h_n diejenige ganzzahlige Zahlenfolge k_n als die zu h_n gehörige bezeichnen, für welche bei jedem n die ganze Zahl k_n der Zahl h_n am nächsten liegt, d. h. für welche $h_n - \frac{1}{2} < k_n \leq h_n + \frac{1}{2}$, ist ferner klar (wegen $\lim (h_n - k_n) = 0$), dass eine pseudoganze Zahlenfolge h_n und ihre zugehörige ganzzahlige Zahlenfolge k_n gleichzeitig an M^* angepasst sind, und dass die beiden Aussagen: »$\varphi(x + h_n)$ konvergiert schwach gegen $\varphi(x)$« und »$\varphi(x + k_n)$ konvergiert schwach gegen $\varphi(x)$« gleichwertig sind. Hieraus folgt, dass wir uns bei der Entscheidung, ob eine Funktion $\varphi(x)$ in bezug auf M^* schwach stationär ist, ohne weiteres auf die Betrachtung von ganzzahligen an M^* angepassten Zahlenfolgen h_n beschränken können. Wann aber eine ganzzahlige Zahlenfolge h_n an M^* angepasst ist, ist unmittelbar zu sehen. Statt alle Zahlen μ des Moduls M^* zu berücksichtigen, brauchen wir nämlich offenbar nur die Zahlen $\mu = \frac{2\pi}{2^m}$ $(m = 0, 1, 2, \ldots)$ zu betrachten (weil jede Zahl μ aus M^* ein ganzzahliges Multiplum einer dieser Zahlen $\frac{2\pi}{2^m}$ ist); dass aber bei festem m eine ganzzahlige Zahlenfolge h_n die Bedingung $\lim_{n \to \infty} \frac{2\pi}{2^m} \cdot h_n = 0 \pmod{2\pi}$

erfüllen soll, ist einfach damit gleichwertig, dass die Zahlen h_n alle von einer gewissen Stelle $n \geqq n_0 = n_0(m)$ ab durch 2^m teilbar sind. Zusammenfassend haben wir also gesehen: Die Forderung, dass eine Funktion $\varphi(x)$ in bezug auf M^* schwach stationär ist, ist mit der folgenden Forderung gleichwertig: Für jede ganzzahlige Zahlenfolge h_n, für welche bei jedem festen m alle Elemente h_n von einer gewissen Stelle an durch 2^m teilbar sind, soll die entsprechende Funktionenfolge $\varphi(x+h_n)$ schwach gegen $\varphi(x)$ konvergieren.

Um bei der nunmehr folgenden Konstruktion der beiden in den Aussagen I bzw. II erwähnten Funktionen $\varphi_1(x)$ bzw. $\varphi_2(x)$ Wiederholungen zu ersparen, werden wir erst eine einzige Funktion $\varphi(x)$ konstruieren, die aber von gewissen Parametern $s_1, s_2, \ldots$ abhängt, und danach durch spezielle Wahl dieser Parameter einerseits zu $\varphi_1(x)$ und andererseits zu $\varphi_2(x)$ gelangen.

Zunächst teilen wir die Menge aller ganzen Zahlen in abzählbar viele Klassen $E_1, E_2, E_3, \ldots$ ein und zwar folgendermassen. In E_1 nehmen wir jede zweite ganze Zahl auf (also entweder alle geraden oder alle ungeraden Zahlen), in E_2 wird jede zweite der übrig gebliebenen Zahlen aufgenommen, in E_3 jede zweite der nunmehr übrig gebliebenen usw.; die Menge E_q besteht also aus allen ganzen Zahlen einer gewissen arithmetischen Progression der Differenz 2^q. Hierbei haben wir nur dafür Sorge zu tragen, dass tatsächlich jede ganze Zahl in einer unserer Klassen untergebracht wird; dies kann in mannigfacher Weise erreicht werden, z. B. in der folgenden: Als E_1 wählen wir die Menge der geraden Zahlen, so dass also 0 schon beim ersten Schritt aufgenommen wird; als E_2 wählen wir diejenige der beiden nunmehr zur Verfügung stehenden arithmetischen Progressionen der Differenz 2^2, welche die kleinste übrig ge-

bliebene positive Zahl enthält, d. h. E_2 ist die Menge der Zahlen $4n+1$; danach wählen wir für E_3 diejenige der beiden zur Verfügung stehenden arithmetischen Progressionen der Differenz 2^3, welche die absolut kleinste übrig gebliebene negative Zahl enthält, also die Menge der Zahlen $8n-1$, und so fort, indem wir abwechselnd das Augenmerk auf die kleinste ledig gebliebene positive und die kleinste ledig gebliebene negative Zahl richten. (Man könnte unmittelbar, z. B. durch Betrachtung der Dualentwicklung der ganzen Zahlen, explizite diejenigen Zahlen charakterisieren, welche bei dem soeben angegebenen Prozess in die Klasse E_q fallen; wir werden aber nicht dabei verweilen, da es für das weitere belanglos ist, in welcher Weise wir die Klassen $E_1, E_2, \ldots$ gewählt haben, falls sie nur die angegebenen allgemeinen Bedingungen erfüllen).[1] Wir werden sagen, dass auf der ganzen Zahl m ein Hügel der Höhe $s\,(\gtrless 0)$ angebracht ist, wenn auf das Intervall $\left(m-\frac{1}{2},\ m+\frac{1}{2}\right)$ als Basis ein gleichschenkliges Dreieck der Höhe $|s|$ aufgesetzt ist, und zwar nach oben oder unten, je nachdem s positiv oder negativ ist. Es sei nun $s_1, s_2, s_3, \ldots$ eine zunächst völlig beliebige Folge von von Null verschiedenen reellen Zahlen. Auf jeder Zahl der Klasse E_1 bringen wir einen Hügel der Höhe s_1 an, auf jeder Zahl der Klasse E_2 einen Hügel der Höhe s_2, usw. Hierdurch wird die ganze Abszissenachse mit einer gewissen Hügelkette bedeckt; die in $-\infty < x < \infty$ definierte und stetige Funktion, welche diese Hügelkette darstellt, soll mit $\varphi(x)$ bezeichnet werden (siehe Fig.). Wir werden zeigen,

[1] In der anfangs zitierten Arbeit von TOEPLITZ wird eine ähnliche Einteilung der ganzen Zahlen in Klassen $E_1, E_2, \ldots$ vorgenommen, wobei aber — im Gegensatz zu unserem Verfahren — die Einteilung so gewählt wird, dass eine einzige Zahl (übrigens die Zahl 0) in keine der Klassen untergebracht wird.

dass diese Funktion — wie auch die Hügelhöhen s_q gewählt sind — eine in bezug auf den Modul M^* schwach stationäre Funktion ist. Hierzu genügt es nach dem oben festgestellten zu zeigen, dass für jede ganzzahlige Folge h_n von der Art, dass bei beliebig gegebenem m die sämtlichen Zahlen h_n der Folge von einer gewissen Stelle an durch 2^m teilbar sind, gilt, dass die entsprechende Funktionenfolge $\varphi(x+h_n)$ schwach (also gleichmässig in jedem endlichen Intervall I) gegen $\varphi(x)$ konvergiert. Es sei also h_n eine beliebige Folge dieser Art und I ein beliebig gegebenes endliches Intervall, das wir von der Form $\left(-l-\frac{1}{2}, l+\frac{1}{2}\right)$ (l positiv ganz) annehmen können. Es sei Q so gewählt, dass jede der (endlich vielen) Zahlen $-l, -l+1, \ldots, l-1$, l einer der Klassen $E_1, \ldots, E_Q$ angehört, und es sei N so gross gewählt, dass jedes h_n mit $n > N$ durch 2^Q teilbar ist. Dann gilt für jedes $n > N$, dass im ganzen Intervall I die Funktion $\varphi(x+h_n)$ sogar mit $\varphi(x)$ identisch ist. Denn durch eine Verschiebung um h_n, also um ein Multiplum von 2^Q geht ja sowohl die Zahlenklasse E_1 wie die Zahlenklasse $E_2, \ldots$ wie die Zahlenklasse E_Q in sich über.

Wir verfügen nun über die bisher völlig beliebigen Zahlen $s_q \neq 0$ und können dadurch sofort zu einer Funktion $\varphi_1(x)$ bzw. zu einer Funktion $\varphi_2(x)$ gelangen.

1). Wählen wir die Hügelhöhen s_q derart, dass $|s_q|$ für $q \to \infty$ gegen Unendlich strebt, so erhalten wir eine Funktion $\varphi_1(x)$, die in bezug auf M^* schwach stationär, aber offenbar nicht schwach normal, sogar weder beschränkt, noch gleichmässig stetig in $-\infty < x < \infty$ ist.

2). Wählen wir etwa $s_q = (-1)^q$, so erhalten wir eine in bezug auf M^* schwach stationäre Funktion $\varphi_2(x)$, die natürlich in $-\infty < x < \infty$ beschränkt und gleichmässig

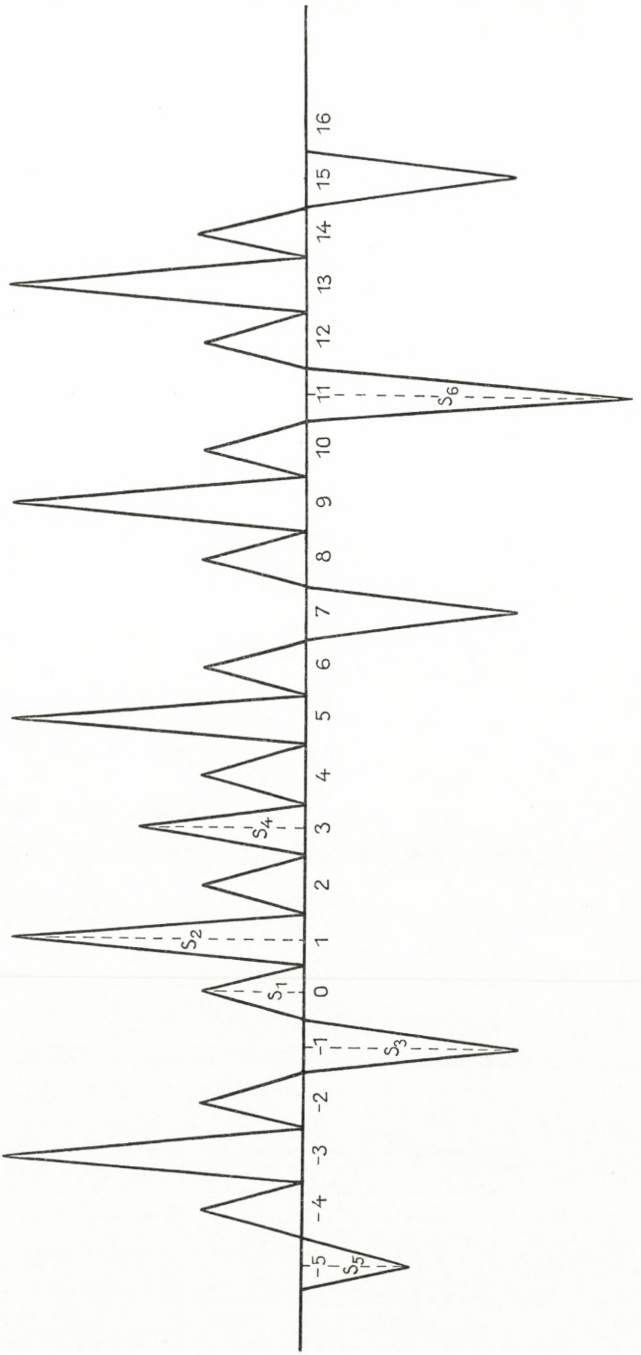
16
15
14
13
12
11
10
9
8
7
6
5
4
3
2
1
0
-1
-2
-3
-4
-5
S_1
S_2
S_3
S_4
S_5
S_6

stetig, also schwach normal ist, die aber nicht stark stationär in bezug auf M^* ist. Denn wäre dies der Fall, so müsste z. B. die Funktionenfolge $\varphi_2(x+2^n)$ stark gegen $\varphi_2(x)$ konvergieren, da ja die Zahlenfolge $h_n = 2^n$ an den Modul M^* angepasst ist, und dies ist gewiss nicht der Fall; es hat sogar bei jedem n die obere Grenze von

$$|\varphi_2(x+2^n) - \varphi_2(x)|$$

in $-\infty < x < \infty$ ihren grösstmöglichen Wert 2; betrachten wir nämlich die Menge $R_n = E_{n+1} + E_{n+2} + \cdots$ aller ganzen Zahlen, welche nicht zu einer der n ersten Klassen $E_1, E_2, \ldots E_n$ gehören, so bilden diese eine arithmetische Progression der Differenz 2^n, und unter den Zahlen dieser Menge R_n gibt es sowohl solche, die »positive« als auch solche, die »negative« Hügel tragen (z. B. sind ja die Hügel auf den Zahlen von E_{n+1} und von E_{n+2} entgegengesetzt gerichtet), also gibt es auch zwei auf einanderfolgende Zahlen in R_n, etwa x_0 und x_0+2^n, für welche $|\varphi_2(x_0+2^n) - \varphi_2(x_0)| = 2$ ist.

VIII.

Über den Logarithmus einer positiven fastperiodischen Funktion.

1°. Es sei $f(x)$ eine für alle x positive, fastperiodische Funktion. Wir bilden die in $-\infty < x < \infty$ reelle stetige Funktion

$$g(x) = \log f(x)$$

und fragen, unter welchen Bedingungen $g(x)$ wiederum fastperiodisch wird.

Eine erste triviale Antwort auf diese Frage lautet:

Damit $g(x) = \log f(x)$ fastperiodisch sei, ist notwendig und hinreichend, dass die untere Grenze m von $f(x)$ grösser als Null (und nicht gleich Null) ist. In der Tat ist die Bedingung $m > 0$ selbstverständlich notwendig, weil sonst $f(x)$ beliebig kleine positive Werte, also $g(x)$ beliebig grosse negative Werte annähme, was mit der Fastperiodizität, also a fortiori Beschränktheit, von $g(x)$ nicht verträglich ist. Und sie ist auch hinreichend, denn für $m > 0$ ist ja $\log y$ in dem abgeschlossenen Intervall $m \leqq y \leqq M$, wo M die obere Grenze von $f(x)$ bezeichnet, stetig, und nach einem bekannten, unmittelbar zu beweisenden Satz ist daher die Fastperiodizität von $\log f(x)$ eine Folge der Fastperiodizität von $f(x)$ selbst.

Diese triviale Bedingung für die Fastperiodizität von

$g(x) = \log f(x)$ lässt sich natürlich auch als eine Bedingung über die Funktion $g(x)$ statt über die Funktion $f(x)$ aussprechen, und zwar lautet sie dann, dass $g(x)$ nach unten beschränkt sein muss.

Von einer in $-\infty < x < \infty$ definierten Funktion $h(x)$ wollen wir sagen, dass sie eine beschränkte Aenderungstendenz besitzt, falls es zu jedem positiven k ein $K = K(k)$ derart gibt, dass für ein beliebiges Punktepaar x', x'' mit $|x' - x''| < k$ die Ungleichung

$$|h(x') - h(x'')| < K$$

gilt. Natürlich bleibt diese Forderung an die Funktion $h(x)$ ihrem Inhalte nach ungeändert, wenn nur für ein einziges k, etwa $k = 1$, die Existenz eines entsprechenden K verlangt wird.

Wir wollen nun den Satz beweisen:

Damit der Logarithmus $g(x) = \log f(x)$ einer positiven fastperiodischen Funktion $f(x)$ wiederum fastperiodisch sei, ist notwendig und hinreichend, dass $g(x)$ eine beschränkte Aenderungstendenz besitzt.

Dass die Bedingung notwendig ist, ist klar; denn falls die Funktion $g(x)$ fastperiodisch ist, ist sie ja auch beschränkt, also selbstverständlich von beschränkter Aenderungstendenz. Dass die Bedingung auch hinreichend ist, erfordert eine kleine Ueberlegung. Nach dem obigen kommt es darauf an zu zeigen, dass das Erfülltsein der Bedingung zur Folge hat, dass $g(x)$ nach unten beschränkt ist. Wäre dieses letztere nun nicht der Fall, d. h. gäbe es Punkte, in denen $g(x)$ beliebig grosse negative Werte annähme, so gäbe es infolge der beschränkten Aenderungstendenz von $g(x)$ gewiss auch beliebig grosse Intervalle, in denen $g(x)$ überall beliebig gross negativ wäre, d. h. in welchen

$f(x) = e^{g(x)}$ überall beliebig nahe an Null herankäme, genau gesprochen: Es liessen sich zu einer vorgegebenen Folge positiver Zahlen ε_n mit $\varepsilon_n \to 0$ entsprechende Intervalle $(x_n, x_n + l_n)$ mit $l_n \to \infty$ derart finden, dass

$$0 < f(x) < \varepsilon_n \text{ für } x_n < x < x_n + l_n.$$

Somit würde

$$\frac{1}{l_n} \int_{x_n}^{x_n + l_n} f(x)\, dx \to 0 \text{ für } n \to \infty,$$

also nach dem »gleichmässigen Mittelwertsatz« für fastperiodische Funktionen der Mittelwert $M\{f(x)\} = 0$ sein. Dies ist aber bekanntlich — wegen der relativen Dichte der Verschiebungszahlen — nicht damit verträglich, dass $f(x) > 0$ ist.

Corollar. Weiss man von dem Logarithmus $g(x)$ einer positiven fastperiodischen Funktion, dass er differenzierbar mit einer beschränkten Ableitung ist, so kann man schliessen, dass $g(x)$ fastperiodisch ist. Denn in diesem Fall ist $g(x)$ natürlich eine Funktion mit beschränkter Aenderungstendenz.

2°. Als eine Anwendung der vorangehenden Ueberlegungen werden wir zeigen, wie aus dem obigen Corollar sich sofort ein Satz ergibt, welchen Bochner in einer Note "On the integration of almost periodic functions" (Journal of the London Math. Soc. Bd. VIII (1933), S. 250—254) mit Hilfe der Normalitätseigenschaften fastperiodischer Funktionen bewiesen hat, und welcher lautet:

Es sei $\varphi(x)$ eine reelle fastperiodische Funktion. Dann ist die Funktion

$$f(x) = e^{\int_0^x \varphi(x)\, dx}$$

nur in dem (trivialen) Fall fastperiodisch, wo schon das Integral $\int_0^x \varphi(x)\,dx$ *fastperiodisch ist.*

In der Tat, falls $f(x)$ fastperiodisch ist, muss nach dem Corollar auch $g(x) = \log f(x) = \int_0^x \varphi(x)\,dx$ fastperiodisch sein, weil ja $g(x)$ die beschränkte (sogar fastperiodische) Ableitung $\varphi(x)$ besitzt.

3°. Nunmehr gehen wir zu einer Anwendung des Satzes in 1°, oder vielmehr des aus ihm unmittelbar folgenden Bochnerschen Satzes in 2°, über, welche Differentialgleichungen betrifft.

Als Verallgemeinerung des fundamentalen Satzes, dass das Integral einer fastperiodischen Funktion immer fastperiodisch ist, falls es nur beschränkt bleibt, haben Neugebauer und der Verfasser bewiesen, dass jede beschränkte Lösung einer linearen Differentialgleichung mit konstanten Koeffizienten und fastperiodischer rechter Seite

$$\frac{d^n y}{dx^n} + k_1 \frac{d^{n-1} y}{dx^{n-1}} + \cdots + k_{n-1} \frac{dy}{dx} + k_n y = \varphi(x)$$

von selbst fastperiodisch ist. Für den allgemeinen Fall einer linearen Differentialgleichung mit fastperiodischen — statt konstanten — Koeffizienten

$$\frac{d^n y}{dx^n} + \varphi_1(x) \frac{d^{n-1} y}{dx^{n-1}} + \cdots + \varphi_{n-1}(x) \frac{dy}{dx} + \varphi_n(x)\, y = \varphi(x)$$

gilt bekanntlich kein entsprechender Satz. Für diese letzte wichtige Tatsache hat Bochner in seiner interessanten Arbeit "Homogeneous systems of differential equations with almost periodic coefficients" (Journal of the London Math.

Soc. Bd. VIII (1933), S. 283—288) ein einfaches explizites Beispiel sogar einer Differentialgleichung erster Ordnung angegeben, und zwar das folgende, in welchem aber zu beachten ist, dass komplexwertige fastperiodische Funktionen zugelassen werden. Es wird die homogene Differentialgleichung

$$\frac{dy}{dx} + i \cdot a(x) \cdot y = 0$$

betrachtet, wo $a(x)$ eine reelle fastperiodische Funktion ist. Die Lösung dieser Differentialgleichung ist durch

$$y(x) = C \cdot e^{-\int_0^x i \cdot a(x)\, dx}$$

gegeben, wo C eine komplexe Konstante bedeutet. Wie auch die reelle fastperiodische Funktion $a(x)$ gewählt wird, ist offenbar die Funktion

$$b(x) = e^{-i\int_0^x a(x)\, dx}$$

beschränkt; sie hat ja den absoluten Betrag 1. Es handelt sich also nur darum, $a(x)$ so zu wählen, dass $b(x)$ nicht fastperiodisch ausfällt. Zu diesem Zwecke wird die fastperiodische Funktion $a(x)$ so gewählt, dass sie die beiden folgenden — bekanntlich mit einander verträglichen — Bedingungen erfüllt.

1) Die Fourierreihe der Funktion $a(x)$ besitzt kein konstantes Glied, d. h. es ist der Mittelwert $M\{a(x)\} = 0$, also $\int_0^x a(x)\, dx = o(|x|)$ für $|x| \to \infty$.

2) Das Integral $\int_0^x a(x)\, dx$ bleibt aber nicht beschränkt.

Es wird nun ein Satz des Verfassers herangezogen, nach

welchem eine Funktion der Gestalt $e^{iF(x)}$, wo $F(x)$ eine stetige reelle Funktion ist, nur dann fastperiodisch sein kann, falls $F(x)$ die Form $c \cdot x + r(x)$ besitzt, wo c eine Konstante (die sogenannte Säkularkonstante) und das Restglied $r(x)$ beschränkt, sogar fastperiodisch ist. Dieser Satz zeigt unmittelbar, dass unsere Funktion $b(x)$ tatsächlich nicht fastperiodisch ist. Denn die im Exponenten dieser Funktion $b(x) = e^{-i\int_0^x a(x)\,dx}$ auftretende Funktion $-\int_0^x a(x)\,dx$ hat sicher nicht die Form $c \cdot x + r(x)$ mit beschränktem $r(x)$, denn wegen $\int_0^x a(x)\,dx = o(|x|)$ müsste c gleich 0 sein, also müsste $\int_0^x a(x)\,dx$ selbst beschränkt sein, was ja nicht der Fall ist.

Das soeben angegebene »Gegenbeispiel« von Bochner beruht in seinem ganzen Aufbau prinzipiell darauf, dass in der betrachteten Differentialgleichung $\frac{dy}{dx} + \varphi(x) \cdot y = 0$ für die fastperiodische Funktion $\varphi(x)$ eine nicht reelle Funktion gewählt wurde. Es mag daher von Interesse sein, auch *ein einfaches Beispiel einer homogenen linearen Differentialgleichung erster Ordnung*

$$(*) \qquad \frac{dy}{dx} + \varphi(x) \cdot y = 0$$

mit einem reellen fastperiodischen Koeffizienten $\varphi(x)$ zu bilden, *deren Lösungen beschränkt, aber nicht fastperiodisch sind.* Wir werden zeigen, dass der in 2° aufs neue bewiesene Satz von Bochner zur Konstruktion eines solchen »Gegenbeispiels« verwendet werden kann. Die Lösungen von (*) werden durch

$$y(x) = c \cdot e^{-\int_0^x \varphi(x)\,dx}$$

gegeben. Es handelt sich also darum, eine reelle fastperiodische Funktion $\varphi(x)$ so zu bestimmen, dass die Funktion

$$\psi(x) = e^{-\int_0^x \varphi(x)\,dx}$$

beschränkt, aber nicht fastperiodisch ausfällt. Eine solche Funktion $\varphi(x)$ wird, behaupte ich, durch die unendliche Reihe

$$\varphi(x) = \sum_{\nu=1}^{\infty} \varepsilon_\nu \sin \delta_\nu x$$

geliefert, wo ε_ν und δ_ν positive Zahlenfolgen sind, welche nur den beiden Bedingungen

$$\sum_{\nu=1}^{\infty} \varepsilon_\nu \text{ konvergent}, \quad \frac{\delta_\nu}{\varepsilon_\nu} \to 0 \text{ für } \nu \to \infty$$

genügen. (Es können also z. B. $\varepsilon_\nu = \frac{1}{2^\nu}$, $\delta_\nu = \frac{1}{\nu \cdot 2^\nu}$ verwendet werden.) Zunächst ist $\varphi(x)$ fastperiodisch, da die Reihe $\sum \varepsilon_\nu \sin \delta_\nu x$ wegen der Konvergenz von $\sum \varepsilon_\nu$ für alle x gleichmässig konvergiert. Bezeichnen wir das Integral $\int_0^x \varphi(x)\,dx$ mit $\chi(x)$, so gilt für jedes feste x die Ungleichung

$$\chi(x) = \sum_{\nu=1}^{\infty} \frac{\varepsilon_\nu}{\delta_\nu}(1 - \cos \delta_\nu x) \geqq 0,$$

da die sämtlichen Glieder der Reihe nicht negativ sind. Also ist $\psi(x) = e^{-\chi(x)}$ sicher beschränkt, nämlich $0 < \psi(x) \leqq 1$. Um schliesslich die Nicht-Fastperiodizität von $\psi(x) = e^{-\chi(x)}$ darzutun, genügt es, nach dem Satz in 2° zu zeigen, dass das im Exponenten von $\psi(x)$ auftretende Integral

$\chi(x) = \int_0^x \varphi(x)\,dx$ nicht fastperiodisch, d. h. nicht beschränkt ist. Dies ist aber offensichtlich nicht der Fall, denn bei jedem festen n gilt (indem wir nur ein einziges Glied in der obigen Reihe von $\chi(x)$ berücksichtigen)

$$\chi\left(\frac{\pi}{2\,\delta_n}\right) \geq \frac{\varepsilon_n}{\delta_n}\left(1 - \cos\,\delta_n \frac{\pi}{2\,\delta_n}\right) = \frac{\varepsilon_n}{\delta_n},$$

und $\frac{\varepsilon_n}{\delta_n}$ wächst ja nach Annahme für $n \to \infty$ über alle Grenzen.

Forelagt paa Mødet den 16. Oktober 1936.
Færdig fra Trykkeriet den 12. November 1936.

Det Kgl. Danske Videnskabernes Selskab.
Mathematisk-fysiske Meddelelser. **XIV**, 8.

OM TAL, SOM PAA TO MAADER KAN SKRIVES SOM EN SUM AF POTENSER AF FEMTE GRAD

AF

A. S. BANG

KØBENHAVN
LEVIN & MUNKSGAARD
EJNAR MUNKSGAARD
1937

Printed in Denmark.
Bianco Lunos Bogtrykkeri A/S

Indledning.

1. A. MARTIN har i Aaret 1887[1] fundet 2 Eksempler paa Potenstal af femte Grad, som er lig med Summen af seks Potenstal af samme Grad, nemlig

$$12^5 = 11^5 + 9^5 + 7^5 + 6^5 + 5^5 + 4^5$$
$$\text{og } 30^5 = 29^5 + 19^5 + 16^5 + 11^5 + 10^5 + 5^5.$$

Han skriver herom i 1896[2]:

Som bekendt kan Summen af to hele Tals femte Potenser ikke være lig en femte Potens, men, saavidt Forfatterens Viden rækker, er det ikke bevist, at Summen af tre, fire eller fem femte Potenser ikke kan være lig en femte Potens. Det er ikke lykkedes Forfatteren at finde færre end seks hele Potenser af femte Grad, hvis Sum er en femte Potens.

2. Det Problem, MARTIN her har opstillet, staar, saavidt mig bekendt, stadig uløst.

Jeg ved heller ikke, om der eksisterer Femte-Potenser, som er lig Summen af tre eller fire Potenser af samme Grad, men jeg har fundet, at der gives uendelig mange Femte-Potenser, som hver er lig Summen af fem Potenser af samme Grad.

Dette Resultat fremgaar af en Identitet, som indeholder seks Femte-Potenser, og er fremsat paa Side 26, og hvoraf man specielt faar

[1] Bull. Phil. Soc. Washington.

[2] Chicago Congr. Papers. Se: Jahrbuch über die Fortschritte der Mathem. 1897. Side 175.

$$107^5 = 100^5 + 80^5 + 57^5 + 43^5 + 7^5;$$
$$17516^5 = 15435^5 + 14175^5 + 11441^5 + 5366^5 + 709^5.$$

3. Det skal tilføjes, at der ogsaa eksisterer Femte-Potenser, som er lig Summen af syv eller af otte Potenser af samme Grad, idet jeg, ved at prøve mig frem, har fundet

$$92^5 = 89^5 + 58^5 + 51^5 + 22^5 + 11^5 + 9^5 + 2^5$$
og $$14^5 = 13^5 + 11^5 + 5^5 + 4^5 + 4^5 + 3^5 + 2^5 + 2^5.$$

4. Man kan stille den mere almindelige Opgave:

At bestemme Tal, som paa to Maader kan skrives som en Sum af Femte-Potenser.

Regner man ogsaa med negative Tal, kan man kortere sige:

At bestemme Femte-Potenser med Summen Nul.

I Stedet for f. Eks.

$$69^5 + 66^5 + 63^5 = 79^5 + 53^5 + 50^5 + 16^5$$

kan skrives

$$79^5 + (-69)^5 + (-66)^5 + (-63)^5 + 53^5 + 50^5 + 16^5 = 0.$$

5. Den stillede Opgave er selvfølgelig ikke løst her i sin Almindelighed.

Den tilsvarende Opgave for Fjerde-Potenser er saaledes ogsaa kun løst i specielle Tilfælde, men i det følgende skal angives en Mængde Identiteter, som umiddelbart giver

9, 8, 7 eller 6 Femte-Potenser med Summen Nul.

Der er angivet 4 Identiteter med 9 Potenser, 7 med 8, 1 med 7 og 1 med 6 Potenser.

Af Identiteterne med 8 Potenser indeholder en 4 Femte- og 4 Tiende-Potenser og en anden 4 Femte- og 4 Femtende-Potenser.

6. Der er angivet 3 Tal, som hver for sig paa 3 Maader, og 1 Tal, som paa 4 Maader kan skrives som en Sum af 4 (positive eller negative) Femte-Potenser.

7. I et Tillæg er samlet de specielle Eksempler, som findes i Afhandlingen, og i hvilke hver enkelt Potens er mindre end 300^5.

1. Kapitel.

9 Femte-Potenser.

1. Vi vil betragte Ligningen

$$(x+m)^5+(x-m)^5+(x+n)^5+(x-n)^5 = \\ =(x+p)^5+(x-p)^5+(x+q)^5+(x-q)^5+y^5,$$

som indeholder 9 Femte-Potenser.

Den reduceres til

$$20x^3(m^2+n^2-p^2-q^2)+10x(m^4+n^4-p^4-q^4)=y^5.$$

Betingelsen for, at Koefficienten til x^3 bliver Nul, er

$$m+p=2ab; \quad m-p=2cd;$$
$$q+n=2ac; \quad q-n=2bd,$$

hvoraf

$$m=ab+cd; \quad p=ab-cd;$$
$$q=ac+bd; \quad n=ac-bd,$$

hvorpaa Indsætning giver

$$80abcd(a^2-d^2)(b^2-c^2)x=y^5.$$

Denne Ligning tilfredsstilles af

$$x=\frac{2s^4}{5e^5}; \quad y=\frac{2s}{e},$$

idet man, for Kortheds Skyld, sætter

$$abcd\,(a^2 - d^2)\,(b^2 - c^2) = s.$$

Ved Indsætning i den oprindelige Ligning fremkommer da Identiteten:

$$A^5 + B^5 + C^5 + D^5 = E^5 + F^5 + G^5 + H^5 + I^5,$$

hvor

$$A = 2s^4 + 5\,(ab + cd)\,e^5; \qquad B = 2s^4 - 5\,(ab + cd)\,e^5;$$
$$C = 2s^4 + 5\,(ac - bd)\,e^5; \qquad D = 2s^4 - 5\,(ac - bd)\,e^5;$$
$$E = 2s^4 + 5\,(ab - cd)\,e^5; \qquad F = 2s^4 - 5\,(ab - cd)\,e^5;$$
$$G = 2s^4 + 5\,(ac + bd)\,e^5; \qquad H = 2s^4 - 5\,(ac + bd)\,e^5;$$
$$I = 10se^4.$$

Ved at indsætte hele Værdier for a, b, c, d og e faar man Eksempler paa 9 Femte-Potenser med Summen Nul.

Specielt faar man, idet man i hvert enkelt Tilfælde dividerer med den højeste Potens af femte Grad, som gaar op i alle 9 Potenser.

for $a = 2,\ b = 2,\ c = 1,\ d = 1,\ e = 12$

$$67^5 + 60^5 + 57^5 + 23^5 = 77^5 + 27^5 + 27^5 + 13^5 + 3^5;$$

for $a = 3,\ b = 2,\ c = 1,\ d = 1,\ e = 24$

$$143^5 + 113^5 + 103^5 + 73^5 = 133^5 + 133^5 + 83^5 + 83^5 + 60^5;$$

for $a = 2,\ b = 2,\ c = 1,\ d = 1,\ e = 18$

$$209^5 + 196^5 + 180^5 + 151^5 = 241^5 + 164^5 + 119^5 + 16^5 + 16^5;$$

for $a = 4,\ b = 4,\ c = 1,\ d = 1,\ e = 360$

$$253^5 + 100^5 + 100^5 + 35^5 = 235^5 + 180^5 + 172^5 + 53^5 + 28^5;$$

for $a = 5,\ b = 3,\ c = 1,\ d = 1,\ e = 288$

$$269^5 + 143^5 + 107^5 + 1^5 = 251^5 + 197^5 + 180^5 + 53^5 + 19^5;$$

for $a = 6,\ b = 5,\ c = 3,\ d = 2,\ e = 3840$

$$441^5 + 266^5 + 166^5 = 391^5 + 366^5 + 300^5 + 66^5 + 41^5 + 9^5.$$

2. Vi vender tilbage til Ligningen

$$(x+m)^5+(x-m)^5+(x+n)^5+(x-n)^5 =$$
$$=(x+p)^5+(x-p)^5+(x+q)^5+(x-q)^5+y^5,$$

som reduceres til

$$20x^3(m^2+n^2-p^2-q^2)+10x(m^4+n^4-p^4-q^4) = y^5.$$

Bestemmer man nu m, n, p og q saaledes, at

$$m^4+n^4=p^4+q^4,$$

faar man

$$20x^3(m^2+n^2-p^2-q^2)=y^5,$$

som tilfredsstilles af

$$x=\frac{250a^3}{b^5};\quad y=\frac{50a^2}{b^3},$$

idet man, for Kortheds Skyld, sætter

$$m^2+n^2-p^2-q^2=a.$$

Ved Indsætning i den oprindelige Ligning fremkommer da Identiteten

$$(250a^3+mb^5)^5+(250a^3-mb^5)^5+(250a^3+nb^5)^5+$$
$$(250a^3-nb^5)^5=(250a^3+pb^5)^5+(250a^3-pb^5)^5+$$
$$(250a^3+qb^5)^5+(250a^3-qb^5)^5+(50a^2b^2)^5.$$

Nu har, som bekendt, Ligningen

$$m^4+n^4=p^4+q^4$$

uendelig mange Løsninger.

Euler har først angivet Identiteter, som giver sammenhørende Værdier af de ubekendte, og senere er mange andre fundet, men nogen almindelig Løsning kendes ikke.

Til hvert Sæt Løsninger af Fjerdegrads Ligningen svarer der altsaa Identiteter, som giver 9 Femte-Potenser med Summen Nul.

De mindste Tal, som passer i Fjerdegrads Ligningen er

$$m = 134; \quad n = 133; \quad p = 159; \quad q = 59.$$

Man faar da

$$144000\,x^3 = y^5,$$

som tilfredsstilles af

$$x = \frac{6\,a^5}{5\,b^5}; \qquad y = \frac{12\,a^3}{b^3},$$

og giver Identiteten

$$(6a^5 + 670b^5)^5 + (6a^5 - 670b^5)^5 + (6a^5 + 665b^5)^5 + (6a^5 - 665b^5)^5 = (6a^5 + 790b^5)^5 + (6a^5 - 790b^5)^5 + (6a^5 + 295b^5)^5 + (6a^5 - 295b^5)^5 + (60a^3b^2)^5.$$

Specielt giver $a = 1$, $b = 1$

$$784^5 + 676^5 + 671^5 + 289^5 = 796^5 + 664^5 + 659^5 + 301^5 + 60^5.$$

3. Ligningen paa Side 5 kan gøres mere almindelig, idet man sætter

$$(\alpha x + m)^5 + (\alpha x - m)^5 + (\beta x + n)^5 + (\beta x - n)^5 = (\alpha x + p)^5 + (\alpha x - p)^5 + (\beta x + q)^5 + (\beta x - q)^5 + y^5.$$

Den reduceres til

$$20\,x^3\,(\alpha^3 m^2 + \beta^3 n^2 - \alpha^3 p^2 - \beta^3 q^2) + 10\,x\,(\alpha m^4 + \beta n^4 - \alpha p^4 - \beta q^4) = y^5.$$

Her kan man bestemme de ubekendte saaledes, at

$$\alpha^3\,(m^2 - p^2) = \beta^3\,(q^2 - n^2).$$

Sætter man $m = p + k$,

fremkommer nemlig en Førstegrads Ligning til Bestemmelse af p, hvorpaa x findes af

$$10\,x\,(\alpha m^4 + \beta n^4 - \alpha p^4 - \beta q^4) = y^5.$$

Fremgangsmaaden skal vises ved 2 Eksempler.

4. Første Eksempel.

Ligningen

$$\alpha^3 (m^2 - p^2) = \beta^3 (q^2 - n^2)$$

tilfredsstilles af

$$\alpha = 2,\ \beta = 3,\ m = 9,\ n = 1,\ p = 0,\ q = 5,$$

som giver

$$112500x = y^5,$$

som tilfredsstilles af

$$x = \frac{a^5}{36b^5};\quad y = \frac{5a}{b}.$$

Ved Indsætning i den oprindelige Ligning fremkommer Identiteten:

$$(2a^5 + 324b^5)^5 + (2a^5 - 324b^5)^5 + (3a^5 + 36b^5)^5 +$$
$$(3a^5 - 36b^5)^5 = (2a^5)^5 + (2a^5)^5 + (3a^5 + 180b^5)^5 +$$
$$(3a^5 - 180b^5)^5 + (180ab^4)^5.$$

Specielt giver $a = 2,\ b = 1$

$$97^5 + 33^5 + 21^5 + 15^5 = 90^5 + 69^5 + 65^5 + 16^5 + 16^5;$$

$a = 3,\ b = 1$ giver

$$90^5 + 85^5 + 77^5 + 18^5 = 101^5 + 61^5 + 60^5 + 54^5 + 54^5;$$

$a = 1,\ b = 1$ giver

$$326^5 + 177^5 + 39^5 = 322^5 + 183^5 + 180^5 + 33^5 + 2^5 + 2^5.$$

5. Andet Eksempel.

Ligningen

$$\alpha^3 (m^2 - p^2) = \beta^3 (q^2 - n^2)$$

tilfredsstilles af

$$\alpha = 1,\ \beta = 2,\ m = 5,\ n = 1,\ p = 1,\ q = 2,$$

som giver

$$5940x = y^5,$$

som tilfredsstilles af

$$x = \frac{72\,a^5}{55\,b^5}; \quad y = \frac{6\,a}{5}.$$

Ved Indsætning i den oprindelige Ligning fremkommer Identiteten

$$(72\,a^5 + 275\,b^5)^5 + (72\,a^5 - 275\,b^5)^5 + (144\,a^5 + 55\,b^5)^5 + (144\,a^5 - 55\,b^5)^5 = (72\,a^5 + 55\,b^5)^5 + (72\,a^5 - 55\,b^5)^5 + (144\,a^5 + 110\,b^5)^5 + (144\,a^5 - 110\,b^5)^5 + (330\,ab^4)^5.$$

Specielt giver $a = 1$, $b = 1$

$$347^5 + 199^5 + 89^5 = 330^5 + 254^5 + 203^5 + 127^5 + 34^5 + 17^5.$$

6. De i dette Kapitel fremsatte Identiteter giver Eksempler paa, at

Summen af fire positive Femte-Potenser er lig Summen af fem positive Femte-Potenser,

eller, at

Summen af tre positive Femte-Potenser er lig Summen af seks positive Femte-Potenser.

At der findes uendelig mange Eksempler af hver Slags, ses f. Eks. af den sidste Identitet, idet man i første Tilfælde tager

$$72\,a^5 > 275\,b^5$$

og i andet Tilfælde

$$275\,b^5 > 72\,a^5 > 55\,b^5.$$

7. Efterfølgende Eksempler skyldes ikke Identiteterne, men de er fundne ved Forsøg:

$$11^5 + 10^5 + 6^5 + 1^5 = 12^5 + 7^5 + 5^5 + 2^5 + 2^5,$$

hvor $11 + 10 + 6 + 1 = 12 + 7 + 5 + 2 + 2$;

$$24^5 + 8^5 + 1^5 + 1^5 = 22^5 + 17^5 + 17^5 + 4^5 + 4^5;$$

$$55^5 + 40^5 + 9^5 + 8^5 = 57^5 + 21^5 + 2^5 + 1^5 + 1^5;$$

$$22^5 + 4^5 + 3^5 = 20^5 + 18^5 + 9^5 + 5^5 + 5^5 + 2^5;$$
$$61^5 + 18^5 + 18^5 = 55^5 + 51^5 + 8^5 + 8^5 + 3^5 + 2^5;$$
$$93^5 + 92^5 + 6^5 + 5^5 = 106^5 + 44^5 + 14^5 + 1^5 + 1^5.$$
$$20^5 + 6^5 = 19^5 + 14^5 + 11^5 + 8^5 + 2^5 + 1^5 + 1^5.$$
$$14^5 = 13^5 + 11^5 + 5^5 + 4^5 + 4^5 + 3^5 + 2^5 + 2^5.$$

2. Kapitel.

8 Femte-Potenser.

1. Vi vil betragte Ligningen

$$(x+m)^5 + (x-m)^5 + (x+n)^5 + (x-n)^5 =$$
$$(x+p)^5 + (x-p)^5 + (x+q)^5 + (x-q)^5,$$

som indeholder 8 Femte-Potenser.

Den reduceres, efter Division med $10x$, til

$$2x^2(m^2 + n^2 - p^2 - q^2) = q^4 + p^4 - m^4 - n^4.$$

Sætter man

$$m = \alpha + \beta;\ p = \alpha - \beta;\ q = \gamma + \delta;\ n = \gamma - \delta,$$

omdannes den til

$$x^2(\alpha\beta - \gamma\delta) = \gamma\delta(\gamma^2 + \delta^2) - \alpha\beta(\alpha^2 + \beta^2).$$

Denne Ligning skal løses i 5 specielle Tilfælde.

2. Første Tilfælde.

Vi sætter

$$\beta = 3\gamma;\ \delta = 2\alpha;\ x = 5y,$$

og faar da

$$\alpha^2 = 5y^2 + 5\gamma^2$$

eller
$$\alpha^2 = (\gamma + 2y)^2 + (2\gamma - y)^2.$$

Denne Ligning tilfredsstilles af

$$a = a^2 + b^2;\ \ 2y + \gamma = 2ab;\ \ y + 2\gamma = a^2 - b^2.$$

Dette giver

$$5\beta = 6a^2 + 6ab - 6b^2; \qquad 5\gamma = 2a^2 + 2ab - 2b^2;$$
$$\delta = 2a^2 + 2b^2; \qquad x = -a^2 + 4ab + b^2;$$

og derefter

$$5m = 11a^2 + 6ab - b^2; \qquad 5n = -8a^2 + 2ab - 12b^2;$$
$$5p = -a^2 - 6ab + 11b^2; \quad 5q = 12a^2 + 2ab + 8b^2.$$

Ved Indsætning i den oprindelige Ligning fremkommer da Identiteten

$$A^5 + B^5 + C^5 + D^5 = E^5 + F^5 + G^5 + H^5,$$

hvor

$$A = 6a^2 + 26ab + 4b^2; \quad B = -16a^2 + 14ab + 6b^2;$$
$$C = -13a^2 + 22ab - 7b^2; \quad D = 3a^2 + 18ab + 17b^2;$$
$$E = -6a^2 + 14ab + 16b^2; \quad F = -4a^2 + 26ab - 6b^2;$$
$$G = 7a^2 + 22ab + 13b^2; \quad H = -17a^2 + 18ab - 3b^2.$$

Her er tillige

$$A + B + C + D = E + F + G + H.$$

Her giver $a = 1,\ b = 0$

$$16^5 + 13^5 + 7^5 = 17^5 + 6^5 + 6^5 + 4^5 + 3^5;$$

$a = 1,\ b = 1$ giver

$$21^5 + 12^5 + 8^5 = 19^5 + 18^5 + 2^5 + 1^5 + 1^5;$$

$a = 3,\ b = 1$ giver

$$68^5 + 51^5 + 49^5 = 71^5 + 48^5 + 29^5 + 18^5 + 2^5;$$

$a = 2,\ b = -1$ giver

$$107^5 + 74^5 + 36^5 + 3^5 = 103^5 + 86^5 + 24^5 + 7^5;$$

$a = 5,\ b = 1$ giver

$$169^5 + 142^5 + 91^5 + 32^5 = 162^5 + 149^5 + 111^5 + 12^5;$$

$a = 4,\ b = 1$ giver

$$213^5 + 194^5 + 127^5 + 34^5 = 204^5 + 203^5 + 137^5 + 24^5;$$

$a = 3,\ b = 2$ giver

$$226^5 + 203^5 + 57^5 = 247^5 + 96^5 + 94^5 + 36^5 + 13^5;$$

$a = 5,\ b = 3$ giver

$$288^5 + 249^5 + 91^5 = 311^5 + 118^5 + 102^5 + 68^5 + 29^5.$$

3. Andet Tilfælde.

Vi gaar tilbage til Ligningen

$$x^2(\alpha\beta - \gamma\delta) = \gamma\delta(\gamma^2 + \delta^2) - \alpha\beta(\alpha^2 + \beta^2),$$

og sætter

$$\beta = 4\gamma;\ \delta = 2\alpha,$$

hvoraf

$$2\alpha^2 - x^2 = 31\gamma^2.$$

Sættes nu

$$\gamma = 2\alpha^2 - b^2,$$

faar man

$$31\gamma^2 = 2(8\alpha^2 + 2\alpha b + 4b^2)^2 - (2\alpha^2 + 16\alpha b + b^2)^2.$$

Denne Ligning er tilfredsstillet af

$$x = 2\alpha^2 + 16\alpha b + b^2; \quad \alpha = 8\alpha^2 + 2\alpha b + 4b^2;$$
$$\beta = 8\alpha^2 - 4b^2;\ \gamma = 2\alpha^2 - b^2;\ \delta = 16\alpha^2 + 4\alpha b + 8b^2,$$

som giver

$$m = 16\alpha^2 + 2\alpha b; \quad n = -14\alpha^2 - 4\alpha b - 9b^2;$$
$$p = 2\alpha b + 8b^2; \quad q = 18\alpha^2 + 4\alpha b + 7b^2.$$

Ved Indsætning i den oprindelige Ligning fremkommer Identiteten

$$A^5 + B^5 + C^5 + D^5 = E^5 + F^5 + G^5 + H^5,$$

hvor

$$A = 18\alpha^2 + 18\alpha b + b^2; \quad B = -14\alpha^2 + 14\alpha b + b^2;$$
$$C = -12\alpha^2 + 12\alpha b - 8b^2; \quad D = 16\alpha^2 + 20\alpha b + 10b^2;$$

$E = 2a^2 + 18ab + 9b^2$; $F = 2a^2 + 14ab - 7b^2$;
$G = 20a^2 + 20ab + 8b^2$; $H = -16a^2 + 12ab - 6b^2$.

Tillige er

$$A + B + C + D = E + F + G + H.$$

Specielt giver $a = 1$, $b = 0$

$$9^5 + 8^5 + 8^5 = 10^5 + 7^5 + 6^5 + 1^5 + 1^5;$$

$a = 1$, $b = -1$ giver

$$32^5 + 27^5 + 8^5 = 34^5 + 19^5 + 7^5 + 6^5 + 1^5;$$

$a = 1$, $b = 1$ giver

$$48^5 + 29^5 + 9^5 + 8^5 = 46^5 + 37^5 + 10^5 + 1^5;$$

$a = 2$, $b = -1$ giver

$$83^5 + 80^5 + 48^5 = 94^5 + 37^5 + 34^5 + 27^5 + 19^5;$$

$a = 1$, $b = -3$ giver

$$106^5 + 103^5 + 46^5 = 120^5 + 47^5 + 32^5 + 29^5 + 27^5;$$

$a = 2$, $b = 1$ giver

$$114^5 + 109^5 + 46^5 = 128^5 + 53^5 + 32^5 + 29^5 + 27^5;$$

$a = 1$, $b = 3$ giver

$$152^5 + 137^5 + 48^5 = 166^5 + 81^5 + 37^5 + 34^5 + 19^5;$$

$a = 3$, $b = -1$ giver

$$167^5 + 152^5 + 128^5 = 186^5 + 109^5 + 94^5 + 31^5 + 27^5;$$

$a = 2$, $b = -3$ giver

$$192^5 + 131^5 + 32^5 + 27^5 = 190^5 + 139^5 + 34^5 + 19^5;$$

$a = 3$, $b = 1$ giver

$$217^5 + 214^5 + 114^5 = 248^5 + 83^5 + 81^5 + 80^5 + 53^5;$$

$a = 5$, $b = -2$ giver

$$243^5 + 226^5 + 166^5 = 272^5 + 137^5 + 120^5 + 59^5 + 47^5;$$

$a = 2$, $b = 3$ giver

$$274^5 + 189^5 + 46^5 + 37^5 = 272^5 + 197^5 + 48^5 + 29^5;$$

$a = 5$, $b = 2$ giver

$$320^5 + 317^5 + 152^5 = 366^5 + 133^5 + 106^5 + 103^5 + 81^5.$$

4. Tredie Tilfælde.

I Ligningen

$$x^2(\alpha\beta - \gamma\delta) = \gamma\delta(\gamma + \delta) - \alpha\beta(\alpha + \beta)$$

sætter man

$$\beta = 3\gamma;\ \delta = 3\varphi;\ \alpha = 2\varphi;\ \gamma = 2\varepsilon,$$

som giver

$$\varphi^2 - x^2 = 68\,\varepsilon^2.$$

Denne Ligning tilfredsstilles af

$$\varphi = 17a^2 + b^2;\ x = 17a^2 - b^2;\ \varepsilon = ab,$$

hvorpaa

$$\alpha = 34a^2 + 2b^2; \quad \beta = 6ab; \quad \delta = 51a^2 + 3b^2;$$
$$m = 34a^2 + 6ab + 2b^2; \quad p = 34a^2 - 6ab + 2b^2;$$
$$q = 51a^2 + 2ab + 3b^2; \quad n = -51a^2 + 2ab - 3b^2.$$

Ved Indsætning i den oprindelige Ligning fremkommer Identiteten

$$A^5 + B^5 + C^5 + D^5 = E^5 + F^5 + G^5 + H^5,$$

hvor

$$A = 51a^2 + 6ab + b^2; \quad B = 17a^2 - 6ab + 3b^2;$$
$$C = 34a^2 + 2ab + 4b^2; \quad D = 68a^2 - 2ab + 2b^2;$$
$$E = 51a^2 - 6ab + b^2; \quad F = 17a^2 + 6ab + 3b^2;$$
$$G = 34a^2 - 2ab + 4b^2; \quad H = 68a^2 + 2ab + 2b^2.$$

Tillige er

$$A + B + C + D = E + F + G + H.$$

Specielt giver $a = 1,\ b = 1$

$$36^5 + 23^5 + 18^5 + 13^5 = 34^5 + 29^5 + 20^5 + 7^5;$$

$a = 1,\ b = 3$ giver

$$46^5 + 32^5 + 31^5 + 21^5 = 40^5 + 39^5 + 38^5 + 13^5;$$

$a = 1,\ b = 5$ giver

$$72^5 + 54^5 + 53^5 + 31^5 = 64^5 + 62^5 + 61^5 + 23^5;$$

$a = 1,\ b = 2$ giver

$$80^5 + 46^5 + 43^5 + 41^5 = 72^5 + 67^5 + 54^5 + 17^5;$$

$a = 1,\ b = 4$ giver

$$108^5 + 90^5 + 89^5 + 43^5 = 106^5 + 92^5 + 91^5 + 41^5;$$

$a = 1,\ b = 7$ giver

$$122^5 + 76^5 + 71^5 + 61^5 = 108^5 + 103^5 + 90^5 + 29^5;$$

$a = 1,\ b = 9$ giver

$$188^5 + 106^5 + 103^5 + 93^5 = 170^5 + 157^5 + 124^5 + 39^5;$$

$a = 1,\ b = 6$ giver

$$190^5 + 128^5 + 123^5 + 89^5 = 166^5 + 161^5 + 152^5 + 51^5;$$

$a = 1,\ b = 11$ giver

$$270^5 + 157^5 + 144^5 + 119^5 = 248^5 + 223^5 + 166^5 + 53^5;$$

$a = 2,\ b = 1$ giver

$$278^5 + 193^5 + 136^5 + 83^5 = 270^5 + 217^5 + 144^5 + 59^5;$$

$a = 2,\ b = 3$ giver

$$302^5 + 177^5 + 160^5 + 131^5 = 278^5 + 249^5 + 184^5 + 79^5.$$

5. Fjerde Tilfælde.

I Ligningen

$$x^2(\alpha\beta - \gamma\delta) = \gamma\delta(\gamma^2 + \delta^2) - \alpha\beta(\alpha^2 + \beta^2)$$

sætter man

$$\alpha = (r^3 + r)\, b;\ \beta = a;\ \gamma = ra;\ \delta = 2b,$$

som giver

$$x^2 (r^3 - r) = a^2 (r^3 - r) - b^2 ((r^3 + r)^3 - 8r).$$

Forudsætter man, at r er forskellig fra $+1$, 0 og -1, kan man bortdividere $r^3 - r$ og faar da

$$a^2 - x^2 = (r^6 + 4\, r^4 + 7\, r^2 + 8)\, b^2.$$

Sætter man nu $b = 2de$ og, for Kortheds Skyld,

$$r^6 + 4r^4 + 7r^2 + 8 = k,$$

faar man

$$a^2 - x^2 = 4kd^2e^2,$$

som tilfredsstilles af

$$a = kd^2 + e^2;\ x = kd^2 - e^2.$$

Dette giver

$$\alpha = (2r^3 + 2r)\, de; \qquad \beta = kd^2 + e^2;$$
$$\gamma = krd^2 + re^2; \qquad \delta = 4de,$$

og derefter

$$m = kd^2 + (2r^3 + 2r)\, de + e^2; \qquad n = rkd^2 - 4de + re^2;$$
$$p = -kd^2 + (2r^3 + 2r)\, de - e^2; \qquad q = rkd^2 + 4de + re^2.$$

Ved Indsætning i den oprindelige Ligning fremkommer Identiteten

$$A^5 + B^5 + C^5 + D^5 = E^5 + F^5 + G^5 + H^5,$$

hvor

$$A = 2kd^2 + (2r^3 + 2r)\, de;$$
$$B = (-2r^3 - 2r)\, de - 2e^2;$$
$$C = (kr + k)\, d^2 - 4de + (r - 1)\, e^2;$$
$$D = (-kr + k)\, d^2 + 4de - (r + 1)\, e^2;$$
$$E = (2r^3 + 2r)\, de - 2e^2;$$
$$F = 2kd^2 - (2r^3 + 2r)\, de;$$

$$G = (kr + k)\, d^2 + 4\, de + (r - 1)\, e^2;$$
$$H = (-kr + k)\, d^2 - 4\, de - (r + 1)\, e^2.$$

Tillige er

$$A + B + C + D = E + F + G + H.$$

Specielt giver $r = 2,\ d = 1,\ e = 2$

$$61^5 + 46^5 + 23^5 = 63^5 + 36^5 + 21^5 + 6^5 + 4^5;$$

$r = 2,\ d = 1,\ e = 6$ giver

$$63^5 + 56^5 + 37^5 = 69^5 + 31^5 + 26^5 + 24^5 + 6^5;$$

$r = 2,\ d = 1,\ e = 10$ giver

$$69^5 + 66^5 + 63^5 = 79^5 + 53^5 + 50^5 + 16^5,$$

som kun indeholder 7 Femte-Potenser:

$r = 2,\ d = 1,\ e = 14$ giver

$$101^5 + 79^5 + 76^5 + 14^5 = 93^5 + 87^5 + 84^5 + 6^5;$$

$r = 2,\ d = 1,\ e = 4$ giver

$$123^5 + 102^5 + 57^5 = 131^5 + 62^5 + 49^5 + 28^5 + 12^5;$$

$r = 2,\ d = 1,\ e = 8$ giver

$$131^5 + 122^5 + 97^5 = 147^5 + 81^5 + 72^5 + 42^5 + 8^5;$$

$r = 2,\ d = 1,\ e = 18$ giver

$$133^5 + 126^5 + 111^5 = 151^5 + 93^5 + 86^5 + 36^5 + 4^5;$$

$r = 2,\ d = 1,\ e = 12$ giver

$$171^5 + 137^5 + 132^5 + 22^5 = 161^5 + 147^5 + 142^5 + 12^5;$$

$r = 2,\ d = 1,\ e = 22$ giver

$$191^5 + 176^5 + 133^5 = 213^5 + 111^5 + 96^5 + 66^5 + 14^5;$$

$r = 2,\ d = 1,\ e = 16$ giver

$$249^5 + 171^5 + 162^5 + 48^5 = 217^5 + 208^5 + 203^5 + 2^5;$$

$r = 2,\ d = 1,\ e = 26$ giver

$$261^5 + 234^5 + 159^5 = 287^5 + 133^5 + 106^5 + 104^5 + 24^5;$$

$r = 2$, $d = 1$, $e = 20$ giver

$$321^5 + 300^5 + 243^5 = 361^5 + 203^5 + 182^5 + 100^5 + 18^5.$$

6. Femte Tilfælde.

I Ligningen

$$x^2(\alpha\beta - \gamma\delta) = \gamma\delta(\gamma^2 + \delta^2) - \alpha\beta(\alpha^2 + \beta^2)$$

sættes $$x = \delta = \frac{\alpha\beta}{2\gamma},$$

hvorved man faar $$\gamma^2 = 2\alpha^2 + 2\beta^2,$$

som tilfredsstilles af

$$\alpha = a^2 + 2ab - b^2; \quad \beta = a^2 - 2ab - b^2;$$

$$\gamma = 2a^2 + 2b^2; \qquad \delta = \frac{a^4 - 6a^2b^2 + b^4}{4a^2 + b^2}.$$

Ved Indsætning i den oprindelige Ligning fremkommer Identiteten

$$A^5 + B^5 + C^5 = D^5 + E^5 + F^5 + G^5 + H^5,$$

hvor

$$\begin{aligned}
A &= 9a^4 - 6a^2b^2 - 7b^4;\\
B &= 8a^4 + 16a^2b^2 + 8b^4;\\
C &= 8a^4 + 16a^2b^2 + 8b^4;\\
D &= 10a^4 + 4a^2b^2 + 10b^4;\\
E &= 7a^4 + 6a^2b^2 - 9b^4;\\
F &= 6a^4 + 28a^2b^2 + 6b^4;\\
G &= a^4 + 16a^3b - 6a^2b^2 + 16ab^3 + b^4;\\
H &= a^4 - 16a^3b - 6a^2b^2 - 16ab^3 + b^4,
\end{aligned}$$

hvor tillige

$$A + B + C = D + E + F + G + H.$$

Specielt giver $a = 1$, $b = 0$

$$9^5 + 8^5 + 8^5 = 10^5 + 7^5 + 6^5 + 1^5 + 1^5;$$

$a = 2$, $b = 1$ giver

$$214^5 + 186^5 + 153^5 + 127^5 = 200^5 + 200^5 + 167^5 + 113^5;$$

$a = 5$, $b = 1$ giver

$$1590^5 + 1129^5 + 1114^5 + 639^5 = 1367^5 + 1352^5 + 1352^5 + 401^5.$$

7. Ligningen

$$(x + \alpha)^5 + (x - \alpha)^5 + 2y^5 = (y + \beta)^5 + (y - \beta)^5 + 2x^5$$

reduceres til

$$\alpha^2 x (2x^2 + \alpha^2) = \beta^2 y (2y^2 + \beta^2).$$

Denne Ligning skal løses i 2 specielle Tilfælde.

8. Første Tilfælde.

Man sætter

$$x = \frac{\beta^2}{2m}; \qquad y = \frac{\alpha^2}{2m},$$

og faar

$$\beta^4 + 2\alpha^2 m^2 = \alpha^4 + 2\beta^2 m^2,$$

som, for $\alpha \gtrless \beta$, giver

$$\alpha^2 + \beta^2 = 2m^2.$$

Denne Ligning tilfredsstilles af

$$a = a^2 + 2ab - b^2; \ \beta = a^2 - 2ab - b^2; \ m = a^2 + b^2,$$

hvoraf

$$x = \frac{(a^2 - 2ab - b^2)^2}{2a^2 + 2b^2}; \qquad y = \frac{(a^2 + 2ab - b^2)^2}{2a^2 + 2b^2}.$$

Ved Indsætning i den oprindelige Ligning fremkommer Identiteten

$$2A^{10} + B^5 + C^5 = 2D^{10} + E^5 + F^5,$$

hvor

$$A = a^2 + 2ab - b^2;$$
$$B = 3a^4 + 2a^2b^2 + 8ab^3 - b^4;$$

$$C = -a^4 - 8a^3b + 2a^2b^2 + 3b^4;$$
$$D = a^2 - 2ab - b^2;$$
$$E = 3a^4 + 2a^2b^2 - 8ab^3 - b^4;$$
$$F = -a^4 + 8a^3b + 2a^2b^2 + 3b^4;$$

Denne Identitet kan ogsaa skrives saaledes

$$(A^2)^5 + (A^2)^5 + B^5 + C^5 = (D^2)^5 + (D^2)^5 + E^5 + F^5,$$

hvor tillige

$$A^2 + A^2 + B + C = D^2 + D^2 + E + F.$$

Specielt giver $c = 2$, $d = 1$

$$71^5 + 49^5 + 49^5 = 69^5 + 59^5 + 39^5 + 1^5 + 1^5;$$

$c = 3$, $d = 2$ giver

$$491^5 + 289^5 + 289^5 = 471^5 + 393^5 + 107^5 + 49^5 + 49^5.$$

9. Andet Tilfælde.

Ligningen

$$\alpha^2 x\,(2x^2 + \alpha^2) = \beta^2 y\,(2y^2 + \beta^2)$$

kan løses ved at man sætter

$$2\alpha^2 x^3 = \beta^4 y; \quad \alpha^4 x = 2\beta^2 y^3,$$

hvoraf

$$x = \frac{\alpha^6}{8b^5}; \qquad \beta = \frac{\alpha^5}{4b^4}; \qquad \alpha = a.$$

Ved Indsætning i den oprindelige Ligning fremkommer Identiteten

$$2A^{15} + B^5 + C^5 = 2D^{15} + E^5 + F^5,$$

hvor

$$A = 2b^2; \quad B = a^6 + 8ab^5; \quad C = a^6 - 8ab^5;$$
$$D = a^2; \quad E = 2a^5b + 8b^6; \quad F = -2a^5b + 8b^6.$$

Denne Identitet kan ogsaa skrives saaledes

$$(A^3)^5 + (A^3)^5 + B^5 + C^5 = (D^3)^5 + (D^3)^5 + E^5 + F^5,$$

hvor tillige

$$A^3 + A^3 + B + C = D^3 + D^3 + E + F.$$

Specielt giver $a = 1$, $b = 1$

$$9^5 + 8^5 + 8^5 = 10^5 + 7^5 + 6^5 + 1^5 + 1^5;$$

$a = 1$, $b = 2$ giver

$$512^5 + 512^5 + 257^5 = 516^5 + 508^5 + 255^5 + 1^5 + 1^5.$$

10. De i dette Kapitel fremsatte Identiteter giver Eksempler paa, at

Summen af fire positive Femte-Potenser er lig Summen af fire andre positive Femte-Potenser

eller at

Summen af tre positive Femte-Potenser er lig Summen af fem positive Femte-Potenser.

At der gives uendelig mange Tilfælde af hver Slags ses f. Eks.

i første Tilfælde af Identiteten paa Side 15 ved at tage $a > b > 0$

og i andet Tilfælde af Identiteten paa Side 13 ved at tage $14a > 15b > 0$.

11. Efterfølgende Eksempler skyldes ikke Identiteterne, men de er fundne ved Forsøg.

$$24^5 + 3^5 + 1^5 + 1^5 = 23^5 + 15^5 + 15^5 + 6^5.$$

$$29^5 + 10^5 + 1^5 + 1^5 = 26^5 + 24^5 + 15^5 + 6^5.$$

$$29^5 + 23^5 + 15^5 + 10^5 = 26^5 + 24^5 + 24^5 + 3^5,$$

hvor $29 + 23 + 15 + 10 = 26 + 24 + 24 + 3$.

$$30^5 + 12^5 + 8^5 + 7^5 = 29^5 + 21^5 + 5^5 + 2^5.$$

$$51^5 + 15^5 + 14^5 + 5^5 = 48^5 + 39^5 + 16^5 + 12^5.$$

$$64^5 + 61^5 + 37^5 + 13^5 = 63^5 + 62^5 + 38^5 + 12^5,$$

hvor $64 + 61 + 37 + 13 = 63 + 62 + 38 + 12$.

$$99^5 + 67^5 + 14^5 + 6^5 = 96^5 + 77^5 + 9^5 + 4^5,$$
hvor $99 + 67 + 14 + 6 = 96 + 77 + 9 + 4.$

$$7^5 + 7^5 + 3^5 = 8^5 + 4^5 + 2^5 + 2^5 + 1^5,$$
hvor $7 + 7 + 3 = 8 + 4 + 2 + 2 + 1.$

$$15^5 + 14^5 + 3^5 = 16^5 + 12^5 + 2^5 + 1^5 + 1^5,$$
hvor $15 + 14 + 3 = 16 + 12 + 2 + 1 + 1.$

$$20^5 + 17^5 + 5^5 = 21^5 + 14^5 + 4^5 + 2^5 + 1^5,$$
hvor $20 + 17 + 5 = 21 + 14 + 4 + 2 + 1.$

$$48^5 + 39^5 + 3^5 = 51^5 + 5^5 + 2^5 + 1^5 + 1^5.$$

$$27^5 + 27^5 = 31^5 + 8^5 + 8^5 + 5^5 + 1^5 + 1^5,$$
hvor $27 + 27 = 31 + 8 + 8 + 5 + 1 + 1.$

$$32^5 + 14^5 = 30^5 + 25^5 + 7^5 + 6^5 + 4^5 + 4^5.$$

$$31^5 + 28^5 = 34^5 + 13^5 + 8^5 + 2^5 + 1^5 + 1^5,$$
hvor $31 + 28 = 34 + 13 + 8 + 2 + 1 + 1.$

$$53^5 + 43^5 = 52^5 + 45^5 + 13^5 + 10^5 + 3^5 + 3^5.$$

$$54^5 + 9^5 = 53^5 + 29^5 + 29^5 + 5^5 + 5^5 + 2^5.$$

$$92^5 = 89^5 + 58^5 + 51^5 + 22^5 + 11^5 + 9^5 + 2^5.$$

12. Af de i dette Kapitel fundne Eksempler kan udledes, at

$$51^5 + 5^5 - 48^5 - 39^5 = 16^5 + 12^5 - 15^5 - 14^5 =$$
$$= 3^5 - 2^5 - 1^5 - 1^5 = 209;$$

$$29^5 + 10^5 - 26^5 - 24^5 = 24^5 + 3^5 - 23^5 - 15^5 =$$
$$= 15^5 + 6^5 - 1^5 - 1^5 = 767149;$$

$$128^5 + 53^5 - 114^5 - 109^5 = 120^5 + 47^5 - 106^5 - 103^5 =$$
$$= 46^5 - 32^5 - 29^5 - 27^5 = 137558488.$$

Tallene 209, 767149 og 137558488 kan da, hver især, paa 3 Maader skrives som en Sum af 4 (positive eller negative) Femte-Potenser.

Man faar endvidere

$$48^5 + 29^5 - 46^5 - 37^5 = 34^5 + 19^5 - 32^5 - 27^5 =$$
$$= 10^5 + 1^5 - 9^5 - 8^5 = 8^5 - 7^5 - 6^5 - 1^5 = 8184 = 2^{13} - 2^3.$$

Tallet 8184 kan altsaa paa 4 Maader skrives som en Sum af 4 (positive eller negative) Femte-Potenser.

3. Kapitel.

7 Femte-Potenser.

1. At der eksisterer 7 Femte-Potenser med Summen Nul, viser MARTINS Tal

$$12^5 = 11^5 + 9^5 + 7^5 + 6^5 + 5^5 + 4^5$$

og
$$30^5 = 29^5 + 19^5 + 16^5 + 11^5 + 10^5 + 5^5.$$

2. Naar man i Identiteten paa Side 17, som indeholder 8 Femte-Potenser, sætter

$$e = -(r^3 + r)\,d \quad \text{og} \quad r = \frac{y}{z},$$

fremkommer følgende Identitet, som kun indeholder 7 Femte-Potenser.

$$A^5 + B^5 + C^5 = D^5 + E^5 + F^5 + G^5,$$

hvor

$$A = y^7 + 3y^5z^2 + y^4z^3 + 2y^3z^4 + 3y^2z^5 + 2yz^6 + 4z^7;$$
$$B = y^7 + 3y^5z^2 - y^4z^3 + 6y^3z^4 - 3y^2z^5 + 6yz^6 - 4z^7;$$
$$C = 2y^6z + 6y^4z^3 + 8y^2z^5 + 8z^7;$$
$$D = y^7 + 3y^5z^2 + y^4z^3 + 6y^3z^4 + 3y^2z^5 + 6yz^6 + 4z^7;$$
$$E = y^7 + 3y^5z^2 - y^4z^3 + 2y^3z^4 - 3y^2z^5 + 2yz^6 - 4z^7;$$
$$F = 2y^6z + 4y^4z^3 + 2y^2z^5;$$
$$G = 2y^4z^3 + 6y^2z^5 + 8z^7.$$

Tillige er

$$A + B + C = D + E + F + G.$$

Specielt giver $y = 2$, $z = 1$

$$69^5 + 66^5 + 63^5 = 79^5 + 53^5 + 50^5 + 16^5.$$

$y = 1$, $z = 2$ giver

$$1332^5 + 789^5 + 443^5 = 1232^5 + 1109^5 + 123^5 + 100^5.$$

3. Forandrer y eller z Fortegn, bliver Identiteten den samme. Man kan da antage y og z for positive.

A, C, D, F og G er da positive.

Da $B > E$, maa enten B og E have samme Fortegn, eller ogsaa maa B være positiv og E negativ. I begge Tilfælde faar man, at

Summen af 3 positive Femte-Potenser er lig Summen af 4 positive Femte-Potenser.

Der er altsaa uendelig mange Tal, som baade er en Sum af 3 og af 4 positive Femte-Potenser.

4. Efterfølgende Eksempler er fundne ved Forsøg:

$$25^5 + 22^5 + 3^5 = 27^5 + 14^5 + 8^5 + 1^5,$$

hvor $25 + 22 + 3 = 27 + 14 + 8 + 1.$

$$34^5 + 10^5 + 1^5 = 33^5 + 20^5 + 20^5 + 2^5.$$

$$22^5 + 1^5 = 21^5 + 16^5 + 7^5 + 5^5 + 4^5.$$

$$64^5 + 45^5 = 58^5 + 57^5 + 11^5 + 9^5 + 4^5.$$

4. Kapitel.

6 Femte-Potenser.

1. I forrige Kapitel viste det sig, at en Identitet med flere Variable, som indeholder 8 Femte-Potenser, specielt kan give en Identitet, ligeledes med flere Variable, som indeholder 7 Femte-Potenser.

Det ligger da nær at antage, at man analogt af de allerede fundne Identiteter kan komme til Identiteter, som

giver 6 Femte-Potenser med Summen Nul, men dette lader sig ikke gøre.

2. At der imidlertid eksisterer 6 Femte-Potenser med Summen Nul, kan man se af følgende Eksempel, som er fundet ved Forsøg.

$$29^5 + 3^5 = 28^5 + 20^5 + 10^5 + 4^5,$$

og her skal nu fremsættes en Identitet, som giver andre Eksempler af samme Art.

3. Vi betragter Ligningen

$$(x^5 + ay^5)^5 + (x^5 - ay^5)^5 =$$
$$(x + by^5)^5 + (x - by^5)^5 + (cx^3y^2)^5 + (dxy^4)^5.$$

Denne Ligning reduceres, hvorefter man dividerer med x^5y^5.

Derved faar man

$$20\,a^2x^{10} + 10\,a^4y^{10} = 20\,b^2x^{10} + 10\,b^4y^{10} + c^5x^{10} + d^5y^{10}.$$

Hvis man nu kan bestemme

$$a,\ b,\ c \text{ og } d$$

saaledes, at

$$20\,(a^2 - b^2) = c^5 \quad \text{og} \quad 10\,(a^4 - b^4) = d^5,$$

bliver den givne Ligning en Identitet.

Jeg har fundet Tallene

$$a = 75;\ b = 25;\ c = 10;\ d = 50,$$

som opfylder disse Betingelser.

Herved fremkommer Identiteten

$$(x^5 + 75\,y^5)^5 + (x^5 - 75\,y^5)^5 =$$
$$(x^5 + 25\,y^5)^5 + (x^5 - 25\,y^5)^5 + (10\,x^3y^2)^5 + (50\,xy^4)^5.$$

Specielt giver $x = 1,\ y = 1$

$$38^5 + 12^5 = 37^5 + 25^5 + 13^5 + 5^5.$$

$x = 5,\ y = 1$ giver

$$64^5 + 61^5 = 63^5 + 62^5 + 25^5 + 5^5.$$

$x = 2,\ y = 1$ giver

$$107^5 = 100^5 + 80^5 + 57^5 + 43^5 + 7^5.$$

$x = 3,\ y = 1$ giver

$$159^5 + 84^5 = 135^5 + 134^5 + 109^5 + 75^5.$$

$x = 5,\ y = 2$ giver

$$221^5 + 29^5 = 200^5 + 160^5 + 157^5 + 93^5.$$

$x = 5,\ y = 3$ giver

$$427^5 + 59^5 = 405^5 + 302^5 + 225^5 + 184^5.$$

$x = 7,\ y = 3$ giver

$$17516^5 = 15435^5 + 14175^5 + 11441^5 + 5366^5 + 709^5.$$

4. Identiteten i dette Kapitel giver enten

en Sum af 2 positive Femte-Potenser, som er lig en Sum af 4 positive Femte-Potenser,

eller

en positiv Femte-Potens, som er lig Summen af 5 positive Femte-Potenser.

5. At der er uendelig mange af hver Slags, ses ved i første Tilfælde at vælge x og y saaledes, at

$$x^5 > 75y^5,$$

og i andet Tilfælde saaledes, at

$$75y^5 > x^5 > 25y^5.$$

Efter at ovenstaaende er skrevet, har jeg set, at Identiteten paa Side 26 ikke er ny, men er fundet af

S. Sastry i »The Journal of The London Mathematical Society« 1934 i en Artikel »On sums of powers«, Side 243.

Tabel over Femte-Potenser.

1.

$11^5 + 10^5 + 6^5 + 1^5 = 12^5 + 7^5 + 5^5 + 2^5 + 2^5.$
$24^5 + 8^5 + 1^5 + 1^5 = 22^5 + 17^5 + 17^5 + 4^5 + 4^5.$
$55^5 + 40^5 + 9^5 + 8^5 = 57^5 + 21^5 + 2^5 + 1^5 + 1^5.$
$67^5 + 60^5 + 57^5 + 23^5 = 77^5 + 27^5 + 27^5 + 13^5 + 3^5.$
$97^5 + 33^5 + 21^5 + 15^5 = 90^5 + 69^5 + 65^5 + 16^5 + 16^5.$
$90^5 + 85^5 + 77^5 + 18^5 = 101^5 + 61^5 + 60^5 + 54^5 + 54^5.$
$143^5 + 113^5 + 103^5 + 73^5 = 133^5 + 133^5 + 83^5 + 83^5 + 60^5.$
$209^5 + 196^5 + 180^5 + 151^5 = 241^5 + 164^5 + 119^5 + 16^5 + 16^5.$
$253^5 + 100^5 + 100^5 + 35^5 = 235^5 + 180^5 + 172^5 + 53^5 + 28^5.$
$269^5 + 143^5 + 107^5 + 1^5 = 251^5 + 197^5 + 180^5 + 53^5 + 19^5.$
$93^5 + 92^5 + 6^5 + 5^5 = 106^5 + 44^5 + 14^5 + 1^5 + 1^5.$

$22^5 + 4^5 + 3^5 = 20^5 + 18^5 + 9^5 + 5^5 + 5^5 + 2^5.$
$61^5 + 18^5 + 18^5 = 55^5 + 51^5 + 8^5 + 8^5 + 3^5 + 2^5.$

$20^5 + 6^5 = 19^5 + 14^5 + 11^5 + 8^5 + 2^5 + 1^5 + 1^5.$

$14^5 = 13^5 + 11^5 + 5^5 + 4^5 + 4^5 + 3^5 + 2^5 + 2^5.$

2.

$24^5 + 3^5 + 1^5 + 1^5 = 23^5 + 15^5 + 15^5 + 6^5.$
$29^5 + 10^5 + 1^5 + 1^5 = 26^5 + 24^5 + 15^5 + 6^5.$
$29^5 + 23^5 + 15^5 + 10^5 = 26^5 + 24^5 + 24^5 + 3^5.$
$30^5 + 12^5 + 8^5 + 7^5 = 29^5 + 21^5 + 5^5 + 2^5.$
$36^5 + 23^5 + 18^5 + 13^5 = 34^5 + 29^5 + 20^5 + 7^5.$
$46^5 + 32^5 + 31^5 + 21^5 = 40^5 + 39^5 + 38^5 + 13^5.$
$48^5 + 29^5 + 9^5 + 8^5 = 46^5 + 37^5 + 10^5 + 1^5.$
$51^5 + 15^5 + 14^5 + 5^5 = 48^5 + 39^5 + 16^5 + 12^5.$
$64^5 + 61^5 + 37^5 + 13^5 = 63^5 + 62^5 + 38^5 + 12^5.$
$72^5 + 54^5 + 53^5 + 31^5 = 64^5 + 62^5 + 61^5 + 23^5.$

$80^5 + 46^5 + 43^5 + 41^5 = 72^5 + 67^5 + 54^5 + 17^5.$
$99^5 + 67^5 + 14^5 + 6^5 = 96^5 + 77^5 + 9^5 + 4^5.$
$101^5 + 79^5 + 76^5 + 14^5 = 93^5 + 87^5 + 84^5 + 6^5.$
$107^5 + 74^5 + 36^5 + 3^5 = 103^5 + 86^5 + 24^5 + 7^5.$
$108^5 + 90^5 + 89^5 + 43^5 = 106^5 + 92^5 + 91^5 + 41^5.$
$122^5 + 76^5 + 71^5 + 61^5 = 108^5 + 103^5 + 90^5 + 29^5.$
$169^5 + 142^5 + 91^5 + 32^5 = 162^5 + 149^5 + 111^5 + 12^5.$
$171^5 + 137^5 + 132^5 + 22^5 = 161^5 + 147^5 + 142^5 + 12^5.$
$188^5 + 106^5 + 103^5 + 93^5 = 170^5 + 157^5 + 124^5 + 39^5.$
$190^5 + 128^5 + 123^5 + 89^5 = 166^5 + 161^5 + 152^5 + 51^5.$
$192^5 + 131^5 + 32^5 + 27^5 = 190^5 + 139^5 + 34^5 + 19^5.$
$213^5 + 194^5 + 127^5 + 34^5 = 204^5 + 203^5 + 137^5 + 24^5.$
$214^5 + 186^5 + 153^5 + 127^5 = 200^5 + 200^5 + 167^5 + 113^5.$
$249^5 + 171^5 + 162^5 + 48^5 = 217^5 + 208^5 + 203^5 + 2^5.$
$270^5 + 157^5 + 144^5 + 119^5 = 248^5 + 223^5 + 166^5 + 53^5.$
$274^5 + 189^5 + 46^5 + 37^5 = 272^5 + 197^5 + 48^5 + 29^5.$
$278^5 + 193^5 + 136^5 + 83^5 = 270^5 + 217^5 + 144^5 + 59^5.$

$7^5 + 7^5 + 3^5 = 8^5 + 4^5 + 2^5 + 2^5 + 1^5.$
$9^5 + 8^5 + 8^5 = 10^5 + 7^5 + 6^5 + 1^5 + 1^5.$
$15^5 + 14^5 + 3^5 = 16^5 + 12^5 + 2^5 + 1^5 + 1^5.$
$16^5 + 13^5 + 7^5 = 17^5 + 6^5 + 6^5 + 4^5 + 3^5.$
$21^5 + 12^5 + 8^5 = 19^5 + 18^5 + 2^5 + 1^5 + 1^5.$
$20^5 + 17^5 + 5^5 = 21^5 + 14^5 + 4^5 + 2^5 + 1^5.$
$32^5 + 27^5 + 8^5 = 34^5 + 19^5 + 7^5 + 6^5 + 1^5.$
$48^5 + 39^5 + 3^5 = 51^5 + 5^5 + 2^5 + 1^5 + 1^5.$
$61^5 + 46^5 + 23^5 = 63^5 + 36^5 + 21^5 + 6^5 + 4^5.$
$63^5 + 56^5 + 37^5 = 69^5 + 31^5 + 26^5 + 24^5 + 6^5.$
$68^5 + 51^5 + 49^5 = 71^5 + 48^5 + 29^5 + 18^5 + 2^5.$
$69^5 + 66^5 + 63^5 = 79^5 + 53^5 + 50^5 + 16^5.$
$71^5 + 49^5 + 49^5 = 69^5 + 59^5 + 39^5 + 1^5 + 1^5.$
$83^5 + 80^5 + 48^5 = 94^5 + 37^5 + 34^5 + 27^5 + 19^5.$

$106^5 + 103^5 + 46^5 = 120^5 + 47^5 + 32^5 + 29^5 + 27^5.$
$114^5 + 109^5 + 46^5 = 128^5 + 53^5 + 32^5 + 29^5 + 27^5.$
$123^5 + 102^5 + 57^5 = 131^5 + 62^5 + 49^5 + 28^5 + 12^5.$
$131^5 + 122^5 + 97^5 = 147^5 + 81^5 + 72^5 + 42^5 + 8^5.$
$133^5 + 126^5 + 111^5 = 151^5 + 93^5 + 86^5 + 36^5 + 4^5.$
$152^5 + 137^5 + 48^5 = 166^5 + 81^5 + 37^5 + 34^5 + 19^5.$
$167^5 + 152^5 + 128^5 = 186^5 + 109^5 + 94^5 + 31^5 + 27^5.$
$191^5 + 176^5 + 133^5 = 213^5 + 111^5 + 96^5 + 66^5 + 14^5.$
$217^5 + 214^5 + 114^5 = 248^5 + 83^5 + 81^5 + 80^5 + 53^5.$
$226^5 + 203^5 + 57^5 = 247^5 + 96^5 + 94^5 + 36^5 + 13^5.$
$243^5 + 226^5 + 166^5 = 272^5 + 137^5 + 120^5 + 59^5 + 47^5.$
$261^5 + 234^5 + 159^5 = 287^5 + 133^5 + 106^5 + 104^5 + 24^5.$

$27^5 + 27^5 = 31^5 + 8^5 + 8^5 + 5^5 + 1^5 + 1^5.$
$32^5 + 14^5 = 30^5 + 25^5 + 7^5 + 6^5 + 4^5 + 4^5.$
$31^5 + 28^5 = 34^5 + 13^5 + 8^5 + 2^5 + 1^5 + 1^5.$
$53^5 + 43^5 = 52^5 + 45^5 + 13^5 + 10^5 + 3^5 + 3^5.$
$54^5 + 9^5 = 53^5 + 29^5 + 29^5 + 5^5 + 5^5 + 2^5.$

$92^5 = 89^5 + 58^5 + 51^5 + 22^5 + 11^5 + 9^5 + 2^5.$

3.

$25^5 + 22^5 + 3^5 = 27^5 + 14^5 + 8^5 + 1^5.$
$34^5 + 10^5 + 1^5 = 33^5 + 20^5 + 20^5 + 2^5.$
$69^5 + 66^5 + 63^5 = 79^5 + 53^5 + 50^5 + 16^5.$

$22^5 + 1^5 = 21^5 + 16^5 + 7^5 + 5^5 + 4^5.$
$64^5 + 45^5 = 58^5 + 57^5 + 11^5 + 9^5 + 4^5.$

4.

$29^5 + 3^5 = 28^5 + 20^5 + 10^5 + 4^5.$
$38^5 + 12^5 = 37^5 + 25^5 + 13^5 + 5^5.$

$64^5 + 61^5 = 63^5 + 62^5 + 25^5 + 5^5.$

$159^5 + 84^5 = 135^5 + 134^5 + 109^5 + 75^5.$

$221^5 + 29^5 = 200^5 + 160^5 + 157^5 + 93^5.$

$107^5 = 100^5 + 80^5 + 57^5 + 43^5 + 7^5.$

Færdig fra Trykkeriet den 13. Februar 1937.

Det Kgl. Danske Videnskabernes Selskab.
Mathematisk-fysiske Meddelelser **XIV**, 9.

THE DISSOCIATION CONSTANT OF THE ANILINIUM ION

BY

KAI JULIUS PEDERSEN

KØBENHAVN
LEVIN & MUNKSGAARD
EJNAR MUNKSGAARD
1937

Printed in Denmark.
Bianco Lunos Bogtrykkeri A/S

In this paper the dissociation constant of the anilinium ion

$$K = (H^+)\,(An) / (AnH^+), \qquad (1)$$

where (H^+), (An), and (AnH^+) are the concentrations of hydrogen ions, aniline, and anilinium ions respectively, is measured electrometrically at different temperatures and salt concentrations.

Measurements were first attempted with the hydrogen electrode in aniline buffer solutions. Hydrogen was passed through a sintered glass filter into the solution, where it formed a large number of tiny bubbles. The e. m. f. was not, however, sufficiently reproducible. Changes as great as one millivolt were found when the current of hydrogen was made quicker or slower. Apparently a reaction takes place at the surface of the platinum electrode altering the composition of the solution in the neighbourhood of the electrode. It was therefore decided to use the glass electrode instead of the hydrogen electrode.

Cells of the following composition were measured

Pt	0.01 *n.* HCl + quinhydrone	glass	solution	3.5 *m.* KCl	0.01 *n.* HCl + quinhydrone	Pt	(2)

The "solution" is either hydrochloric acid of known hydrogen ion concentration or an aniline buffer solution.

The glass electrodes were of the type described by Mac Innes.[1] They consisted of a plane diaphragm of Corning glass no. 015 which formed the bottom of a piece of ordinary glass tubing whose upper part was covered with a layer of paraffin wax. Inside was a solution of quinhydrone in 0.01 normal hydrochloric acid into which dipped a bright platinum electrode.

As container for the solution under investigation a vessel was employed of the same kind as those used in this laboratory for calomel electrodes.[2] It was completely filled with the solution. Instead of the glass stopper, the glass electrode was placed in the opening, and fixed by means of a short piece of rubber tubing forming a belt round the tube of the glass electrode. The liquid-liquid junction was formed by sucking bridge solution half way up into the perpendicular part of the side tube. This is an easy way of obtaining a stable and reproducible diffusion potential.[3]

The other half cell, a quinhydrone electrode in 0.01 normal hydrochloric acid, was made in a vessel of the same kind as that used for the solution under investigation. The two vessels, and a test tube containing bridge solution into which they both dipped, were placed in an electrically regulated liquid paraffin thermostat.

As null instrument for the electrometric measurements a Lindemann electrometer was used. A sensitivity of 0.1 millivolt was obtained by carefully balancing the voltages

[1] MacInnes and Dole, J. Amer. Chem. Soc. **52** (1930) 29. MacInnes and Belcher, J. Amer. Chem. Soc. **53** (1931) 3315.

[2] Lewis, Brighton and Sebastian, J. Amer. Chem. Soc. **39** (1917) 2245. J. K. Gjaldbæk, Kgl. Danske Vid. Selsk., Math.-fys. Medd. **5** (1924) no. 9.

[3] Guggenheim, J. Amer. Chem. Soc. **52** (1930) 1315. Unmack and Guggenheim, Kgl. Danske Vid. Selsk., Math.-fys. Medd. **10** (1930) no. 8.

of the quadrants. The needle terminal of the electrometer was connected with the quinhydrone electrode inside the glass electrode. The potential of the other quinhydrone electrode was adjusted by means of a potentiometer until the needle showed no deflection when earthed. The accuracy of the measurements was ± 0.1 millivolt.

Before the actual measurements the glass electrode was tested by measuring the following combination

Pt | 0.01 *n*. HCl + quinhydrone | glass | solution X + quinhydrone | Pt,

where solution X is 1) 0.01 normal hydrochloric acid, 2) a dilute acetate buffer solution of pH about 5, and 3) a dilute phosphate buffer solution of pH about 7. If we find that all the cells have the potential zero, we may conclude that the glass and quinhydrone electrodes have the same potential for all the solutions, that is, that the law of the reversible hydrogen electrode holds for the glass electrode in the interval examined. This was actually found to be the case with an accuracy of ± 0.1 millivolt, when a constant asymmetry potential of a few tenths of a millivolt was subtracted.

The aniline buffer solutions were freshly prepared for each day's measurements by mixing appropriate amounts of aniline and normal hydrochloric acid and diluting with water. These buffer solutions were in most cases further diluted with sodium chloride solution of the same ionic concentration. The aniline used was the middle fraction obtained by distillation *in vacuo* of KAHLBAUM's aniline for analytical purposes. Sodium chloride and hydrochloric acid for analytical purposes were used without further purific-

ation. All the solutions were made from redistilled water. The quinhydrone solutions were renewed every day.

Cells of the type given in scheme 2 were measured at the three temperatures 14.8°, 25.0°, and 34.9°. The aniline buffer solution, which we may call solution 1, contained anilinium chloride and aniline (usually of nearly equal concentrations), and in addition sodium chloride. Within a series of measurements the concentrations of anilinium chloride and aniline were varied, while the total salt concentration s was kept constant by adding sodium chloride. A solution of known hydrogen ion concentration, which we may call solution 2, was always measured along with each series of aniline buffer solutions. Solution 2 was a mixture of hydrochloric acid (about 0.01 normal) and sodium chloride, generally of the same total salt concentration as solution 1. The difference E between the e. m. f. measured for solutions 1 and 2 does not contain the asymmetry potential of the glass electrode. We may consider E as the e. m. f. of the cell

$$H_2 \mid \text{solution 1} \mid 3.5\ m.\ KCl \mid \text{solution 2} \mid H_2.$$

According to the thermodynamic considerations of Guggenheim[1] the e. m. f. of cells of this type may be written as a sum of three terms

$$E = E_{El} + E_D + E_S, \tag{4}$$

where E_{El} is the ideal electrode potential, E_D is the ideal diffusion potential, and E_S is the salt effect potential. E_S vanishes when both solution 1 and 2 are infinitely dilute.

If we use the abbreviation

[1] Guggenheim, J. Phys. Chem. **34** (1930) 1758.

$$\varrho \equiv \frac{RT}{F \log e}, \tag{5}$$

the ideal electrode potential is

$$E_{El} = -\varrho \log \frac{(H^+)_1}{(H^+)_2}. \tag{6}$$

The ideal diffusion potential may be written

$$E_D = E_{1\,D} - E_{2\,D}, \tag{7}$$

where $E_{1\,D}$ is the ideal diffusion potential of the junction solution 1 | 3.5 *m.* KCl, and $E_{2\,D}$ that of the junction solution 2 | 3.5 *m.* KCl. For convenience we may write

$$E_{1\,D} \equiv \varrho\delta_1, \qquad \text{and} \qquad E_{2\,D} \equiv \varrho\delta_2. \tag{8}$$

The salt effect potential may be written

$$E_S = -\varrho \log \frac{f_1}{f_2}, \tag{9}$$

where f_1 and f_2 are characteristic of the combinations solution 1 | 3.5 *m.* KCl and solution 2 | 3.5 *m.* KCl respectively. They are generally called activity coefficients of the hydrogen ion, a misleading expression. Equation 9 defines only the relative values of f_1 and f_2, not their absolute values. In the last part of this paper we shall discuss the question of an absolute definition.

From equations 4, 6, 7, 8, and 9 we obtain

$$-\log (H^+)_1 - \log \frac{f_1}{f_2} = \frac{E}{\varrho} - \delta_1 + \delta_2 - \log (H^+)_2.$$

If we introduce equation 1 we get

$$-\log K - \log \frac{f_1}{f_2} = \frac{E}{\varrho} - \delta_1 + \delta_2 - \log (H^+)_2 - \log \frac{(An)}{(AnH^+)},$$

which equation may also be written as follows

$$-\log K - \log \frac{f_1}{f_{(\mathrm{NaCl})_1}} = \frac{E}{\varrho} - \delta_1 + \delta_2 - \log (\mathrm{H}^+)_2 - \log \frac{(\mathrm{An})}{(\mathrm{AnH}^+)} - \log \frac{f_2}{f_{(\mathrm{NaCl})_1}}. \qquad (10)$$

Here $f_{(\mathrm{NaCl})_1}$ is the value of f for a pure sodium chloride solution of the same ionic concentration as solution 1.

The ideal diffusion potential for the kind of junction used here may, according to Guggenheim[1], be calculated to a good degree of approximation from Henderson's formula.[2] Values of the ionic conductivities all corresponding to one and the same solution must be introduced into this formula.[3]

For the junction: electrode solution | 3.5 *m.* KCl, the formula may be written

$$\delta = \frac{3.5\,(u_{\mathrm{Cl}} - u_{\mathrm{K}}) + \sum_{+} c_i u_i - \sum_{-} c_i u_i}{3.5\,(u_{\mathrm{Cl}} + u_{\mathrm{K}}) - \sum_{+} c_i u_i - \sum_{-} c_i u_i} \log \frac{3.5\,(u_{\mathrm{Cl}} + u_{\mathrm{K}})}{\sum_{+} c_i u_i + \sum_{-} c_i u_i}, \qquad (11)$$

where c_i and u_i are respectively the concentration and conductivity of an ion i. $\sum_{+}$ and $\sum_{-}$ denote respectively summation over all positive and over all negative ions in the electrode solution.

In Table 1 values of δ calculated from this formula are given for the junctions used in this paper. All the conductivities used for the calculation correspond to the electrode solution at 25°. If we make the sufficiently precise assumption that the ratio between the ionic conductivities

[1] Guggenheim, J. Amer. Chem. Soc. **52** (1930) 1315.

[2] Henderson, Z. physik. Chem. **59** (1907) 118, **63** (1908) 325.

[3] Guggenheim and Unmack, Kgl. Danske Vid. Selsk., Math.-fys. Med. **10** (1931) no. 14, pag. 16.

is independent of the temperature from 15° to 35°, we may use the calculated values throughout the whole temperature interval. For hydrochloric acid and for solutions of sodium and potassium chloride we have used the conductivities given in the International Critical Tables, and the transference numbers determined by LONGSWORTH.[1] For mixtures of hydrochloric acid and sodium chloride we assume that the mixture law holds. For anilinium chloride we use the conductivities determined by SIDGWICK and WILSDON[2], together with the assumption that the chloride ion has the same conductivity in equally concentrated solutions of anilinium chloride and potassium chloride.

The remaining term on the right hand side of equation 11, namely $-\log \frac{f_2}{f_{(NaCl)_1}}$, is found from measurements with

Table 1.

Ideal diffusion correction δ for the junction: solution of given composition | 3.5 *m.* KCl calculated from formula 11.

c	c molar AnHCl	c molar NaCl	0.001 *m.* HCl + (c−0.001) *m.* NaCl	0.002 *m.* HCl + (c−0.002) *m.* NaCl	0.005 *m.* HCl + (c−0.005) *m.* NaCl	0.01 *m.* HCl + (c−0.01) *m.* NaCl	c molar HCl
0.001	..	0.0688	..	..	..	..	0.0603
0.002	0.0637	0.0627	0.0580	..	..	..	0.0560
0.005	0.0562	0.0554	0.0539	0.0530	..	..	0.0524
0.01	0.0506	0.0501	0.0499	0.0489	0.0504	..	0.0525
0.02	0.0433	0.0436	0.0441	0.0446	0.0463	0.0492	0.0554
0.05	0.0317	0.0342	0.0350	0.0359	0.0383	0.0422	0.0691
0.10	0.0194	0.0250	0.0258	0.0267	0.0293	0.0334	0.0905
0.20	0.0025	0.0139	0.0148	0.0156	0.0180	0.0221	0.1265
0.21	..	..	0.0140	..	0.0172	0.0213	..
0.30	—0.0117	0.0057	..	..	..	0.0126	..

[1] LONGSWORTH, J. Amer. Chem. Soc. **54** (1932) 2741, **57** (1935) 1185.
[2] SIDGWICK and WILSDON, J. Chem. Soc. **99** (1911) 1118.

Table 2.

Electromotive force E at 14.8° of the cell H_2 | solution 1 | 3.5 *m*. KCl | solution 2 | H_2 measured by means of the glass electrode.

Solution 1			Solution 2		E volts	$-\log \frac{f_2}{f_{(NaCl)_1}}$	$-\log K - \log \frac{f_1}{f_{(NaCl)_1}}$
(AnHCl)	(An)	(NaCl)	(HCl)	(NaCl)			
0.3025	0.3066	0.000	0.01025	0.290	0.1591	0.000	4.793
0.2017	0.2044	0.100	0.01025	0.290	0.1607	0.000	4.815
0.1008	0.1022	0.200	0.01025	0.290	0.1623	0.000	4.836
0.0504	0.0511	0.250	0.01025	0.290	0.1629	0.000	4.844
0.01891	0.01916	0.280	0.01025	0.290	0.1634	0.000	4.851
0.2513	0.0522	0.0505	0.01025	0.290	0.1215	0.000	4.819
0.0506	0.2530	0.2512	0.01025	0.290	0.2022	0.000	4.840
0.2017	0.2044	0.000	0.01025	0.190	0.1591	0.000	4.788
0.1008	0.1022	0.100	0.01025	0.190	0.1608	0.000	4.812
0.0390	0.0395	0.161	0.01025	0.190	0.1617	0.000	4.824
0.01833	0.01858	0.182	0.01025	0.190	0.1621	0.000	4.829
0.1012	0.1004	0.000	0.01025	0.090	0.1584	0.002	4.781
0.0506	0.0502	0.050	0.01025	0.090	0.1593	0.002	4.794
0.02024	0.02008	0.080	0.01025	0.090	0.1599	0.002	4.802
0.0506	0.0502	0.000	0.01025	0.040	0.1580	0.008	4.777
0.02024	0.02007	0.030	0.01025	0.040	0.1586	0.008	4.786
0.02024	0.02007	0.000	0.01024	0.010	0.1574	0.023	4.777
0.01012	0.01004	0.010	0.01024	0.010	0.1577	0.023	4.781
0.01012	0.01004	0.000	0.01024	0.010	0.1570	0.038	4.776
0.00405	0.00402	0.000	0.01024	0.010	0.1570	0.052	4.780

the hydrogen electrode in solutions of hydrochloric acid and sodium chloride, as described later in this paper.

We are now able to calculate $-\log K - \log \frac{f_1}{f_{(NaCl)_1}}$ from equation 10. The experimental data and the results of the calculation are given in the tables 2, 3, and 4. As can be seen from these tables $-\log K - \log \frac{f_1}{f_{(NaCl)_1}}$ varies even when

Table 3.

Electromotive force E at 25.0° of the cell H_2 | solution 1 | 3.5 *m*. KCl | solution 2 | H_2 measured by means of the glass electrode.

Solution 1			Solution 2		E volts	$-\log \frac{f_2}{f_{(NaCl)_1}}$	$-\log K \frac{f_1}{f_{(NaCl)_1}}$
(AnHCl)	(An)	(NaCl)	(HCl)	(NaCl)			
0.3015	0.2965	0.000	0.01011	0.290	0.1522	0.000	4.600
0.2010	0.1977	0.100	0.01011	0.290	0.1537	0.000	4.619
0.1005	0.0988	0.200	0.01011	0.290	0.1554	0.000	4.642
0.0504	0.0496	0.250	0.01011	0.290	0.1561	0.000	4.651
0.01977	0.01944	0.280	0.01011	0.290	0.1566	0.000	4.657
0.2010	0.1977	0.000	0.01011	0.190	0.1524	0.000	4.598
0.1005	0.0988	0.100	0.01011	0.190	0.1540	0.000	4.620
0.0502	0.0494	0.150	0.01011	0.190	0.1548	0.000	4.630
0.01977	0.01944	0.180	0.01011	0.190	0.1553	0.000	4.636
0.1005	0.0988	0.000	0.01011	0.090	0.1522	0.002	4.592
0.1009	0.1026	0.000	0.01011	0.090	0.1532	0.002	4.594
0.1013	0.0995	0.000	0.01024	0.090	0.1526	0.002	4.590
0.0502	0.0494	0.050	0.01011	0.090	0.1531	0.002	4.604
0.05047	0.05133	0.050	0.01011	0.090	0.1541	0.002	4.606
0.05066	0.04974	0.050	0.01024	0.090	0.1535	0.002	4.605
0.01977	0.01944	0.080	0.01011	0.090	0.1538	0.002	4.613
0.02027	0.01990	0.080	0.01024	0.090	0.1540	0.002	4.611
0.08098	0.01974	0.0202	0.01011	0.090	0.1171	0.002	4.600
0.06751	0.03316	0.0337	0.01011	0.090	0.1354	0.002	4.606
0.05060	0.05000	0.0506	0.01011	0.090	0.1530	0.002	4.600
0.03371	0.06682	0.0675	0.01011	0.090	0.1711	0.002	4.603
0.02027	0.08021	0.0809	0.01011	0.090	0.1889	0.002	4.603
0.05047	0.05133	0.000	0.01011	0.040	0.1529	0.008	4.591
0.0506	0.0499	0.000	0.01011	0.040	0.1520	0.008	4.589
0.0506	0.0497	0.000	0.01025	0.040	0.1522	0.008	4.588
0.01990	0.02022	0.030	0.01011	0.040	0.1535	0.008	4.599
0.02020	0.01992	0.030	0.01011	0.040	0.1526	0.008	4.597
0.02027	0.01990	0.030	0.01025	0.040	0.1530	0.008	4.600
0.01990	0.02022	0.000	0.01011	0.010	0.1522	0.023	4.589
0.02020	0.01992	0.000	0.01011	0.010	0.1516	0.023	4.592
0.02021	0.01999	0.000	0.01011	0.010	0.1513	0.023	4.586

Table 3 (continued).

Solution 1			Solution 2		E volts	$-\log \frac{f_2}{f_{(NaCl)_1}}$	$\frac{-\log K}{-\log \frac{f_1}{f_{(NaCl)_1}}}$
(AnHCl)	(An)	(NaCl)	(HCl)	(NaCl)			
0.02052	0.02012	0.000	0.01025	0.010	0.1516	0.023	4.586
0.00998	0.00984	0.010	0.01011	0.010	0.1520	0.023	4.598
0.01026	0.01006	0.010	0.01025	0.010	0.1521	0.023	4.593
0.00998	0.00984	0.000	0.01011	0.040	0.1509	0.044	4.586
0.01011	0.01000	0.000	0.01011	0.010	0.1512	0.038	4.591
0.01026	0.01006	0.000	0.01025	0.010	0.1513	0.038	4.590
0.00498	0.00493	0.000	0.01011	0.010	0.1511	0.049	4.592
0.00405	0.00399	0.000	0.01011	0.040	0.1513	0.058	4.596
0.00410	0.00402	0.000	0.01025	0.010	0.1512	0.052	4.592
0.00200	0.00200	0.000	0.01011	0.010	0.1516	0.060	4.591

the total salt concentration s is constant. Unfortunately, it is impossible to decide from measurements of this kind how the variation is distributed over the two terms. It is therefore in principle impossible to determine the dissociation constant K of an acid in its buffer solution by means of electrometric measurements of cells with liquid-liquid junctions without making an arbitrary assumption concerning the salt effect potential. However, it is possible, without making any such assumption, to find K for a sodium chloride solution containing only an infinitesimal amount of anilinium chloride and aniline. We plot $-\log K - \log \frac{f_1}{f_{(NaCl)_1}}$ against the concentration of anilinium chloride for the solutions in which (AnHCl) is approximately equal to (An). In Fig. 1 we have drawn straight lines through points corresponding to the same total salt concentration s. By means of the straight lines we extrapolate to (AnHCl) $= 0$, that is, to s molar sodium chloride solution. The ordinate is $-\log K$ for the sodium chloride solution, because for this solution $f_1 = f_{(NaCl)_1}$. This computation includes

Table 4.

Electromotive force E at 34.9° of the cell H_2 | solution 1 | 3.5 *m*. KCl | solution 2 | H_2 measured by means of the glass electrode.

Solution 1			Solution 2		E volts	$-\log \frac{f_2}{f_{(NaCl)_1}}$	$-\log K - \log \frac{f_1}{f_{(NaCl)_1}}$
(AnHCl)	(An)	(NaCl)	(HCl)	(NaCl)			
0.3028	0.3034	0.000	0.01024	0.290	0.1477	0.000	4.430
0.2018	0.2022	0.100	0.01024	0.290	0.1492	0.000	4.449
0.1009	0.1011	0.200	0.01024	0.290	0.1508	0.000	4.469
0.0501	0.0502	0.250	0.01024	0.290	0.1516	0.000	4.478
0.01442	0.01444	0.286	0.01024	0.290	0.1521	0.000	4.484
0.2513	0.0522	0.0505	0.01024	0.290	0.1078	0.000	4.456
0.0506	0.2530	0.2512	0.01024	0.290	0.1936	0.000	4.468
0.2018	0.2022	0.000	0.01025	0.190	0.1479	0.000	4.428
0.1006	0.0991	0.101	0.01025	0.190	0.1492	0.000	4.451
0.0505	0.0498	0.150	0.01025	0.190	0.1500	0.000	4.460
0.0203	0.0200	0.180	0.01025	0.190	0.1505	0.000	4.466
0.1010	0.0996	0.000	0.01025	0.090	0.1470	0.003	4.418
0.0505	0.0498	0.050	0.01025	0.090	0.1481	0.003	4.432
0.0203	0.0200	0.080	0.01025	0.090	0.1488	0.003	4.442
0.08116	0.02110	0.0202	0.01024	0.090	0.1129	0.003	4.434
0.06750	0.03473	0.0337	0.01024	0.090	0.1306	0.003	4.429
0.05062	0.05158	0.0506	0.01024	0.090	0.1489	0.003	4.432
0.03375	0.06842	0.0675	0.01024	0.090	0.1670	0.003	4.428
0.02025	0.08189	0.0810	0.01024	0.090	0.1857	0.003	4.434
0.05050	0.04978	0.000	0.01025	0.040	0.1467	0.011	4.417
0.02020	0.01991	0.030	0.01025	0.040	0.1476	0.011	4.430
0.02050	0.01861	0.000	0.01025	0.010	0.1443	0.021	4.418
0.01025	0.00930	0.010	0.01025	0.010	0.1449	0.021	4.425
0.01025	0.01002	0.000	0.01025	0.010	0.1462	0.037	4.424
0.00512	0.00501	0.000	0.01025	0.010	0.1461	0.048	4.424
0.00202	0.00197	0.000	0.01025	0.010	0.1466	0.059	4.426

two extrapolations to pure sodium chloride solution, 1) from mixtures of aniline buffer solution and sodium chlo-

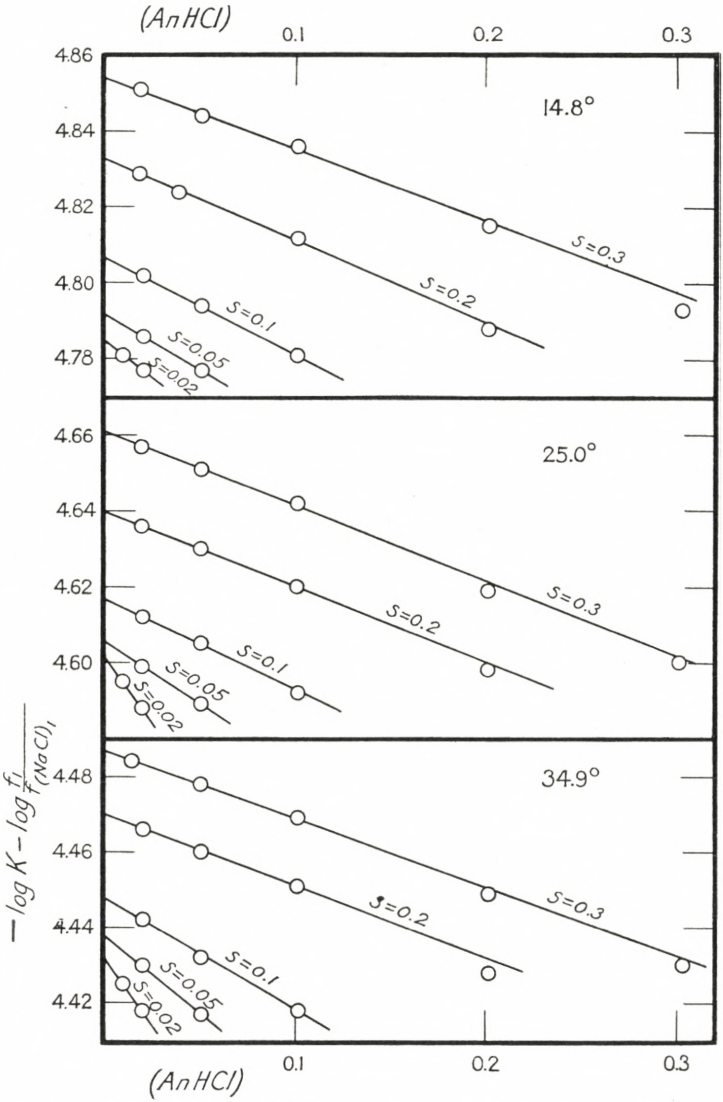

Fig. 1. The dissociation constant in mixtures of aniline buffer solution and sodium chloride of total salt concentration s. Extrapolation to pure sodium chloride solution.

ride solution, and 2) from mixtures of hydrochloric acid and sodium chloride solution (see later), that is, we have extrapolated to a cell of the composition

$$H_2 \mid s \text{ molar NaCl} \mid 3.5\ m.\ KCl \mid s \text{ molar NaCl} \mid H_2,$$

for which both E_D and E_S vanish. The dissociation constant of the anilinium ion in pure sodium chloride solutions found in this way is therefore independent, not only of the salt effect potential, but also of the special way in which we have corrected for the ideal diffusion potential.

If we wish to find K for finite concentrations of the buffer constituents we must, as already pointed out, make an assumption as to the way in which the variation of $-\log K - \log \frac{f_1}{f_{(NaCl)_1}}$, within a series of buffer solutions of constant s, is distributed over the two terms. The simplest assumption is that either $-\log K$ or $-\log \frac{f_1}{f_{(NaCl)_1}}$ is constant and has the same value as that of the pure s molar sodium chloride solution. We prefer the former alternative because the influence of salts on f, as will be seen in the last part of this paper, is of a very specific nature.

In Fig. 2 the values of $-\log K$ for sodium chloride solutions are plotted against the concentration. For each temperature the points fall on a straight line corresponding to the following expressions for the dissociation constant K of the anilinium ion in an s molar sodium chloride solution ($s < 0.3$):

$$\left.\begin{array}{ll} \text{at } 34.9^\circ & -\log K = 4.428 + 0.20\ s \\ \text{at } 25.0^\circ & -\log K = 4.596 + 0.22\ s \\ \text{at } 14.8^\circ & -\log K = 4.780 + 0.26\ s. \end{array}\right\} \qquad (12)$$

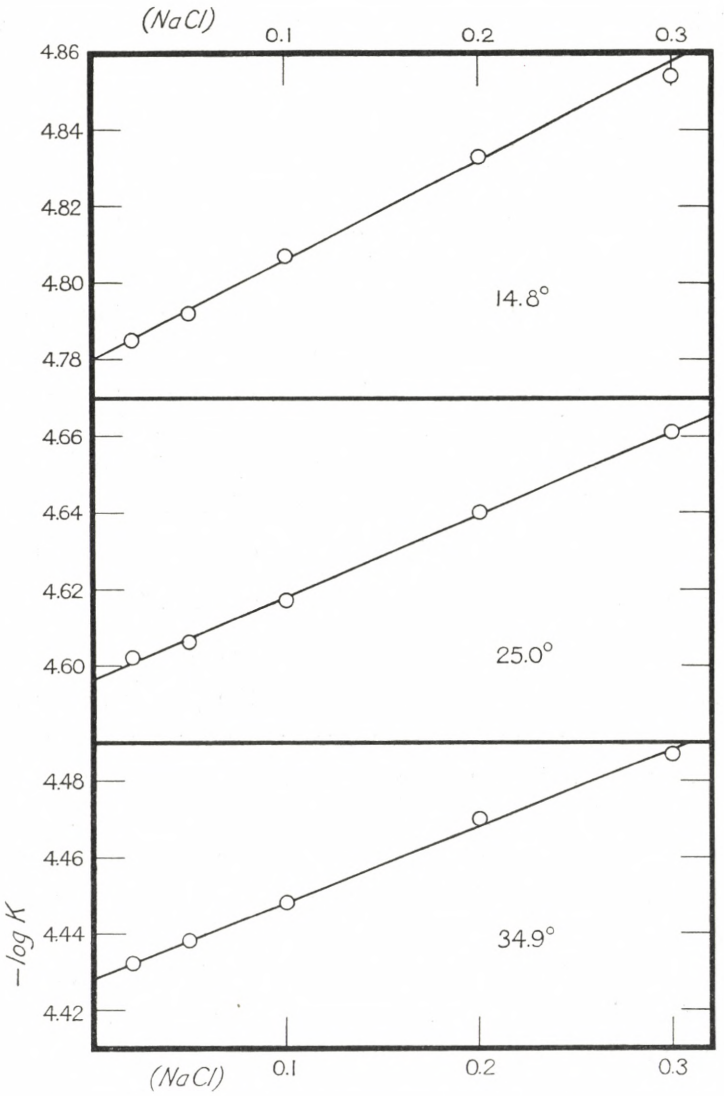

Fig. 2. The dissociation constant of the anilinium ion in sodium chloride solutions.

By setting $s = 0$ we find K^0, the dissociation constant at infinite dilution. If we plot $-\log K^0$ against $\frac{1}{T}$, the reciprocal of the absolute temperature, we get the points indicated by circles in Fig. 3. They fall on a straight line of equation

$$-\log K^0 = 1.553 \frac{10^3}{T} - 0.614. \qquad (13)$$

From the slope we find the heat of dissociation of the anilinium ion at infinite dilution

$$C_6H_5NH_3^+ + H_2O \rightarrow C_6H_5NH_2 + H_3O^+ - 7105 \text{ cal.}$$

In order to find the heat of neutralization of the anilinium ion we combine this result with the heat of neutralization of the hydroxonium ion

$$H_3O^+ + OH^- \rightarrow 2\,H_2O + 13692 \text{ cal.}$$

found by HARNED and HAMER[1] for infinite dilution at 20° by electrometric measurements of cells without liquid-liquid junction. We thus find

$$C_6H_5NH_3^+ + OH^- \rightarrow C_6H_5NH_2 + H_2O + 6587 \text{ cal.}$$

We may compare this value with a calorimetric determination by THOMSEN.[2] He found that 6450 cal./equiv. are evolved when approximately 0.3 normal solutions of anilinium sulphate and sodium hydroxide are mixed at about 18°.

The dependence of K^0 on the temperature may also be expressed by the following equation which is more convenient for interpolation than equation 13

[1] HARNED and HAMER, J. Amer. Chem. Soc. **55** (1933) 2194.

[2] THOMSEN, Thermochemische Untersuchungen I (1882) 408.

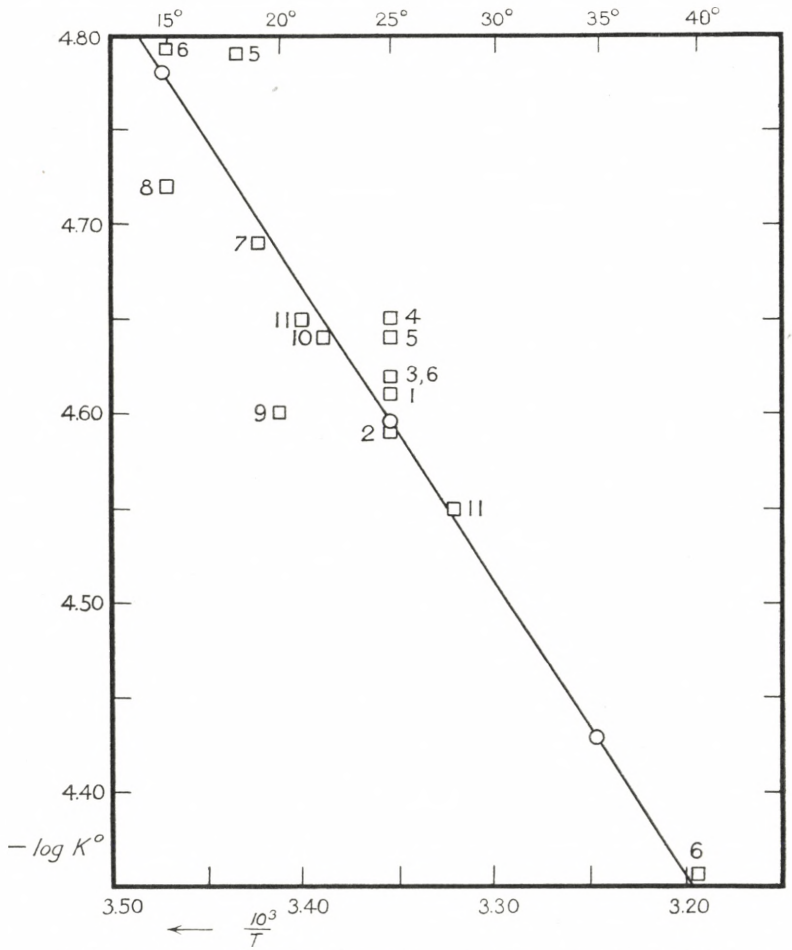

Fig. 3. The dissociation constant of the anilinium ion. Circles, this paper. Squares, other determinations.

[1] Bredig, conductivity of anilinium chloride solutions. [2, 3] Löwenherz, solubility of cinnamic acid ([2]) and of p-nitrobenzoic acid ([3]) in solutions of aniline, recalculated. [4] Farmer and Warth, partition equilibria between benzene and aqueous solutions of anilinium chloride. [5] Denison and Steele, a special conductivity method. [6] Lundén, conductivity of anilinium chloride solutions. [7, 8] Brønsted and Duus, hydrogen electrode ([7]) and catalysis ([8]). [9] Hahn and Klockmann, potentiometric titration, hydrogen electrode. [10] Flexser, Hammett and Dingwall, ultraviolet spectrophotometry. [11] Hall and Sprinkle, hydrogen electrode.

[1] Z. physik. Chem. **13** (1894) 322. [2 3] ibid. **25** (1898) 394. [4] J. Chem. Soc. **85** (1904) 1713. [5] ibid. **89** (1906) 999. [6] Medd. från Vet.-Akad:s Nobelinstitut **1** (1907) no. 7. [7 8] Z. physik. Chem. **117** (1925) 299. [9] ibid. A **146** (1930) 373. [10] J. Amer. Chem. Soc. **57** (1935) 2103. [11] ibid. **54** (1932) 3469.

$$-\log K^0 = 4.596 - 0.0175\,(t-25) + 0.00005\,(t-25)^2 \quad (14)$$

Here t is the temperature in degrees centigrade.

In Fig. 3 we have plotted both the determinations in this paper (circles) and those of other investigators (squares). The numbers refer to the list under the figure. The determinations of LÖWENHERZ have been recalculated (Table 5). He determined the solubility s at 25° of a sparingly soluble acid HS (dissociation constant K_1) in b molar aniline. We assume that the concentration of the undissociated form of the sparingly soluble acid is the same (s_0) in all the solutions. s_0 is calculated from the solubility in pure water and K_1. The dissociation constant ratio is given by the equation

Table 5.

Recalculation of LÖWENHERZ's determination of the dissociation constant of the anilinium ion at 25°.

	Cinnamic Acid $K_1^0 = 3.8 \times 10^{-5}$ * $s_0 = 0.00297$		p-Nitrobenzoic Acid $K_1^0 = 4.0 \times 10^{-4}$ ** $s_0 = 0.00100$	
b	s	$-\log \frac{K^0}{K_1^0}$	s	$-\log \frac{K^0}{K_1^0}$
0.000	0.00331	..	0.00164	..
0.005	0.00610	0.175	..	..
0.010	0.00804	0.169	0.00841	1.226
0.020	0.01100	0.167	0.01379	1.239
0.040	0.01543	0.165	0.02172	1.201
0.080	0.0222	0.170	0.0347	1.204
	Mean...	0.169	Mean...	1.218
	$-\log K^0 =$	4.59	$-\log K^0 =$	4.62

* LARSSON, Z. anorg. Chem. **155** (1926) 247.

** OSTWALD, Z. physik. Chem. **3** (1889) 259.

$$\frac{K}{K_1} = \frac{(An)\,(HS)}{(AnH^+)(S^-)} = \frac{[b-(s-s_0)+(H^+)]\,s_0}{[s-s_0-(H^+)]\,(s-s_0)}.$$

In Table 5 are given the values of

$$-\log\frac{K^0}{K_1^0} = -\log\frac{K}{K_1} - 2\,\alpha\sqrt{s-s_0},$$

where $\alpha = 0.504$ is the Debye-Hückel coefficient. They are approximately constant for each of the two acids. From the average value and the value of K_1^0 given at the top of the table we find the value of $-\log K^0$ given at the bottom.

The activity coefficient of the hydrogen ion in solutions of hydrochloric acid and sodium chloride.

In order to find the last term of equation 10, cells of the following composition were measured with the hydrogen electrode

$$H_2 \mid X \mid 3.5\ m.\ KCl \mid S \mid H_2.$$

Here X denotes a solution containing hydrochloric acid and (in most cases) sodium chloride at known concentrations, while S is always 0.01011 normal hydrochloric acid. We calculate the ideal diffusion potential from Henderson's formula (Table 1) and compute

$$-\log\frac{f_{(X)}}{f_{(S)}} = \frac{E}{\varrho} - \delta_X + \delta_S + \log(H^+)_X - \log 0.01011, \quad (15)$$

where $f_{(X)}$ and $f_{(S)}$ are the so called activity coefficients of the hydrogen ion characteristic of the combination X | 3.5 *m.* KCl and S | 3.5 *m.* KCl, respectively.

Table 6 contains the experimental data and the results of the computation. The composition of solution X is given in the two first columns. The next two columns give the e.m.f. measured at 25.0° and 34.9°, respectively. The values of $-\log \frac{f_{(X)}}{f_{(S)}}$ calculated from the experimental data by means of equation (15) are given in last two columns. The dif-

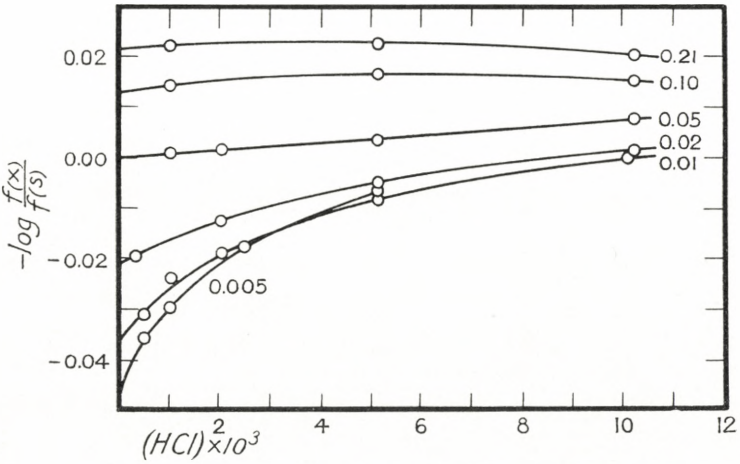

Fig. 4. $-\log \frac{f_{(X)}}{f_{(S)}}$ in mixtures of hydrochloric acid and sodium chloride at 25°. The corresponding total salt concentrations are written beside the curves.

ference between the values at the two temperatures is hardly greater than the experimental error. In Fig. 4 and 5 $-\log \frac{f_{(X)}}{f_{(S)}}$ has been plotted against the concentration of hydrochloric acid, and curves drawn through points corresponding to the same total salt concentration s. In this way an attempt has been made to extrapolate to X = pure s molar sodium chloride solution. When $s \geq 0.02$ the extrapolation seems safe. When $s = 0.01$, and even more so when $s = 0.005$, the extrapolation is less accurate owing

to the greater curvature. The values of $-\log \frac{f_{(X)}}{f_{(S)}}$ for sodium chloride solutions found in this way are also given in Table 6.

The last term of equation 10 is now found from Table 6 by writing $-\log \frac{f_2}{f_{(NaCl)_1}} = -\log \frac{f_2}{f_{(S)}} - \left(-\log \frac{f_{(NaCl)_1}}{f_{(S)}}\right)$. At 15° we have used the values found for 25°.

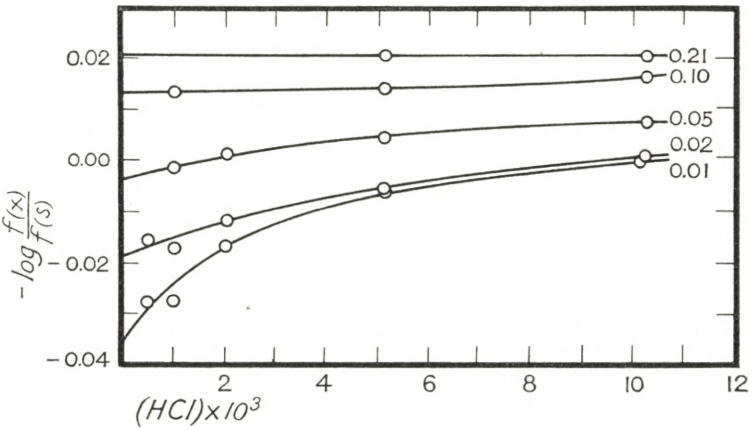

Fig. 5. $-\log \frac{f_{(X)}}{f_{(S)}}$ in mixtures of hydrochloric acid and sodium chloride at 35°. The corresponding total salt concentrations are written beside the curves.

In this paper we have given only the ratios between values of f for different solutions. We have not followed the usual procedure of defining a standard state relative to which f is measured. From a theoretical point of view it is most natural to set f as unity for an infinitely dilute electrode solution. The practical availability of this definition depends on an extrapolation to infinite dilution, and here we meet difficulties. As pointed out by Guggenheim[1]

[1] Guggenheim, J. Phys. Chem. **34** (1930) 1758. Unmack and Guggenheim, Kgl. Danske Vid. Selsk., Math.-fys. Med. **10** (1930) no. 8.

Table 6.

Measurements of the cell

H_2 | Solution X | 3.5 *m.* KCl | Solution S | H_2,

where Solution X has the composition given in the table, while Solution S is always 0.01011 normal hydrochloric acid.

Solution X		$E \times 10^3$ 25.0°	$E \times 10^3$ 34.9°	$-\log \frac{f_{(X)}}{f_{(S)}}$ 25.0°	$-\log \frac{f_{(X)}}{f_{(S)}}$ 34.9°
(HCl)	(NaCl)				
0.01025	0.200	— 0.97	— 1.00	0.021	0.021
0.005125	0.205	16.72	17.15	0.023	0.021
0.001038	0.209	57.52	..	0.022	..
..	0.210	..	..	0.021*)	0.021**)
0.01025	0.090	— 0.56	— 0.53	0.015	0.016
0.005125	0.095	17.07	17.48	0.017	0.014
0.001030	0.099	57.94	59.80	0.014	0.013
..	0.100	..	..	0.013*)	0.013**)
0.01025	0.040	— 0.50	— 0.52	0.008	0.008
0.005125	0.045	16.83	17.45	0.004	0.005
0.002052	0.048	40.10	41.40	0.002	0.002
0.001029	0.049	57.7	59.50	0.001	— 0.001
..	0.050	..	..	0.000*)	— 0.003**)
0.01025	0.0102	— 0.45	— 0.48	0.002	0.001
0.005125	0.0152	16.80	17.32	— 0.005	— 0.005
0.002050	0.0182	39.78	41.14	— 0.012	— 0.012
0.001029	0.0191	..	59.10	..	— 0.017
0.0005133	0.0197	..	77.64	..	— 0.015
0.0003451	0.0202	85.1	..	— 0.019	..
..	0.0203	..	..	— 0.021*)	— 0.019**)
0.01011	0.000	0	0	0.000	0.000
0.005055	0.0051	17.20	17.90	— 0.008	— 0.006
0.002022	0.0081	40.02	41.48	— 0.019	— 0.017
0.001016	0.0092	57.46	59.15	— 0.024	— 0.027
0.0005072	0.0096	74.90	77.60	— 0.031	— 0.027
..	0.0101	..	..	— 0.036*)	— 0.036**)

*) By graphical extrapolation (Fig. 4).
**) By graphical extrapolation (Fig. 5).

Table 6 (continued).

Solution X		$E \times 10^3$ 25.0°	$E \times 10^3$ 34.9°	$-\log \frac{f_{(X)}}{f_{(S)}}$ 25.0°	$-\log \frac{f_{(X)}}{f_{(S)}}$ 34.9°
(HCl)	(NaCl)				
0.005055	0.0000	17.40	..	— 0.007	..
0.002528	0.0025	34.60	..	— 0.018	..
0.001016	0.0040	57.37	..	— 0.029	..
0.000507	0.0045	74.88	..	— 0.036	..
..	0.0050	..	..	— 0.047*)	..
0.1010	..	— 56.78	— 58.61	0.002	0.002
0.05050	..	— 39.72	— 41.10	0.010	0.009
0.02030	..	— 17.24	— 17.88	0.008	0.007
0.01011	..	0	0	0.000	0.000
0.005055	..	17.40	17.88	— 0.007	— 0.008
0.002030	..	40.18	41.73	— 0.021	— 0.018
0.001020	..	57.75	60.27	— 0.028	— 0.018
0.000508	..	75.45	78.86	— 0.040	— 0.025

*) By graphical extrapolation (Fig. 4).

f is a function of the mean activity coefficients of all the salts and the transference numbers of all the ions in the electrode solution, throughout the transition layer and in the bridge solution. We have therefore no reason to believe that f follows the laws holding for the real activity coefficients of the salts. In spite of this, it is not unusual to extrapolate to infinite dilution by means of Debye-Hückel's law in the form $-\log f = \alpha \sqrt{s} - \beta s$, where s is the salt concentration, α is the Debye-Hückel coefficient (0.504 at 25° for a univalent ion), and β is a constant characteristic of the salt in the solution. From a treatment of the data in Table 6 we shall see that this procedure may give a meaningless result.

At the end of Table 6 are given the results of measurements in hydrochloric acid of different concentration. In

Fig. 6 we have plotted $-\log \frac{f_{(X)}}{f_{(S)}} - 0.504\sqrt{s}$ against s, both for X = hydrochloric acid (open circles) and for X = sodium chloride solutions (solid circles). Only the results at 25° have been used. The straight lines drawn in the figure

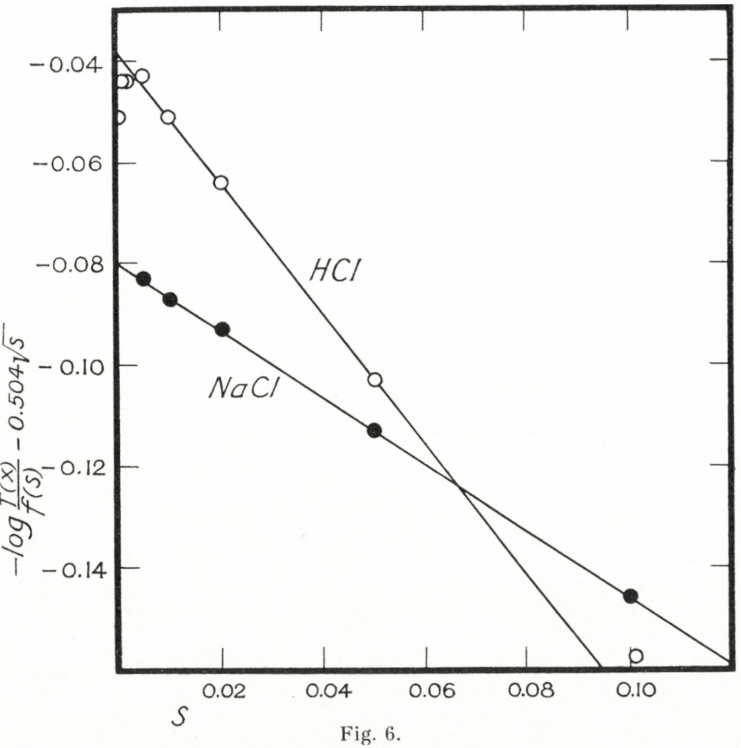

Fig. 6.

fit well to each set of points. Only for the most dilute solutions of hydrochloric acid are there considerable deviations, but here the experimental accuracy is smaller. If we determine $-\log \frac{f_{(X)}}{f_{(S)}}$ at infinite dilution from the straight line through the points for hydrochloric acid we get −0.038, while we get −0.080 when we extrapolate from the points for sodium chloride, that is, we find that $-\log f$

for a 0.01 normal hydrochloric acid is 0.038, when we use the results for hydrochloric acid, and 0.080, when we use those for sodium chloride. Of course, the curves for sodium chloride and hydrochloric acid solutions must approach each other in more dilute solution. However, even for the most dilute solutions used here, where we might expect Debye-Hückel's law to hold to a good approximation for the mean activity coefficients, the difference between the values of f in sodium chloride solution and hydrochloric acid is very considerable. According to Guggenheim this individual effect is closely connected with the deviation from 0.5 of the transference numbers of sodium chloride and hydrochloric acid. For these electrolytes the transference numbers of the cations are respectively 0.396 and 0.821 at 25° and infinite dilution. The correct value for the extrapolation is therefore probably between those found in Fig. 6 for sodium chloride and hydrochloric acid, but nearer the former than the latter. However, for practical purposes it is of no use making an accurate extrapolation to infinite dilution. Instead of an infinitely dilute solution we may choose any other standard state. The determinations of f in the literature are all based on such conventional standard states, although they have always been chosen in such a way that f is about unity in infinitely dilute solution. A convention of this kind is included in Sørensen's[1] definition of $\mathrm{pH} = -\log [(\mathrm{H}^+) f]$. Bjerrum and Unmack[2] use another convention, based partly on an extrapolation of the relative values for sodium chloride solutions in a similar way to that shown in Fig. 6.

[1] Sørensen, Compt. rend. trav. lab. Carlsberg **8** (1909) no. 1.

[2] Bjerrum and Unmack, Kgl. Danske Vid. Selsk., Math.-fys. Med. **9** (1929) no. 1.

Det Kgl. Danske Videnskabernes Selskab.
Mathematisk-fysiske Meddelelser. **XIV**, 10.

ON THE TRANSMUTATION OF ATOMIC NUCLEI BY IMPACT OF MATERIAL PARTICLES

I. GENERAL THEORETICAL REMARKS

BY

N. BOHR AND F. KALCKAR

KØBENHAVN
LEVIN & MUNKSGAARD
EJNAR MUNKSGAARD
1937

Printed in Denmark.
Bianco Lunos Bogtrykkeri A/S.

PREFACE

As indicated by the title the present paper was intended to form the first part of a treatise consisting of three parts to appear in immediate succession. The second part was planned as a more detailed elaboration of the theory of nuclear collisions on the general lines discussed here while the third part should contain an analysis on such lines of the available experimental evidence about nuclear transmutations. The publication of the present paper which was in print in January 1937 was, however, postponed and the completion of the other parts of the treatise delayed due to a visit of the authors to American universities in order to attend a number of conferences where nuclear problems were discussed. In the meantime the subject has been in rapid development due to the publication of several important papers during the last few months. Moreover an admirable complete report of the present state of nuclear dynamics has been published by H. BETHE in "Reviews of Modern Physics", **9**, 69, (1937), in which are included detailed comments on some of the considerations here presented, based on verbal communications from the authors at a conference in Washington, February 1937. Under these circumstances the plan of publishing a more comprehensive treatise has been temporarily abandoned, and in order to bring the present paper up to date it has been completed by an addendum written in October 1937 and containing references and brief comments of the most important recent contributions to the subject.

TABLE OF CONTENTS

§ 1. Basic Ideas.

In a recent paper[1] it was pointed out that the extreme facility of energy exchanges between the densely packed particles in atomic nuclei plays a decisive role in determining the course of nuclear transmutations initiated by impact of material particles. In fact, the assumption underlying the usual treatment of such collisions, that the transmutation consists essentially in a direct transfer of energy from the incident particle to some other particle in the original nucleus leading to its expulsion, cannot be maintained. On the contrary, we must realize that every nuclear transmutation will involve an intermediate stage in which the energy is temporarily stored in some closely coupled motion of all the particles of the compound system formed by the nucleus and the incident particle. On account of the strong forces which come into play between any two material particles at the small distances in question, the coupling between the particles of this compound system is

[1] N. Bohr, Neutron capture and nuclear constitution, Nature **137**, 344 and 351, (1936), cited for brevity in the following as (A).

Added in proof. In a more recent article (Science **86**, 161, 1937) a brief account of the later developments of the views presented in the paper cited is given. A fuller account with more detailed references to the previous litterature on the subject is further contained in an address at the International Physical Congress in Paris, October 1937, which will soon appear in the congress communications.

in fact so intimate that its eventual disintegration — whether it consists in the release of an "elementary" particle like a proton or a neutron, or of a "complex" nuclear particle like a deuteron or an α-ray — must be considered as a separate event, independent of the first stage of the collision process. The final result of the collision may thus be said to depend on a free competition between all the various disintegration and radiation processes of the compound system consistent with the general conservation laws.

From this point of view the treatment of nuclear transmutations initiated by collisions will imply in the first place an examination of the balance between the separate processes involved in the formation and disintegration of the semistable intermediate system. Notwithstanding the suggestiveness of simple mechanical analogies (A, p. 351) the discussion of this problem obviously demands proper quantum theoretical considerations. In fact, not only are the possible energy states of the compound system generally restricted by the laws of quantum mechanics, but also the formation or disintegration of this system will often involve characteristic quantum mechanical effects of the kind well known from the successful explanations of the laws of radioactive decay due to Condon and Gurney, and especially to Gamow. Considerable modifications in the usual treatment of such problems, which rest upon the assumption that the incident particle within the nucleus to a first approximation moves in a fixed field of force, are necessitated, however, by the intimate coupling here assumed between the motion of the particles in nuclei. Still we shall see that the extreme thoroughness of this coupling actually introduces certain simplifications which permit one to draw a number of simple conclusions of a comprehensive character about nuclear reactions.

Results of great interest on the constitution of atomic nuclei have been obtained, as is well known, by treating such nuclei as quantum mechanical systems built up entirely of neutrons and protons. This offers not only an explanation of the fact revealed by the study of band spectra and of the hyperfine structure of series lines that the intrinsic spin of the nucleus of any isotope is an odd or even multiple of the unit $h/4\pi$, according as its mass number is odd or even respectively, but also allows a general understanding of the way in which the stability of nuclei, and hence the occurrence of isotopes and the values of their mass defects, vary with mass and charge number. In this connection it may be especially noted that the important information about the forces between nuclear particles at close distances obtained in this way by HEISENBERG and his collaborators rests essentially upon an estimate of the average kinetic energy of these particles in the normal state of nuclei. Since protons as well as neutrons obey the Pauli exclusion principle, this kinetic energy will in fact be nearly independent of the conditions of motion assumed for the nuclear particles and, as regards its order of magnitude, will always be comparable with what would be obtained if each particle was assumed to move in a separate cell within the nucleus.

Any closer examination of the constitution of atomic nuclei based on the usual procedure in which, like the extranuclear electrons in atoms, each particle is assumed in the first approximation to move independently in a conservative field of force cannot, however, on account of the far more intimate coupling between nuclear particles, be expected to yield results which may be directly compared with the actual properties of nuclei. Notwithstanding the

promising attempts at a more rigorous treatment of the constitution of very light nuclei, we must for the moment be content to consider atomic nuclei as a state of matter of extreme density and electrisation, whose properties can only be explored by the analysis of the experimental evidence on nuclear reactions. Still, the circumstance that the excitation energy of the compound nucleus involved in ordinary experiments on nuclear transmutations is very small compared with the total energy necessary for the complete separation of all its constituent particles permits, as we shall see, a simple comparison to be made between many properties of nuclear matter and the properties of ordinary liquid and solid substances.

§ 2. Nuclear Level Distribution.

As shown in (A), the distribution of energy levels of excited nuclei exhibits a striking difference from what would be expected if such excitations, as ordinarily assumed, were due to an abnormally high energy state of a single nuclear particle. Thus the experimental evidence concerning the capture of fast and slow neutrons by heavy nuclei with emission of radiation shows that the distance between the energy levels of such nuclei decreases rapidly with increasing excitation, with the result that the distribution of energy levels becomes practically continuous, even for excitation energies which — although sufficient for the escape of a neutron with great kinetic energy — are far too small to alter essentially the semistable character of the compound system. Even within the region of continuous distribution the mean life time of the compound system is probably more than a hundred thousand times as long as the time interval which a fast neutron would use in passing through a region

of nuclear dimensions. The typical features of the nuclear level distribution are easily understood, however, if we realize that the stationary states of a nucleus must correspond to some quantized collective type of motion of all its constituent particles. In fact the rapid approach of neighbouring nuclear levels with increasing energy resembles (comp. A p. 346) the characteristics of the multitude of the linear combinations which may be formed by a number of independent quantities (see Addendum I). The nuclear level distribution has therefore very much the same character as that of the quantum states of a solid body, well known from the theory of specific heats at low temperatures (see Addendum II).

This analogy suggests a more direct comparison between the excitation of a nucleus and the vibrations of elastic substances, a comparison which is much simplified by the circumstance that apart from the very lightest nuclei the density of matter and energy is practically the same in all nuclei. Denoting by N the total number of protons and neutrons in such a nucleus, the volume will in fact be approximately given by

$$V = N\delta^3, \tag{1}$$

where δ is about $3 \cdot 10^{-13}$ and may be taken as the diameter of the cell occupied by an individual nuclear particle. Further the average kinetic energy of each particle in such nuclei will be given approximately by the simple formula

$$K = \frac{h^2}{8\delta^2\mu}, \tag{2}$$

where h is Planck's constant, and μ the nearly equal mass of a proton or a neutron. This gives for K approximately

20 M. e. V. and, since from measurements of mass defects the average binding energy of a neutron or a proton in a nucleus is found to be approximately 10 M. e. V., the average potential energy loss per nuclear particle becomes nearly 30 M. e. V. Just as δ may be considered as a characteristic unit of length in nuclear problems, a suitable unit of time in such problems is given by the interval τ, which an elementary particle of kinetic energy K would use in covering the distance δ. This time interval which is approximately given by

$$\tau = 2\frac{\mu\delta^2}{h}, \tag{3}$$

is of the order of magnitude of 10^{-22} sec.

The circumstance that the excitation energy of heavier nuclei is always very small compared with the total kinetic energy NK in the normal state of the nucleus invites us now to compare the nuclear excitations with the oscillations in volume and shape of a sphere under the influence of an elasticity ε or surface tension ω given by expressions of the type of

$$\varepsilon = C_\varepsilon K\delta^{-3}; \quad \omega = C_\omega K\delta^{-2}, \tag{4}$$

where the dimensionless factors C_ε and C_ω must be expected to be approximately constant for all but the lightest nuclei. Thus the frequences ν_ε and ν_ω of the oscillations of the simplest character of a sphere of volume V and density σ are given by the familiar formulas

$$\nu_\varepsilon \backsimeq \varepsilon^{1/2} V^{-\frac{1}{3}} \sigma^{-\frac{1}{2}}; \quad \nu_\omega \backsimeq \omega^{1/2} V^{-\frac{1}{2}} \sigma^{-\frac{1}{2}}, \tag{5}$$

which are easily tested by dimensional considerations. Putting $\sigma = \mu\delta^{-3}$ we obtain from (5) by means of (1), (2), and (4)

for the energy differences between successive quantum states of the nucleus corresponding to such oscillations

$$\Delta_\varepsilon E = h\nu_\varepsilon \backsimeq \sqrt{8 C_\varepsilon}\, N^{-\frac{1}{3}} K; \quad \Delta_\omega E = h\nu_\omega \backsimeq \sqrt{8 C_\omega}\, N^{-\frac{1}{2}} K. \quad (6)$$

Due to the difficulty of estimating the numerical values of the constants C_ε and C_ω the main interest of these formulas is the variation of the energy differences with N. Thus the fact that the average energy differences between the lower excited states of nuclei varies decidedly faster than $N^{-\frac{1}{3}}$ and even somewhat more rapidly than $N^{-\frac{1}{2}}$ shows that, at any rate for heavier nuclei, simple elastic vibrations corresponding to $\Delta_\varepsilon E$ are not responsible for the lowest excited states and can only be expected to be present for higher excitations. The circumstance, however, that $\Delta_\omega E$ corresponds more closely to the way the average distance of the lower levels decreases with N, suggests a more direct comparison of surface oscillations with the fundamental modes of nuclear excitation responsible for the main features of the level distribution. Still the fact that the proper surface energy of nuclei estimated from the mass defect curves[1] give, when introduced in (4) and (6), values for $\Delta_\omega E$ of more than a million volts even for heavy nuclei, where the average level distance is certainly not more than a few hundred thousand volts, shows the great difficulty involved in such a comparison (see Addendum III).

Obviously any such simple considerations can at most serve as a first orientation as regards the possible origin of nuclear excitations. In a closer discussion of this problem more detailed considerations regarding the specific character of the interactions between the individual nuclear particles on the stability as well as of the exci-

[1] cf. C. F. v. Weizsäcker, Die Atomkerne, Leipzig 1937.

tation mechanism of nuclei are needed. This is in fact not only indicated by the well known periodicities in the mass defect curve but also by the marked difference observed between the distances of the ground level and the excited levels for nuclei with even and odd mass and charge numbers. These effects must obviously be ascribed to the different degrees of saturation of the forces between pairs of nuclear particles obtainable in such nuclei on account of the restrictions implied by the Pauli principle in a more rigorous quantum mechanical treatment of the many body systems concerned. Due to the close coupling of the motion of the nuclear particles it would seem difficult, however, at the moment to discern to what extent conclusions concerning the exchange character or the spin dependence of the specific nuclear forces are reliable, when based on considerations of nuclear models with weak coupling between the particles.

In particular any attempt of accounting for the spin values by attributing orbital momenta to the individual nuclear particles seems quite unjustifiable. We must in fact assume that any orbital momentum is shared by all the constituent particles of the nucleus in a way which resembles that of the rotation of a solid body. Denoting by J the moment of inertia, we obtain

$$\Delta_r E = \frac{h^2}{8\pi^2 J} \backsimeq N^{-\frac{5}{3}} K \qquad (7)$$

as an estimate of the energy differences between the lowest quantum states of such rotations. For heavy nuclei (7) gives values small compared with the average level distance and may therefore possibly explain the fine structure observed for many energy levels of such nuclei. Part of

this fine structure and perhaps many other of the characteristic features of the structure of the lower level distribution may, however, be attributed to the orientations of the intrinsic spins of the nuclear particles relative to each other and to the resulting angular momentum of the nuclear motions (see Addendum IV).

§ 3. Radiative Properties of Nuclei.

As first revealed from the study of so-called internal conversion of γ-rays, the radiation emitted from excited nuclei will often show polarity properties differing essentially from that of an excited atom containing an electron in an abnormally high quantum state. While in the atomic case the intense radiations are always of dipole type, nuclear radiations corresponding to poles of higher order are found to be relatively intense. It is true that this is just what should be expected if nuclei could be considered as composed entirely of constituents like α-particles, all having the same charge and the same mass, because in that case the electric center would always coincide with the mass center and exclude the appearance of any dipole moment[1]. In the more general case, however, where nuclei must be considered to be built up of protons and neutrons, the appearance of dipole moments must — quite independent of the character of the forces between the particles — obviously be expected to appear, if the coupling is assumed to be so small that the state of the nucleus can be described by attributing well defined quantum states to each particle.

If, on the contrary, the coupling between the motions of the individual particles is assumed to be so intimate that we have only to do with collectively quantized states of the

[1] Comp. N. Bohr, Journ. Chem. Soc. p. 381 (1932).

whole nucleus, the situation will obviously be very different. In fact, unless the excitation is so high that the relative position of neighbouring particles is essentially affected, the radiative properties of the nucleus must be expected to show a close resemblance with that of a rotating or oscillating body with practically uniform electrisation and, due to the approximate coincidence of the charge and the mass center, dipole moments will under such conditions be absent or at any rate much suppressed. Such a comparison also makes possible a quantitative estimate of the probabilities of the radiative processes responsible for neutron capture. In fact, for an oscillation of the nuclear matter with frequency ν and relative amplitude α the quadrupole radiation emitted per unit time will be approximately

$$R \eqsim (2\pi\nu)^6 \frac{E^2}{c^5} \alpha^2 d^4, \tag{8}$$

where $E = Ze$ is the total electric charge, and $d = \delta N^{1/3}$ the diameter of the nucleus. Further we have for a low quantum state

$$h\nu \eqsim (2\pi\nu)^2 \alpha^2 d^2 M, \tag{9}$$

where $M = N\mu$ is the total mass of the nucleus. Eliminating α from (8) and (9) we get for the probability of a radiative transition in unit time

$$\Gamma_r = \frac{R}{h\nu} \eqsim \tau^{-1} (2\pi\nu)^4 \frac{e^2}{hc} \frac{Z^2 \delta^4}{N^{1/3} c^4}. \tag{10}$$

Now the life time of the excited nuclear states formed by slow neutron impact on heavy nuclei corresponds to a value of Γ_r about $\tau^{-1} 10^{-7}$ and this agrees with (10), if $h\nu$ for the most probable radiative transition is of the order of a million volts, as would seem consistent with general experimental evidence.

Formula (10) holds of course only in the case of a transition actually accompanied by a quadrupole radiation. For nuclear excitations corresponding to radial pulsations or to simple rotations even the quadrupole moment will, however, disappear and radiative transitions will become still more improbable[1]. As regards the question of radiative transitions between any two levels of an excited nucleus, it must also be noted that the various possible types of oscillations can generally not be expected to be independent of each other. In fact an estimate by means of (9) of the amplitudes of these oscillations shows that even for heavy nuclei such amplitudes will be small compared with nuclear dimensions only for the lowest quantum states. In general there will therefore probably be a close coupling between the elastic vibrations of the different types, which may explain the observation of the frequent appearance of comparatively hard radiation from excited nuclei corresponding to transitions between distant nuclear levels[2]. In this connection it may be hoped that further experiments on the radiation emitted from excited nuclei as well as on nuclear disintegrations produced by γ-rays will help to clear up the question of the mechanisms of the excitation of nuclei (see Addendum V).

[1] C. F. v. Weizsäcker, Naturwiss. **24**, 813, (1936) has recently suggested that the appearance of so-called isomeries among the artificial radioactive elements may be explained by the extremely small probabilities which radiative transitions with a change of angular momentum of several times $h/2\pi$ would have on any nuclear model. In this connection it may be of interest to call attention to the possibility that the uniformity of the electrisation of the densely packed nuclear matter may also make the probabilities of radiative transitions as well as of internal conversion processes between certain other pairs of nuclear states extremely small.

[2] Comp. esp. S. Kikuchi, K. Husimi and H. Aoki, Nature **137**, 992, (1936).

§ 4. Escape of Neutrons from Excited Nuclei.

As already mentioned in § 1, the disintegration of the compound system involved in nuclear transmutations must be considered as an event depending only on the state of this system and not on the way in which it is formed. Such disintegrations demand in fact a so to speak fortuitous concentration on the individual particle released of an essential part of the energy temporarily stored in intrinsic motions of the nuclear matter. These characteristic features of nuclear dynamics appear especially clearly in the case of the disintegration of the compound system which results in neutron escape. In fact, in the case of release of charged particles the electric repulsion extending beyond the range of the proper nuclear forces may under certain circumstances have a considerable influence on the probability of the disintegration, and this essentially quantum mechanical effect cannot always, as we shall see in § 6 be unambiguously seperated from the kinematical conditions for the liberation of a particle from the nuclear matter. Even in the case of neutron collisions classical mechanical considerations cannot be unambiguously applied to the motion of the neutrons outside the nucleus, unless the de Broglie wave length

$$\lambda = \frac{h}{\mu v} \tag{11}$$

is shorter than or at any rate comparable with nuclear dimensions. Strictly we cannot speak of a definite establishment of interaction between a free neutron and some particle within the nucleus, unless λ is comparable with δ. The formation of a semistable compound system, which under such conditions will in almost every case result from contact

between the incident neutron and the surface of the nucleus, closely resembles in fact the adhesion of a vapour molecule to the surface of a liquid or solid body. Conversely the disintegration of the compound system with neutron release exhibits a suggestive analogy to the evaporation of such substances at low temperatures.

This analogy has been emphasized by FRENKEL in a recent paper[1] in which he has derived, by a comparison with the well-known evaporation formula, an expression for the probability of neutron escape from an excited nucleus which, in our notation, can be written

$$\Gamma_n = N^{2/3} \tau^{-1} e^{-\frac{W}{kT}}, \tag{12}$$

where W is the work necessary for the liberation of a neutron from the nuclear matter, T the effective temperature and k Boltzmann's factor. This temperature energy of the nucleus FRENKEL estimates by assuming that the excitation energy is distributed according to Planck's formula over a multitude of oscillators equal in number with the intrinsic degrees of freedom of a system consisting of N particles. If U is the total excitation energy of the nucleus, this gives

$$U = \sum_i \frac{h\nu_i}{e^{h\nu_i/kT} - 1}, \tag{13}$$

where the summation is extended over all the oscillators. Assuming further that the frequencies of these oscillators are all comparable with the lowest frequencies of the radiation emitted from excited nuclei, he obtains for the

[1] J. FRENKEL, Sow. Phys. 9, 533, (1936).

compound system formed by the collision between a neutron and a heavy nucleus values for kT of a few hundred thousand electron volts. Introduced in (12), this gives values for Γ_n considerably smaller than the probability of neutron escape estimated from experiments. Since W is about 10 M. e. V. the formula is, however, very sensitive to the estimate of T and a far better agreement with experimental values is actually obtained, if we take into account that the possible oscillations of the nuclear matter have very different frequencies varying from the values given by formulas like (7) up to values of the same order of magnitude as K/h.

Practically all the excitation energy of the compound system is therefore stored in a few oscillations of the nuclear matter of smallest frequencies and accordingly the temperature of the nucleus calculated by (13) will be several times as high as that estimated by Frenkel, and becomes quite sufficient to secure an approximate agreement with the observed disintegration probabilities in the cases where a reasonable accuracy of formula (12) can be expected. A quantitative comparison between ordinary evaporation and neutron escape from the compound system is in fact limited not only by the difficulty involved in an accurate estimate of the effective temperatures of this system but also by the circumstance that the excitation of the residual nucleus left after the escape of a neutron will generally be much smaller than that of the compound system, in contrast with usual evaporation phenomena where the change in the heat energy of the bodies concerned, during the escape of a single vapour molecule, is negligibly small. A formula like (12) can therefore only be expected to give approximately correct results when the average excitation of the

residual nucleus, although always smaller than that of the compound system, is still of the same order of magnitude. (See Addendum VI).

In such cases a comparison between neutron escape from the compound system and ordinary evaporation offers, too, a simple explanation of the relative probabilities of different disintegration processes leading to different excited states of the residual nucleus. In fact, formula (12) gives primarily an estimate of the probability of those disintegration processes in which the energy of the escaping neutron is approximately the same as that of a gas molecule at the temperature concerned, and the relative probabilities of the escape of neutrons with higher velocities must be expected to be smaller in approximate conformity with Maxwell's velocity distribution of gas molecules. Actually such a comparison offers a simple explanation of the observation that in nuclear reactions resulting in neutron release the probability of a neutron leaving the nucleus with the total energy available is generally very small, if this energy is large compared with the temperature energy. (See Addendum VII).

Similar considerations are also in qualitative agreement with the observed great probability of energy transfer in collisions between nuclei and neutrons of kinetic energy greater than the energy difference between the normal and the lowest excited states of the nucleus. While this effect contrasts so strikingly with the usual ideas of nuclear collisions it is (compare (A), p. 347) nevertheless readily explained by the smaller demands on the concentration of the energy stored in the nuclear matter necessary for neutron escape in such disintegrations of the compound system as leave the residual nucleus in an excited state

than in such as leave it in its normal state. In very violent collisions, where the energy of the compound system is comparable or even larger than K, we should further expect that several particles would leave this system in successive separate disintegration processes[1]. If such a disintegration process results in the escape of a neutron its most probable energy will be of the same order of magnitude as the temperature energy of the compound system, while, if a charged particle is released, its energy will be higher on account of the additional effect of the electrical repulsion beyond the nuclear surface, which in a case like this has only a minor influence on the liberation process itself. (See § 6).

§ 5. Slow Neutron Collisions.

In the case of collisions between nuclei and neutrons with such small kinetic energies that the de Broglie wave length (11) is very long compared with nuclear dimensions we cannot, as has been mentioned, speak in an unambiguous way about contact between the neutron and the nucleus. Accordingly every simple basis is evidently lost for an ordinary mechanical description of the formation of the compound system or its disintegration. This is also shown most strikingly by the remarkable phenomena of capture of slow neutrons for which effective cross sections have been found amounting to several thousand times of simple nuclear cross sections. In these highly selective phenomena we have obviously to do with a typical quantum mechanical resonance effect where, although the collision process can

[1] The escape of more than one neutron in nuclear collision has recently been observed in fast neutron collisions by F. Heyn, Nature **138**, 723, (1936).

still be separated in well defined stages, the probabilities of successive stages cannot be estimated independently of each other.

In the first attempts to explain the appearance of such resonance the neutron was supposed to move within the nucleus in a fixed field forming a so-called potential hole. On account of the great fall in potential, the kinetic energy of the neutron within the hole would in fact be so large that its wave length became smaller than the diameter of the hole, although the wave length outside was much larger. This great change in wave length therefore effects an almost complete reflection of the neutron wave from the inner walls of the hole, allowing a standing wave of considerable intensity to be built up for suitable energy values of the neutron. As a consequence of the existence of such a semistable state of motion of the neutron within the nucleus there will appear for these energy values both an abnormally large scattering effect corresponding to the reemission of the neutron from this state and a considerable probability of capture of the neutron resulting from a radiative transition to a lower energy state within the potential hole. Although this picture in a very instructive way illuminates essential features of the resonance effect, it was soon found quite insufficient to account for the details of the phenomena observed. In particular an estimate of the probability of radiative effects in such simple collision processes shows that the probability of scattering will always be greater than or comparable with the probability of capture in contrast with the experimental results, according to which the often extraordinarily large capture probability of slow neutrons is in no case found to be accompanied by an excessively high scattering effect.

To overcome this difficulty, G. Breit and E.Wigner[1] have proposed a modification of the explanation of the resonance effects in slow neutron collisions according to which, in the intermediate state another nuclear particle through its interaction with the incident neutron is lifted from its normal state to a higher quantum state at the same time as the neutron becomes itself bound in some stationary state in the nuclear field with an energy too low to allow its immediate escape. On account of the small power of penetration of the incident neutron wave into a potential hole of nuclear dimensions even a relatively small probability of energy transfer from the neutron to another particle bound in the nucleus is in fact, as they showed, sufficient to reverse the balance between the scattering and the radiative processes in such collisions. Still, as was already pointed out in (A), the observed extraordinary sharpness of the resonance phenomena and their comparatively frequent occurrence demand a much longer life time of the intermediate system and a much closer distribution of its energy levels than any nuclear model with weak coupling between the individual particles can give.

The decisive progress in the treatment of the resonance problems by Breit and Wigner consists, however, in the establishment of general formulas for the variation of the cross sections of neutron scattering and capture in the resonance region, which are of great value for the analysis of the experimental evidence. Denoting by Γ_n and Γ_r the probabilities of neutron disintegration and of radiative transitions of the compound system respectively these cross section formulas can be written

[1] Breit and Wigner, Phys. Rev. **49**, 519, (1936).

$$\sigma_{sc} = \frac{\lambda^2}{4\pi} \frac{\Gamma_n^2}{(E-E_0)^2 h^{-2} + \frac{1}{4}(\Gamma_n+\Gamma_r)^2} \tag{14}$$

and

$$\sigma_r = \frac{\lambda^2}{4\pi} \frac{\Gamma_n \Gamma_r}{(E-E_0)^2 h^{-2} + \frac{1}{4}(\Gamma_n+\Gamma_r)^2}, \tag{15}$$

where λ and E are the wave length and kinetic energy of the incident neutron respectively, and E_0 is the energy value to be ascribed to the semistable stationary state of the compound system.

The remarkable resemblance of (14) and (15) with well known optical dispersion formulas is most suggestive and illustrates in particular the difficulties of separating simply in resonance collisions the probability of the formation of the compound system from the probabilities of the competing disintegration and radiation processes of this system. While the ratio between the latter probabilities as always alone determines the relative yields of scattering and capture, we see from the dependence of the absolute values of these yields on Γ_n and Γ_r how these probabilities also influence the degree of resonance obtainable and thereby the probability of the formation of the compound system.

As regards the discussion of the experimental evidence by means of (14) and (15), it is especially important that it in principle is possible from measurements of the breadth of the resonance region

$$\beta = h(\Gamma_n + \Gamma_r) \tag{16}$$

and of the maximum capture cross section

$$\sigma_r^{\max} = \frac{\lambda^2}{\pi} \frac{\Gamma_n \Gamma_r}{(\Gamma_n+\Gamma_r)^2} \tag{17}$$

to determine Γ_n as well as Γ_r. The closer analysis of the phenomena shows that for heavier elements Γ_r is of the order of

10^{14} $\sec^{-1}$, and that the ratio of Γ_γ and Γ_n for neutrons of temperature velocity is about 10^3. While Γ_γ over a considerable energy region must be expected to vary only slowly with energy, Γ_n will, as follows from quite simple quantum mechanical arguments, be directly proportional to the velocity of the incident neutron in the energy region, where the neutron wave length is large compared with nuclear dimensions, because in such a case the balance between the processes will depend only on the probability of the presence of a neutron close to the nucleus[1].. We shall therefore expect that Γ_n and Γ_γ will be of the same order of magnitude for neutron energies of about 10^5 volts. For still higher energies Γ_n must be expected to increase still more rapidly and soon become much greater than Γ_γ in conformity with the experimental evidence regarding fast neutron collisions[2].

In the formulas (14) and (15) it is presumed that only one semistable state of the compound system is responsible for the anomalous variation of the cross sections for capture

[1] As pointed out by O. R. Frisch and G. Placzek, Nature **137**, 357, (1936), and by P. Weekes, M. Livingstone and H. Bethe, Phys. Rev. **49**, 471 (1936), such simple arguments offer a direct method of gauging small neutron velocities. In fact the cross section for nuclear disintegrations initiated by slow neutron impacts and resulting in the release of fast α-rays will over a large energy region with high approximation be inversely proportional to the neutron velocity, since in such a case the life time of the compound system will be very small and all typical resonance effects will disappear as also shown by formula (15), if β given by (16) is very large compared with the energy of the incident neutrons in the whole region concerned.

[2] In a recent paper by H. Bethe and G. Placzek, Phys. Rev. **51**, 450, (1937), a detailed discussion of the experimental evidence regarding slow neutron collisions is given. In this paper formulas of somewhat more general type than (14) and (15) are developed, in which an explicit account is taken of the influence on the resonance phenomena of the spin properties of the nuclei concerned.

and scattering. Just as in the case of optical dispersion it is possible, however, to account for the combined effects of several resonance levels, if only the breadth of each level is small compared with the distance between neighbouring levels. In case the compound system in the energy region concerned has a continuous level distribution such an analysis cannot be unambiguously performed, but — if in this region the wave length of the incident neutron is still large compared with nuclear dimensions — the cross section for scattering and capture will be given by the simple expression (17), if the Γ's are identified with the slowly varying probabilities of disintegration and radiation of the compound system. In fact, in contrast to the case of collisions with fast neutrons, the cross sections will in this region be determined by a balance between the processes of formation and disintegration of the compound system which quite resembles that in complete resonance. (Addendum VIII).

§ 6. Release of Charged Particles from Nuclei.

As is well known from the quantum mechanical explanation of α-ray disintegration of radioactive nuclei, a charged particle may escape from a nucleus even if its potential energy in the region just outside the proper nuclear surface would be larger than its kinetic energy at great distances. In fact, a most instructive explanation of the characteristic relation between the energy with which α-rays are expelled from radioactive nuclei and the average life time of such nuclei has been obtained by comparing these disintegrations with the escape of a particle through a fixed potential barrier around the nucleus formed by the combined action of the attraction between the nuclear particles at small distances and their electrostatic repulsion

beyond the range of these forces. As well known from Gamow's theory, we get in this way for the probability of disintegration per unit time

$$\Gamma_\alpha \backsimeq \tau^{-1} e^{-\frac{4\pi}{h}\int_a^b \sqrt{2m\,(P(r)-E)}\,dr}, \qquad (18)$$

where m and E are the mass of the particle and the energy with which it is expelled, $P(r)$ is the potential of the particle at the distance r from the center of the nucleus, a is the inner radius of this barrier, and b the classical distance of closest approach.

Formula (18) has in particular been used as a basis for estimates from the known disintegration constants of the radii of radioactive nuclei. The recognition of the decisive influence of energy exchanges between the individual nuclear particles on the probability of the release of uncharged particles from the compound system formed by nuclear collisions raises, however, the question to what extent such estimates are reliable. In fact we have to consider that the α-particle before its expulsion does in no way move freely in a fixed potential hole but that its escape from the nucleus must rather be considered as composed of two more or less sharply separated steps, of which the first consists in the release of the α-particle from the nuclear matter, and the second in its penetration as a free particle through a potential barrier. Comparing the first step of this process with the escape of fast neutrons from highly excited nuclei, Bethe[1] has in a recent paper concluded that the penetrability of the α-particle barrier must be many times larger than hitherto assumed and has thus arrived at values for nuclear radii which are considerably larger than those

[1] H. Bethe, Phys. Rev. **50**, 977 (1936).

ordinarily adopted and which would require a radical change in all estimates of the effect of the extranuclear electric forces in charged particle reactions.

As regards such an argumentation it must be remembered, however, that while the outer slope of the barrier is determined entirely by the electric repulsion between the nuclear particles at large distances, its inner rise is essentially due to the peculiar nuclear forces at small distances. The disintegration of the imaginary nucleus, which would remain after the complete elimination of the barrier, would therefore not be opposed by the nuclear forces in the same way as the escape of neutral particles from real nuclei, and the difference between two such processes will obviously be the larger the more the top of the potential barrier is raised over the energy of the escaping particle. In the particular case of radioactive nuclei in their normal state, where the height of the α-ray barrier is of the same order of magnitude as K, the instability of the nuclear system which remains after the elimination of this barrier would thus seem to be so large that the probability of disintegration of the nucleus would be practically determined by the barrier effect alone. Notwithstanding the ambiguity inherent in all estimates of nuclear radii without a closer discrimination between various possible types of nuclear reactions, it would therefore seem that estimates of the radii of radioactive nuclei by means of formulas of the type of (18) can hardly be changed greatly by taking the many body aspects of the problem into account. (See Addendum IX.)

Compared with α-ray decay of radioactive nuclei in their normal state the relative influence of the repulsive forces and the energy exchange between the individual nuclear particles on the disintegration probabilities is com-

pletely reversed in the highly excited compound nuclei formed by collisions where, as already remarked in § 4, the direct effect of the repulsive forces will often simply be a subsequent acceleration of the charged particles evaporating from the nuclear matter. This effect is especially clearly shown in the much studied nuclear transmutations initiated by α-ray impact on light nuclei and resulting in the expulsion of high speed protons. Resembling the circumstances of neutron escape from excited nuclei it is found that, as soon as the energy is large enough, it is more likely that the nucleus after the proton expulsion is left in an excited state than in its normal state. The only difference between the relative abundance of the various proton groups appearing in such transmutations and that of the corresponding neutron groups is, in fact, that due to the repulsion even the slowest protons have energies markedly higher than the temperature of the compound nucleus. Still, as regards the estimate of the absolute values of the disintegration probabilities by means of evaporation formulas of the type (12), it must be remembered that the latent heat of evaporation cannot be simply identified with the energy necessary to remove a proton in the normal state of the compound nucleus to infinite distance, but that the potential of the proton just outside the nuclear surface must be added to this energy.

§ 7. Collisions between Charged Particles and Nuclei.

In nuclear transmutations initiated by impacts of charged particles we can, if the energy of these particles is sufficiently large as in fast neutron collisions, consider the formation of the compound system as a direct consequence of a contact between the incident particle and the original nucleus. In case of charged particles, however, the energy

must of course be so large that even after the penetration through the electrostatic repulsive field around the nucleus the wave length of the incident particle is still small compared with nuclear dimensions. For impacts of high speed α-particles on lighter nuclei the approximate fulfilment of these conditions for a simple treatment of the formation of the compound system is proved by the fact that the total yield of the disintegration processes is nearly independent of the velocity of the incident particles. This is particularly clearly shown in certain cases where as well protons as neutrons can be released in comparable abundance as a result of the collision, and where it is found that the sum of the yield of protons and neutrons is remarkably constant over a large region of α-ray energy, even if their relative abundance may vary considerably within this region[1]. At the same time this observation shows most strikingly that in such collisions we have not to do with any direct coupling between the individual protons and neutrons expelled and the incident α-ray, but that the proton and neutron release represents competing disintegration processes of the compound system[2].

In α-ray impacts with smaller energies we meet with a more complicated situation, partly because the energy levels of the compound system are no longer continuously distributed but more or less sharply separated and partly because the establishment of contact between the incident particle and the original nucleus presents in itself a typical quantum mechanical problem. As regards the latter question it is

[1] See O. Haxel, Z. f. Phys. **93**, 400, (1935).

[2] Added in proof. This point has recently also been emphasized by W. D. Harkins, Proc. Nat. Acad. of Sci. **23**, 120, (1937), who, without entering more closely on the question of the mechanism of nuclear reactions, already several years ago has advocated the view that nuclear transmutations are always initiated by the formation of a compound system.

well known that Gamow's theory for the penetration through the potential barrier around the nucleus allows one, in many cases of nuclear disintegrations initiated by α-ray impact, to account satisfactorily for the variation of the output with increasing α-ray energy. It is, however, obvious that the remarkable maxima for certain α-ray energies observed in several nuclear disintegrations giving rise to the expulsion of high speed protons cannot be explained in the usual way by attributing such maxima to the presence of a semistable quantum state of the incident α-particle within the barrier, from which it may fall to some lower quantum state accompanied by the rise of the proton from its normal energy level within the nucleus to a level sufficiently high to allow its escape. In fact, no such explanation of the resonance effects, where in the first approximation the α-particle as well as the proton is supposed to move in a fixed nuclear field, can be reconciled with the large probability of proton emission by impact of faster α-particles, which may be assumed easily to penetrate into the interior of the nucleus. Indeed, as remarked incidentally by Mott[1] already some years ago, this fact implies a coupling between the α-particle and a proton, which would be far too close to permit a resonance to develop even for lower α-ray energies, where the penetration of the α-particle into the nucleus is assumed to be essentially influenced by the potential barrier, but where the excess energy is still sufficient to permit the proton to pass unhindered over the top of the barrier.

The resonance effect in question must clearly be attributed to a coincidence of the sum of the energies of the free α-particle and the original nucleus with that of a stationary state of the compound system corresponding to some quan-

[1] N. F. Mott, Proc. Roy. Soc. **133**, 228, (1931).

tized collective type of motion of all its constituent particles. The sharpness of these states and accordingly of the resonance effects will depend on the life time of the compound system, which will be determined by the sum of the probabilities of the various competing disintegration processes of this system. Apart from exceptional cases the release of protons will be far the most probable and will, as clearly shown by the velocity distribution of the emitted protons mentioned in § 6, depend on an evaporation like process of the nuclear matter which only indirectly will be influenced by the presence of the repulsive forces outside the nucleus. This is not only in conformity with the existence of resonance in the energy region, where a proton would be able to escape without difficulty from the potential barrier, but also explains the fact that the width of the resonance levels for not too fast α-rays varies only slowly with increasing α-ray energy, although the ease with which an α-particle passes through the potential barrier should increase very rapidly with increasing α-ray energy.

In a more detailed discussion of nuclear transmutation initiated by α-ray impacts it must further be taken into account that the wave length of the α-particle even in the resonance region is generally of the same order as nuclear dimensions and that therefore special attention must be paid to the possibilities of different values of its angular momentum relative to the nucleus and their influence on the absolute values of the effective cross sections for the disintegration process. This circumstance will in particular influence an estimate of the relative importance of the potential barrier and of energy exchange within the nucleus on the release probability of α-particles in the region concerned. It is in this connection also of interest to note that the

phenomenon of so called anomalous scattering of α-rays in close nuclear collisions may not, as in the usual treatment, be entirely attributed to a deflection of the α-ray in a fixed field of force but may be essentially influenced by the possibility that an α-particle is temporarily taken up in the compound nucleus and subsequently emitted by a separate disintegration process.

In nuclear transmutations initiated by artificially accelerated protons the repulsive forces will on account of the comparatively small energy of the incident particle have a preponderent influence on the whole phenomenon. This is also shown by the great accuracy with which the relative variation of the output with proton energy, apart from cases of exceptional sharp resonance, is given by Gamow's theory. Simple calculations of the probability of penetration of the protons through the potential barrier can, however, not explain the often remarkably large differences between the absolute values of the output of transmutation processes by impact on different nuclei. These specific effects show in fact in a striking way the great extent to which the probability of the formation of the compound system in the proper quantum mechanical region may depend on the probabilities of disintegration processes of this system itself, which probabilities may again depend largely on the spin properties of the original nucleus and the disintegration products.[1]

In the particular case of highly selective capture of slow protons by certain light nuclei we meet, as regards the way in which the capture cross section depends on the probabilities of proton escape and of radiative transitions,

[1] Compare M. Goldhaber, Proc. Camb. Phil. Soc. **30**, 361 (1934); L. R. Hafstad, N. P. Heydenburg and M. A. Tuve, Phys. Rev. **50**, 504 (1936). (See also Addendum IV).

with an especially instructive analogy to slow neutron capture, at the same time as the two phenomena exhibit extreme differences in mechanical respects. In fact the cross section for proton capture and the breadth of the resonance region can obviously be expressed by general formulas of the same type as (15) and (16), but while the probability of neutron release Γ_n depends solely on energy exchanges within the nuclear matter the corresponding probability for proton escape Γ_p will also largely depend on the extra-nuclear repulsion. Still due to the high excitation of the compound system the situation is essentially different from α-ray disintegration of radioactive nuclei in their normal state, discussed in paragraph 6, and the influence on Γ_p of the mechanism of release of the proton from the nuclear matter will here be comparable with the barrier effect.

Essential new features are exhibited by transmutations initiated by deuteron collisions where the output over larger energy regions is often very much greater than estimated by the quantum mechanical probability of a material point with charge and mass like that of the deuteron in reaching the surface of the nucleus. As pointed out by OPPENHEIMER and PHILLIPS[1] we must, however, here take into consideration that on account of the comparatively large size and small stability of the deuteron it may be disrupted during the collision with the result that the neutron is captured by the nucleus and the proton repelled by the extra nuclear field. For the smallest deuteron velocities this view seems actually to offer a satisfactory explanation of the experimental evidence. For larger deuteron velocities, where still the energy is too small to allow a sufficiently probable penetration of a charged mass point into the interior of the nucleus,

[1] J. R. OPPENHEIMER and M. PHILLIPS, Phys. Rev. 48, 500 (1935).

it is, however, necessary to assume that even a partial overlapping of the regions, to be ascribed to the motions of the elementary particles of which the nucleus and the deuteron respectively are composed, may result in a complete fusion of the two systems into a semistable compound nucleus.

On account of the weak binding energy of the deuteron the excitation of the compound nucleus will here be almost double as high as that which results from a neutron or proton impact. Still — except in the extreme case of mutual collisions between deuterons where the total energy approaches that of two free protons and two free neutrons too closely to allow an intermediate state of sufficient stability — the excitation energy of the compound system will be so small compared with the total binding energy of its particles that, like in other nuclear transmutations, the collisions can be separated into two well defined stages. In fact just the great variety of the disintegration processes of the compound system made possible by the high excitation in deuteron collisions offers many instructive examples of the competition responsible for the final result of nuclear reactions.

Addendum.

I. Under the simplifying assumption that each level represents a combination of a number of nearly equidistantly distributed quantities the density of nuclear levels for high excitation can be simply estimated by means of an asymptotic formula for the number of possible ways $p(n)$ any integer may be written as a sum of smaller positive integers which has been derived by G. H. Hardy and S. Ramanujan (Proc. London Math. Soc. (2) XLII, 75, 1918) and to which

our attention has recently be drawn. This formula can for large values of n be approximately written

$$p(n) = \frac{1}{4\sqrt{3}\,n} e^{\pi\sqrt{2/3\,n}} .$$

If now for the unity we assume an energy value of $2 \cdot 10^5$ e. V. corresponding approximately to the average distance between the lowest levels of heavier nuclei, we get for the number of combinations with which an excitation energy of $8 \cdot 10^6$ e. V. can be obtained $p(40) \cong 2 \cdot 10^4$, meaning an average level distance of about 10 e. V. which roughly corresponds to the densities of the level distribution estimated from slow neutron collisions.

II. A closer theoretical discussion of the characteristic features of the nuclear level distribution has been given by H. Bethe (Phys. Rev. **50**, 332, 1936, and Rev. mod. Phys. **9**, 69, 1937) who, on the basis of general theorems of statistical mechanics connecting the entropy of a thermodynamical system with the average energy, has estimated the density of energy levels of a highly excited nucleus for two different simplified models of nuclear excitation. In the first of these the coupling between the motion of the individual particles is entirely neglected for the sake of simplicity and the excitation energy is compared with that of a so called Fermi gas at low temperatures; in the second model the coupling is assumed to be close and the excitation energy is supposed to have its origin entirely in capillarity oscillations of the nuclear matter of the type discussed briefly in the text. Although none of these models can be assumed to reproduce the actual conditions in nuclei correctly, the calculations of Bethe offer instructive examples of the ways in which the typical character of the level scheme of nuclei

follows from the assumption that the excitation energy is shared by the nuclear particles in a way corresponding to a thermal equilibrium.

Further interesting contributions to this problem have been given by L. Landau (Sow. Phys. **11**, 556, 1937) and V. Weisskopf (Phys. Rev. **52**, 295, 1937) who, without introducing any special assumptions as regards the origin of nuclear excitation, have calculated the nuclear level density by thermodynamical methods, assuming that the mean value of the excitation energy for a heavy nucleus is proportional to the square of its absolute temperature. This condition, which also is fulfilled in the first of the two special cases discussed by Bethe, does actually mean that the fundamental modes of motion in nuclei have energy values which are nearly equidistant. It is therefore interesting to note that the formulas for the nuclear level density derived from thermodynamical analogies are — at any rate as regards the exponential dependence on the total excitation energy of the nucleus — practically identical with the expression for $p(n)$ in Addendum I, if we by the number n understand the measure of the total energy with the energy differences between the lowest states, as unit.

III. The question of the origin of nuclear excitation involves great difficulties due not only to the scarcity of our knowledge of the specific nuclear forces but also to the complications of the quantum mechanical problem concerned. The aim of the simple remarks in the text is therefore in the first line to discuss certain possibilities of a simplified semi-empirical treatment. While in this respect the existence of quasi elastic oscillations of nuclei suggests itself by a straightforward correspondence argument, it is,

however, very doubtful whether such an argument can be legitimately applied to an analogy of nuclear excitation with capillary oscillations. In fact the comparison with a non viscous fluid involved in this analogy can hardly be maintained in view of the close coupling between the motions of the individual nuclear particles. Besides such a comparison would — as kindly pointed out to us by Prof. PEIERLS at a recent discussion in Copenhagen — force us to consider other types of inner nuclear motions as well, which in particular would be inconsistent with the comparison mentioned in the text of the rotational motion within a nucleus and that of a rigid body.

IV. The problem of the interaction between the orbital momenta and spin vectors of the nuclear particles has often been discussed not only in connection with the spin values of nuclei but also in attempts of accounting for the remarkable selection rules for various nuclear transmutations. Usually these effects are ascribed to a loose coupling between the orbital momenta of the individual particles and their spin vectors like that in atoms. In a recent paper by F. KALCKAR, J. R. OPPENHEIMER and R. SERBÉR (Phys. Rev. **52**, 279, 1937) it is shown, however, that it seems possible to explain these rules merely by assuming that the total angular momentum and the resulting intrinsic spin of the nuclear particles are coupled sufficiently loosely to allow a well defined quantum mechanical specification of their relative orientations.

V. A treatment of the nuclear photoeffect consistent with the views on nuclear excitation and radiation here discussed is attempted in a recent paper by F. KALCKAR, J. R. OPPENHEIMER and R. SERBER, (Phys. Rev. **52**, 273,

1937). In particular it is shown how it is possible from the remarkable experiments by W. Bothe and W. Gentner with high energy γ-rays (Naturwiss., 25, 90, 126, 191, 1937), to estimate the probabilities of radiative transitions from excited states to the normal state of the nucleus. For nuclei of medium atomic weight and 17 M. e. V. excitation these probabilities are in certain cases found to be of the order $\tau^{-1} \cdot 10^{-9}$ sec^{-1}, i. e., about $^1/_{100}$ of the most probable radiation probabilities for such nuclei. This comparatively large probability of such distant transitions contrasts strikingly with what might at first sight be expected from a simple comparison (see L. Landau, Sow. Phys. **11**, 556, 1937) of the radiation from an excited nucleus and a black body with the temperature of about a million volt per degree of freedom (see § 4). Still it may be remarked that such a comparison involves difficulties due to the high degree of polarity of nuclear radiation and the close coupling between the various modes of excitation mentioned in the text. Moreover the apparently capricious way in which the yield of the nuclear photoeffects varies from element to element suggests that we have in transitions from these highly excited nuclear states to the normal state to do with some peculiar features of the radiative mechanism connected perhaps with the appearance of dipole moments.

VI. A closer examination of the conditions for the application of an evaporation formula of the usual type to nuclear disintegration problems is given by V. Weisskopf in a recent paper cited in Addendum II. On the basis of general methods of statistical mechanics a detailed discussion is given there not only of the limitation of simple thermodynamical analogies in nuclear problems due to

the comparatively few degrees of freedom of the system concerned, but also of the generalisations of the usual thermodynamical procedure required for the proper treatment of such systems.

VII. The energy distribution of neutrons escaping from highly excited nuclei has been especially closely studied in the case of the usual neutron source of Beryllium bombarded with α-rays. While here the distribution of the fast neutrons is found to agree closely with the theoretical expectations, an apparent deviation is exhibited by the relative abundance of neutrons with energies far below the estimated temperature of the compound nucleus. This apparent difficulty disappears, however, if we assume that the slow neutrons in question must, as first suggested by P. AUGER (Journ. de Physique, **4**, 719, 1933), be ascribed to a more complex process, the first stage of which is the escape of an α-ray from the compound system leaving a beryllium nucleus in an excited state, while the second stage consists in the subsequent breaking up of this nucleus into two α-particles and a slow neutron. This view is further strongly supported by a recent experimental investigation by T. BJERGE (Proc. Roy. Soc., in print).

VIII. The question of the quantum mechanical resonance effects in case of continuous level distribution has recently been more closely discussed by F. KALCKAR, J. R. OPPENHEIMER and R. SERBER in the paper cited in Addendum V, on the nuclear photoeffect, which presents special features analogous to the problem of nuclear transmutations initiated by impact of slow particles. A more comprehensive quantum mechanical treatment of nuclear reactions will further be given in a paper by F. KALCKAR to appear shortly and

in which it will especially be attempted to develop general arguments resembling the correspondence treatment of atomic radiation problems.

IX. The question of the proper estimate of the nuclear radii to be derived from the analysis of α-ray disintegration of radioactive nuclei is further discussed by Bethe in his recent report on nuclear dynamics (Rev. of Mod. Phys., **9**, 69, 1937), where he makes extensive use of the enlarged values of such radii which he has proposed in the paper cited on page 26. In this connection Bethe also comments on the criticism of this procedure of estimating nuclear radii given in the text and presented at the Conference in Washington (see Preface). Meanwhile an important contribution to this problem has been given by Landau in his paper cited in Addendum II, where he has succeeded from very general arguments in deducing a comprehensive formula for the dependence of the probability of nuclear disintegrations under release of charged particles on the external repulsion as well as on the density of the level distribution of the nucleus in the energy region concerned. In the case of radioactive decay, where the levels are widely separated, Landau's formula leads to values for the nuclear radii which differ only little from those derived from ordinary potential barrier formulas but which are essentially different from those proposed by Bethe. The closer connection between Landau's treatment and the argumentation given in the text will be discussed in the forthcoming paper of Kalckar which was mentioned above.

Færdig fra Trykkeriet den 27. November 1937.

Det Kgl. Danske Videnskabernes Selskab.
Mathematisk-fysiske Meddelelser. **XIV**, 11.

THE STABILITY OF CRYSTALLINE PEPSIN

BY

JACINTO STEINHARDT

KØBENHAVN
LEVIN & MUNKSGAARD
EJNAR MUNKSGAARD
1937

A preliminary account of these measurements was presented to the Kemisk Forening of Copenhagen on 19 May, 1936, and appeared in abbreviated form in *Nature*, 11 July, 1936.

Printed in Denmark.
Bianco Lunos Bogtrykkeri A/S.

THE STABILITY OF CRYSTALLINE PEPSIN

BY

JACINTO STEINHARDT*

(from the Institute of Physical Chemistry of the University of Copenhagen)

I. Alkaline Inactivation.

The availability of crystalline enzyme preparations which are well-defined and homogeneous to degree offers obvious incentives to renew physico-chemical investigations of enzyme behaviour. The results of such investigations should be relatively free of the uncertainties which necessarily attended the many ingenious experiments with grossly impure and undefinable solutions, in the last decade. Examination of the variation of activity, stability, and certain convenient physical properties over a wide range of conditions may not only elucidate the mechanism of enzyme action, but also furnish indications of their chemical structure. Further incentive lies in the great advances in solution theory during the last fifteen years. These have a special importance for the crystallizable enzymes which, as with other proteins, must be regarded as highly polyvalent acids entering into involved electrolytic equilibria; their departure from ideal behaviour will be as great, or greater, than any the physical-chemist has already studied. Finally, the accumulation, in recent years, of accurate and essential physico-chemical protein data facilitates and compels unambiguous interpretation of enzyme experiments.

* Fellow of the Nation Research Council, and of the General Educational Board, U. S. A. during the course of this research.

Although purification of an enzyme makes possible its analytical and thermodynamic investigation, its kinetic properties are still most characteristic and most significant. Unfortunately the substrates of the most easily available crystalline enzymes are themselves proteins and undergo reaction in many successive steps. Study of such systems is extraordinarily difficult, practically and theoretically; one must not only succeed in distinguishing the effects of the experimental variables on each of two complex substances, but must also isolate experimentally a single link in the chain of successive reactions — for which at present there is no certain procedure — and must find conditions under which the accumulating diversity of reaction products will not alter the initial state of the system beyond definition. The instability of both enzyme and substrate create other difficulties (NORTHROP has shown that some kinetic experiments merely measure the rate of destruction of the enzyme, and give little information about its reaction with the substrate). Knowledge of the stability of both components is a necessary prerequisite for kinetic studies on the reaction between them. Such knowledge can only result from other, simpler kinetic experiments.

Study of the kinetics of enzyme inactivation, because it avoids the difficulties just cited and furnishes necessary information for later work, is thus a logical first step in a general investigation of enzyme kinetics. Here there is no other substance under examination than the enzyme itself.

Pepsin was selected for the present research because it is easily and cheaply prepared, and because it has been subjected to more thorough tests of homogeneity (including ultracentrifugal analysis: PHILPOT and ERIKSSON-QUENSEL, 1933; PHILPOT, 1935) than other crystalline preparations.

Unlike trypsin, its destruction is almost completely irreversible under ordinary conditions (NORTHROP, 1930—31). Methods of measurement therefore involve fewer assumptions or complications of procedure.

Earlier inactivation experiments with impure pepsin have led to a number of unusual conclusions. It has been reported that a definite fraction of the total enzyme (the size of the fraction varying with the hydrogen-ion concentration) is instantly inactivated on bringing a solution to a neutral or alkaline pH; the remainder then becomes inactive unimolecularly at a measurable rate (GOULDING, WASTENEYS, and BORSOOK, 1926—27). The inactivation rate has been shown to depend greatly on the acidity, as in protein denaturation, but different investigators have reported different degrees of dependence. MICHAELIS and ROTHSTEIN (1920) who believed the kinetics to follow a three-halves order, found the rate to vary inversely with the fourth power of the hydrogen-ion concentration over a wide range. EGE (1925) found a third power dependence; the less extensive data of GOULDING, et al., indicate an exponent between these two, although these authors describe the inverse relation to hydrogen ions as linear. It is shown in the present paper that all these results are partly fortuitous, but a large exponent relating the rate to hydrogen-ions is common to all and requires explanation. Interest also attaches to the large thermal increments, also characteristic of protein denaturation, reported for pepsin by ARRHENIUS (75,000 calories) and by MICHAELIS and ROTHSTEIN (58,000 calories) since, as in many cases of denaturation, these large values require much slower rates of reaction at ordinary temperatures than are actually observed if the thermal increment is to be given its usual theoretical significance.

In the present research the course of inactivation has been followed over the widest possible range of acidity and salt concentration with four different buffers. In addition, the effect of temperature has been studied by measuring the dependence of velocity on acidity at a second temperature as well.

II. Experimental.

Pepsin. — The enzyme was crystallized from PARKE, DAVIS pepsin, 1 : 10,000, by PHILPOT's modification (1935) of NORTHROP's method.[1] In a few experiments pepsin crystallized once only, by NORTHROP's unmodified method (1930), was used, but most experiments were made with pepsin crystallized three times according to PHILPOT's directions, except for the occasional omission of stirring in the second and third crystallizations. Some 25 stock-solutions were prepared at various times, as described below, from 8 different preparations; the non-protein nitrogen impurity, estimated by precipitation of the protein with 10 volumes of 0,15 M trichloracetic acid at 80° and KJELDAHL analysis of the filtrate, varied from 4 to 25 per cent. of the total nitrogen. In spite of these differences the kinetic data obtained with all the stock solutions are a homogeneous body of data, and it is impossible to correlate minor individual variations with particular batches of crystals, or with the amount of impurity.

The specific activity, measured by the hemoglobin method, was always somewhat higher than the figure given by ANSON and MIRSKY (1932—33). This is partly due to the high dilution in which the activity was tested, since the hemoglobin method is not entirely independent of concentration (see Measurement of Pepsin Concentration, below). When calculated by the method described below, different solutions prepared from the same or different batches of crystals showed the same range of variation in specific activity, about 10 per cent.

After thorough washing with 0.001 M HCl, stock solutions were prepared by stirring the crystals in small volumes of 0.005 M HCl until no more would dissolve. After filtering off the residual crystals this procedure was repeated with fresh solvent, in some cases

[1] I am indebted to Mr. PHILPOT for kindly making available to me before publication his convenient method for crystallizing pepsin.

as often as 30 times. The apparent solubility falls off rapidly with successive extractions of the same crystals, and appears to approach a limiting value; the exact determination of this limit is difficult since the small quantity of crystals which remain for the last extractions do not permit the rapid attainment of equilibrium. The apparent change in solubility is not accompanied by any significant change in specific activity, if the latter is calculated on the basis of pepsin nitrogen. Non-protein nitrogen drops to about 0.04 mg. per ml. after three or four extractions. This is a satisfactorily small fraction of the 'soluble' extract (about 5 per cent.), but since the later extracts are very much less concentrated, this constant level of non-protein nitrogen finally represents a quarter or more of the total nitrogen. Analyses in solutions are thus a poor indication of the amount of impurity in the crystals, for non-protein nitrogen is a larger fraction of the total nitrogen when the latter is small than when it is great, as can also be shown by using buffers in which pepsin is very soluble, — here non-protein nitrogen may be reduced to a negligible fraction. Conversely, non-protein nitrogen rises to some 50 per cent., in more concentrated HCl (at the isoelectric point) where the enzyme is less soluble.

The apparent fractionation with respect to solubility is very similar to the protein fractionations reviewed by SØRENSEN (1930) but appears to have a simple explanation, — gradual removal of electrolyte from the crystals by successive portions of solvent. This may be complicated to some extent by removal of acid from the solvent by the crystals in the first few exposures to solvent. When the solvent contains somewhat higher HCl concentrations and a sufficient amount of salt this drift in solubility is never observed after one or two washings. The constant amount of non-protein N always present may be due to admixture of slightly soluble solid nitrogenous material; it is noteworthy that tyrosine (in which pepsin is rich, and which is often seen in crystalline form in old denatured pepsin suspensions) would contribute the amount of non-protein nitrogen always found (WINNEK and SCHMIDT, 1935). If the first hypothesis suggested here is accepted, the solubility of pepsin in dilute HCl is lower than previously reported (NORTHROP, 1929—1930 b), at this concentration about 0.07 mg. N per ml. In 0.1 MKCl the solubility is approximately three times as great.

The first, more concentrated extracts sometimes but not always contained a quantity of inactive protein (from 15 to 35 per cent. in the first extract) which, like pepsin, is precipitated by 0.15 M

trichloracetic acid, but, unlike pepsin, is not rendered insoluble at the isoelectric point in the presence of half-saturated sodium sulfate by previous treatment with strong base. This material is usually largely removed in the first few extractions (25 ml. portions of solvent to an initial 6 gr. filter cake). Its occasional presence in kinetics experiments was without effect.

The stock solutions were kept at 3°—4° until needed. They underwent only slight deterioration in periods of 2—3 weeks before use.

Choice of buffers. — Pepsin is inactivated at measurable rates at pH between 5.7 and 7.1. Since the reaction velocity depends on the buffer, it was desirable to cover as much of the range as possible with single buffers. Phosphate excepted, none of the buffers conventionally used are available in this range, and phosphate was eliminated by the choice of monobasic acids to facilitate ease of calculation and control of ionic strength, and to avoid other buffered regions which might interfere with adjustment of pH for subsequent activity measurements. With the exception of a few orienting experiments with citrate, the buffers were made from *p*-nitrophenol (most frequently), trimethylacetic acid, and trimethyl-*o*-aminophenol halide. The classical dissociation constant of these acids (on the conventional acidity scale defined below) at $\mu = 0.1$ and 25°, are given in Table 1[1]. All four buffers were purified by

[1] I am grateful to Professor J. N. BRØNSTED for a highly purified sample of trimethylacetic acid, and for suggesting the use of trimethylaminophenols. These monobasic acids carry a positive charge, owing to the methylated nitrogen; their conjugate bases, the form in which they occur uncombined, are zwitterions. The charged group causes the phenolic group to dissociate at much higher hydrogen-ion concentrations than in phenol, and the methylation avoids the complications of polybasicity:

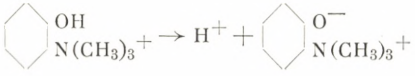

The meta- and para-acids are approximately equally strong (ca. 1×10^{-8}). All three forms have the useful property of crystallizing, on half neutralization of the base, as "basic salts" which can be dissolved to give solutions containing equal concentrations of acid and its conjugate base. The hydrogen-ion concentration of these solutions is thus equal to the dissociation constant. The dissociation constants and heats of dissociation (5165 calories for the ortho-compound) were measured by Mr. THOMAS ROSENBERG and by Fru cand. polyt. AGNES DELBANCO.

Table I.

Classical dissociation constants of acids used in preparing the buffers. Values refer to 25° and ionic strength 0.1.

Acid	K	pK
p-nitrophenol	1.12×10^{-7}	6.95
trimethylacetic	1.0×10^{-5}	5.00
trimethyl-*o*-aminophenol halide	3.81×10^{-8}	7.42

repeated recrystallization. The total concentration of acid plus base in the reaction mixture was kept at 0.02 M, except in the experiments with the aminophenol, in which the concentration was varied. In every case sufficient KCl (in a few experiments KNO_3, or KCl + NaCl) was added to bring the ionic strength up to the desired value (in the experiments at $\mu = 0.5$, in Table III only, the same amount of salt was used at every pH, μ rising in the more alkaline solutions to 0.51). Since *p*-nitrophenol is less than half dissociated at the more alkaline pH used, ionic-strengths much below 0.02 could be used with this buffer.

pH measurement. — Acidity measurements were made in triplicate at the conclusion of each experiment, with a quinhydrone electrode connected through saturated KCl to a 1 M KCl calomel half-cell. These were mounted in the thermostat used for the kinetic experiments; this precaution was required because two of the buffers used have a high temperature sensibility. The reaction velocity is so greatly dependent on pH and salt concentration that the comparative accuracy of the data is limited by the pH measurement rather than by the velocity-constant. Thus, it was also necessary to correct the observed potentials for the small differences of liquid junction potential in solutions of different ionic strength. The procedure used was similar to that of GUGGENHEIM and SCHINDLER (1934), but the potential of the calomel half-cell was assigned by measuring it against the quinhydrone electrode immersed in a solution, 0.005 M in HCl and 0.095 M in NaCl. The pH of this solution, at both temperatures, was arbitrarily defined as 2.339, in accordance with the older SØRENSEN scale; it is recognized that the true p_{aH} scale probably lies .065 units higher. The correction for liquid-junction potential, based on recent determinations of the transport numbers of K^+ and Cl^-

(McINNES and DOLE, 1931) becomes uncertain to the extent of one millivolt in the most alkaline solutions of ionic strength below 0.03, owing to the relatively large content of buffer anion of unknown mobility. In all calculations of pH, allowance was made for the effect of the ion concentration on the normal potential of the quinhydrone electrode (SØRENSEN, SØRENSEN, and LINDERSTRØM-LANG, 1921).

The quinhydrone electrode gives slightly drifting potentials in nitrophenol buffers. The presence of this drift has offered no difficulty in practise; the potentials obtained in the interval between 3 and 8 minutes are reproducible to 0.3 millivolts.

The solutions with $\mu = 0.5$ included in Table III were not measured at 25° but at room temperature. The pH has been corrected to 25° from the known heat of dissociation.

Kinetic procedures. — 40 ml. of 0.04 M buffer were placed in a 150 ml. glass-stoppered flask in the thermostat. Another flask contained the enzyme solution (diluted with 0.0005 M HCl to contain from 0.005 to 0.028 mg. pepsin N per ml.). Both solutions had been adjusted to the same ionic-strength with salt, and the buffer solution contained sufficient extra base to neutralize the acid in the enzyme solution. After half an hour, 40 ml. of enzyme solution were run into the buffer, a stop-watch being started at the time of half-delivery (usually 7—8 seconds). The vessel was whirled for a few seconds and allowed to stand in thermostat without further shaking except in certain experiments described later. At the desired intervals 3 ml. samples were pipetted off and discharged into small test-tubes containing sufficient HCl to neutralize all the buffer base, and to bring the free acid concentration to 0.0005 M. These samples keep in the cold for many hours without noticeable change; activity tests were usually made in from one to three hours, but in very slow experiments the solutions were tested a few minutes after sampling. A zero-time sample was also taken, in the same way, from enzyme that had been run into an equal volume of dilute HCl, or, as a further check, into the buffer acid. Comparison of these controls with one another and with the calculated effect of dilution is described in the discussion of the data.

This procedure was varied slightly in a number of experiments. Those involving very low ionic-strengths required that all the added salt should be in the enzyme solution and none in the buffer. In one series (Table III) the vessels were shaken regularly by a horizontal movement of 5 cms. 170—185 times per minute.

Measurement of pepsin concentration. — Pepsin was estimated by measurement of its catalytic activity, using two different test-proteins. In most experiments the enzyme in 1 ml. of the diluted sample was measured in duplicate by the hemoglobin method of ANSON and MIRSKY (1932—33), using commercial denatured hemoglobin (MERCK's). This change from the purified native hemoglobin solution of these authors necessitated redetermination of blanks, and calibration of the relation between colorimeter readings and enzyme concentration. Plotting the logarithm of the tyrosine equivalent determined colorimetrically, after subtraction of the reading with solutions containing no enzyme, against the enzyme concentration results in a straight line; but the slope of this line is not 1, as it should be for a linear relation. The 'proportionality blank' of ANSON and MIRSKY was not used, since tests with actual dilutions of a tyrosine standard added to the filtrates showed that it was not required. The relation between enzyme concentration and tyrosine equivalents in the digest is accurately given by the equation:

$$E = kTy^{1.265} \qquad (1)$$

with enzyme concentrations between 0.0003 and 0.01 mg. pepsin N per ml. If the concentration of the tyrosine standard is doubled, and higher enzyme concentrations are used, the relation is more nearly linear, and holds over a correspondingly higher range of concentrations with the exponent 1.150 instead of 1.265. Both concentration ranges have been used with completely consistent and comparable results.

Eq. 1 shows that, if the reaction kinetics are of the first order, the logarithm of the tyrosine reading is interchangeable with the logarithm of the enzyme concentration in giving a straight line against time. If the velocity constant is calculated from the slope this must be divided by the appropriate exponent. This procedure has been followed in calculating the velocity constants given in the tables.

Calculation of specific activities of pepsin preparations on the assumption that tyrosine readings obtained with this modification of the hemoglobin method are linearly related to enzyme concentration will give a result depending on the dilution of the enzyme tested. If, however, the activity is defined as the reciprocal of k in Eq. 1, and E and Ty are expressed in the same units as in ANSON and MIRSKY's definition, the figure obtained, 0.045 — 0.049,

is independent of concentration. The residual random variation is not greater than the limits of error in pepsin N measurements in the dilute stock solutions employed.

In order to get results of the highest reproducibility it was necessary to time all operations, i. e., the precipitated digestion mixture was filtered rapidly after standing for six minutes, the colour developed with the Folin reagent was measured after waiting one hour, etc. A deep red filter, inserted in the eyepiece of the colorimeter eliminated the interference of the yellow colour of nitrophenol.

In a few experiments KAHLBAUM's casein was used as test-protein. Here the amount of digestion after one hour was estimated by KJELDAHL analysis of the filtrate after precipitation with trichloracetic acid, as described by NORTHROP (1932—33), but the protein solution was prepared according to HOLTER (1930). Blanks were deducted for the quantity of nitrogen introduced by the buffer (with *p*-nitrophenol this blank is uncertain, owing to partial loss of nitrogen from the buffer during destructive digestion). Velocity constants determined in this way were entirely consistent with those obtained with the hemoglobin method (See Fig. 3, in which the points obtained with casein are marked by a thin vertical line).

Temperature control. — The experiments were carried out at 25° and 15°. A large mercury-toluol regulator and efficient stirring kept the temperature constant to better than 0.01°.

III. The Data.

The results of 85 experiments at 25° are given in Tables II and III, the division corresponding to whether or not the reaction-vessels were shaken during the experiment. Owing to the large number, it is impractical to present detailed data for each experiment; only the logarithm of the unimolecular velocity-constant, and the initial enzyme concentration are given for each set of experimental conditions. Each velocity constant represents duplicate analyses after at least ten time-intervals spaced over at least 80 per cent. completion of the reaction in over half the experiments (in many,

Table II.

Velocity of inactivation at 25° when the reaction-vessel was not shaken.

Ionic Strength	pH	$\log_{10} k_{10}^{\text{min.}}$	Initial Enzyme (mg. N/ml.)
(a) *p*-nitrophenol buffers			
0.50	6.012	— 3.708	0.00364
	6.250	— 2.489	.00368
	6.663	— 0.838	.00349
0.30	5.994	— 3.642	0.00338
	6.147	— 2.854	.00376
0.20	3.81	— 5.614	0.00579
	5.706	— 5.188	.00254
	5.830	— 4.322	.00604
	5.894	— 4.207	.00254
	6.290	— 2.273	.00577
	6.442	— 1.484	.00222
0.10	5.861	— 4.598	0.00388
	6.178	— 2.968	.00378
	6.502	— 1.470	.00391
0.05	5.964	— 4.390	0.00359
	6.095	— 3.752	.00378
	6.205	— 3.101	.00415
	6.382	— 2.307	.00435
	6.529	— 1.777	.00411
	6.668	— 1.628	.00437
0.0317	6.097	— 3.920	0.00307
	6.290	— 3.126	.00381
	6.325	— 2.907	.00370
	6.526	— 2.155	.00405
	6.895	— 0.945	.00376
0.0248	5.994	— 4.742	0.00418

(continued on next page)

Table II.

(continued)

Ionic Strength	pH	$\log_{10} k_{10}^{min.}$	Initial Enzyme (mg. N/ml.)
0.02	6.043	— 4.745	0.00290
	6.099	— 4.439	.00326
	6.356	— 3.152	.00311
	6.70	— 2.070	.00296
	6.94	— 1.303	.00319
0.012	6.044	— 5.117	0.00460
	6.374	— 3.452	.00456
	6.69	— 2.502	.00452
	7.03	— 1.534	.00458
0.0317	6.013	— 4.189	0.00341
(KNO_3 as salt)	6.475	— 2.232	.00340
0.20	5.838	— 4.305	0.00376
(with 1 % HCHO)	6.279	— 2.108	.00376
(b) Trimethylacetic acid buffers			
0.20	5.994	— 4.344	0.00363
	6.079	— 3.844	.00328
	6.476	— 2.041	.00359
0.05	6.176	— 3.919	0.00346
(c) Trimethyl-*o*-aminophenol buffers			
0.20	6.297	— 2.620	0.00337
	6.571	— 1.517	.00372
0.042	6.438	— 2.791	0.00322

over 95 per cent.). As indication of the adequacy of the data, and as justification of the employment of unimolecular constants as a description of the individual experiments, detailed results for three experiments from Tables II and III are shown in Fig. 1. These three representative runs have been selected only because their rates (at the same ionic-

Table III.

Velocity of inactivation at 25° with the reaction-vessel shaken. Data marked (′) were obtained with casein as test-protein: all others with hemoglobin.

Ionic Strength	pH	$\log_{10} k_{10}^{\text{min.}}$	Initial Enzyme (mg. N/ml.)
(a) *p*-nitrophenol buffers			
0.50—0.51	5.91	— 3.187	0.00800
	5.97	— 3.333	.0131
	5.99	— 3.211	.0130
	6.04	— 3.325	.0131
	6.08	— 3.003	.00939
	6.16	— 2.614	.0126
	(′) 6.28	— 2.326	.025
	6.33	— 2.142	.0119
	6.35	— 1.888	.0131
	6.38	— 1.860	.00735
	(′) 6.38	— 1.880	.025
	6.46	— 1.542	.00980
	6.49	— 1.604	.00936
	6.56	— 1.175	.0130
	6.64	— 0.882	.0111
0.30	6.044	— 3.051	0.0125
	6.145	— 2.767	.00806
	6.234	— 2.643	.00806
	6.316	— 2.076	.0139
	6.408	— 1.772	.00799
	6.452	— 1.483	.0127
	6.587	— 1.047	.0127
0.20	3.789	— 3.494	0.00578
	5.780	— 3.388	.00678
	5.851	— 3.454	.00596
	5.910	— 3.366	.0122
	6.034	— 3.305	.0126
	6.284	— 2.327	.0129
	6.631	— 0.931	.0139

(continued on next page)

Table III.

(continued)

Ionic Strength	pH	$\log_{10} k_{10}^{min.}$	Initial Enzyme (mg. N/ml.)
0.10	6.071	— 3.364	0.0102
	6.225	— 2.618	.00950
	6.436	— 1.642	.0104
0.05	5.958	— 3.676	0.00360
0.0248	5.980	— 3.582	0.00395
0.02	6.040	— 3.671	0.00320
0.012	6.028	— 3.420	0.00295

(b) Trimethyl-*o*-aminophenol buffers. Concentration 0.025 M at pH 6.73 and 0.05 for the others.

0.50	(') 6.410	— 2.072	0.025
	(') 6.73	— 0.77	0.025
	(') 6.79	— 0.67	0.025

(') Test protein was casein

strengths and in the same buffer) are not too far apart to be shown on a single graph; even so, there is an approximately fifty-fold variation in the half-periods of these three experiments, in the narrow pH interval between 6.290 and 6.631. The ordinates represent a quantity proportional to the logarithm of the pepsin concentration (as described under Methods), and the half-periods are shown by broken vertical lines.

It is clear that the data are well represented by kinetic equations of the first order, at least until the reaction is almost complete. The slight slowing at over 80 per cent completion is insufficient to permit application of three-halves order kinetic equations, as in the analysis of MICHAELIS and ROTHSTEIN. When the 52 experiments of Tables II and V are tested with both equations, 27 are satisfactorily fitted by

first order to over 80 per cent. completion, and only 2 appear to be better fitted by the fractional order; the remainder are indeterminate, either because they were not followed far enough, or in a few cases because the points scatter too

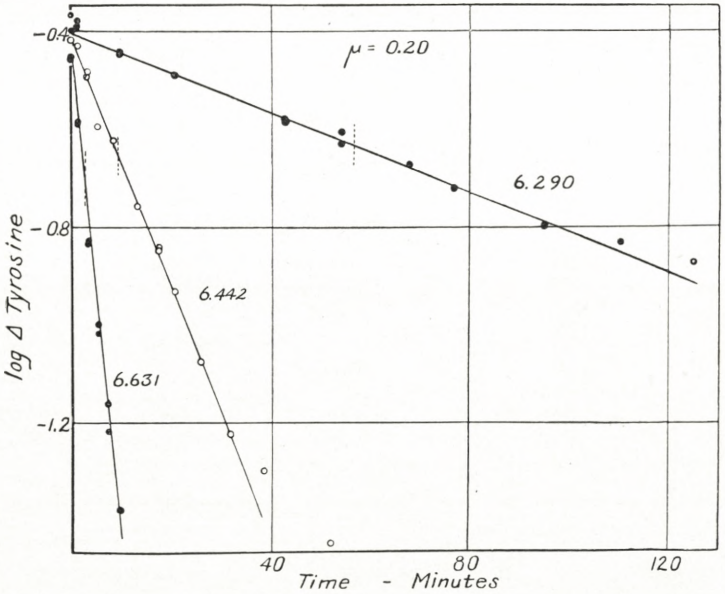

Fig. 1. The individual kinetic experiments at an ionic-strength of 0.2 at 25°. The buffer was *p*-nitrophenol. The experiment at pH 6.442 is from Table I, the others from Table II (reaction-vessels shaken). Broken vertical lines show the half-periods.

widely. An even more conclusive reason for rejecting the fractional order is that a fivefold variation in initial enzyme concentration fails to change the time for half completion. Thus, the slowest reaction shown in Fig. 1 (plotted as though it had the same ordinates as the other two sets of data) had an initial enzyme concentration only one-quarter that of the others; however, its rate stands in the same relation to pH as the others, as later described (see Fig. 2). In general, ex-

periments at this salt concentration fall into two groups of widely different initial concentrations, with no corresponding differences in velocity.

The deviations from first-order kinetics at the end cannot be due to approaching equilibrium, for the position of these deviations varies from one experiment to another, apparently at random, with no relation to pH. Similar absence of correlation with particular enzyme preparations likewise excludes the possibility of a small admixture of a more stable active substance. The progressive absorption of very small amounts of carbon dioxide during sampling would, in view of the great pH dependence, produce such deviations, but it is also possible that these effects indicate insufficient standardization in the complicated analytical procedure. When an almost completely inactivated pepsin solution is allowed to stand at pH 5 there is a slight recovery of activity for some days (NORTHROP, 1932—33, and unpublished experiments of the author). The amount recovered is small, but when 90 per cent. or more of the pepsin initially present in these very dilute solutions has been destroyed this amount is a considerable fraction of the remaining activity. The apparent falling off in inactivation rate when nearly all the pepsin has been destroyed may be due to such recovery of activity in the interval between acidifying the sample and testing its activity. The necessary addition of acid before each test introduces an unavoidable ambiguity[1].

Whatever their cause, these deviations are too small to

[1] PHILPOT has suggested (1935) that base does not denature pepsin but changes it to something more susceptible to subsequent acid denaturation. Should this be true, the present measurements nevertheless refer to the reaction initiated by base, but there might well be competing reactions on addition of acid before the tests. One of these may sligthly reverse the effect of base.

have an appreciable effect on the velocity-constants, which are fixed by the data to within 5 per cent. (in a few bad cases, 10 per cent.). This accuracy is ample for estimation of the effects of acidity, ionic-strength, and temperature, since the range of effects produced by variation in these conditions is very wide: there is a factor of about 88,000 between the fastest and slowest rates listed in Tables II and III.

The three experiments shown in Fig. 1 exhibit no instant inactivation of the kind describerd by GOULDING, BORSOOK, and WASTENEYS (1926). No such effects were found in any of the experiments. Effects of this kind can be detected only by comparing the enzyme concentration of the stock solution (corrected by the factor of dilution), or the enzyme concentration found in a blank dilution (with dilute HCl, or the buffer acid) against the enzyme concentration extrapolated to the beginning of the experiment from the straight line fitted to the experimental points. No better agreement can be expected than the closeness with which the ordinary experimental points fit the best straight line. In practise discrepancies of as much as 10 per cent. are occasionally found between extrapolated and calculated zeros; usually the agreement is better. The extrapolated figure is often higher than that calculated from the stock solution rather than lower the discrepancies seem therefore to be without special significance. It is reasonable to find slightly greater scattering in the zero time measurement since the procedure in sampling and estimating this solution is not exactly the same as the procedure for all the others. There is also reason for believing, in view of the discussion of the experiments of Table III in a later section, that some slight inactivation may occur at the start of an experiment from the act of mixing the solutions; a few per cent. of inactivation has been demon-

strated by comparison of the calculated zero (from measurement of the stock solution) and control dilutions with the acid of the buffer. Such inactivation, due to a heterogeneous reaction at air interfaces, is naturally not reproducible.

Although Northrop (1930 *a*) and Herriott and Northrop (1934) have published data on crystalline pepsin which appear to confirm the existence of instantaneously inactivated fractions varying with pH, the procedure described — analysis after a single time-interval a few minutes after mixing — could not distinguish between such effects and continuous inactivation at a rate increasing with pH. For crystalline pepsin, at least, it seems safe to conclude that this instantaneous inactivation does not exist, and need not be allowed for or explained.[1]

This description of the data of Table II applies equally to Table III, with a single reservation. The latter data, obtained in experiments during which the reaction-vessel was shaken, are of two kinds, as will be shown in the following pages: experiments pH 6.1 and above are in no way different from those already described, — unimolecular, and with no instant inactivation; below this pH, the velocity observed is predominantly that of a heterogeneous reaction, and is independent of pH. This reaction is likewise of the first order, but its velocity can be altered by the speed of shaking. This sometimes increased at night when the laboratory voltage rose; the precise value of the constants in the more acid solutions is therefore sometimes uncertain, and the results of different experiments are not all strictly comparable.

[1] The explanation proposed by Goulding and his collaborators requires the assumption that both active and inactive pepsin can act as a single chemical species in determining an equilibrium.

Since NORTHROP has shown that the inactivation of pepsin can be reversed, to a very small extent, at pH between 5.0 and 5.6, indications of an equilibrium point were sought in the more acid experiments. No marked deviations from first-

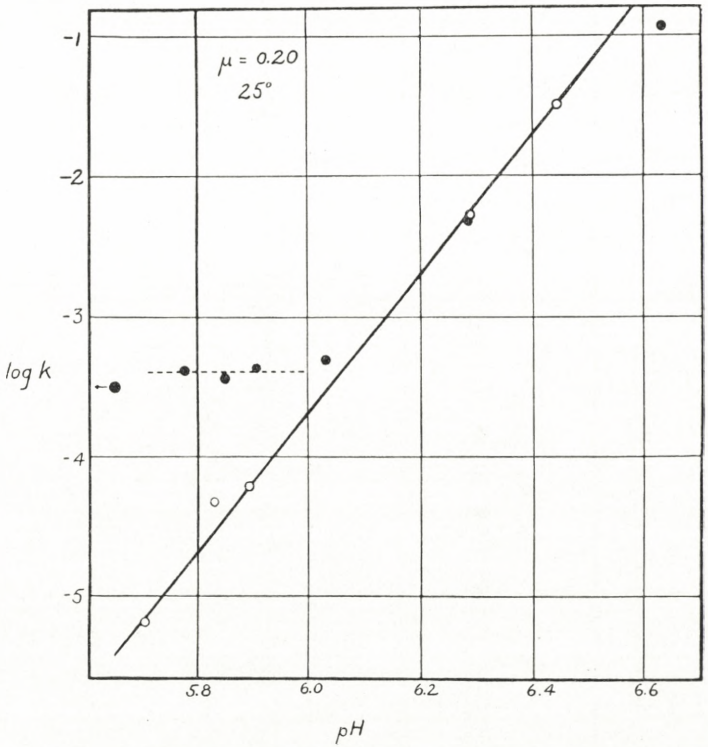

Fig. 2. The relation of the logarithm of the velocity-constant to pH at an ionic-strength of 0.2 at 25° with *p*-nitrophenol buffers. The open circles represent experiments from Table I (no shaking), the filled circles data from Table II (vessels shaken). The point marked with an arrow represents at experiment at pH 3.79.

order kinetics were shown at over 80 per cent. completion even in the slowest experiment in Table II (pH 5.706). Thus, even at acidites only sligthly above those used by NORTHROP, the equilibrium point lies far over on the side of total

destruction at this temperature; other experiments at sligthtly higher pH show that this is also true at 3°—4°.

Dependence of velocity on pH. — These experiments not only confirm the existence of an enormous effect of acidity on the velocity of inactivation, but show that this effect is even greater than has been reported. Since the series with *p*-nitrophenol buffers at $\mu = 0.2$ covers a wider range than the others, data for this ionic-strength from both tables are combined in Fig. 2. Because the points represent half-periods differing by a factor of 20,000 (2.5 minutes to 36 days) the logarithms of the decadic velocity constants in reciprocal minutes are plotted instead of the constants themselves. This method of plotting shows strikingly the great regularity of the pH relationship. All the points from Table II (open circles) lie on a straight line, the slope of which is exactly five. The points from Table III (filled circles) representing experiments in which the vessels were shaken, lie on the same line, except at pH below 6.1, where the reaction rate becomes entirely indenpedent of pH and is presumably that of a different reaction path, involving phase interfaces[1]. The first of the filled circles, marked with an arrow, represents an experiment at pH 3.79 — it is included here to show how far this independence of pH extends. At the intersection of the horizontal and slanting

[1] The product of the heterogeneous reaction is much less soluble than that of the homogeneous reaction in dilute salt solutions at pH below 6.3. The lower pH limit for the solubility of the latter is not known, since it is formed so slowly at pH below 6.1 that there may be time for it to be hydrolysed by the remaining pepsin; but it is soluble in more acid solutions than the product of the heterogeneous reaction, which appears as a finely divided suspension almost as soon as shaking commences, in the more acid solutions. The conclusion that the heterogeneous reaction occurs at air interfaces depends on failure to effect its velocity by coating the inside of the reaction-vessel with various waxes.

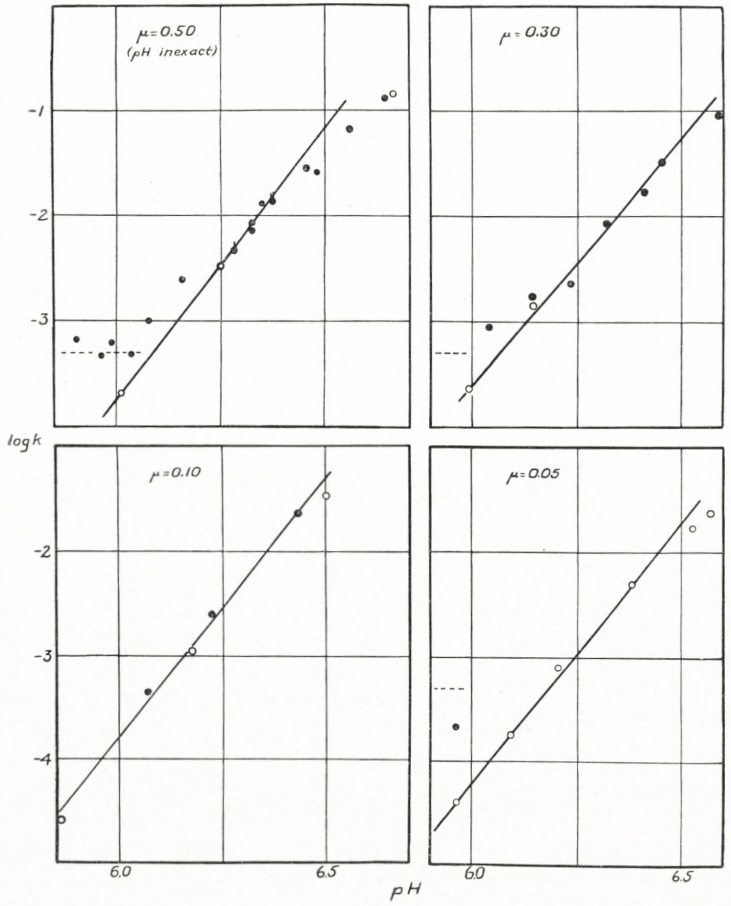

Fig. 3. The relation of the logarithm of the velocity-constant to pH at ionic-strenghts of 0.5, 0.3, 0.1, and 0.05 at 25° with *p*-nitrophenol buffers. Open circles are data obtained without shaking (Table I), filled circles data with the vessels shaken (Table II). In the set for $\mu = 0.5$, two experiments with casein as test-protein are marked by thin vertical lines.

lines the velocity of both homogeneous and heterogeneous reactions is comparable; at higher and lower pH one or the other reaction is so much the faster that the contribution of the second to the total velocity can be neglected.

It will be observed that the highest point lies a little

below the line; this is shown later to be true of every series of experiments. At the highest velocities, the proportionality of velocity to the inverse fifth power of the hydrogen-ion concentration no longer prevails; further increase in pH produce a relatively smaller increase in velocity. At this temperature and salt concentration this limit is reached only at the highest measurable velocities, but a lower temperatures and and in more dilute solutions, these deviations can be followed further; just noticeable here, they are shown later to be important for the theory of the fifth-power dependence which covers a velocity-interval of about 1 to 5000 in these data.

Data for all other ion-concentrations show the same relationship to pH. In Fig. 3 the results, with and without shaking, for four different ionic-strenghts (*p*-nitrophenol buffers) are shown separately. In all four sets the fifth-power dependence holds over a wide range; as with the data of Fig. 2 the velocity becomes independent of pH in the more acid solutions — when the vessels are shaken. In each case, again, the points for highest velocities always lie a little below the straight line — which should evidently curve off in this region. Three of the four sets of data have practically the same coordinates, but in the fourth set ($\mu = 0.05$) the velocities at the same pH are considerably lower. These effects of salt concentration are described more fully in a later section, in which data for still lower ionic-strengths are also presented.

The data for $\mu = 0.5$ scatter more than the others because temperature was not controlled during measurement of pH in part of this series (see Methods). These data show how slight errors in pH measurement, combined with the normal deviations from the straight line at high pH, and the results of shaking at low pH, can appear to give a line of

lower slope than five. MICHAELIS and ROTHSTEIN reported a slope of four; possibly, failure to control ionic-strength also contributed to this fortuitous result in their experiments, as well as in those of EGE, and of GOULDING, et al.

It has been shown by EGE, and confirmed by unpublished experiments of the author, that inactivation of pepsin by acids is directly proportional to the hydrogen-ion concentration. By extrapolating the line of slope 5 in Fig. 2, and drawing a line of slope -1 through the point for pH 3.81 (Table II), the pH of maximum stability is found at the intersection of the two lines at pH 5.28, close to where NORTHROP found maximum reversal of inactivation. At this pH the extrapolated value for the half-period of each inactivation reaction is approximately eight years. In more dilute salt solutions and at lower temperatures the enzyme is even more stable.

Significance of the fifth-power. — A dependence on acidity so great as to change the velocity of inactivation 10,000 times in one pH unit suggests how proteins may sometimes appear to possess sharp, almost discontinuous pH-stability regions (SVEDBERG, 1930). It also demands that secondary effects on acidity of such other experimental variables as salt concentration and temperature must be estimated and allowed for before interpretation of their primary effects on protein denaturation is undertaken. For this it is necessary to postulate a mechanism of this unusual pH dependence.

The view that denaturation of proteins is catalyzed by hydrogen and hydroxyl ions (in the sense of P. S. LEWIS, 1926, 1927; W. C. M. LEWIS, 1931) must be rejected as a primary mechanism in this case because of the large ex-

ponent; the salt effect, discussed later, helps to exclude it also. Catalysis by the basic ions of the buffer (BRØNSTED, 1928) is inapplicable for the same reasons, and can be further excluded in other ways. The high exponent admits only explanations involving equilibria, and the fact that hydrogen-ions are involved in the proportionality suggests that the equilibria concern dissociation of acid groups in the enzyme molecule.

Pepsin, a highly polyvalent amphoteric electrolyte, undergoes many stages of acid dissociation; consequently, many different kinds of pepsin ion coexist in the solutions in which the reaction was studied. It is necessary to assume that of the many groups which dissociate a hydrogen-ion in this range of acidity, the dissociation of a certain 5 groups greatly increases the susceptibility of the enzyme to inactivation. It is an essential part of this assumption that the dissociation of five groups and not fewer is required for the great increase in instability. Nothing can be postulated about the stability of intermediate ions in which one, two, three, or four of the five groups have given off a hydrogen-ion except that they are much more stable. At the level of stability observed, it it the dissociation of the fifth hydrogen-ion which causes the significant change.

The five groups involved are probably not the only groups which dissociate in this range of acidity; it is only assumed that the dissociation of the fifth of these groups has a much greater effect on the stability than the dissociation of any other group in this range. Since it is known that pepsin bears both positive and negative charges, and that its net charge is already strongly negative in the lowest pH interval of these experiments, the effect of these 5 dissociations is not likely to be unspecific and due solely to a change in

net charge[1]. It is more likely that this effect on the stability is produced by 5 specific chemical groups, probably of one kind: however, this last supposition is not an essential part of the explanation of the fifth-power dependence proposed here.

If all other stages of dissociation than the 5 in question are ignored, and the dissociation constants K_1, K_2, K_3, K_4, and K_5, are assigned to the successive stages, then the fraction of the total pepsin (in all ionic forms) present as ions of the fifth kind can be expressed in the following mass-law identity, in which P_1, $P_2 \ldots P_5$ represent pepsin ions formed by the 5 stages of dissociation, and P_0 represents all the other possible species of pepsin ions, on the more acid side of these dissociations:

$$\left.\begin{aligned} \frac{P_5}{P_0+P_1+P_2+P_3+P_4+P_5} &= \\ = \frac{1}{\frac{a_H^5}{K_1K_2K_3K_4K_5}+\frac{a_H^4}{K_2K_3K_4K_5}+\frac{a_H^3}{K_3K_4K_5}+\frac{a_H^2}{K_4K_5}+\frac{a_H}{K_5}+1}&. \end{aligned}\right\} \quad (2)$$

The left-hand member of this equation is proportional to the reaction-rate only when the respective ratios of activities to concentrations for the several ionic species remain fixed, as in the case of measurements made at constant ionic-strength in dilute solutions. The right-hand member is multiplied by a complex but constant factor in changing the Ps from activities to concentrations, under these conditions, to get an expression proportional to velocity.

[1] The related assumption that dissociation of any five groups out of a larger available number produces the decisive effect on the stability suffices to give the slope of five, and cannot be excluded. It leads to much more complicated equations for the exact pH-velocity function. For this reason, and because it is inherently less probable, its possibilities are not further developed.

When $K_1 << a_H$ it follows that $K_2, \ldots K_5 << a_H$, and only the first term of the series in the right-hand denominator need be considered; this is equivalent to the condition that the strongest ot the 5 groups is only slightly dissociated. The equation then becomes:

$$\frac{P_5}{\sum_0^5 P_i} \cong \frac{K_1 K_2 K_3 K_4 K_5}{a_H^5} \qquad (2')$$

omitting the additional constant factor mentioned above, The region over which the straight line adequately represents the data in the logarithmic plots (Figs. 2 and 3) is the region over which the condition for this approximation prevails.

Further conclusions are more easily drawn by considering the relations that the *K*s may bear to one another (theoretically, given a wide enough range of data, it is deducible from the curvature at the alkaline end). Accepting the presumption that all 5 groups are chemically identical, the fact that there are at least three carbon atoms, and usually a nitrogen atom also, between the nearest neighboring protein acid groups, will cause these groups, unless placed under special steric influences, to have apparent dissociation constants which differ only by limiting statistical factors (ADAMS, 1916). When these factors are assigned in the usual way, Eq. 2 can be rewritten:

$$\frac{P_5}{\sum_0^5 P_i} = \frac{1}{\frac{1}{\alpha^5} + \frac{5}{\alpha^4} + \frac{10}{\alpha^3} + \frac{10}{\alpha^2} + \frac{5}{\alpha} + 1} \qquad (3)$$

when the constant factor is omitted as before. In this equation, $\alpha = \frac{K_0}{a_H}$ where K_0 is a constant which is the same for each acid group (its apparent dissociation constant

separated from the purely statistical effect due to the presence of the others in the same molecule). This equation is a special case of (2) and will therefore give the approximate Eq. 2′, but greater interest attaches to the exact form, which should

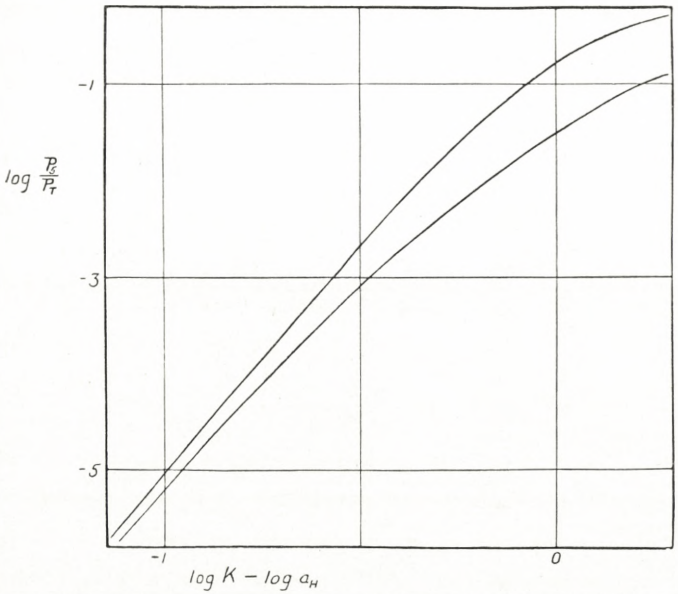

Fig. 4. Graphical representation of Eqs. 3 (lower) and 3′ (upper) on the coordinate system of Figs. 2 and 3.

describe the curved as well as the linear portions of Figs. 2 and 3, if this interpretation of the fifth-power effect is correct.

If no allowance is made for statistical factors, the numerical factors drop out of Eq. 3:

$$\frac{P_5}{\sum_0^5 P_i} = \frac{1}{\frac{1}{\alpha_5}+\frac{1}{\alpha_4}+\frac{1}{\alpha_3}+\frac{1}{\alpha_2}+\frac{1}{\alpha}+1}. \qquad (3')$$

Both (3) and (3′) are shown plotted, on the same coordinates as the data, in Fig. 4 — the abscissa has been made

independent of particular values of pH or K_0. Both equations have been shown, because the overlapping of other dissociating groups in pepsin in the same pH range makes the assignment of statistical factors uncertain. Overlapping tends to make the apparent *K*s more nearly alike. Since the factors may even tend to approach unity, their omission may be preferable to their inclusion, which would be strictly necessary only if the 5 groups were the only acid radicals in the molecule. As the figure shows, the result is not greatly affected; when factors are included the curve turns off from a straight line more gradually. It is interesting to observe to what extent dissociation of the first group may proceed before marked deviations from a straight line appear: when one-sixth of the total enzyme has dissociated at least one hydrogen-ion from one or more of the five groups, the velocity predicted by Eq. 3′ is only 20 per cent. lower than the corresponding value on the straight line, a just appreciable difference on this scale.

Figs. 5 and 8, which follow (further discussed later) illustrate the satisfactory way in which one of these two equations (3′) fits the data — the fit with (3) is definitely less satisfactory. The two lowest ionic-strengths (0.02 and 0.012) are less well fitted, but it is probably without significance that (3) describes them better since there is reason for believing that data for very dilute salt solutions should depart form the simple theoretical relationship (this is given in discussion of the salt effect). The decision between the alternative forms therefore rests on the more concentrated solutions. None of the data extend as far into the region of curvature as would be desirable for the most critical test of fit. Consequently, the coordinates assigned to the theoretical curve are, within narrow limits, somewhat arbitrary; cal-

culations which follow, based on these fitted coordinates, are uncertain to the extent of this arbitrariness. It should be possible to avoid this in future work by extending the data into the region of curvature, by working at lower temperatures; but the present measurements are sufficiently unambiguous to permit some conclusions.

The antilogarithm of the pH (with sign changed) which corresponds, for each set of data, with the abscissa zero of the curve in Fig. 4, is equal to K_0 which enters into α in Eq. 3′. At all ionic-strengths between 0.1 and 0.5 almost identical values are found; the maximum uncertainty in fitting any one set of data is 0.1 pH unit (usually it is half of this); the maximum difference between the most probable valuef or each ionic strengths is under 0.4 unit. The mean value of the pH at the abscissa zero is 6.76, corresponding to $K_0 = 1.74 \times 10^{-7}$.

This constant falls in a range occupied by very few types of acids. Of the limited number of acid radicals in proteins (carboxyl, imino, ammonium $\left(R - NH_3^+\right)$, phenylhydroxy, thiol, imido, and guanido) only imino groups, as in histidine, and ammonium groups, are near enough in strength to this value to be considered. In most amino-acids and polypeptides, the charged ammonium groups have much smaller acid constants than are required here, but the constant increases 40—60 times with increasing length of the polypeptide chain to a limiting value of pK at approximately 7.8 (Cohn, 1931). This limit agrees very well the figure 7.5 calculated by Linderstrøm-Lang (1935) for the protamine clupein — a polypeptide of 28 amino-acids residues. Since the clupein chain is studded with 20 well-spaced positive charges from its guanido groups, Lang's finding probably represents the greatest acidity which protein amino groups can attain,

when they are derived from aliphatic monoamino-acids. They are thus 5 or 6 times too weak to fit the requirements of this analysis.

The imino group of histidine has pK = 6.0 or 6.1 (LEVY, 1935, and other investigators). Its strength has been measured in the polypeptides histidyl-histidine, in which the mean value for the two imino groups is hardly affected and histidylglycine, in which there is a slight increase (GREENSTEIN, 1931; 1933). It therefore appears unlikely that it could be weakened sufficiently in any combination; the group is fairly remote from the amide linkage.

The strength of amino groups in the tetravalent sulfur-containing amino-acid, cystine, is 15—40 times greater than that of amino groups from other aliphatic amino acids. No measurements are available in polypeptides, but in the amino-acid pK is about 7.65 (CANNAN and KNIGHT, 1927). By analogy with the behavior of the same group in other amino-acids, its strength in polypeptides and proteins may easily equal or go below the value, 6.76, required by the present interpretation of the kinetic data. This tentative identification of the 5 groups with amino groups of cystine is consistent with NORTHROP's chemical analysis of pepsin which shows that the enzyme contains ten atoms of sulfur, which could correspond to five cystine residues. The analytical data of HERRIOTT and NORTHROP (1934) also show that there are from 3 to 5 primary amino groups per molecule — a remarkably small number, doing much to explain the very acid isoelectric point of the enzyme. Recently, GORTER, VAN ORMONDT, and MEIJER (1935) have shown, by analysis of the pH dependence of surface spreading of pepsin, that the number of amino groups is very small. There is no difficulty in assigning these amino groups to

cystine rather than to lysine, which contributes many of the amino groups of other proteins.

These comparisons neglect the possibility that the constants derived from the kinetic data may be compound, and include a constant for a secondary tautomeric equilibrium. The fact that the analysis has suggested dissociations localized in cystine, already known to be involved in changes accompanying protein denaturation (HOPKINS, 1930; ANSON and MIRSKY, 1935—36) encourages credence in its conclusions. To test them further, experiments were made in buffer solutions containing 1 per cent. formaldehyde (this concentration is without effect on the hemoglobin method). In the simplest case, combination of one HCHO molecule per amino group, and assuming that only the uncombined amino groups govern the stability, the reaction rate should be hardly changed in acid solutions, but should be increasingly diminished with rising pH. The effect actually found was very small — but was greater rather than smaller in more acid solutions. Since it is known that as many as three HCHO molecules can combine with a single amino group, since 5 groups are involved, and since no confident prediction can be made about the reactivity of the various complexes, these tests must be considered to have resulted inconclusively.

The salt effect. — The effect of changes in ionic strength, shown in Fig. 5, is extraordinarily great. Between ionic-strengths of 0.012 and 0.10 the velocity at a given pH increases about 40 times; above this the effect is much smaller and finally reverses. If the explanation proposed for the pH dependence is correct, the ionic-strength can affect the velocity in two ways, corresponding to primary and

secondary salt effects (Brønsted, 1928). The latter is not a direct effect on the velocity, but only displaces the dissociation equilibrium which determines the concentration of the

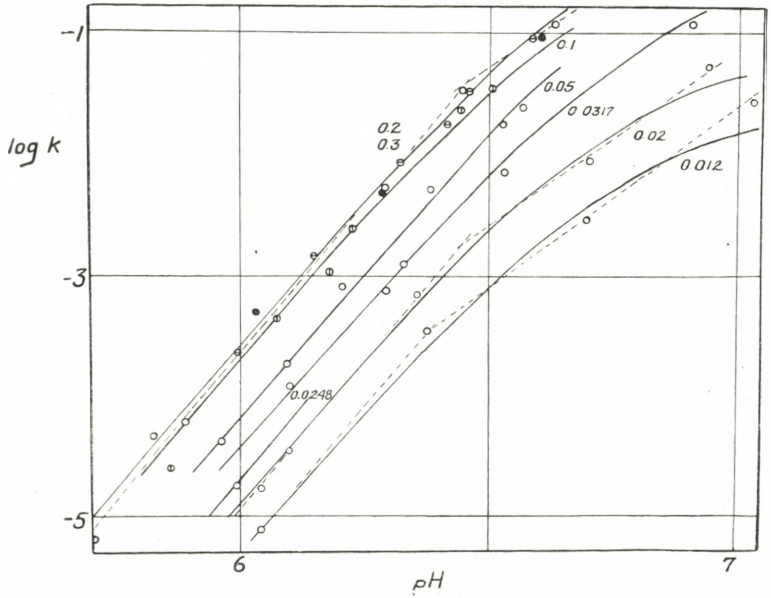

Fig. 5. The assembled data for *p*-nitrophenol buffers at all ionic-strength except 0.5, omitted to avoid crowding. Data from Table II (filled circles) are omitted at pH at which the heterogeneous reaction predominated. The fitted curves are from Eq. 3′; the broken straight lines are an alternative method of determining the relative positions of each set of data, — the upper branch has a slope of three.

reactive pepsin ion. A first-order calculation of the size and sign of this displacement in terms of the foregoing views, may be tested against the displacement along the abscissa of the theoretical curves fitted to the data.

The 5 stages of dissociation may be represented as a single process:

$$PH_5 \rightarrow P_5^- + 5H^+$$

for which the following mass-law equation is valid:

$$\frac{a_{H+}^{5} f_{P_5^-} C_{P_5}}{f_{PH_5} C_{PH_5}} = K'. \qquad (4)$$

The same argument used for justifying the assignment of identical values to the 5 dissociation constants also requires that the activity-coefficients will be governed by the charge on each group (here + 1 on the acid, and zero on the conjugate base), rather than by the net charge of the entire molecule. The subscripts in the equation are misleading in this connection, since the species written PH_5 actually bears a negative charge, and P_5^- differs from it by having 5 positive charges the fewer, so that the ion becomes 5 charges more negative. That the localized charge on a group rather than the net charge on the protein determines the dissociation behaviour of that group as a function of changes in the medium is effectively shown by the succesfull use of alcohol-water mixtures as a solvent in which to titrate the amino groups of proteins with base, as introduced by FOREMAN (1920) and WILLSTATTER and WALDSCHMIDT-LEITZ (1921); there is a different effect of the medium on the relative strengths of amino groups and indicator, — directly referable to the positive charge which changes to zero on dissociation of a hydrogen ion from the amino group in the course of the titration. The fact that the net charge of the protein is negative is without effect.

Eq. 4 may be written (subscripts now indicate postulated charges; P_0 is the former P_5)

$$\frac{C_{P_0}}{C_{PH_5+}} = K' \frac{f_{PH_5+}}{f_{P_0}} \frac{1}{a_{H+}^{5}} \qquad (4')$$

Over the range in which the 5th-power relation between velocity and pH prevails, the left-hand member differs inappreciably from the fraction which enters into the apparent velocity-constant, $\frac{C_{P_0}}{\sum_0^5 C_{P_i}}$, and in a small pH-interval this difference is nearly a constant factor, close to unity. With only slight approximation, then:

$$\log \frac{C_{P_0}}{\Sigma C_{P_i}} + \log k + \log F \cong \log K' + 5\,pH + \log f_{PH_5^+} - \log f_{P_0} \quad (4'')$$

where k is the constant factor, and F combines all other factors entering into the velocity-constant, including dimensional factors, the primary effect of temperature, and the primary salt effect. The final term is practically independent of ionic-strength in dilute solutions and its variation may be neglected. By writing (4'') for two different ion concentrations, and chosing values of pH at which the same ion ratio is found in the two sets of data, the ion ratio and certain other terms may be eliminated by subtraction, with the result:

$$pH_{\mu_2} - pH_{\mu_1} \cong \frac{1}{5}\left[\log \frac{(f_{PH_5^+})_{\mu_1}}{(f_{PH_5^+})_{\mu_2}} + \log \frac{F_{\mu_2}}{F_{\mu_1}}\right] \quad (5)$$

in which the numerical subscripts refer to the two ionic-strengths.

If, on the contrary, a zero charge on the acid groups were asssumed the final result, arrived at in an analogous manner, would be:

$$pH_{\mu_1} - pH_{\mu_2} \cong \frac{1}{5}\left[\log \frac{(f_{P^-})_{\mu_1}}{(f_{P^-})_{\mu_2}} + \log \frac{F_{\mu_1}}{F_{\mu_2}}\right]. \quad (5')$$

At constant temperature the second term in the bracket

represents, by definition, the primary salt effect, and may be eliminated by determining $pH_{\mu_2} - pH_{\mu_1}$ from the horizontal component of the displacement in the fitted theoretical curve (Eq. 3′) instead of from the pH-interval between the two sets of data for the same velocity (the vertical component of the shift corresponds to the primary salt effect). The remaining term may then be approximately evaluated by analogy with the familiar variation of activity coefficients for the same charge-types as these in simpler ions. On increasing the salt concentration from high dilution to $\mu = 0.1$, the activity coeffients of such ions most often fall from values near unity down to abont 0.7. Using these figures in (5) and (5′) the calculated value for $\triangle$ pH in the horizontal component of the displacement over this interval of ionic-strengths is -0.031 or $+0.031$ respectively, when μ_1 is taken as the higher concentration. This is an extremely small displacement, at the limit of certainty with which the theoretical curves can be fitted to the data.

Table IV.

Relation of apparent pK_0 to ionic-strength, determined by superposition of the theoretical curve (upper curve, Fig. 4) to the data.

Ionic Strength	Apparent pK_0 (middle value of possible range)	Displacement (from $\mu_1 = 0.3$)
0.50	6.800	.044
0.30	6.756	...
0.20	6.765	.009
0.10	6.755	— .001
0.05	6.838	.082
0.0317	6.779	.023
0.02	6.771	.015
0.012	(6.755)	(— .001)

The horizontal displacements represented by the curves in Fig. 5 are given in Table IV.[1] The figures are hardly consistent enough to warrant certainty as to sign (they favour sligthly Eq. 5, consistent with amino or imidizole groups), but they agree very well with the requirement, arrived at by the use of the fraction $\frac{1}{5}$, that the displacement should be very small.[2] The result also justifies the approximation made when the factor k was introduced as a constant; over so small a pH interval it cannot vary appreciably.

The greater part of the large effect of ionic-strength shown in Fig. 5 is thus a primary one. In BRØNSTED's theory of the primary salt effect the formation of an intermediate complex preceding reaction is postulated. When this complex and the ions that form it (the reacting species of the stoichiometric equation) are of unlike charge type, their respective activity-coefficients vary in different ways with the ionic-strength, and the concentration of the complex, on which depends the velocity, varies with the resulting ratio. When the reacting species have other than zero charge this leads to prediction of an exponential salt effect over the range in which the DEBYE-HÜCKEL limiting law is valid, according to the following equation (20°):

$$\log \frac{k}{k_0} = Z_A Z_B \sqrt{\mu} \qquad (6)$$

where k_0 is the velocity-constant at infinite dilution, and Z_A and Z_B are the charges on the ions forming the critical

[1] The broken straight lines of slopes 5 and 3 in Figs. 5 and 8 show an alternative approximate method for determining these displacements. In every case the displacements of their intersections have closely agreed with the displacements of the coordinates of the theoretical curve.

[2] Were the velocity dependent on the concentration of hydroxyl-ions as MICHAELIS and ROTHSTEIN thought possible, this displacement should be much greater.

complex. This equation shows that a straight line of integral slope should result when the logarithms of the velocity-constants are plotted against the square root of the ionic-strength, and that the slope of this line should be positive if the ions

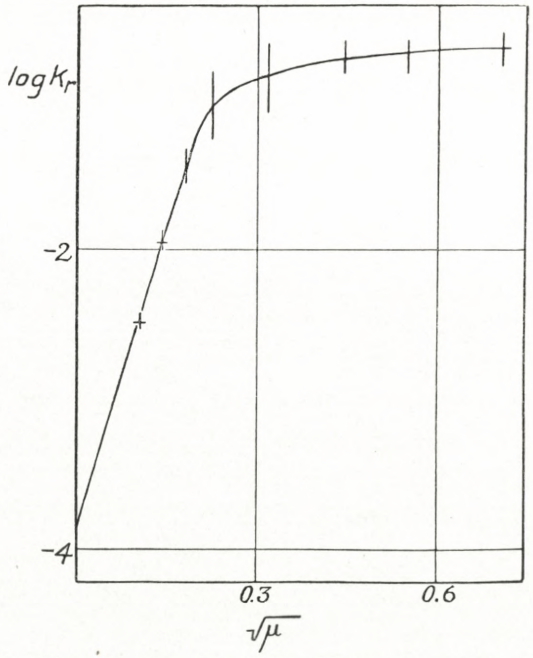

Fig. 6. The primary salt effect with *p*-nitrophenol buffers at 25°. The vertical lines show the range of uncertainty resulting from freedom in fitting Eq. 3′ to the data for each ionic-strength.

are of like sign, and negative otherwise. The equation has been applied successfully to a large number of reactions with values of $Z_A Z_B$ between -4 and $+4$. Outside this range it has been less succesfull, probably because the limiting law itself fails for ions of large charges.

Application of Eq. 6 to the present data must take account only of the change in ordinates between each of the fitted theoretical curves in Fig. 5. In Fig. 6 these ordinates are

plotted against the square root of the ionic-strength, with the length of each vertical line indicating the limits of uncertainty due to curve-fitting. The result is consistent with a linear relationship in the range of dilution in which agreement with Eq. 6 may be expected. The slope, however, is very great, approximately + 13. This figure need not imply charges of more than 5 or 6 since ions of high charges sometimes produce limiting slopes of two or even three times the theoretical value. This distinctively large effect, reminiscient of the large salt effects that have been demonstrated in other protein phenomena, notably solubility, is apparently inconsistent with the preceding assignment of activity coefficients on the basis of single group charges. It remains obscure at the present time.

In one respect it requires further consideration: an unusually high sensitivity to ionic-strength entails a high sensitivity to specific ion effects at lower concentrations than those at which they are usually manifested, and the exact application of the principle of the ionic-strength is then limited to even lower salt concentrations than those to which it is generally applied. A practical consequence for these experiments is that mixtures of buffer-ions and neutral salt in different proportion to give the same "ionic-strength" will not give equivalent ionic effects. This is particularly likely at low concentrations, where the ratio of neutral salt to (for example) sodium nitrophenolate, varies over wide extremes. To estimate the magnitude of such specific effects, two experiments were made at $\mu = 0.0317$, substituting KNO_3 for KCl; the nitrate was chosen as most likely among common ions to manifest specific difference from the chloride. The velocities obtained at pH 6.013 and 6.475 were about 50 per cent. and 35 per cent. greater than

when KCl was used. Substitution of small amount of NaCl for KCl was without effect at $\mu = 0.5$, where sensitivity to changes in concentration is also low. These experiments show that no appreciable distortion of the pH-velocity relationship is to be expected from specific ion effects except at the lowest salt concentrations, where a very small distortion may result at the least acid end of the data. Higher velocities will be found, owing to the specific effect of the large concentration of the larger nitrophenol ion. This is the direction in which the experimental data deviate from the theoretical curve at $\mu = 0.02$ and 0.012.

The specific effects of buffers. — Any explanation of the fifth-power relation which depends on a catalytic mechanism is very unlikely; the small secondary salt effect more specifically excludes hydroxyl-ion catalysis. General basic catalysis (by the buffer anion) can only be excluded rigidly by showing that the velocity does not depend on the concentration of the buffer, or on the strength of the buffer acid. The pH relationship itself is incompatible with such a dependence on the concentration of the anion, provided the dissociation constant of the buffer is not the same as the dissociation constant used in calculating the theoretical curve. Nevertheless, in order to obtain good buffering, the buffer selected will tend to have a constant close to this.

In most of the experiments the buffer was *p*-nitrophenol; the pK of this acid in 0.1 M KCl is 6.95 while that of the postulated pepsin groups is 6.76. The difference, though small, is much outside the limits of error, but to exclude the possibility of basic catalysis beyond a doubt experiments were made with other buffers of widely differing strengths,

If basic catalysis is involved, the pH range over which an inverse fifth-power relation to acidity is found should differ with each buffer.

Fig. 7 shows data obtained with trimethyl-*o*-aminophenol

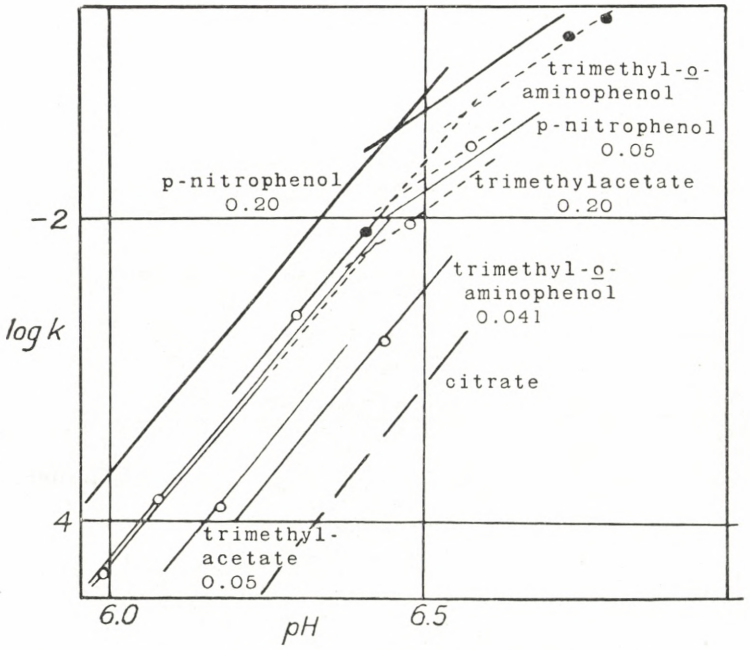

Fig. 7. Data for other buffers compared with the results with *p*-nitrophenol at 25°. The latter are represented by broken lines of slope 5 and 3, taken from Fig. 5. The position of the citrate data, indicated by a line, is only approximate.

halide (pK $\cong$ 7.4) at μ = ca. 0.20 and 0.041, and with trimethylacetic acid (pK $\cong$ 5.0) at μ = 0.20 and 0.05. For reference, curves representing the data for nitrophenol at μ = 0.20 and 0.05 are included. The general position of very much rougher results with poorly buffered citrate solutions is also shown by a broken line. Although there are few points, and they do not all represent strictly com-

parable experimental conditions, it is clear that the relation of velocity to pH is not changed, although the three acids differ in strength by about 200 times. It is also evident that comparable salt effects are found with all the buffers.

The absolute rate of reaction differs with each buffer; even disregarding the results with citrate there is a factor of three between two of the others, though with no relation to the acid strength. *p*-Nitrophenol, which gives the fastest rate, has a strength between that of the other two. The latter differ in strength by about 200 times and give almost identical rates.

The experiments of MICHAELIS and ROTHSTEIN, with phosphate buffers, add further detail to the situation shown in Fig. 7, if the effect of impurities in their solutions may be neglected. The velocities reported are much lower than any in Tables II and III, and are comparable with the results obtained with citrate. This specific influence of the buffer cannot be explained at present.

The effect of temperature. — The large temperature coefficients hitherto reported for protein denaturation have been obtained by comparing the velocity at two different temperatures at the same pH. When values so obtained are transformed into "energies of activation" through the ARRHENIUS equation, they invariably lead to such large figures (with two enzymes, trypsin and ptyalin, the values are about 150,000 and 120,000 calories respectively; trypsin, at least, is a protein) that the observed rate of reaction cannot be accounted for by any known process for the redistribution of energy between molecules in gases or in solution. This method of calculating activation energies is incorrect if the view of the pH-velocity dependence set forth in this

paper is accepted, for the concentration of the reactive ionic species also increases at higher temperatures, and this increase contributes to the total kinetic temperature effect. This is made plain by Fig. 8, which shows the reaction rates as a

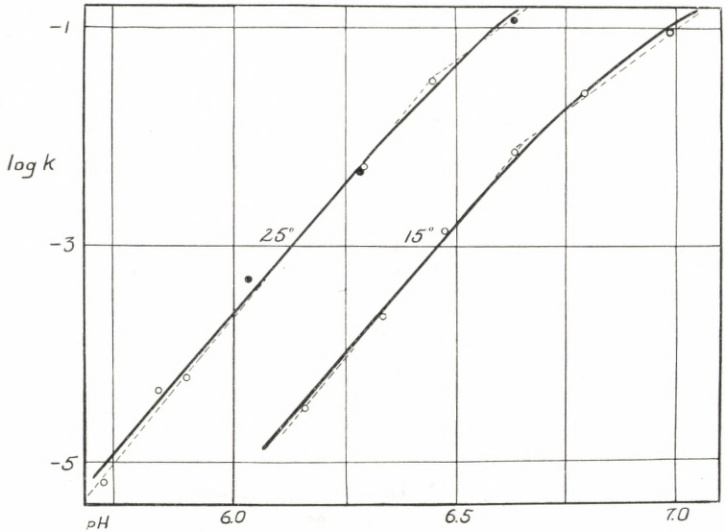

Fig. 8. A comparison of the pH-dependence of the velocity-constant at two temperatures. The curves are from Eq. 3′. The broken straight lines are included as an additional method of appraising the shift in the coordinates of the sets of data, as in Fig. 5.

function of pH at 15° and 25° at the same ionic strength, and with the same buffer. The data for the lower temperature are given in Table V. Even casual inspection shows that the greater part of the temperature effect consists of a horizontal shift in the curves, and that only a small part of the increase in velocity at the same pH is due to a vertical change in coordinates, — i. e. an increase in the rate at which the unstable ion decomposes. Precise appraisal of the two components of the total effect is handicapped by failure of the data to extend to more alkaline solutions.

Table V.

Velocity of inactivation at 15° and ionic strength 0.20; *p*-nitrophenol buffers. No shaking.

pH	$\log_{10} k_{10}^{min}$	Initial Enzyme (mg. N/ml.)
6.161	— 4.483	0.00288
6.333	— 3.638	.00290
6.473	— 2.851	.00309
6.630	— 2.120	.00328
6.788	— 1.593	.00266
6.982	— 1.021	.00341

Within the limits of uncertainty imposed by this circumstance, the most probable value for the horizontal shift can be set as 0.23 pH units. This is equivalent to a heat of dissociation for each of the five groups (again assumed to be alike) of 9040 calories.[1] While this figure is only approxi-

[1] $\triangle H = 4.571 \triangle pH \cdot \frac{T_2 T_1}{T_2 - T_1}$ by assuming $\triangle H$ to be constant over the 10° temperature interval. This equation is not affected by the simultaneous functioning of 5 groups. This is easily shown over the range in which the logarithmic graph is linear:

$$\log \frac{P_5}{\sum_0^5 P_i} \cong 5 \log K_0 + 5 pH .$$

Combining this with the familiar equation for the deqendence of K on T, it becomes:

$$\log \frac{P_5}{\sum_0^5 P_i} \cong 5 \left[\frac{\triangle H}{4.571 T} + C \right] + 5 pH .$$

For equal values of the left-hand member, at two temperatures:

$$5 \left[\frac{\triangle H}{4.571 T_1} + C \right] + 5 pH_1 = 5 \left[\frac{\triangle H}{4.571 T_2} + C \right] + 5 pH_2 .$$

The factor 5 and the constant C thus cancel out. Use of the exact equation 3′ does not affect the result. The only assumption required is identity of the dissociation constants and their heat effects.

mate, it clearly favours the previous identification of the acid constants with ammonium-like groups. In amino-acids these groups have heats varying from about 9000 calories (in histidine and tyrosine) to 12,800 calories. The highest value characteristic of other groups is 7000 calories for the imino group of histidine.

In regions where both curves are approximately straight lines, $Q_{10} = 40$, corresponding to an apparent energy of activation of 63,500 calories. This is fairly near to the figure, 58,000, given by the data of MICHAELIS and ROTHSTEIN. Of this quantity, 45,200 (5×9040) is the heat of dissociation of the stages determining the concentration of the unstable ion. Thus, the true value of E (activation energy) for decomposition of the reacting ion is the remainder, 18,300 calories. The same figure is given by direct estimation of the vertical displacement between the two curves. The relative uncertainty in E is necessarily larger than in $\triangle$ H; this does not affect the main point of interest here which is the great difference between the apparent and true energies of activation, and the fact that the true value, 18,300, is a magnitude commonly met with in ordinary chemical processes.[1]

This difference has manifest significance for kinetic calculations since it removes the paradox associated with the larger value .When the ARRHENIUS equation is rewritten in the form:

$$k = Ze^{\frac{-E}{RT}}$$

[1] MICHAELIS and ROTHSTEIN suggested from their temperature data that practically the entire effect of temperature could be accounted for by its influence on C_{OH} at fixed pH, if the reaction-mechanism was catalysis by hydroxyl ions. This suggestion involves the assumption that the inverse kinetic relation to C_H signifies direct dependence on C_{OH}. Were this true, in light of their data, E should be zero, and the recation should be immeasurably fast.

in which k is the natural velocity-constant expressed in reciprocal seconds, and Z is a factor which may be regarded, to a first approximation, as the number of molecular collisions per second per unit volume, — its most common value in simple bimocular gas-reactions is aproximately 10^{11} in close agreement with the predictions of the kinetic theory of gases. Recent surveys of reactions in solutions (MOELWYN-HUGHES, 1933 *b*; CHRISTIANSEN, 1924) have shown that in many cases comparable values of Z are found, and that in most cases Z, regarded as an empirical factor seldom departs from 10^{11} [by a factor of more than 100. Values of $\log Z$ over 14 or 15 are paradoxical because the number of collisions between reactant molecules and other molecules is not likely to exceed 10^{14}; even this value can be attained only by very large molecules with large persistence of velocity after collision (MOELWYN-HUGHES, 1933 *a*). No mechanism is then provided for the initiation of individual molecular reactions, nor even for the maintenance of a number of molecules with sufficient energy to react.

Z has been calculated for the present data, using alternatively the apparent and corrected values of E. The velocity-constant has been taken from the *p*-nitrophenol data extrapolated to infinite dilution (Fig. 6) at a pH corresponding to $\frac{K}{a_H} = 0.446$. Use of data for the other buffers would give lower values, but a factor of 3 is of little importance in these calculations.

Log k (extrapolated) is -3.9, which, after correction to reciprocal seconds and Napierian logarithms, becomes $ln\, k_{sec.} = -13.1$. This number must still be transformed from a decadic to a natural base (in the first order kinetic equation), on which it becomes -12.26. The reaction-rate is still

expressed in terms of the total pepsin; on changing to the amount present as the reactive ion (P_5), $ln\, k'^{Nap.}_{sec.} = -9.74$. Since E is 18,300 $\frac{E}{RT}$ is 31.2. Combining these numbers, $ln\, Z = 21.46$, or $\log Z = 9.3$. This result is well within the range of values commonly found. Interpreted literally, it signifies that approximately one out of one hundred collisions between unstable ions possessing the activation energy and solvent molecules, result in reaction. Even the use of the fastest data (nitrophenol buffers) and correction for the very small amount of reactive ions, has given a result that is low rather than high.

If a straightforward calculation is made with the uncorrected value, 63,500 calories, $\log Z$ is approximately 41, and the observed rate is thus at least 10^{26} times too fast to be accounted for by ordinary kinetic considerations. This anomaly is present in all earlier kinetic data on protein denaturation or enzyme destruction and various proposals (among others, the existence of reaction chains and contributions to the activation energy from many degrees of freedom) have been advanced to account for it (see, for example, MOELWYN-HUGHES, 1933*a*, and LEWIS, 1931). Other authors have tried to account for the high energy without recognizing the paradox associated with it (MIRSKY and PAULING, 1936, among others). Should the present calculations prove applicable to other proteins, the difficulties arising from the large temperature effect in denaturation may prove to be illusory.[1] Data on ptalin (EGE, 1932) and hemoglobin (P. S. LEWIS, 1926, 1927) show that the occurrence of a large exponent in the kinetic depen-

[1] Theories of the mechanism of denaturation which partly rest on large values for E (such as MIRSKY and PAULING's) may then require some revision.

dence on acidity, on which these calculations are based, is common.

The foregoing computations, though limited in exactness, support the interpretation of the pH effect which underlies them. They can also be extended to explain the frequently observed variation of the apparent Q_{10} or E with pH in protein denaturation (it is readily seen in Fig. 8, at pH above 6.5). The observation that E appears to become smaller and approaches a limiting value at high temperatures (LEWIS's recalculation of the data of CHICK and MARTIN) when measured at a single pH is also understandable from the shift of the curves left-ward with increasing temperature, — regions of smaller slope, therefore smaller vertical separation, coming to lie at the pH of the experiment (most of the protein becoming transformed to the unstable ion). The limits found, with serum proteins about 23,000 calories, are only slightly higher than the 18,300 computed here. It is noteworthy that the temperature effect in acid denaturation is frequently much smaller than in alkaline solutions (see, for example, EGE, 1925, 1934). In acid solutions only carboxyl groups can be dissociating, and the effect of temperature on their dissociation is vanishingly small.

The author wishes to record his indebtedness to Professor J. N. BRØNSTED for generous provision of laboratory facilities and assistance, and for affording frequent opportunities to discuss the ideas developed in this paper. He is likewise grateful to Dr. KAI LINDERSTRØM-LANG and Dr. HEINZ HOLTER of the Carlsberg Laboratories, to Professor J. A. CHRISTIANSEN of the Chemical Laboratory, Danmarks tekniske Højskole, and to Mr. EINAR GÜNTELBERG of the Institute of Physical Chemistry, for much fruitful advice information. The kind interest of Dr. J. N. NORTHROP of the

Rockefeller Institute for Medical Research at Princeton was an important factor in encouraging the author to undertake this work.

Experimental assistance was rendered by Miss TOVE PONTOPPIDAN THOMSEN.

VI. Summary.

Crystalline pepsin, in solutions of constant ionic-strength on the alkaline side of its pH stability maximum inactivates unimolecularly at a rate which is inversely proportional to the fifth power of the hydrogen-ion concentration. This relation has been found to apply over a range of velocity of 1 to 5000 in the results of nearly 100 kinetic experiments at two temperatures with four different buffers, and at various ionic-strengths. The rate varies with the buffer but the fifth-power dependence does not. Over a still wider range the results are in quantitative agreement with the view, supported by other evidence, that the rate depends on the concentration of a single pepsin ion in which all 5 of the primary amino groups of the enzyme have lost their positive charges. If all five groups are of equal strength, their acid dissociation constant is 1.74×10^{-7}. Evidence is submitted for localizing these groups in cystine residues.

On shaking the reaction-vessels, a heterogeneous reaction, independent of pH and μ, obscures the results at pH below 6.1. Above this, the homogeneous reaction predominates, and shaking cannot modify the results otherwise obtained. Experiments without shaking show that at the pH stability maximum (5.28 at $\mu = 0.2$) the half-period of inactivation is approximately 8 years.

With increasing salt concentration ($\mu = 0.012$ to $\mu = 0.1$) the velocity at constant pH increases nearly ex-

ponentially about 40 times. At higher ion-concentrations the change is smaller, and finally reverses. The virtual absence of a secondary salt effect is consistent with the theory of the pH dependence.

If account is taken of the effect of temperature on the size of pepsin fraction present as the unstable ion, the temperature effect on the rate of the actual reaction (decomposition of this ion) is much smaller than the observed change in velocity. When the ratio $\frac{k_{25°}}{k_{15°}}$ (about 40) is used to calculate the critical increment, the result is 63,500 calories, — a high figure, characteristic of protein denaturation. When the shift in the pH dependence is allowed for, assuming all five groups alike, an ordinary value, 18,300, is obtained. The exponent produces a large disparity, though the heat of dissociation of each group is only 9040 calories. The latter value favours the view that primary amino groups are involved.

The observed reaction rates stand in reasonable relation to the number of molecular collisions with activated unstable pepsin ions, when the corrected figure, 18,300, is used for the energy of activation. They are too high by a factor of 10^{26} when the uncorrected figure, 63,500, is used. Should this result apply to the proteins generally, the theoretical difficulties arising from the great temperature effect in denaturation may prove to be illusory. The frequently observed variation of critical increment with pH, and its decline to a limiting value at high temperatures, can also be explained.

Citations.

Adams, E. Q., Journ. Am. Chem. Soc., 1916, **38,** 1503.
Anson, M. L., and Mirsky, A. E., Journ. Gen. Physiol. 1932—33, **16,** 59; Journ. Gen. Physiol. 1935—36, **19,** 427, 439, 451, 559, 571.
Arrhenius, S., Quantitative Laws in Biological Chemistry, New York, 1915.
Brønsted, J. N., Chem. Rev., 1928, **5,** 231.
Cannan, R. K., and Knight, B. C. J. G., Biochem. Journ. 1927, **21,** 1384.
Christiansen, J. A., Zts. physik. chem., 1924, **113,** 35.
Cohn, E. J., Ergebn. d. phsiol., 1931, **33,** 781.
Ege, R., Zts. f. phsiol. chem. 1925, **143,** 159; Biochem. Zts. 1932, **244,** 243; Zts. f. phsiol. chem., 1934, **224,** 129.
Foreman, F. W., Biochem. Journ., 1920, **14,** 451.
Gorter, E., Van Ormondt, H., and Meijer, T. M., Biochem. Journ., 1935, **29,** 38.
Goulding, A. M., Wasteneys, H., and Borsook, H., Journ. Gen. Physiol., 1926—27, **10,** 451.
Greenstein, J. P., Journ. Biol. Chem., 1931, **93,** 479; Journ. Biol. Chem., 1933, **101,** 603.
Guggenheim, E. A., and Schindler, T., Journ. Phys. Chem., 1934, **38,** 533.
Herriott, R. M., and Northrop, J. H., Journ. Gen. Physiol., 1934—35, **18,** 35.
Holter, H., Zts. f. phsiol. chem., 1931, **196,** 1.
Hopkins, F. G., Nature, 1930, **126,** 328.
Levy, M., Journ. Biol. Chem., 1935, **109,** 361.
Lewis, P. S., Biochem. Journ., 1926, **20,** 965, 978, 984; 1927, **21,** 46.
Linderstrøm-Lang, K., Trans. Farad. Soc., 1935, **31,** 324.
McInnes, D. A., and Dole, M., Journ. Am. Chem. Soc., 1931, **53,** 1357.
Michaelis, L., and Rothstein, M., Biochem. Zts., 1920, **105,** 60.
Mirsky, A. E., and Pauling, L., Proc. Nat. Ac. Sci., 1936, **22,** 439.

MOELWYN-HUGHES, E. A., Erg. d. Enzymforsch., 1933 *a*, **2**, 1; Kinetics of Reactions in Solution. Oxford, 1933 *b*.

NORTHROP, J. H., Journ. Gen. Physiol., 1929—30, **13**, 739; Journ. Gen. Physiol., 1929—30, **13**, 767; Journ. Gen. Physiol., 1930—31, **14**, 713; Journ. Gen. Physiol., 1932—33, **16**, 33.

PHILPOT, J. ST. L., and ERIKSON-QUENSEL, I.-B., Nature, 1933, **132**, 82.

PHILPOT, J. St. L., Biochem. Journ., 1935, **29**, 2458.

SVEDBERG, T., Trans. Farad. Soc., 1930, **26**, 740.

SØRENSEN, S. P. L., Cont. rend. d. trav. d. Lab. Carlsberg, 1930, **18**, 5.

SØRENSEN, S. P. L., SØRENSEN, M., and LINDERSTRØM-LANG, K., Cont. rend. d. trav. d. Lab. Carlsberg, 121, **14**.

WILLSTATTER, R., and WALDSCHMIDT-LEITZ, E., Ber. d. deutsch. chem. Gesell., 1921, **54**, 2988.

WINNEK., P. S., and SCHMIDT, C. L. A., Journ. Gen. Physiol., 1934—35, **18**, 889.

Færdig fra Trykkeriet den 7. August 1937.

Det Kgl. Danske Videnskabernes Selskab.
Mathematisk-fysiske Meddelelser **XIV**, 12.

ON THE SELECTIVE CAPTURE OF SLOW NEUTRONS

BY

O. R. FRISCH

KØBENHAVN
LEVIN & MUNKSGAARD
EJNAR MUNKSGAARD
1937

Printed in Denmark.
Bianco Lunos Bogtrykkeri A/S.

We deal in this paper with the selective capture of slow neutrons (1, 2) in arsenic, iodine, and gold (3). On capturing a neutron, the nuclei of these elements are transformed into unstable ones, which revert to stable nuclei again by the emission of a beta-particle:

$^{75}_{33}\mathrm{As} + {}^{1}_{0}\mathrm{n} = {}^{76}_{33}\mathrm{As}$ $\quad {}^{76}_{33}\mathrm{As} \xrightarrow{\beta} {}^{76}_{34}\mathrm{Se}$ half-value period 27 hours

$^{127}_{53}\mathrm{J} + {}^{1}_{0}\mathrm{n} = {}^{128}_{53}\mathrm{J}$ $\quad {}^{128}_{53}\mathrm{J} \xrightarrow{\beta} {}^{128}_{54}\mathrm{X}$ „ „ „ 25 min.

$^{197}_{79}\mathrm{Au} + {}^{1}_{0}\mathrm{n} = {}^{198}_{79}\mathrm{Au}$ $\quad {}^{198}_{79}\mathrm{Au} \xrightarrow{\beta} {}^{198}_{80}\mathrm{Hg}$ „ „ „ 2.8 days

These elements were selected because they show the phenomenon of selective capture in a marked degree, because only one stable isotope is known in each case, and because the corresponding unstable isotopes have periods which are convenient for measurement.

Samples of the substance under investigation were exposed under various conditions to the neutrons emerging from a block of paraffin wax, containing a source of fast neutrons (Ra + Be or radon + Be). The samples were then transferred to a GEIGER-MÜLLER counter, and the activity shown by the counter was taken as a measure of the number of neutrons captured within the sample.

The observations have been interpreted on the assumption (4, 5) that the capturing nucleus together with the incoming neutron forms a "compound nucleus" with well

defined energy levels whose width is small compared with their separation, in the energy region concerned. In the first instance, however, we shall only assume one such level in each case, and the evidence for and against this assumption will be discussed.

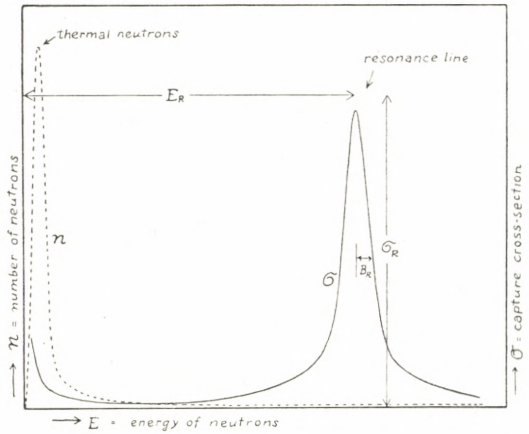

Fig. 1.

The conditions in the one level case are shown schematically in fig. 1. The full line indicates the dependance of the capture cross-section σ on the kinetic energy E of the incoming neutrons; this dependence (5) is given by the formula

$$\sigma = \frac{\sigma_R}{1 + \left(\frac{E - E_R}{B_R}\right)^2} \cdot \sqrt{\frac{E_R}{E}}$$

E_R = Resonance energy
σ_R = Resonance cross-section
$2B_R$ = Half-value width of resonance line.

In all cases so far investigated the "resonance cross-section" σ_R is much larger than the corresponding value of σ for neutrons of thermal energy; still the thermal neutrons contribute considerably to the activation of the sample, on

account of their large number (the estimated energy distribution of the neutrons emerging from a paraffin block (6, 7) is indicated by the dotted line). A screen of cadmium was therefore used to remove the thermal neutrons in the usual way; the main part of the activity is then due to neutrons with energies near E_R. In what follows, these neutrons will simply be called "resonance neutrons".

In order to determine the resonance energy E_R, the absorption of the resonance neutrons in boron was compared with the absorption of thermal neutrons in boron (8). Theoretical arguments have been given for the assumption that the absorbing cross-section of boron is inversely proportional to the velocity of the neutrons (8, 9). This "$\frac{1}{v}$-law" should hold for neutron velocities up to at least 10^7 cm./sec. (energies of $\sim$ 50 eV.) when the capture cross-section becomes of the order of ordinary nuclear cross-sections. Experimental checks are in qualitative agreement with this assumption (10, 11). In this paper the validity of the $\frac{1}{v}$-law will be taken as established. We have made no attempt to verify it.

The resonance cross-section σ_R was determined by measuring the absorption of the resonance neutrons in the element under investigation. Absorption curves under various geometrical conditions have been obtained and compared with theory.

Two different ways of obtaining an estimate of the width of the resonance level are discussed in the case of gold. An attempt has been made to discover a broadening of the absorption line on increasing the temperature of the absorber (thermal Doppler-effect) but no conclusive result has been obtained so far.

1. Determination of Resonance Energies.

Experimental procedure. The neutron source (500 mg. radium in the form of $RaSO_4$, mixed with beryllium) was placed at the centre of a cube of paraffin wax of side 13 cms. To investigate the resonance energy of gold, four gold discs (15 mms. diameter, 0.1 mm. thick) were placed 2 cms. below the lower face of the cube and arranged at the corners of a square of 3 cms. sides, situated symmetrically with respect to the cube. Absorbers of 3 cms. in diameter of amorphous boron (pressed without binding material) were placed on three of the gold plates, the absorber thicknesses being 0.10, 0.20, and 0.40 gr./cm.^{2}, respectively. On comparing the activities induced in the four gold plates, an absorption curve, in boron, of the resonance neutrons of gold is obtained. A shield of 0.4 gr./cm.^{2} cadmium was placed immediately below the paraffin to cut off the thermal neutrons, and a double shield (0.4 gr./cm.^{2} cadmium + 0.5 gr./cm.^{2} gold) against stray neutrons was placed under the gold. After two days exposure the activity of the gold plates was measured by means of Geiger-Müller counters having a 10 mms. diameter window of mica (0.0065 gm./cm.^{2}). In order to reduce the time necessary for a sufficiently high count three counters were used simultaneously; small differences in the counting rates of the counters were eliminated by measuring the activity of every disc on each of the three counters and taking the average.

Information on the behaviour of neutrons filtered through about 0.15 gr./cm.^{2} gold was obtained by measuring the activity both of the lower and the upper sides of the gold plates; since the electrons emitted by gold are very

soft the activity of the lower side is almost entirely due to neutrons which have penetrated nearly the whole thickness of the gold plate.

In the case of arsenic this simple method could not be used since the electrons emitted by active arsenic are much harder. Eight plates of As_2O_3 of 15 mms. diameter, each containing 0.200 gr. As_2O_3, were therefore placed in pairs,

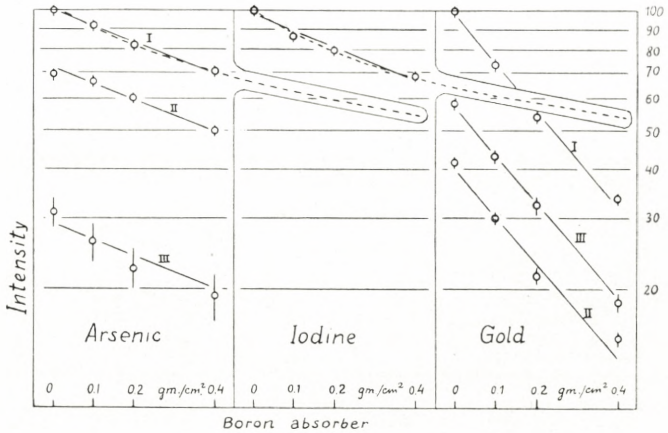

Fig. 2.

one on top of another, at the corners of a square, as in the case of the gold. The boron absorbers and the upper cadmium shield were the same, but there was no shield underneath; there are, however, reasons to believe that this makes little or no difference in the case of arsenic. Only the activity of the upper sides of the plates was measured.

With iodine, similar plates, each containing 0.500 gm. I_2O_5 were used; only one plate was placed under each boron filter. The lower shield consisted of 0.4 gm./cm.^{2} cadmium + 2 gm./cm.^{2} iodine. Only the activities of the upper sides were measured.

Results of measurements. The results are summarized in fig. 2 where the activities are plotted on a logarithmic scale against the thickness of the boron absorber; the units are such that the intensity without any absorber is always 100. (I = unfiltered neutrons, II = filtered, III = I—II).

In the case of gold, the absorption in boron is seen to be fairly well exponential, and the ratio of the activities of the upper and lower sides does not change appreciably with increasing boron thickness. This supports the view that most of the activity in gold is produced by one narrow range of neutron velocities, or in other words, that one nuclear level is responsible for most of the activation.

In the case of arsenic, the reduction in activity by the thickest boron absorber used was only 30 %, so no definite conclusion can be drawn from the straightness of the absorption curves. Furthermore the difference between curves I and II is only a small one (the arsenic filter was too thin) so too much weight should not be laid on the constancy of their ratio. In the case of iodine the points might suggest a slight curvature in the absorption curve.

Absorption of thermal neutrons in boron. The absorption of thermal neutrons in boron was determined using, as detector, a boron lined ionisation chamber, connected to a linear amplifier and mechanical counter. The sensitive boron layer covered a circle of 15 mms. diameter and was brought into the same position relative to the paraffin as the plates to be activated in the foregoing experiments; in this way identical geometrical conditions were secured[1]. A screen of cadmium was used to discriminate between thermal and faster neutrons. The pro-

[1] The chamber was placed above instead of below the paraffin block.

cedure was the usual one: counts were made (a) without absorber, (b) with 0.4 gm./cm.^{2} cadmium, (c) with 0.020 gm./cm.^{2} boron, (d) with cadmium and boron. The ratio $(c - d) : (a - b)$ gives the transmission in boron of the neutrons stopped by cadmium (C-neutrons); it was found to be (51.5 ± 1.5) %.

Some doubt may arise as to the degree of temperature equilibrium of the neutrons defined in the way described above, although a large part of the C-neutrons has certainly got thermal velocities as may be deduced from temperature variation (12, 13) and rotating wheel (14) experiments. The following experiment was therefore carried out: counts were taken, in the way described above, with the difference that the cadmium was not placed on top of the paraffin but at a certain depth below the surface. The ratio $(c - d) : (a - b)$ then gives the absorption, in boron, of those neutrons which were slow enough at that depth to be stopped by cadmium but had, however, to diffuse through a certain layer of paraffin wax before reaching the boron absorber and the ionisation chamber. We should expect those neutrons to be more nearly in temperature equilibrium than the C-neutrons. As a matter of fact, the ratio $(c - d) : (a - b)$ was found to be unchanged, for depths up to 3 cms. of paraffin, within the limit of error of about 5 %. It seems therefore reasonable to assume that this ratio would be essentially the same for a beam of neutrons in perfect temperature equilibrium.

The effective velocity of neutrons with a Maxwellian velocity distribution, that is, the velocity of homogeneous neutrons showing the same absorption in boron, depends somewhat on the thickness of the boron absorber used. For thin boron absorbers it corresponds to an energy of

$\frac{\pi}{4} kT$; when about 50 % of the neutrons are absorbed a slightly higher energy of very nearly kT has to be used (15).

Oblique Incidence. Under the geometrical conditions employed, oblique neutrons from directions forming angles up to about 70° with the normal were involved. The determination of the mass absorption coefficient of boron would therefore require a serious correction and thereby become rather inaccurate. The determination of E_R, however, requires a knowledge of the ratio only of two mass absorption coefficients, which is, in the first instance, equal to the inverse ratio of the respective boron thicknesses required to obtain equal absorption.

The geometrical conditions are, however, not quite identical since the different detectors used respond in a different way to oblique neutrons so that a small correction has to be applied. In the boron chamber, the probability of a neutron being counted is larger for oblique neutrons since their path inside the effective boron layer (that is, the layer from which disintegration alpha-particles may escape into the chamber) is longer ("thin detector"). In gold, however, most of the resonance neutrons are absorbed in a layer which is thin compared with the mean range of the electrons emitted by the active gold; therefore, the probability of a resonance neutron being counted is almost independent of the angle of incidence ("Thick detector"). In the case of gold, therefore, a correction of 5 % has been applied (see appendix I) while in the case of arsenic and iodine the detectors used were regarded as thin, and consequently the uncorrected values were taken.

Discussion of Resonance Energies. The final results are summarised in table 1. The results of H. H.

Table 1.

	C-neutrons	Arsenic	Iodine	Gold	Units
Half-value thickness H..	0.0205 ± 0.001	0.75 ± 0.07	0.71 ± 0.07	0.25 ± 0.01	gr./cm.^{2}
$\frac{H_R}{H_C} = q'$		37 ± 3.5	35 ± 3.5	12.2 ± 0.5	
$q_{\text{corr}} = \frac{\mu_{(C)}}{\mu_{(R)}}$ ...		37 ± 4	35 ± 4	11.6 ± 0.7	
$E_R = kT \cdot q^2$ ...	$(kT = 0.026)$	35 ± 8	32 ± 8	3.5 ± 0.5	eV.
E_R (Goldsmith and Rasetti)		84	80	2.5	eV.

Goldsmith and F. Rasetti (15) which were published after our measurements were finished have been included for comparison. While in the case of gold the agreement is tolerable the authors find considerably higher energy values for arsenic and iodine than we do. This difference seems to indicate that, in fact, more than one level contributed to the activation, both in arsenic and iodine. The difference between the values obtained by Goldsmith and Rasetti and our values is then probably due to the fact that Goldsmith and Rasetti used thicker boron absorbers than we, and thereby suppressed the low energy levels relative to the higher ones. In fact the introduction of their values into our fig. 2 (a rather arbitrary procedure, on account of the different geometrical conditions) suggests a definite curvature of the absorption curves (indicated by the dotted lines) which is, however, quite compatible with the points measured by us. It would therefore appear that the energy values given both by Goldsmith and Rasetti and in this paper are just different average values, and that at least one level somewhat below 30 eV. and at least one above 80 eV. are involved (and possibly levels in between), both in arsenic and iodine.

It seems very doubtful whether much additional imformation may be expected from this type of experiments since the boron absorption method is rather ineffective as soon as more than one component is involved, like all methods where absorption curves are analysed into exponentials (e. g. gamma ray analysis by absorption).

2. Determination of Resonance Cross Sections.

Determinations of resonance cross sections by different authors have so far not been very consistent among themselves. This is probably due to the phenomenon of self-reversal (16): neutrons with velocities near to the centre of the absorption line are quickly absorbed, those at the sides showing a smaller absorption. The apparent absorption coefficient will, therefore, depend on the thickness of the absorber used, decreasing with increasing absorber thickness; in other words, the absorption curve is not exponential but flattens out at large absorber thicknesses.

We shall first discuss the shape of the absorption curve theoretically and then compare it with experiment. Our calculation is based on the assumptions that only one resonance level is involved the width of which is small compared with the resonance energy, and that the neutrons have a uniform energy distribution in the energy region concerned. The first assumption permits us to neglect the $\frac{1}{v}$-factor in the capture cross section which becomes important, anyhow, only for very slow neutrons which in the experiments have been removed by a cadmium screen. We take therefore

$$\sigma = \frac{\sigma_R}{1 + \left(\frac{E - E_R}{B_R}\right)^2}$$

or, introducing the mass absorption coefficient

$$\mu = \frac{\sigma \cdot N}{A} \quad \begin{pmatrix} N = \text{Avogadro's number} \\ A = \text{Atomic Weight} \end{pmatrix}$$

$$\mu = \frac{\mu_R}{1 + \left(\frac{E - E_R}{B_R}\right)^2}.$$

Assuming that $n \cdot dE$ neutrons of energies between E and $E + dE$ fall normally on a plate of the absorber, the number present after passage through a thickness x will be $n \cdot e^{-\mu x} dE$. The number of neutrons which are absorbed between x and $x + dx$ is then found by differentiating the last expression. Finally one has to integrate over all neutron energies, to obtain the total number of neutrons absorbed in a thin detector of thickness dx behind an absorbing layer of thickness x. We find this to be

$$\text{const.}\, e^{-z} \cdot J_0(iz) \left(z = \frac{\mu_R x}{2},\ J_0 = \text{Bessel function of order zero}\right).$$

This function is tabulated in column A of table 2 and shown graphically in fig. 3. The function starts off like an exponential, the corresponding absorption coefficient μ_0 being, however, only half the value μ_R at resonance. For larger absorber thicknesses the curve flattens out and approaches asymptotically the function $\frac{1}{\sqrt{\pi \mu_R x}}$.

The same calculation has been carried out numerically in the case where the neutrons do not enter the plate normally but are distributed in angle according to a cosine law. (B in table 2 and fig. 3.) For completeness the figures corresponding not to a resonance line but to a fixed absorption coefficient μ_0 are included (C and D), both for normal and cosine incidence.

Table 2.

$\mu_0 x$	A	B	C	D
0.01	0.990	0.950	0.990	0.950
02	980	914	980	913
05	951	832	951	828
1	907	737	905	723
2	827	629	819	574
3	758	546	741	467
4	697	..	670	..
5	..	..	607	327
6	600	395	549	275
8	523	..	449	..
1.0	466	296	368	148
1.5	367	234	223	..
2	308	198	135	038
3	243	158	050	011
4	207	137	018	..
5	183	122	007	..
6	166	111	003	..
7	152	099	001	..

In plotting the experimental points one has to add to each absorber thickness a certain fraction of the detector thickness, the effective depth of the detector. For a thin detector this is just half its thickness; for a thick detector

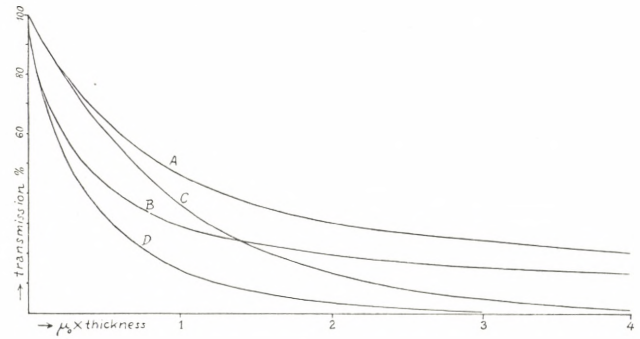

Fig. 3.

of thickness a the absorption of the electrons emitted in the detector has to be taken into account. We have done this in a rough way by measuring the absorption coefficient μ_e of the electrons in the detector material and by using for the effective depth the expression $\frac{1}{\mu_e}\left(1 - a\,\mu_e \frac{e^{-a\,\mu_e}}{1 - e^{-a\,\mu_e}}\right)$.

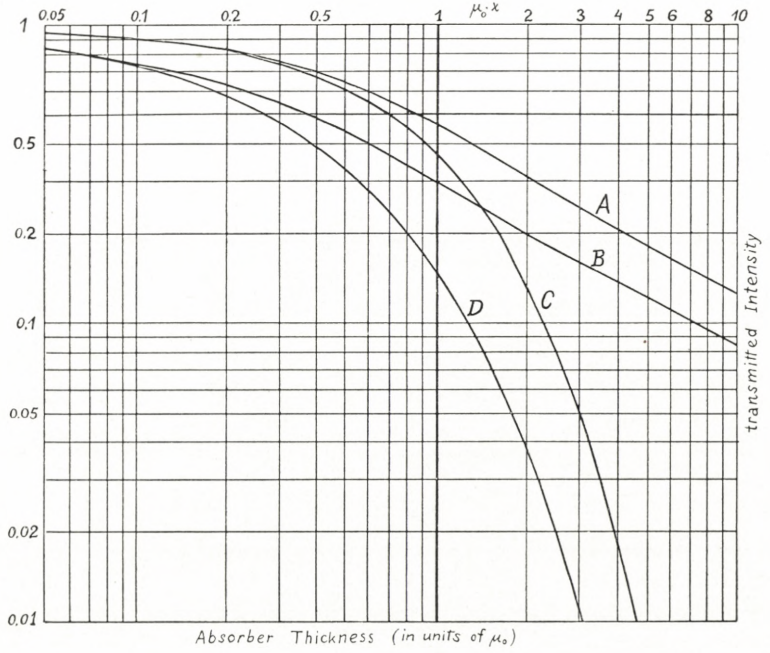

Fig. 4.

In comparing the theoretical curves with the experiments we must remember the following point. The scales of the ordinate and abscissa of the theoretical and experimental curves are not the same. The adjustment of the scales can be most easily effected by plotting both the ordinate and abscissa logarithmically, for then a change of scale merely causes a shifting of the origin. The theoretical curves are

first plotted (fig. 4); comparison is then carried out by plotting the experimental points on the same scale on a piece of transparent paper and by attempting to obtain coincidence by means of vertical and horizontal translations of the paper.

Experimental procedure. A nearly parallel beam of neutrons would obviously be the best for measuring their absorption, but intensity considerations force one to content oneself with rather bad geometrical arrangements. We have used two types. In one of them, a block of paraffin wax shaped like a cone was used as a source of slow neutrons, and the detector was placed in such a way that only neutrons forming angles of about 45°, or less, with the normal were able to reach it. In the other one, the absorbers and the detector were placed immediately on top of a flat paraffin block. For the determination of the initial absorption coefficient the "conical" arrangement was always used; the "flat" arrangement, yielding larger intensity, was used to obtain, in some cases, the shape of the absorption curve up to higher absorbing thicknesses.

In the case of iodine, plates of 15 mms. diameter, each containing 0.200 gr. I_2O_5, where used as detectors; the absorber plates consisted also of I_2O_5. The activity of both sides was measured in all cases and the average was taken (the difference was always small); the effective depth could then be taken as equal to half the thickness of the detector, corresponding to 0.043 gr./cm.^{2} iodine. On plotting the points, this amount was always added to the absorber thickness. The distance of the detector from the paraffin varied by about one mm.,

depending on the absorber used; to allow for this, a small correction of 4 % at most was applied.

The points obtained are plotted, on a double logarithmic scale, in fig. 5. The effective absorber thickness (in gr./cm.^{2}) has been written under each point while the corrected intensity is written on top of it, in arbitrary units. On comparing the points with different curves of type A (see fig. 4) one sees that none of them fits all the observed points. Doppler

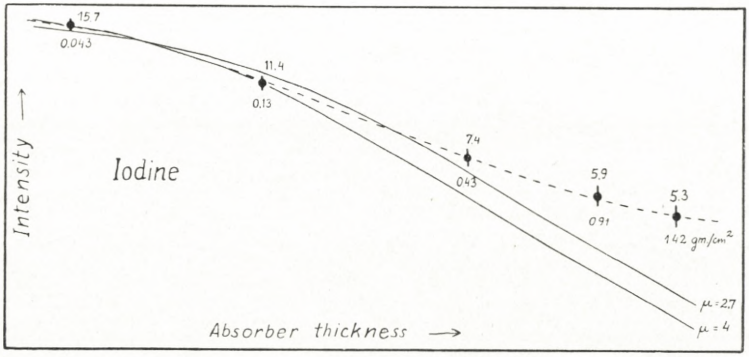

Fig. 5.

broadening of the line would make the absorption still steeper and thereby make the discrepancy still worse. The only possibility seems again to be to assume that more than one level is involved. If we assume, for example, that about 20 % of the activation of the detector without absorber is due to some group of neutrons which are only weakly absorbed in iodine and that 80 % is due to a line with $\mu_0 = 5$ cm.^{2}/gr. ($\sigma_R = 2.1 \cdot 10^{-21}$ cm.^{2}) then we get the dotted line which fits the observed points perfectly. It should be emphasized that, of course, many other combinations of neutron groups with different absorption

coefficient could be found which would fit the points equally well. A small part of the activation might be due to the primary neutrons from the (Ra + Be) source; this might account for some of the weakly absorbable neutrons.

In the case of arsenic, the absorption coefficient was determined in a similar way, using detectors of 15 mms.

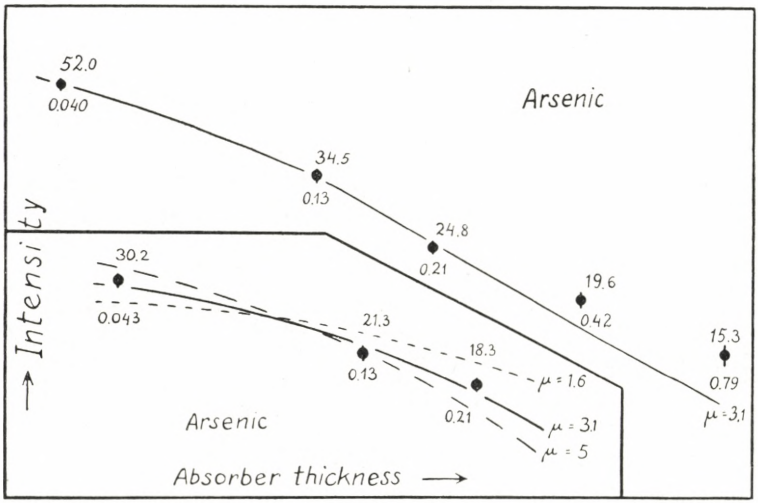

Fig. 6.

diameter, each containing 0.200 gr. As_2O_3, and the conical paraffin arrangement. The results are plotted in fig. 6. An additional experiment in which larger absorbing thicknesses were employed was carried out with the flat arrangement. The first three points of this fit the corresponding curve with the same value of μ_0 (3.1 cm.^{2}/gr.) determined in the conical arrangement. The other two points deviate from the curve in a similar way to the case of iodine, but the deviation seems to be smaller.

Both with arsenic and iodine, the oxygen contained in

the absorbers had no measurable influence; this was checked by special experiments.

In the case of gold, the initial absorption coefficient μ_0 was determined by using gold foils of about 0.004 mm. thickness as detector and absorber. Two such foils (of 15 mms. diameter) were simultaneously exposed to the neutrons with the conical arrangement, on top of one another, and the activity induced in both of them was measured. A small correction of 3 % was applied to the activity ratio measured since in a preliminary experiment it had been found that one of the foils showed 3 % more activity when both had been exposed under identical conditions. Since only two points are measured and the intensity ratio is small one may work out the absorption coefficient assuming an exponential absorption law. In this way one gets $\mu_0 = 41$ cm.²/gr. (oblique incidence having been allowed for). Some uncertainty, however, arises from the inhomogeneity of the gold foils used; if, instead of 3 %, a correction of 7 % is applied to the ratio measured, in view of the fact that there was a 7 % difference in weight between the foils, one gets $\mu_0 = 35$ cm.²/gr. As a safe estimate we would propose the value $\mu_0 = (40 \pm 5)$ cm.²/gr. (corresponding to $\sigma_R = 2.6 \cdot 10^{-20}$ cm.²).

On account of this high value, together with the high density of gold, it has been possible to follow the absorption curve of gold for a very large range of thicknesses, varying in ratio from 1 to 5000. For this purpose, a pile of 29 gold plates of different thickness, the total thickness being about 6 mms., was placed on top of the flat paraffin block. To prevent neutrons from entering the pile from the sides, a "guard ring" of gold, of 15 mms. internal and 25 mms. external diameter, was placed round the pile. After three

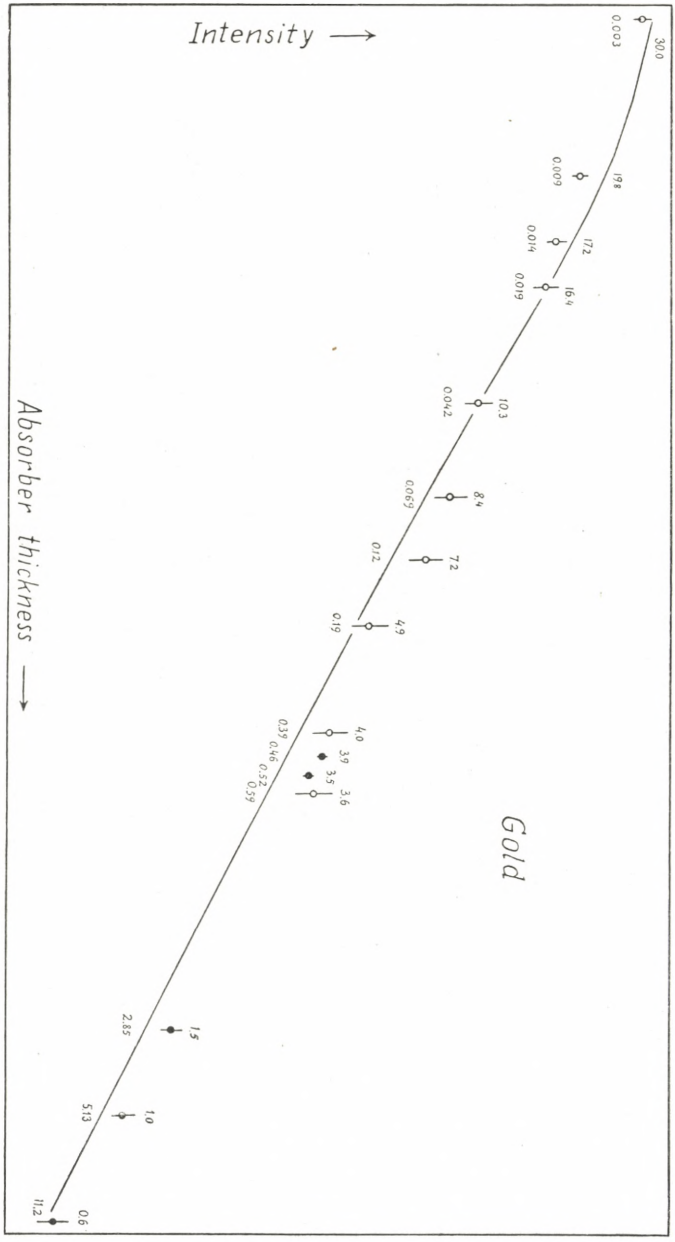
Intensity ⟶
Absorber thickness ⟶
Gold
30.0
0.003
198
0.009
172
0.014
164
0.019
103
0.042
84
0.063
72
0.12
49
0.19
4.0
3.9
3.5
3.6
0.39
0.46
0.52
0.59
1.5
2.85
1.0
5.13
0.6
11.2

Fig. 7.

days exposure the activities of a suitable selection of foils were measured, the corresponding absorbing thicknesses having a fairly uniform distribution on a logarithmic scale.

Ten of the gold foils selected for measurement were of nearly equal thickness (0.004 mm.); small differences in thickness were allowed for by dividing the measured activity by the weight of each foil. For thicker absorbing layers, however, the intensity becomes too small to be measured by such thin detectors; plates of 0.1 mm. thickness were therefore used and their activity was divided by the empirical figure seven, to match them with the thin detectors. The results are shown in fig. 7. The curve drawn through the points is a curve of type B (see fig. 4), for $\mu_0 = 40$ cm.^{2}/gr. The fit is remarkably good, considering the great range of thickness, and offers a very conclusive proof of the "resonance shape" of the absorption line. The deviations present are too small to offer a basis for discussion.

3. Width of Resonance Level.

From the formula $\mu = \dfrac{\mu_R}{1 + \left(\dfrac{E - E_R}{B_R}\right)^2} \cdot \sqrt{\dfrac{E_R}{E}}$ the half-value width $2B_R$ can be calculated if E_R, μ_R and the absorption coefficient at another velocity, e. g. for thermal neutrons (μ_T) is known. In the case of gold, taking $E_R = 3.5$ eV., $\mu_R = 2\mu_0 = 80$ cm.^{2}/gr., and $\mu_T = 0.29$ cm.^{2}/gr., we obtain $2B_R = 0.12$ eV. This result is, however, uncertain because other levels might contribute to the absorption coefficient μ_T at thermal energies, possibly also levels below "zero", that is, levels with smaller energies than would correspond to an incoming neutron with zero velocity.

From measurements on the relative intensity of activation due to thermal and resonance neutrons one may obtain information on the width of resonance (17, 11) without assuming only one level. A very rough estimate on this basis gave a width of about 0.1 eV. which is the same order of magnitude as had been obtained in silver and rhodium (11).

In the case of such narrow absorption lines the Doppler broadening, due to the thermal agitation of the capturing nuclei, is not at all negligible. For a infinitely sharp level the Doppler half-value width of the absorption line would be $4\sqrt{ln\,2}\cdot\sqrt{kT\cdot\frac{E_R}{A}}$ (A = atomic weight) which, in the case of gold at room temperature, is equal to 0.06 eV. An attempt was therefore made to find an influence of temperature on the width of the absorption line.

Gold foils of 0.01 mm. thickness were exposed to slow neutrons filtered with cadmium, the gold being either at room temperature or at a faint red glow (about 600° C). Since neutrons near the centre of the absorption line are almost completely absorbed in that thickness of gold the broadening of the line with increasing temperature was expected to result in increased activity. The experiments are rendered laborious by the smallness of the differences to be measured and by the inhomogeneity of the gold foils. Still, from four runs carried our with different gold foils and arrangements, a difference in activity, in favour of the hot foil, of $(7.5 \pm 1.5)\,\%$ seemed to be fairly well established.

A check experiment, however, in which the cadmium screen was removed, showed about the same difference in activity between the hot and the cold foil. Since about

three-quarters of the activity obtained under these conditions was due to thermal neutrons, this result is hard to understand. For thermal neutrons the rate of capture per unit time should be independent of the velocity $\left(\frac{1}{v}\text{-law!}\right)$ and consequently there should be no temperature effect. It is therefore doubtful wether the effect observed with the cadmium screen present is genuine, and it may be that all the effects observed are due to some still undetected source of error.

APPENDIX I.

Obliquity Corrections.

Calculations have been carried out regarding the absorption curve of radiation with a given absorption coefficient μ, under geometrical conditions roughly the same as those actually used. For the directional distribution of the neutrons emerging from the paraffin, the expression

$$J_2 \sin\vartheta\, d\vartheta\, d\varphi = \left(\cos\vartheta + \sqrt{3}\cdot\cos^2\vartheta\right) \sin\vartheta\, d\vartheta\, d\varphi$$

was taken (11). This is also the number of neutrons from different directions, indicated by a "thick" detector which responds equally well to neutrons from all directions. In a "thin" detector, however, oblique neutrons have a probability of being detected, larger by a factor $1/\cos\vartheta$. In this case, the directional distribution of indicated neutrons is given by

$$J_1 \sin\vartheta\, d\vartheta\, d\varphi = \left(1 + \sqrt{3}\cdot\cos\vartheta\right) \sin\vartheta\, d\vartheta\, d\varphi.$$

If the detector is not placed directly on top of the paraffin, no neutrons emerging at a very flat angle will hit the detector. The directional distribution of indicated

$$F_1 = \frac{e^{-k}\left[2+\sqrt{3}\,(1-k)\right] - e^{-\frac{k}{a}}\left[2a+\sqrt{3}\,(a^2-ak)\right] - \left[E(k) - E\left(\frac{k}{a}\right)\right](2k-\sqrt{3}\cdot k^2)}{2\,(1-a)+\sqrt{3}\,(1-a^3)}$$

$$F_2 = \frac{e^{-k}\left[3\,(1-k)+\sqrt{3}\,(2-k+k^2)\right] - e^{-\frac{k}{a}}\left[3\,(a^2-ak)+\sqrt{3}\,(2a^3-a^2k+ak^2)\right] + \left[E(k)-E\left(\frac{k}{a}\right)\right](3k^2-\sqrt{3}\cdot k^3)}{3\,(1-a^2)+2\sqrt{3}\,(1-a^3)}$$

$$\left(a = \cos\vartheta_0, \quad k = \mu x, \quad E(y) = \int_y^\infty \frac{e^{-z}}{z}\,dz\right).$$

neutrons becomes, then, very complicated, depending on the shape of the paraffin surface and the distribution of neutron brightness along it. In the calculation the assumption was made, for the sake of simplicity, that for $\vartheta < \vartheta_0$ the directional distribution given above is valid while for $\vartheta > \vartheta_0$ no neutrons are indicated at all, where ϑ_0 is a suitably chosen angle.

The relative number of neutrons indicated behind an absorbing plate of thickness x is then given by

$$F = \frac{\int_0^{\vartheta_0}\int_0^{2\pi} J \cdot e^{-\frac{\mu x}{\cos\vartheta}} \cdot \sin\vartheta \, d\vartheta \, d\varphi}{\int_0^{\vartheta_0}\int_0^{2\pi} J \cdot \sin\vartheta \, d\vartheta \, d\varphi} .$$

If the integration is carried out, taking either J_1 or J_2 for the distribution of indicated neutrons, the expressions on page 24 are obtained.

These formulae have been kindly evaluated by Mr. FRODE HJERTING; the results are given in table 3.

For practical purposes, the set of curves given in fig. 8 may be found convenient. Each curve corresponds to a value of ϑ_0; the abscissae are the observed transmissions (absorptions), and the ordinate gives, then, the factor f by which one has to multiply the absorber thickness in order to obtain a thickness which would, in the case of a parallel beam, give the transmission observed. In other words: if one has calculated the "apparent" absorption coefficient from an absorption experiment, neglecting obliquity, then one has to divide it by f in order to obtain the true one. For not too bad geometrical conditions (ϑ_0 not larger than about 60°) the absorption is nearly exponential and, there-

Table 3.

	ϑ_0	$\cos\vartheta_0$	$\mu x = 0.01$	0.02	0.05	0.1	0.2	0.5	1.0	2.0
F_1 thin detector	90°	0	0.964	0.936	0.866	0.774	0.634	0.381	0.181	0.048
	84°	0.1	978	957	899	812	671	404	193	051
	77°	0.2	982	964	913	835	703	432	207	055
	71°	0.333	985	969	929	856	734	470	232	062
	60°	0.5	987	973	934	874	764	512	267	080
	48°	0.667	988	976	942	886	786	548	302	093
	0°	1	990	980	951	905	819	607	368	135
F_2 thick detector	90°	0	983	967	920	849	728	471	240	068
	84°	0.1	984	968	922	852	731	474	242	069
	77°	0.2	985	970	926	858	739	481	246	070
	71°	0.333	986	972	931	867	753	498	257	074
	60°	0.5	987	974	937	878	771	525	279	082
	48°	0.667	988	977	942	888	788	553	307	096
	0°	1	990	980	951	905	819	607	368	135

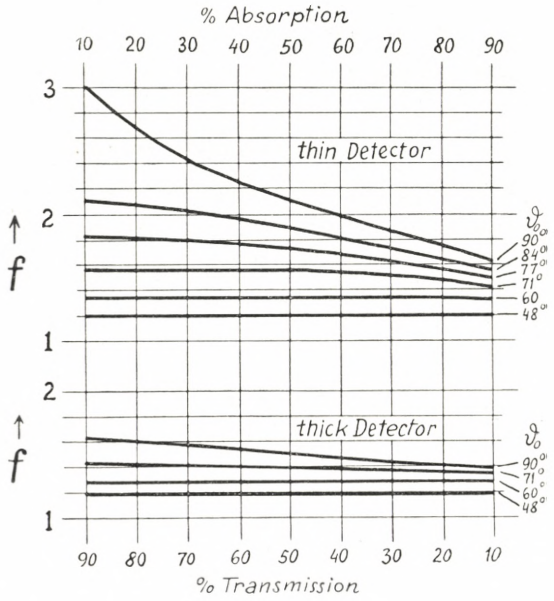

Fig. 8.

fore, f is fairly independent of the absorber thickness. For ϑ_0 smaller than 45°, f is nearly equal to $\frac{2}{(1+\cos\vartheta_0)}$, both for thin and thick detectors.

In applying the obliquity correction to the experiments with the paraffin cube, a value of $\vartheta_0 = 71°$ has been adopted. Consequently the apparent absorption coefficient has to be divided by 1.42 in the case of gold, and by 1.52 in the case of the other detectors used. This would result in a correction of 7 % in the value of q, for gold; for various reasons, this correction was lowered to 5 %.

APPENDIX II.

Cut-off Energy of Cadmium.

In order to obtain some information on the energy limit up to which the high absorbing power of cadmium extends (cut-off energy) the absorption in boron of those neutrons which penetrate through cadmium (as detected by a boron chamber) has been compared with the absorption of thermal neutrons in boron (9). The residual neutrons were found to be about six times less absorbable than the thermal ones, and it was concluded from this that cadmium is fairly transparent for neutrons with energies as small as 1 eV.

These experiments have been repeated and extended over a large range of boron thicknesses without, however, changing very much the result which was obtained first. In table 4 the results of an experiment are collected where the absorption in boron of neutrons detected by a boron chamber was studied with and without a screen of 1 gr./cm.^{2} cadmium. The source of neutrons was a tin can filled with water (17 cms. diameter and 18 cms. high), with 200 mgr.

Table 4.

boron absorber thickness in gr./cm.^{2}	*A* without cadmium	*B* with a screen of 1 gr./cm.^{2} Cd (unit as in *A*)	*C* same as *B*	*D* *A* — *B*
			(unit changed to make first value = 100)	
0	100 $\pm$ 2	6.9 $\pm$ 0.15	100 $\pm$ 2	100 $\pm$ 2
0.020	59 $\pm$ 2	(6.6)	..	56.5 $\pm$ 2
0.030	45 $\pm$ 2	(6.4)	..	41.5 $\pm$ 2
0.049	32 $\pm$ 1.5	6.1 $\pm$ 0.2	89 $\pm$ 3	28 $\pm$ 1.5
0.10	13.3 $\pm$ 0.6	5.6 $\pm$ 0.2	81 $\pm$ 3	8.3 $\pm$ 0.7
0.20	..	4.4 $\pm$ 0.2	64 $\pm$ 3	..
0.40	3.1 $\pm$ 0.3	2.9 $\pm$ 0.15	42 $\pm$ 2	0.2 $\pm$ 0.4
1.0	..	1.8 $\pm$ 0.15	26 $\pm$ 2	..

Ra + Be placed in its centre; the detecting boron layer had a diameter of 15 mms., as in the experiments described above, and was placed 8 cm. above the water surface.

The absorption curves both for the residual neutrons and those stopped by the cadmium screen are shown in fig. 9. The fact that the half value thickness for the residual

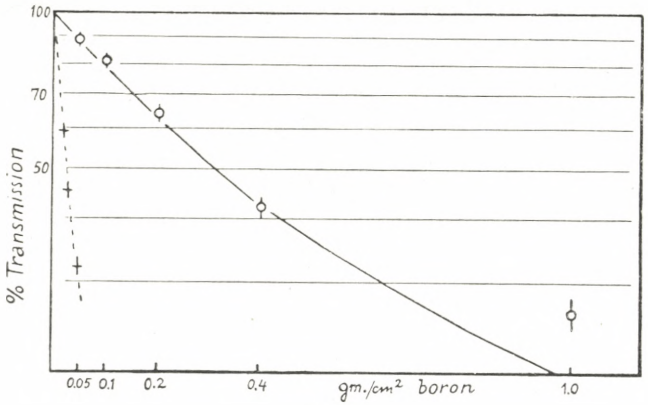

Fig. 9.

neutrons is seen to be about 15 times larger than for thermal neutrons shows that they are absorbed like a homogeneous group of about 5 eV. energy. This value may be regarded as a kind of average energy of the residual neutrons.

As a rough approximation to the velocity distribution of the residual neutrons one may assume that no neutrons are present with velocities below a certain limit v_L, while above this limit the number of neutrons entering the boron chamber per unit time with velocities between v and $v + dv$ is proportional to $\frac{dv}{v}$ (7, 11).

The absorption curve for this distribution has been calculated, taking into account the $\frac{1}{v}$-sensitivity of the boron chamber, and the result is

$$J = J_0 \frac{1 - e^{-\mu_L \cdot x}}{\mu_L \cdot x} \qquad \left(\begin{array}{l} x = \text{boron thickness} \\ \mu_L = \text{absorption coefficient of boron} \\ \qquad \text{for neutrons of velocity } v_L \\ \qquad (\text{energy } E_L). \end{array} \right)$$

Taking E_L equal to 0.87 eV. we obtain the curve shown in fig. 9. From the good agreement of this curve with the points measured we may deduce that the cut-off energy of a screen of 1 gr./cm.^{2} cadmium is slightly below one volt. Of course, the cut-off is not a sharp one; there will be still lower energies transmitted, to some extent, and higher energies will still be somewhat absorbed. A careful study of the cadmium absorption curve combined with measurements of the absorption in boron of the transmitted neutrons may give more information on this point.

SUMMARY

The selective capture of slow neutrons in gold can be attributed mainly to one resonance level. The resonance

energy is found to be 3.5 ± 0.4 eV. (using the "boron absorption method"), the resonance cross-section is $(2.6 \pm 0.3) \cdot 10^{-20}$ cm.². The half-value width of the absorption line is estimated to be of the order of 0.1 eV. An attempt of finding an influence of temperature on the line width (thermal Doppler effect) gave no conclusive results.

In the case of arsenic and iodine there are indications that more than one level contributes to the activation; in both cases, the boron absorption method gives a value of about 30 eV. for the average resonance energy if fairly thin boron absorbers are used, while Goldsmith and Rasetti find a value of about 80 eV., using thicker absorbers. It is concluded that at least one level below 30 eV. and one above 80 eV. contribute to the activation both of arsenic and iodine.

Absorption curves obtained in the element under investigation also indicate the presence of more than one level in the case of arsenic and iodine, while the absorption curve of gold is in accord with the assumption of one level only.

The influence of oblique incidence on absorption measurements is discussed in detail, and a diagram is given by means of which the corrections can be carried out readily.

The "cut-off" energy of a screen of 1 gr./cm². cadmium is found to be nearly 1 eV.

In conclusion, I wish to thank Prof. Dr. N. Bohr for his kind interest in this work, and Dr. G. Placzek, Dr. V. Weisskopf and Dr. G. Wick for many helpful and stimulating discussions. Furthermore, my thanks are due to the Rask-Ørsted foundation for a grant which enabled me to carry out this investigation at the Institut for teoretisk Fysik at Copenhagen.

REFERENCES

1) E. Amaldi, E. Fermi, Ric. Scient. VI—II, 344 (1935).
2) L. Szilard, Nature **136**, 950 (1935).
3) O. R. Frisch, H. A. C. McKay, G. Hevesy, Nature **137**, 149 (1936).
4) N. Bohr, Nature **137**, 344 (1936).
5) G. Breit, E. Wigner, Phys. Rev. **49**, 519 (1936).
6) T. Bjerge, C. H. Westcott, Proc. Roy. Soc. A **150**, 709 (1935).
7) P. B. Moon, Proc. Phys. Soc. **48**, 648 (1936).
8) D. F. Weekes, M. S. Livingston, H. A. Bethe, Phys. Rev. **49**, 471 (1936).
9) O. R. Frisch, G. Placzek, Nature **137**, 357 (1936).
10) H. v. Halban, P. Preiswerk, Nature **137**, 905 (1936).
11) E. Amaldi, E. Fermi, Phys. Rev. **50**, 899 (1936).
12) P. B. Moon, J. R. Tillman, Proc. Roy. Soc. A **153**, 476 (1936).
13) P. Preiswerk, H. v. Halban, Nature **136**, 1027 (1935).
14) J. R. Dunning, G. B. Pegram, G. A. Fink, D. P. Mitchell, E. Segrè, Phys. Rev. **48**, 704 (1935).
15) H. H. Goldsmith, F. Rasetti, Phys. Rev. **50**, 328 (1936).
16) H. v. Halban, P. Preiswerk, Nature **138**, 163 (1936), J. de Phys. **8**, 36 (1937).
17) E. Amaldi, E. Fermi, Ric. Scient. VII—I, 310 (1936).

Færdig fra Trykkeriet den 21. Juni 1937.

Det Kgl. Danske Videnskabernes Selskab.
Mathematisk-fysiske Meddelelser. **XIV**, 13.

ÜBER DIE THEORIE DES ABSOLUTEN MANOMETERS VON MARTIN KNUDSEN

VON

SOPHUS WEBER

KØBENHAVN
LEVIN & MUNKSGAARD
EJNAR MUNKSGAARD
1937

Printed in Denmark.
Bianco Lunos Bogtrykkeri A/S.

§ 1. In den letzten Jahren sind viele Fragen über die Wirkung des Radiometers geklärt worden, einerseits durch die grundlegenden Arbeiten von MARTIN KNUDSEN[1] über den »Knudsen-Zustand« der Gase, andererseits durch die theoretischen Untersuchungen über die bei grösserer Dichte im Gase entstehenden Strömungen, herrührend von den Temperaturunterschieden in der Oberfläche der Radiometerflügel; diese Strömungen und die hierdurch entstehenden Druckspannungen werden beherrscht von der Grenzbedingung an der Oberfläche, worin die Temperaturunterschiede vorkommen. MAXWELL[2] hat in seiner Arbeit über die hydrodynamischen Gleichungen in einem ungleichmässig erwärmten Gase diese Grenzbedingung untersucht und formuliert; er findet, wenn die mittlere freie Weglänge im Gase, λ, klein ist im Verhältniss zu den Abmessungen, dass ein Temperaturgradient, $\frac{dT}{dx_2}$, in der Oberfläche eines festen Körpers eine tangentiale Strömung hervorruft, so dass eine tangentiale Gleitgeschwindigkeit, u_2, an der Oberfläche entsteht; diese ist nach MAXWELL bestimmt durch die Gleichung:

$$u_2 - \gamma_M \cdot \frac{du_2}{dx_1} = \frac{3}{4} \cdot \frac{\eta}{\varrho \cdot T} \cdot \frac{dT}{dx_2}, \qquad \text{(I)}$$

[1] MARTIN KNUDSEN: Ann. d. Ph., Bd. 28, 1909, p. 75, Bd. 32, 1910, p. 809.

[2] I. CLERK-MAXWELL: Phil. Trans., 170, I, 1879, p. 231.

wo $\gamma_M = \sqrt{\frac{\pi}{2}} \cdot \frac{\eta}{p\sqrt{_1\varrho}}$ der gewöhnliche Gleitungskoefficient des Gases ist; η und ϱ sind die innere Reibung und die Dichte des Gases, während $\frac{du_2}{dx_1}$ die Variation der Geschwindigkeit in der Richtung der Normale des Oberflächenelementes ist.

Hettner[1] hat später die Berechnung wiederholt und hat die Bezeichnung »thermische Gleitung« für das Glied in der rechten Seite der Gleichung (I) eingeführt.

In einer Untersuchung über die thermomolekulare Druckdifferenz haben wir[2] die Grenzbedingung näher untersucht und experimentell gefunden, dass diese geschrieben werden muss:

$$u_2 - k_2 \cdot \gamma_M \cdot \frac{du_2}{dx_1} = k_1 \cdot \frac{3}{4} \cdot \frac{\eta}{\varrho \cdot T} \cdot \frac{dT}{dx_2}, \qquad \text{(II)}$$

wo $k_1 = k_2 = \text{ca.}\ \frac{4}{3}$; ausserdem muss, wenn λ nicht mehr klein den Abmessungen gegenüber ist, das Glied für die thermische Gleitung mit einem Faktor, A, multipliciert werden. A ist bestimmt durch das Verhältniss zwischen der freien Weglänge, λ, und den Abmessungen des Apparates; für ein kreisförmiges Rohr mit Radius R und ein Temperaturgefälle $\frac{dT}{dx_2}$ in der Richtung der Achse wird die Grenzbedingung:

$$u_2 - k_2 \cdot \gamma_M \cdot \frac{du_2}{dx_1} = k_1 \cdot \frac{3}{4} \cdot \frac{\eta}{\varrho T} \cdot \frac{dT}{dx_2} \cdot A \qquad \text{(III)}$$

oder annäherungsweise:

$$u_2 - \frac{4}{3} \cdot \gamma_M \cdot \frac{du_2}{dx_1} = \frac{\eta}{\varrho T} \cdot \frac{dT}{dx_2} \cdot \frac{1}{1 + \frac{\lambda}{R}};$$

[1] G. Hettner: Z. f. Ph., Bd. 30, 1924, p. 258.

[2] Sophus Weber, W. H. Keesom und G. Schmidt: Comm. Kamerlingh Onnes Lab., Leiden, No. 246[a], p. 9 und Sophus Weber: Comm. Kamerlingh Onnes Lab., Leiden, No. 246[b], p. 7.

für parallele Platten mit dem Abstand, d, wird mit derselben Annäherung: $A = \frac{1}{1+\frac{\lambda}{d}}$.

Diese einfache Form für A kann nur betrachtet werden als eine erste Annäherung von einem komplicierten Ausdruck, der aber mathematisch nicht einfach zu behandeln ist.

§ 2. Beim Durchlesen der Literatur stellt es sich heraus, dass das Verständniss von der Wirkung des Radiometers im Allgemeinen sehr erschwert worden ist, weil die experimentell untersuchten Radiometer früher so wenig rationell konstruiert worden sind. Hierdurch wird der Einfluss von den festen Wänden, welche den beweglichen Teil des Radiometers umgeben, sehr unübersichtlich, so dass der Einfluss von den bei grösserer Dichte des Gases entstehenden Strömungen nicht mathematisch zu berechnen ist; die meisten früheren experimentellen Untersuchungen über das Radiometer sind darum nicht für die Vergleichung zwischen Theorie und Experiment zu verwenden.

Die verschiedenen Radiometererscheinungen können wir am besten in fünf Hauptgruppen einteilen:

1) Untersuchungen über das absolute Manometer von Martin Knudsen und das Zweiplattenradiometer von Hettner.
2) Untersuchungen über das Flügelradiometer, bezw. das Einplattenradiometer.
3) Untersuchungen über das Quarzfadenradiometer von Westphal.
4) Untersuchungen über die Knudsen'sche Radiometerkraft, welche in verschiedenen Werten des Akkom-

modationskoefficienten der Gasmoleküle an den beiden Seiten des Radiometersystems ihre Ursache hat.

5) Untersuchungen über Photophorese oder Radiometerwirkungen an kleinen Körpern, z. B. Kugeln, und verwandten Erscheinungen.

§ 3. In dem Folgenden werden wir die Gruppen 1 und 2, besonders das absolute Manometer von Martin Knudsen, betrachten, weil das absolute Manometer von Knudsen in der Ausführung, welche Knudsen die rationelle absolute Manometerform genannt hat, das einfachste, rationelle Radiometer ist; in dieser Ausführung sind alle physikalischen Verhältnisse genau festgelegt, und jede Grösse von Bedeutung für die theoretische Diskussion kann experimentell gemessen werden; in der Knudsen'schen Konstruktion haben wir eine dicke, flache, cirkulare Kupferplatte A (das Ende von einem Kupfercylinder mit inwendiger elektrischer Heizung) mit einer bekannten konstanten Temperatur T_1; dieser cirkulare Cylinder ist von einem dicken kupfernen Schutzringcylinder, C, mit der Temperatur, T_3, umgeben. T_1 und T_3 können genau gemessen werden; gegenüber der warmen Platte A, umgeben von dem Schutzringcylinder, C, ist die schwere kupferne Platte B drehend aufgehängt, und die Temperatur, T_2, von B kann genau gemessen werden; sind $T_1 = T_2 = T_3$, ist die Oberfläche von B genau parallel mit den Oberflächen von A und C, die in einem Plan liegen. — Die Aussenseite von B ist berusst, während die Innenseite von B, wie auch die Oberfläche von A und C, blanke Kupferplatten sind.

Wir dürfen also annehmen, dass der Akkommodationskoefficient für diese Oberfläche derselbe ist; ausserdem

dürfen wir annehmen, dass die Platte B, wie auch die Oberfläche von A und C, überall dieselbe Temperatur bezw. T_2, T_1 und T_3 haben, und dass keine Temperaturgradienten in diesen Metallmassen anwesend sind; in diesem System ist also nur ein Temperaturgradient vorhanden, am Rande der Oberfläche A bei dem Übergang zwischen A und dem Schutzring C; dieses ist erläutert in Fig. 1.

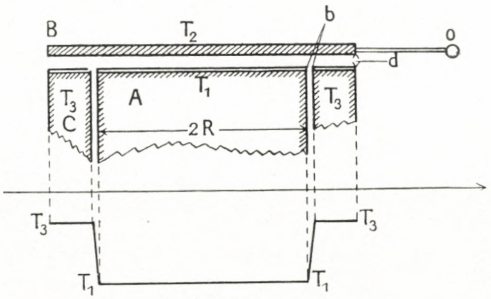

Fig. 1.

In den Versuchen waren die Temperaturen T_2 und T_3 nur sehr wenig verschieden, jedenfalls bei kleinen Temperaturunterschieden, und dieselbe wie die Temperatur des umgebenden Gases.

Für das absolute Manometer ist der Zustand und die Radiometerkraft, K, sowohl theoretisch als experimentell ausführlich von Martin Knudsen behandelt für den Fall, dass die freie mittlere Weglänge des Gases, λ, sehr gross gegenüber dem Abstand, d, zwischen den Platten A und B ist, also für den Fall: $\frac{d}{\lambda} \gtrsim 0$.

In diesem Falle erhält man, jedenfalls wenn der Akkommodationskoefficient $a = 1$ ist, dass unabhängig von den Eigenschaften des Gases die Radiometerkraft, K, per cm^2, ist gegeben durch:

$$K = p_1 - p_2 = \frac{1}{2} \cdot p_2 \left(\sqrt{\frac{T_1}{T_2}} - 1 \right),$$

wo p_1 der Druck zwischen den Platten A und B ist, während p_2 der Druck von dem umgebenden Gase ist; ausserdem muss für die strenge Gültigkeit dieser Formel der Akkommodationskoefficient für die inneren Oberflächen von A und B, $a = 1$ sein; ist aber der Temperaturunterschied, $T_1 - T_2$, sehr klein den Temperaturen T_1 und T_2 gegenüber, ist die Korrektion wegen des Einflusses des Akkommodakoefficient unbedeutend[1]; für kleine Werte von $T_1 - T_2$ erhalten wir für die Radiometerkraft pro cm^2:

$$K = \frac{1}{2} p_2 \left(\sqrt{\frac{T_1}{T_2}} - 1 \right) = \frac{1}{4} \cdot p_2 \cdot \frac{T_1 - T_2}{T_2}.$$

Diese einfache Lösung ist aber nur gültig für den Fall, $\frac{d}{\lambda} \geqq 0$; die allgemeine Lösung der Radiometerkraft für dieses System muss untersucht werden um zu bestimmen, wie die Radiometerkraft, K, in dem ganzen Gebiet $0 \leqq \frac{d}{\lambda} \leqq \infty$ verlauft.

Wir werden nun zuerst untersuchen, wie der Zustand wird, wenn $\frac{d}{\lambda} \to \infty$, wobei wir aber voraussetzen, dass der Abstand, d, immer so klein bleibt, dass sich zwischen den Platten A und B nur laminare und keine Konvektionsströmungen ausbilden werden, weil hierdurch das ganze Bild von dem Verlauf der Radiometerkraft vollständig geändert werden kann.

§ 4. Betrachten wir nun das absolute Manometer in der rationellen Ausführung (Fig. 1), dann erhalten wir die Temperaturverteilung für die Oberfläche CAC, wie diese in dem Temperaturdiagram (Fig. 1) angegeben ist; wir haben nur

[1] Vgl. J. H. A. ter Heerdt: Dissertation, Utrecht 1924, p. 204.

einen Temperaturgradienten[1] $\frac{dT}{dr} = \frac{T_1 - T_2}{b}$ am Rande der Oberfläche A; b ist der Abstand zwischen dem Kupfercylinder A und dem Schutzringcylinder C; durch diesen Temperaturgradienten entsteht eine thermische Gleitströmung am Rande der Platte A, der Oberfläche CAC entlang und in der entgegengesetzten Richtung von dem Temperaturgefälle, also von dem Rande nach der Mitte der Platte A; bei der Oberfläche der Platte B geht die Strömung in die entgegengesetzte Richtung. Hier strömt die einströmende Gasmenge wieder zurück, so dass die gesammte durch den Rand strömende Gasmenge gleich an Nul sein muss.

Infolge der inneren Reibung im Gase entsteht durch diese Strömung ein Druckunterschied, so dass der Druck im Gase zwischen den Platten grösser wird als im Gasraum ausserhalb der Platten; die Platten werden sich also abstossen.

Weil der Diameter von der Platte A, $2R = 1{,}63$ cm, im Verhältniss zu dem Abstand $b = 0{,}0174$ cm, zwischen A und C sehr gross ist, können wir bei der Berechnung von der entstandenen Strömung von der Krümmung des Randes von A wegsehen und ein Randelement der Platte A als geradlinig ansehen; wir betrachten also den Strömungszustand am Rande von zwei parallelen Platten A_1 und B_1, wenn in der Platte A_1 ein Temperaturgefälle auf einer Stelle, R, vorhanden ist (vgl. Fig. 2).

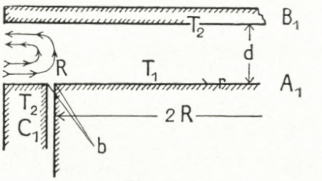

Fig. 2.

[1] T_1 und T_2 sind die Temperaturen von der Gasschicht an der Oberfläche der Kupferplatten; bei grösserer Dichte sind sie dieselben wie von den Kupferplatten selbst. (Vgl. pag. 28, Fussnote 1).

Nennen wir die Strömungsgeschwindigkeit w, so erhalten wir ein Geschwindigkeitsdiagram, wie in der Zeich-

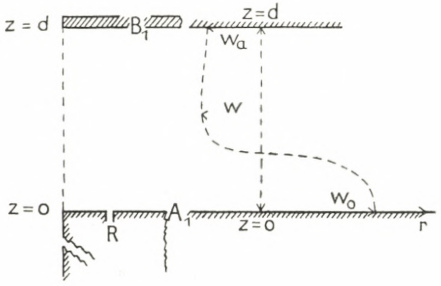

Fig. 3.

nung, Fig. 3, angegeben, mit der Bedingung, wenn der Abstand zwischen den Platten, d, ist, dass:

$$d \cdot \int_0^d w \cdot dz = 0 . \qquad \text{(IV)}$$

Für diese laminare Strömung haben wir nach Lamb[1], wenn η die innere Reibung und p der Druck des Gases sind:

$$\eta \cdot \frac{d^2 w}{dz^2} = \frac{dp}{dr},$$

oder nach Integration:

$$w = A_0 + B_0 z + C_0 z^2 \quad \text{mit} \quad C_0 = \frac{1}{2\eta} \cdot \frac{dp}{dr}.$$

Berücksichtigen wir die Gleitung des strömenden Gases bei den Oberflächen von A_I und B_I, erhalten wir die folgenden Grenzbedingungen:

$$w_0 - k_2 \cdot \gamma_M \cdot \left(\frac{dw}{dz}\right)_{z=0} = \frac{3}{4} \cdot k_1 \cdot \frac{\eta}{\varrho \cdot T} \cdot \frac{dT}{dr} \cdot \frac{1}{1 + \frac{\lambda}{d}} = c_1, \qquad \text{(V)}$$

[1] H. Lamb: Hydrodynamics, Cambridge 1906, p. 542.

und weil kein Temperaturgradient in der Platte B vorhanden ist:

$$w_a + k_2 \cdot \gamma_M \cdot \left(\frac{dw}{dz}\right)_{z=d} = 0, \quad \text{wo} \quad \gamma_M = \sqrt{\frac{\pi}{2}} \cdot \frac{\eta}{p\sqrt{{}_1\varrho}}. \qquad \text{(VI)}$$

In diesen Ausdrücken sind k_1 und k_2 Konstanten, die einander gleich sind und unabhängig von den Eigenschaften und Temperatur des Gases; $\varrho = {}_1\varrho_0 \cdot p \cdot \frac{273{,}1}{T}$ ist die Dichte des Gases, während nach S. Chapman[1]:

$$p \cdot \lambda = \frac{1}{0{,}499} \sqrt{\frac{\pi}{8}} \cdot \frac{\eta_0}{\sqrt{{}_1\varrho_0}} \left(\frac{T}{T_0}\right)^{1+n},$$

oder praktisch gesprochen:

$$p \cdot \lambda = \sqrt{\frac{\pi}{2}} \cdot \frac{\eta_0}{\sqrt{{}_1\varrho_0}} \left(\frac{T}{273{,}1}\right)^{1+n} = {}_1\lambda = {}_1\lambda_0 \left(\frac{T}{273{,}1}\right)^{1+n}$$

weil

$$\frac{\eta}{\eta_0} = \left(\frac{T}{T_0}\right)^{\frac{1}{2}+n}.$$

Hierzu kommt also die Bedingung (IV), dass die totale Gasmenge, welche durch den Rand zwischen $z = 0$ und $z = d$ strömt, gleich Null sein muss, woraus:

$$\int_0^d (A_0 + B_0 z + C_0 z^2)\, dz = 0.$$

Hieraus erhalten wir nach einfacher Umstaltung:

$$c_1 = \frac{1}{3} c_0 \cdot d \left(1 + 6 k_2 \cdot \frac{\gamma_M}{d}\right)$$

oder:

$$\frac{dp}{dr} = \frac{9}{2} k_1 \frac{\eta^2}{{}_1\varrho \cdot p \cdot d^2 \left(1 + 6 k_2 \cdot \frac{\gamma_M}{d}\right)\left(1 + \frac{\lambda}{d}\right)} \frac{1}{T} \frac{dT}{dr} \qquad \text{(VII)}$$

[1] Vergl. J. H. Jeans: The dynamical Theory of Gases, 1925, p. 276.

woraus:

$$\frac{dp}{dT} = \frac{1}{2} \cdot \frac{p}{T} \cdot \frac{1}{\frac{\pi}{18 k_1}\left(\frac{d}{{}_1\lambda}\right)^2 \cdot p^2 + \frac{\pi}{3 k_1}\left(k_2 + \frac{1}{6}\right)\left(\frac{d}{{}_1\lambda}\right) p + \frac{\pi}{3}\frac{k_2}{k_1}}. \quad \text{(VIII)}$$

Die analoge Formel für die thermomolekulare Druckdifferenz war[1]:

$$\frac{dp}{dT} = \frac{1}{2} \cdot \frac{p}{T} \cdot \frac{1}{\frac{\pi}{24 k_1}\left(\frac{R}{{}_1\lambda}\right)^2 \cdot p^2 + \frac{\pi}{6 k_1}\left(k_2 + \frac{1}{4}\right)\left(\frac{R}{{}_1\lambda}\right) p + \frac{\pi}{6}\frac{k_2}{k_1}}.$$

Nach Vergleichung mit den Experimenten wurden $k_1 = k_2 =$ ca. $\frac{4}{3}$ und $\frac{\pi}{6} \cdot \frac{k_2}{k_1} = \mu =$ ca. 1,25 gefunden, so dass die numerische Übereinstimmung für den Wert von μ nicht befriedigend ist; es ist also auch nicht zu erwarten, dass dies der Fall für den Wert von $\frac{\pi}{3}\frac{k_2}{k_1} = \mu_1 = 2\mu$ in der Formel (VIII) sein wird. Vorläufig werden wir die Formel (VIII) schreiben:

$$\frac{dp}{dT} = \frac{1}{2} \cdot \frac{p}{T} \cdot \frac{1}{\alpha_1\left(\frac{d}{{}_1\lambda}\right)^2 \cdot p^2 + \beta_1\left(\frac{d}{{}_1\lambda}\right) \cdot p + \mu_1}, \quad \text{(IX)}$$

worin wir annehmen dürfen, dass α_1 und β_1 bekannt sind, und $\alpha_1 = \frac{\pi}{18 k_1} = \frac{\pi}{24}$, während $\beta_1 = \frac{\pi}{3 k_1}\left(k_2 + \frac{1}{6}\right) = \frac{3\pi}{8}$.

§ 5. Um die totale Radiometerkraft, K, zwischen den Platten A und B zu bestimmen, müssen wir durch Integration von (VIII) den Wert von p bestimmen; da in diesem Falle das Temperaturgefälle nur am Rande der Oberfläche, $O = \pi R^2$, liegt, und in der Platte A kein Temperaturgefälle vorkommt, dürfen wir annehmen, dass die

[1] Comm. Kamerlingh Onnes Lab., Leiden, No. 246[b], p. 7.

thermische Gleitströmung praktisch gesprochen nur am Rande der Platte A liegt, so dass der Druck p_1 zwischen A und B überall konstant ist, weil die Gleitströmung praktisch gesprochen, jedenfalls wenn der Abstand d klein ist, nicht zwischen den Platten A und B durchdringen wird; anders wäre es aber, wenn in der Platte A ein Temperaturgefälle von der Mitte bis zum Rande der Platte vorliegen würde (vgl. später § 11). In unserem Falle erhalten wir also, auch weil b sehr klein gegenüber R ist:

$$K_{\text{total}} = \pi R^2 (p_1 - p_2),$$

wo p_1 aus (VIII) bestimmt werden kann.

Wenn wir nur kleine Temperaturdifferenzen haben, und also nur kleine Druckunterschiede erhalten, können wir (VIII) schreiben:

$$\frac{dp}{dr} = M \cdot \frac{dT}{dr}.$$

Integrieren wir also über die Strecke, b, wo das ganze Temperaturgefälle liegt, und setzen wir in diesem Gebiet voraus, dass M als eine Konstante angesehen werden kann, so erhalten wir:

$$\frac{dp}{dT} = \frac{p_1 - p_2}{T_1 - T_2} = M$$

oder:

$$\frac{K_{\text{tot.}}}{\pi R^2} = K = p_1 - p_2 = \frac{1}{2T} \frac{T_1 - T_2}{\alpha_1 \left(\frac{d}{{}_1\lambda}\right)^2 \cdot p + \beta_1 \left(\frac{d}{{}_1\lambda}\right) + \mu_1 \cdot \frac{1}{p}}$$

oder:

$$\frac{K}{T_1 - T_2} = \frac{p_1 - p_2}{T_1 - T_2} = \frac{1}{2T} \cdot \frac{1}{\alpha_1 \left(\frac{d}{{}_1\lambda}\right)^2 \cdot p + \beta_1 \left(\frac{d}{{}_1\lambda}\right) + \mu_1 \cdot \frac{1}{p}}.$$

Wir ersehen hieraus, dass die Grösse $\frac{K}{T_1 - T_2}$ ein Maximun bei einem bestimmten Druck, $p_{\max}$, haben muss. Wir

finden leicht die Werte für die Lage und für die Grösse des Maximums:

$$p_{\max} = \frac{{}_1\lambda}{d}\sqrt{\frac{\mu_1}{\alpha_1}} \text{ und } \left(\frac{p_1 - p_2}{T_1 - T_2}\right)_{\max} = \frac{1}{2\,T}\cdot\frac{{}_1\lambda}{d}\cdot\frac{1}{2\sqrt{\mu_1\,\alpha_1} + \beta_1}. \quad \text{(X)}$$

Ausserdem haben wir auch für das Maximum: $p_{\max}\cdot\lambda_{\max} = {}_1\lambda$ und also:

$$\frac{d}{\lambda_{\max}} = \sqrt{\frac{\mu_1}{\alpha_1}} \quad \text{oder} \quad \lambda_{\max} = d\sqrt{\frac{\alpha_1}{\mu_1}}. \quad \text{(XI)}$$

In seinen experimentellen Versuchsreihen hat Martin Knudsen für bekannte Werte von p_2, dem Druck des Gases, die Werte von der abstossenden Radiometerkraft, K, sowohl für Wasserstoff als auch für Sauerstoff gemessen.

Nennen wir:

$$P' = 4\,T_2\cdot\frac{K}{T_1 - T_2},$$

haben wir aus Gleichung (IX)

$$P' = 4\,T_2\cdot\frac{p_1 - p_2}{T_1 - T_2} = \frac{2}{\alpha_1\left(\frac{d}{{}_1\lambda}\right)^2\cdot p + \beta_1\left(\frac{d}{{}_1\lambda}\right) + \mu_1\cdot\frac{1}{p}}.$$

Aus dem obenstehenden Wert von $\left(\frac{p_1 - p_2}{T_1 - T_2}\right)_{\max}$ erhalten wir:

$$P'_{\max} = 2\cdot\frac{{}_1\lambda}{d}\cdot\frac{1}{2\sqrt{\alpha_1\,\mu_1} + \beta_1};$$

woraus:

$$\frac{P'}{P'_{\max}} = \frac{2+\delta}{\frac{p}{p_{\max}} + \frac{p_{\max}}{p} + \delta} = \frac{2+\delta}{e^x + e^{-x} + \delta}, \quad \text{(XII)}$$

wo $\delta = \frac{\beta_1}{\sqrt{\mu_1\cdot\alpha_1}}$ und $ln\cdot x = \frac{p}{p_{\max}}$.

Wir ersehen hieraus, dass der Ausdruck für $\frac{P'}{P'_{\max}}$ im Bezug auf sein Maximum bei $x = 0$ symmetrisch ist, weil der Wert von $\frac{P'}{P'_{\max}}$ für $x = m$ und $x = -m$ derselbe ist.[1]

§ 6. Wir gehen nun dazu über das experimentelle Versuchsmaterial für das rationelle absolute Manometer zu betrachten; das einzigste vorliegende Material[2] ist eine ausgebreitete Versuchsreihe mit Wasserstoff und eine kleinere mit Sauerstoff (Martin Knudsen: Ann. d. Ph., Bd. 32, 1910, p. 831 u. w.); diese sind wiedergegeben in den Tabellen I und II; $T_1 - T_2$ ist die Temperaturdifferenz der Platten A und B; α der durch Spiegelablesung beobachtete Ausschlag in cm (ein Centimeter hat eine Veränderung des mittleren Abstandes der warmen und kalten Platte von 0.005 cm zu Folge).[3]

p_2 ist der mit MacLeod's Gauge gemessene Druck zuzüglich des Druckes der Quecksilberdämpfe und P' der aus der Formel:

$$K = \frac{P'}{4} \cdot \frac{T_1 - T_2}{T_2} \quad \text{oder} \quad P' = 4\,T_2 \cdot \frac{K}{T_1 - T_2}$$

berechnete Druck, wo K die gemessene Radiometerkraft per cm^2 bedeutet. In der vierten Kolonne der Tabelle ist $\log_{10} p_2$ angegeben und in Fig. 4 und Fig. 5 ist P' als Funk-

[1] Für die vollständige mathematische Behandlung, auch für den Fall, dass die Gleichung (VIII) integriert werden muss, verweise ich nach den Rapporten 6, 7 und 8 von dem 7. internationalen Kälte-Kongres 1936. (La Haye — Amsterdam, Juin 1936).

[2] Vgl.: E. Fredlund: Ann. d. Ph., Bd. 13, 1932, p. 802 und 808.

[3] Bei neuen Versuchsreihen würde man sich so einrichten, dass die Lage von B und also der Abstand zwischen A und B sich nicht änderte, z. B. durch eine kompensierende Torsionskraft; während der Messung würden also B und A genau parallel sein, und der Abstand konstant bleiben.

Tabelle 1.

Wasserstoff, H_2, Temperatur T_2 = ca. 22° C.

(Die Drücke sind in Dyn/cm² = Bar angegeben.)

$T_1 - T_2$	α	p_2	$\log_{10} p_2$	$P' = 4\,T_2 \cdot \frac{K}{T_1 - T_2}$	$\frac{P'}{P'_{max}}$	$\log_{10} \frac{p_2}{p_{2\,max}}$
46.1	0.40	2.60	0.415	2.57	0.01115	— 2.685
46.4	0.45	2.89	.461	2.87	0.01248	— 2.639
45.4	0.58	3.95	.597	3.78	0.01645	— 2.503
44.1	0.68	4.87	.688	4.57	0.01985	— 2.412
42.8	0.86	6.51	.814	5.95	0.02585	— 2.286
40.5	1.03	8.35	.922	7.53	0.03270	— 2.178
37.5	1.24	11.03	1.043	9.80	0.0425	— 2.057
31.4	1.40	15.5	1.190	13.2	0.0575	— 1.910
40.7	2.62	23.1	1.364	19.1	0.0830	— 1.736
13.9	0.88	23.5	1.371	19.2	0.0835	— 1.729
9.6	0.92	36.7	1.565	29.0	0.1260	— 1.535
6.6	0.84	52.0	1.716	38.0	0.1650	— 1.384
4.8	0.88	82	1.914	56	0.2435	— 1.186
4.3	0.87	83	1.919	55	0.2390	— 1.181
3.0	0.96	138	2.140	88	0.383	— 0.960
3.5	1.38	191	2.281	118	0.513	— 0.819
3.2	1.50	250	2.398	141	0.613	— 0.702
3.0	1.50	309	2.490	148	0.643	— 0.610
3.0	1.67	381	2.581	165	0.717	— 0.519
3.1	1.93	476	2.678	185	0.805	— 0.422
3.1	2.05	576	2.760	196	0.852	— 0.340
2.5	1.83	945	2.975	217	0.945	— 0.125
2.4	1.80	1366	3.136	222	0.966	+ 0.036
2.2	1.43	2185	3.340	242	1.050	+ 0.240
2.1	1.10	3353	3.526	155	0.675	+ 0.426
2.2	1.00	5016	3.700	135	0.587	+ 0.600
1.5	0.40	11706	4.070	79	0.343	+ 0.970

$P'_{max} = 230$, $\log_{10} p_{2,max} = 3.100$, $p_{2,max} = 1250$.

tion von $\log_{10} p_2$ graphisch dargestellt, bezw. für die Wasserstoff- und Sauerstoff-reihe. Wir ersehen hieraus, dass mit beiden Gasen eine symmetrische Kurve für grössere Werte von p_2 gefunden wird; leider ist die Anzahl von observier-

Tabelle 2.

Sauerstoff, O_2, Temperatur T_2 = ca. 22° C.

(Die Drücke sind in Dyn/cm² = Bar angegeben.)

$T_1 - T_2$	α	p_2	$\log_{10} p_2$	$P' = 4\,T_2 \cdot \frac{K}{T_1 - T_2}$	$\frac{P'}{P'_{max}}$	$\log_{10} \frac{p_2}{p_{2,max}}$
44.9	0.42	2.77	0.443	2.77	0.0425	— 2.107
40.7	0.46	3.56	0.551	3.55	0.0515	— 1.999
47.0	0.70	4.79	0.680	4.41	0.0680	— 1.870
41.3	0.77	6.47	0.811	5.52	0.0850	— 1.739
40.1	0.87	7.85	0.895	6.43	0.0990	— 1.655
38.5	1.05	10.52	1.022	8.08	0.1240	— 1.528
38.2	1.30	14.0	1.146	10.1	0.1555	— 1.404
33.1	1.56	21.1	1.324	14.0	0.216	— 1.226
27.4	1.65	28.2	1.449	17.8	0.274	— 1.101
21.4	1.82	43.9	1.643	25.2	0.388	— 0.907
16.6	2.22	84.0	1.924	39.6	0.610	— 0.626
10.4	1.98	139	2.143	56.4	0.868	— 0.407
8.0	1.85	603	2.780	69.0	1.061	+ 0.230
4.4	0.36	2013	3.304	24.0	0.369	+ 0.754
4.8	0.17	4921	3.633	14.3	0.218	+ 1.083

$P'_{max} = 65$, $\log_{10} p_{2,max} = 2.550$, $p_{2,max} = 355$.

ten Punkten bei den höheren Drücken nicht sehr zahlreich, wodurch die Grösse und die Lage des Maximums nicht so genau, wie zu erwünschen wäre, bestimmt werden können.

Wir erhalten aus den experimentellen Kurven (P', $\log_{10} p_2$):

für Wasserstoff: $p_{2,max} = 1250$ Bar; $P'_{max} = 230$,

für Sauerstoff: $p_{2\,max} = 355$ „ ; $P'_{max} = 65$,

woraus für H_2: $\frac{P'_{max}}{p_{2,max}} = 0.184$, und für O_2: $\frac{P'_{max}}{p_{2,max}} = 0.183^5$.

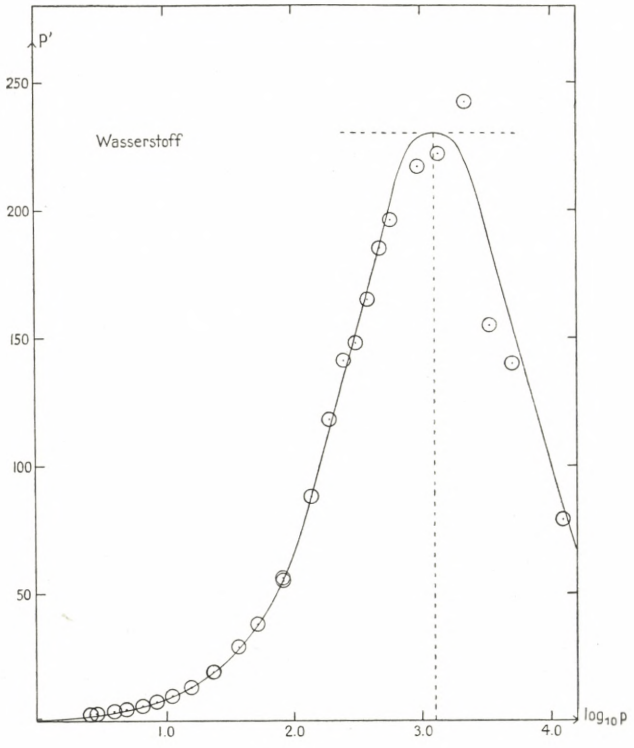
p'
250
200
150
100
50
Wasserstoff
1.0
2.0
3.0
4.0
log10p

Fig. 4.

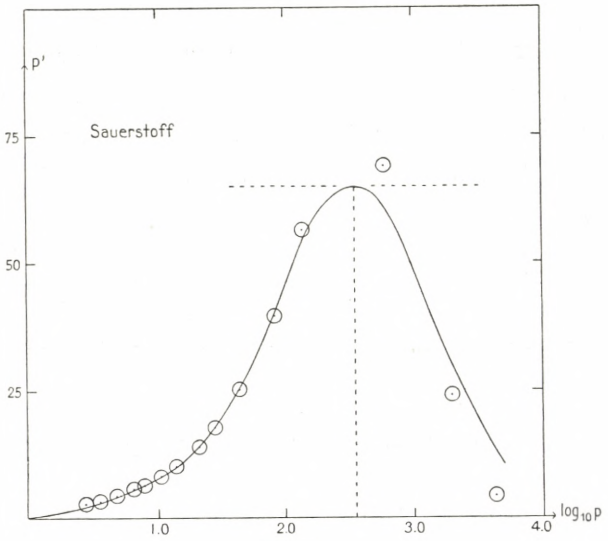
p'
75
50
25
Sauerstoff
1.0
2.0
3.0
4.0
log10p

Fig. 5.

Wir haben aber nach der obenstehenden Theorie:

$$p_{2,\max} = \frac{1}{d}\lambda \sqrt{\frac{\mu_1}{\alpha_1}}$$

und

$$P'_{\max} = 4\, T_2 \left(\frac{p_1 - p_2}{T_1 - T_2}\right)_{\max} = \frac{1}{d}\lambda \cdot \frac{1}{\sqrt{\mu_1 \alpha_1} + \frac{\beta_1}{2}},$$

woraus:

$$\frac{P'_{\max}}{p_{2,\max}} = 0.184 = \frac{1}{\mu_1 + \frac{1}{2}\beta_1 \sqrt{\frac{\mu_1}{\alpha_1}}}.$$

Mit:

$$\alpha_1 = \frac{\pi}{18 k_1} = \frac{\pi}{24} = 0.1309 \text{ und } \beta_1 = \frac{3\pi}{8} = 1.1781$$

finden wir hieraus $\mu_1 = 2.70$, also praktisch gesprochen den Wert von $2\mu = 2 \cdot 1.25 = 2.50$, den wir erwarten müssten nach dem Resultat, das wir für die thermomolekulare Druckdifferenz gefunden haben; bei dem absoluten Manometer haben wir also dieselbe Unübereinstimmung zwischen Theorie und Experiment wie in der thermomolekularen Druckdifferenz.[1]

Aus den Werten für α_1 und μ_1 können wir den mittleren Plattenabstand, d, für die Wasserstoffserie bestimmen und erhalten:

[1] Die Ursache der Unübereinstimmung zwischen dem experimentellen und theoretischen Wert von μ muss ohne Zweifel darin gesucht werden, dass der verwendete Ausdruck:

$$A = \frac{1}{1 + \varphi\left(\frac{\lambda}{d}\right)} = \frac{1}{1 + q \cdot \frac{\lambda}{d}}, \text{ mit } q = 1.$$

in dem Gebiet $\frac{d}{\lambda} \to \infty$ nur eine grobe Annäherung für den Faktor A in der Maxwell'schen Grenzbedingung (III) gibt; für $\frac{d}{\lambda} \to 0$ muss $q = 1$ sein; um aber Übereinstimmung zwischen $\mu_{\text{theor.}}$ und $\mu_{\text{beob.}}$ für $\frac{d}{\lambda} \to \infty$ zu erhalten, musste $q =$ ca. 2 sein (Vgl. Sophus Weber: Comm. Kamerlingh Onnes Lab., Leiden, No. 246b, p. 7 und auch Martin Knudsen und Sophus Weber: Ann. d. Ph. 1911, Bd. 36, p. 981).

$$d_{H_2} = \lambda'_{max} \sqrt{\frac{\mu_1}{\alpha_1}} = \frac{11.32}{1250} \sqrt{\frac{\mu_1}{\alpha_1}} = 0.041 \text{ cm},$$

während wir in derselben Weise für die Sauerstoffreihe finden:

$$d_{O_2} = \lambda''_{max} \sqrt{\frac{\mu_1}{\alpha_1}} = \frac{6.36}{355} \sqrt{\frac{\mu_1}{\alpha_1}} = 0.081 \text{ cm}.$$

Diese Abstände, die leider nicht in den Versuchsreihen während der Messung bestimmt sind, und vielleicht auch nicht in derselben Messungsreihe ganz konstant gewesen sind, werden aber von der richtigen Grössenordnung sein (vgl. M. Kn. loc. cit. p. 834); bei neuen Messungen ist diese Abstandsmessung während des Versuches von grösster Bedeutung; bei den Abständen, bezw. 0.041 cm und 0.081 cm, ist aber zu erwarten, dass die Bestimmungen bei grösserer Dichte, besonders in der Sauerstoffreihe, etwas von Konvektionsströmungen beeinflüsst sein können; der letzte Punkt, bezw. die letzten Punkte, der Sauerstoffreihe sind wahrscheinlich nicht ganz frei von diesem Einfluss.

§ 7. Wenn wir die obengefundenen Werte für $p_{2,\,max}$ und P'_{max} für die Wasserstoff- und Sauerstoffreihe als Einheiten für die gemessenen Werte von p_2 und P' nehmen, können wir die »reducierten« Werte von $\frac{P'}{P'_{max}}$ als Funktion von $\log_{10} \frac{p_2}{p_{2,\,max}}$ darstellen und erhalten hierdurch eine reducierte Kurve; diese Werte sind angegeben in den Kolonnen 6 und 7 von den Tabellen. Wenn die Messungen und die Theorie richtig sind, müssen diese reducierten Punkte liegen auf der theoretischen »reducierten« Kurve, nämlich:

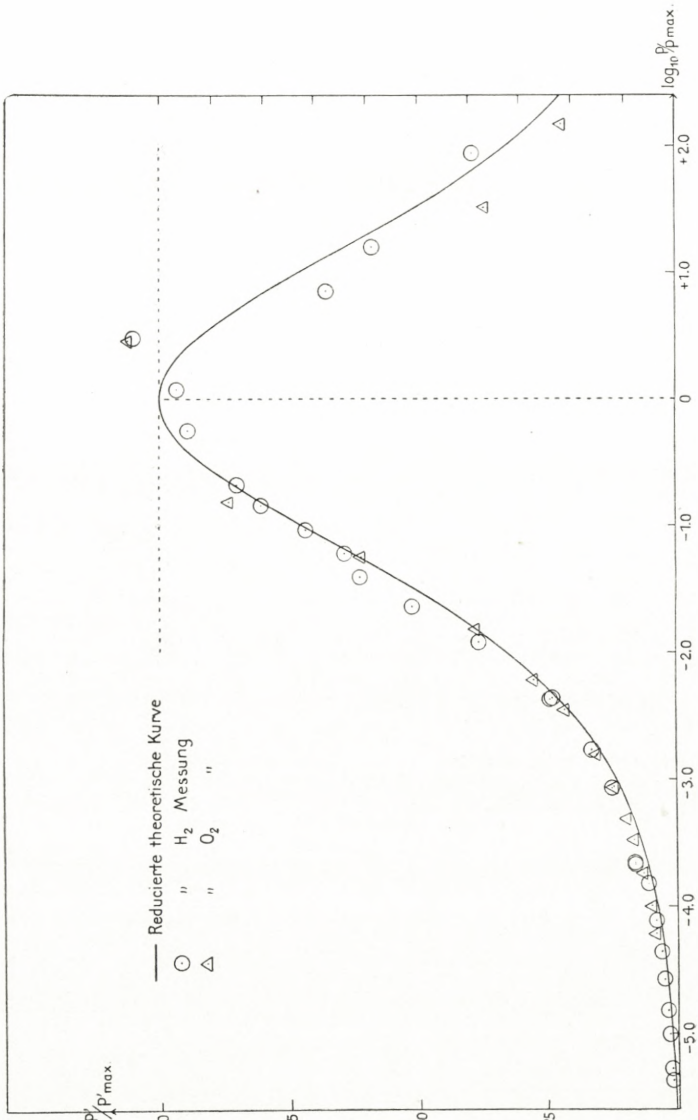
p'/p'max.
1.00
0.75
0.50
0.25
Reducierte theoretische Kurve
H2 Messung
O2 "
-5.0
-4.0
-3.0
-2.0
-1.0
0
+1.0
+2.0
log10 p'/p'max.

Fig. 6.

$$\frac{P'}{P'_{\max}} = \frac{2+\delta}{e^x + e^{-x} + \delta} = \frac{2+\delta}{\frac{p_2}{p_{2,\max}} + \frac{p_{2,\max}}{p_2} + \delta},$$

wo $x = ln \frac{p_2}{p_{2,\max}}$ und $\delta = \frac{\beta_1}{\sqrt{\mu_1 \alpha_1}} = 1.983.$

Diese reducierte theoretische Kurve, welche unabhängig von dem Abstand, d, zwischen den Platten A und B wird, ist in Fig. 6 eingezeichnet[1] (die gezogene Kurve), während die gemessenen reducierten Wasserstoffpunkte (Kreis mit Punkt) und die gemessenen reducierten Sauerstoffpunkte (Dreieck mit Punkt) eingetragen sind.

Wenn die Genauigkeit, womit diese experimentellen Bestimmungen ausgeführt sind, in Betracht gezogen wird, ist die Übereinstimmung befriedigend und eine Stütze für die entwickelte Theorie; die vorliegenden Abweichungen bei den niedrigen Drücken sind dadurch zu erklären, dass μ_1 bei den niedrigen Drücken keine Konstante bleibt, sondern kleiner wird. Um die Grenzbedingung für $\frac{d}{\lambda} \to 0$ zu befriedigen, muss μ_1 zwischen $\mu_1 = 2$ für $\frac{d}{\lambda} \gtreqless 0$ und $\mu_1 = 2{,}70$ für $\frac{d}{\lambda} \gtreqless \infty$ variieren.

Die einfachste Interpolationsformel für diesen Fall ist:

$$\mu_1 = 2 \cdot \frac{1 + m \cdot \frac{d}{\lambda}}{1 + n \cdot \frac{d}{\lambda}}, \text{ mit } 2 \cdot \frac{m}{n} = 2.70 = \mu_{1,\infty}.$$

Die Abweichungen bei den grösseren Drücken sind wohl entweder durch einsetzende Konvektionsströmungen — be-

[1] Einfachkeitshalber haben wir nicht $ln \frac{p_2}{p_{2,\max}}$, sondern $\log_{10} \frac{p_2}{p_{2,\max}}$ als Abscisse verwendet.

sonders in der Sauerstoffreihe — zu erklären, oder vielleicht auch dadurch, dass der Abstand zwischen den Platten A und B sich während der Versuchsreihe etwas geändert hat; dies wäre wohl möglich, weil für die drehbare Platte ein Platinaufhängungsdraht und kein Quarzdraht gebraucht wurde; im Allgemeinen muss aber festgestellt werden, dass die zwei Versuchsreihen eine befriedigende Bestätigung von der entwickelten Theorie geben.

§ 8. Wie bereits oben erwähnt, befriedigt die Formel:

$$\frac{dp}{p} = \frac{1}{2}\frac{dT}{T}\frac{1}{\mu_1 + \beta_1\left(\frac{d}{\lambda}\right) + \alpha_1\left(\frac{d}{\lambda}\right)^2}$$

nicht die Grenzbedingung für $\frac{d}{\lambda} \doteq 0$, weil wir in diesem Falle die Grenzformel:

$$K = p_1 - p_2 = \frac{1}{4}\cdot p_2 \frac{T_1 - T_2}{T_2}, \quad \text{oder} \quad \frac{dp}{p} = \frac{1}{4}\cdot\frac{dT}{T}$$

erhalten müssen; wir verwenden am einfachsten, wie oben erwähnt, in diesem Falle die Interpolationsformel:

$$\mu_1 = 2\frac{1 + m\cdot\frac{d}{\lambda}}{1 + n\cdot\frac{d}{\lambda}}, \quad \text{mit} \quad \frac{m}{n} = \frac{1}{2}\mu_{1,\infty} = 1.35$$

und erhalten hierdurch aus Formel (VIII) für $\frac{d}{\lambda} \to 0$:

$$\frac{dp}{p} = \frac{1}{2}\cdot\frac{dT}{T}\frac{1}{2\left[1 + (m-n)\right]\cdot\frac{d}{\lambda} + \beta_1\frac{d}{\lambda}} =$$

$$= \frac{1}{4}\cdot\frac{dT}{T}\frac{1}{1 + \left(m - n + \frac{1}{2}\beta_1\right)\frac{d}{\lambda}}.$$

Es wird nun, weil β_1 und $\frac{m}{n}$ bekannt sind, von Interesse zu untersuchen, ob man durch theoretische Überlegungen den Faktor, $m-n+\frac{1}{2}\beta_1$, bestimmen kann; dieses ist bereits annäherungsweise ausgeführt von P. Debye[1], der laut seiner angenäherten Berechnung fand:

$$K = \frac{1}{2} p_2 \left\{ \sqrt{\frac{T_1}{T_0}} - 1 \right\} \frac{1}{1+\left(\frac{T_0}{T_1}\right)^2 \left(e^{\frac{d}{\lambda}} - 1\right)},$$

oder in erster Annäherung und für kleine Temperaturunterschiede:

$$K = \frac{1}{4} \cdot \frac{p}{T} \frac{\Delta T}{1+\frac{d}{\lambda}\left(1-2\frac{\Delta T}{T}\right)+\cdots} = \frac{1}{4} \cdot \frac{p}{T} \cdot \frac{\Delta T}{1+\frac{d}{\lambda}}.$$

Hieraus würde folgen, dass $m-n+\frac{1}{2}\beta_1 =$ ca. 1; es ist aber möglich die Berechnung mit etwas grösserer Annäherung, als von Debye verwendet, durchzuführen; wir finden hierdurch:

$$m-n+\frac{1}{2}\beta_1 = \frac{3}{4}.$$

§ 9. Betrachten wir zu diesem Zweck (Fig. 7) zwei grosse planparallele Platten A und B mit dem Abstand, d, und den Temperaturen T_1 und T_2; der Abstand, d, ist sehr klein im Vergleich mit den Abmessungen der Platten; wir setzen weiter voraus, dass die Platten A und B sich befinden in einem unendlich grossen Behalter, in welchem die Anzahl der Moleküle in der Raumeinheit N, der Druck p_2 und die Temperatur T_2 sind. Einfachkeitshalber neh-

[1] P. Debye: Phys. Zeitschrift 32, p. 809, 1910.

men wir an, dass der Akkommodationskoefficient a des Gases gegenüber den Platten A und B ist: $a = 1$. Wir werden nun zuerst den stationären KNUDSEN-Zustand untersuchen; in diesem Falle ist $\frac{d}{\lambda} = 0$. Ein Element dS von der Platte B empfängt eine totale Bewegungsmenge, M, in der Richtung der Normale; ein Teil, M_1, dieser Bewegungsmenge rührt von den einfallenden Molekülen her und diese kommen alle direkt von der Platte A; ein anderer Teil der

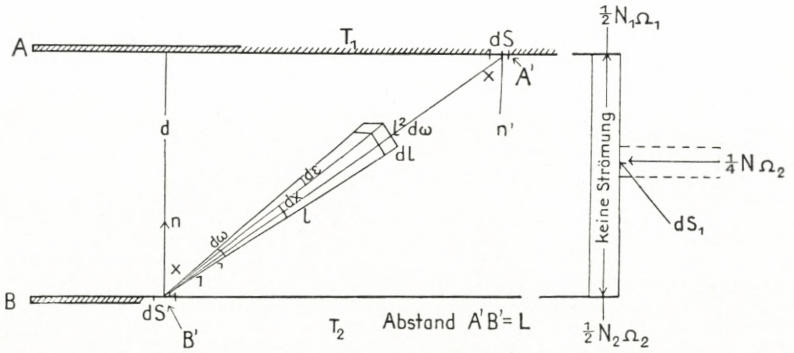

Fig. 7.

Bewegungsmenge, M_2, empfängt dS dadurch, dass die einfallenden Moleküle von dem Element dS nach dem Cosinusgesetz und mit der mittleren Geschwindigkeit Ω_2 zurückgeworfen werden; ausserdem empfängt die andere Seite des Elementes, dS, von dem Aussenraum eine Bewegungsmenge, M_3.

Verwenden wir die Terminologie von KNUDSEN und TER HEERDT[1], dann erhalten wir, wenn in der Raumeinheit zwischen den Platten N_1 Moleküle mit der Geschwindigkeit, Ω_1, und Richtung von der Platte A hinweg, und N_2 Moleküle mit der Geschwindigkeit, Ω_2, und Richtung von

[1] MARTIN KNUDSEN: Ann. d. Ph., Bd. 28, 1909, p. 103 und J. H. A. TER HEERDT: Dissertation, Utrecht, 1923.

der Platte B hinweg, sich befinden, dass die totale Bewegungsmenge, welche das Element dS von beiden Seiten empfängt, wird $M_1 + M_2 + M_3$, wo:

$$M_1 = \int \frac{1}{2\pi} \cdot N_1 \Omega_1 \cos x \, d\omega \cdot m \Omega_1 \cdot \cos x$$

$$M_2 = \int \frac{1}{2\pi} \cdot N_2 \Omega_2 \cos x \, d\omega \cdot m \Omega_2 \cdot \cos x$$

$$M_3 = -\int \frac{1}{2\pi} \cdot N \Omega_2 \cos x \, d\omega \cdot m \Omega_2 \cdot \cos x .$$

Weil $d\omega = \sin x \, dx \, d\varepsilon$ und $p_2 = \frac{1}{3} mN \overline{\Omega}_2^2$, wird:

$$M_1 + M_2 + M_3 = \text{die Radiometerkraft } K =$$
$$= \frac{1}{3} mN_1 \overline{\Omega}_1^2 + \frac{1}{3} mN_2 \overline{\Omega}_2^2 - \frac{1}{3} mN \overline{\Omega}_2^2 .$$

Betrachten wir ein Randelement, dS_1, erhalten wir in dem stationären Zustand, dass die Gleichgewichtsbedingung für den Massentransport gibt:

$$\frac{1}{2} \cdot N_1 \Omega_1 = \frac{1}{2} \cdot N_2 \Omega_2 = \frac{1}{4} \cdot N \Omega_2 .$$

Wir finden hieraus:

$$K = \frac{1}{3} mN_2 \overline{\Omega}_2^2 \left(\frac{\Omega_1}{\Omega_2} - 1 \right) = \frac{1}{2} \cdot p_2 \left(\sqrt{\frac{T_1}{T_2}} - 1 \right),$$

also die bekannte Formel von Martin Knudsen für das absolute Manometer, wenn $\frac{d}{\lambda} = 0$ ist.

Wenn die Dichte des Gases zwischen den Platten A und B so gross wird, dass die Zusammenstösse zwischen den Molekülen einsetzen, erreichen also nicht alle Moleküle, die von der Platte A ausgehen, die Platte B ohne Zusam-

menstoss gelitten zu haben; nennen wir die mittlere freie Weglänge von den Molekülen der Gruppe N_1, λ_1, wird die Anzahl, n_1, die zwischen den Platten Zusammenstoss gelitten haben:

$$\int dn_1 = \int \frac{1}{2\pi} N_1 \Omega_1 \left(1 - e^{-\frac{L}{\lambda_1}}\right) \cos x \, d\omega, \quad \text{wo} \quad L = \frac{d}{\cos x}.$$

Die Korrektion, die hierdurch für die obengenannte Bewegungsmenge, M_1, entsteht, wird also:

$$dM_1 = \int (-dn_1 \cdot m \Omega_1 \cos x + dn_1 \cdot m \Omega_x \cos x)$$

oder, wenn $\frac{d}{\lambda_1} \to 0$:

$$dM_1 = -\frac{1}{2\pi} N_1 \Omega_1 \cdot m (\Omega_1 - \Omega_x)$$

$$\cdot \frac{d}{\lambda_1} \int \left(\cos x \sin x - \frac{1}{2} \frac{d}{\lambda_1} \sin x \ldots\right) dx \, d\varepsilon$$

$$= -\frac{1}{2} N_1 \Omega_1 \cdot m (\Omega_1 - \Omega_x) \frac{d}{\lambda_1} \left(1 - \frac{d}{\lambda_1} \cdots\right).$$

In derselben Weise finden wir, wenn wir ein Element dS' in der Platte A betrachten, und wenn M_1' die Bewegungsmenge bezeichnet, die dS' von den einfallenden Molekülen der Gruppe, N_2, empfängt, dass die Korrektion für die Bewegungsmenge M_1' wird:

$$dM_1' = \frac{1}{2} N_2 \Omega_2 \cdot m (\Omega_2 - \Omega_x) \frac{d}{\lambda_2} \left(1 - \frac{d}{\lambda_2} + \cdots\right).$$

Hieraus erhalten wir, weil in dem stationären Zustand $dM_1 - dM_1' = 0$ und weil $\lambda_1 = \lambda_2$, welches z. B. sehr leicht aus dem Ausdruck für die mittleren freien Weglängen in diffundierenden Gasen gesehen wird:

$$N_1 \Omega_1 (\Omega_1 - \Omega_x) + N_2 \Omega_2 (\Omega_2 - \Omega_x) = 0,$$

woraus:

$$\Omega_x = \frac{N_1 \Omega_1^2 + N_2 \Omega_2^2}{N_1 \Omega_1 + N_2 \Omega_2}$$

und also die Korrektion für die Radiometerkraft, K:

$$dK = -\frac{1}{2} m \cdot N_1 \Omega_1 (\Omega_1 - \Omega_x) \frac{d}{\lambda} \left(1 - \frac{d}{\lambda} \cdots\right).$$

Wenn wir sehr dicht in der Nähe von der Grenzbedingung $K = \frac{1}{2} p \left(\sqrt{\frac{T_1}{T_2}} - 1\right)$ sind, dann können wir in dem Ausdruck für die Korrektion dK als Annäherung die Grenzbedingung für $\frac{d}{\lambda} = 0$, $N_1 \Omega_1 = N_2 \Omega_2$, einsetzen und erhalten hieraus:

$$\Omega_x = \frac{1}{2} (\Omega_1 + \Omega_2)^{1}$$

[1] In diesem Falle kann man also die Gasmasse zwischen den Platten auffassen als eine Gasmasse mit der Temperatur T_x und mit N_x Molekülen pr. cm^3. T_x ist bestimmt durch:

$$\Omega_x = \frac{1}{2} (\Omega_1 + \Omega_2),$$

oder:

$$\sqrt{T_x} = \frac{1}{2} (\sqrt{T_1} + \sqrt{T_2}).$$

Betrachten wir ein Randelement, dS_1, zwischen den Platten, so muss in dem Grenzzustand $\frac{d}{\lambda} \rightarrow 0$ die Gleichgewichtsbedingung sein:

$$\frac{1}{4} N_x \Omega_x = \frac{1}{4} N \Omega_2,$$

woraus

$$\frac{p_x}{p_2} = \frac{\Omega_x}{\Omega_2} = \frac{1}{2} \left(\sqrt{\frac{T_1}{T_2}} + 1\right)$$

oder

$$K = p_x - p_2 = \frac{1}{2} \cdot p_2 \left(\sqrt{\frac{T_1}{T_2}} - 1\right),$$

in Übereinstimmung mit der Formel von Knudsen.

und

$$dK = -\frac{1}{2} m \cdot N_2 \Omega_2 \left(\frac{\Omega_1}{2} - \frac{\Omega_2}{2}\right) \cdot \frac{d}{\lambda}\left(1 - \frac{d}{\lambda} + \cdots\right)$$

$$= -\frac{3}{8} p_2 \left(\sqrt{\frac{T_1}{T_2}} - 1\right) \cdot \frac{d}{\lambda}\left(1 - \frac{d}{\lambda} + \cdots\right).$$

Wir erhalten hieraus für die Radiometerkraft K':

$$K' = K + dK = \frac{1}{2} p_2 \left(\sqrt{\frac{T_1}{T_2}} - 1\right)\left[1 - \frac{3}{4}\frac{d}{\lambda} + \frac{3}{4}\left(\frac{d}{\lambda}\right)^2 \cdots\right]$$

oder in erster Annäherung:

$$K' = \frac{1}{2} p_2 \left(\sqrt{\frac{T_1}{T_2}} - 1\right) \frac{1}{1 + \frac{3}{4} \cdot \frac{d}{\lambda}}.$$

Diesen Ausdruck können wir durch die Präcisionsmessungen von Martin Knudsen[1] für das absolute Manometer nachprüfen; wir sehen in der Tabelle 3 in der ersten Kolonne den wahren und gemessenen Wert des Druckes, p, und in der zweiten Kolonne den Wert p', berechnet aus den gemessenen Werten von K durch die Formel:

$$K = \frac{1}{2} p' \left(\sqrt{\frac{T_1}{T_2}} - 1\right), \qquad \text{(b)}$$

während wir den Wert p'' in Kolonne 3 berechneten aus:

$$K = \frac{1}{2} p'' \left(\sqrt{\frac{T_1}{T_2}} - 1\right) \frac{1}{1 + \frac{3}{4} \cdot \frac{d}{\lambda}}, \qquad \text{(a)}$$

wo K die gemessene Radiometerkraft per cm^2 bezeichnet.

Wir ersehen hieraus, dass die in dieser Weise theoretisch abgeleitete Radiometerkraft in befriedigender Übereinstim-

[1] Martin Knudsen: Ann. d. Ph., Bd. 32, 1910, p. 835.

Tabelle 3.

Der Abstand zwischen den Platten in den Versuchsreihen: $d = 0.07$ cm.

Wahrer Wert für p	berechnet nach Formel (b)	berechnet nach Formel (a)
Versuch Nr. 1. Wasserstoff. $p\lambda = 11.5$.[1]		
$p =$ 2.46 Bar.	$p' =$ 2.46 Bar.	$p'' =$ 2.46 Bar.
4.88 —	4.86 —	4.95 —
6.23 —	6.25 —	6.38 —
8.54 —	8.37 —	8.65 —
10.58 —	9.95 —	10.40 —
11.74 —	11.11 —	11.70 —
Versuch Nr. 2. Sauerstoff. $p\lambda = 6.45$.		
$p =$ 2.45 Bar.	$p' =$ 2.45 Bar.	$p'' =$ 2.45 Bar.
4.80 —	4.70 —	4.88 —
7.13 —	6.74 —	7.13 —
8.97 —	8.24 —	8.84 —
11.25 —	9.92 —	10.82 —
11.70 —	10.21 —	11.18 —
Versuch Nr. 3. Kohlensäure. $p\lambda = 4.0$.		
$p =$ 2.33 Bar.	$p' =$ 2.33 Bar.	$p'' =$ 2.33 Bar.
3.74 —	3.63 —	3.79 —
6.09 —	5.78 —	6.20 —
7.93 —	7.24 —	7.96 —
9.31 —	8.23 —	9.24 —
10.68 —	9.13 —	10.41 —

mung mit der experimentellen Untersuchung von Knudsen ist, und dass hierdurch die Abhängigkeit des absoluten Manometers von dem benutzten Gase in der Nähe der

[1] Hier wird verwendet die mittlere Weglänge nach S. Chapman; die Änderung von λ mit der Temperatur kann in dieser Berechnung vernachlässigt werden, jedenfalls wenn T_1 und T_2 nur wenig verschieden sind.

Grenzbedingung bekannt ist, so dass unter Umständen das »absolute« Manometer in einem grösseren Druckgebiet verwendet werden kann. Wenn der Akkommodationskoeffizient für die Innenseite der zwei Platten A und B verschieden von $a = 1$ ist, muss dieses in bekannter Weise berücksichtigt werden.[1]

Aus den Werten $2\frac{m}{n} = \mu_{1,\infty} = 2.70$ und $m - n - \frac{1}{2}\beta_1 = \frac{3}{4}$ erhalten wir für die Formel (IX):

$$\frac{dp}{dT} = \frac{1}{2} \cdot \frac{p}{T} \cdot \frac{1}{2 \cdot \dfrac{1+0.621\,\dfrac{d}{\lambda}}{1+0.460\,\dfrac{d}{\lambda}} + 1.1781\,\frac{d}{\lambda} + 0.1309\left(\frac{d}{\lambda}\right)^2}$$

oder für kleine Temperaturdifferenzen in erster Annäherung:

$$p_2 = 4\,T_2\,\frac{K}{T_1 - T_2}\left\{\frac{1+0.621\,\dfrac{d}{\lambda}}{1+0.460\,\dfrac{d}{\lambda}} + 0.589\,\frac{d}{\lambda} + 0.0655\left(\frac{d}{\lambda}\right)^2\right\}$$

worin, $K = p_1 - p_2$, die gemessene Radiometerkraft per cm^2 ist; dieser Ausdruck für p_2 ist leider nicht explizit, weil p_2 auch in λ eingeht, und die Gleichung kann also nur durch sukzessive Annäherungen gelöst werden.

Die Messungsreihen von Martin Knudsen mit Wasserstoff und Sauerstoff, Tabelle 1 und 2, sind mit dieser Formel in befriedigender Übereinstimmung, wenn für Wasserstoff $d = 0.041$ cm und für Sauerstoff $d = 0.081$ cm verwendet werden; bei niedrigen Drücken sind aber die berechneten Werte aus der Formel etwas zu gross, weil in diesen Versuchsreihen mit einer Mischung von Gas und Quecksilberdampf gearbeitet ist, wodurch der Wert von λ nicht so ganz

[1] E. Fredlund: Ann. d. Ph., Bd. 13, 1932, p. 802, Ann. d. Phys., Bd. 14, 1932, p. 617.

gut bekannt ist; dieses ist auch die Erklärung dafür, dass diese Messungsreihen in dem niedrigen Druckgebiet nicht ganz in Übereinstimmung sind mit den späteren, oben benutzten Präcisionsmessungen von Knudsen, in welchen der Quecksilberdampf ausgefroren war; es wäre aber sehr wünschenswert neue Versuchsreihen, worin alle Dämpfe ausgefroren wurden, zu unternehmen, und worin die Aufmerksamkeit besonders auf die Abstandsmessung zwischen den Platten gelenkt wurde, bezw. diese Versuche so einzurichten, dass der Abstand, d, während der Versuchen konstant gehalten wurde (System Brüche und Littwin).

§ 10. Aus dem vorhergehenden geht deutlich die grosse Analogie zwischen dem absoluten Manometer von Knudsen und der thermomolekularen Druckdifferenz hervor, und dass diese Erscheinungen von analogen Formeln beherrscht werden; dasselbe ist auch der Fall für andere Radiometer und Radiometererscheinungen, wenn diese so eingerichtet sind, dass die physikalischen Zustände in dem Versuch hinreichend festgelegt sind und so eingerichtet, dass der entstehende Strömungszustand übersehen werden kann. In dem folgenden werde ich noch kurz ein Paar von den bekannten Radiometerausführungen besprechen und besonders das Flügelradiometer oder Einplattenradiometer im Wärmestrom.

Die angemessene rationelle Ausführung von diesem Radiometer ist m. E. von E. Brüche und W. Littwin[1] angegeben; in dieser Untersuchung war ein kleiner Radiometer-flügel oder -platte, F, drehend aufgehängt zwischen zwei grossen parallelen Platten, W und K, mit den Temperaturen T_1 und T_2; die auf der Platte, F, ausgeübte

[1] E. Brüche und W. Littwin: Z. f. Ph., Bd. 67, 1931, p. 333. — Vgl. auch: E. Fredlund, loc. cit.

Radiometerkraft wurde kompensiert durch eine bekannte Torsionskraft, so dass die Platte, F, ihre Lage zwischen W und K und also ihre Abstände von W und K nicht änderte; ausserdem war der Radiometerflügel, F, in einigen von den Versuchen von einem Schutzring, S, umgeben; der Apparat ist in Fig. 8 zu sehen. Wir können annehmen, dass die Platte F gut wärmeleitend ist, so dass die zwei Seiten dieser dünnen Platte dieselbe Temperatur haben, oder jedenfalls nur eine ganz kleine Temperaturdifferenz. Weiter nehmen wir an, in Übereinstimmung mit den Versuchen, dass der Akkommodationskoefficient für alle Oberflächen derselbe ist.

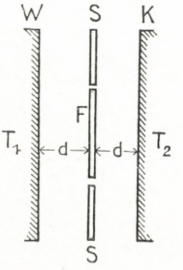

Fig. 8.

Es stellte sich in dieser Untersuchung experimentell heraus, dass der Einfluss von dem Schutzring des drehbaren Flügels F sehr klein war, und dass die Messresultate mit und ohne Schutzring praktisch gesprochen dieselben waren, woraus folgt, dass die thermische Gleitströmung zwischen F und W und zwischen F und K mit und ohne Schutzring praktisch gesprochen dieselben waren. Wir können also auch für das Einplattenradiometer im Wärmestrom die oben entwickelte Theorie für das absolute Manometer verwenden. Nennen wir die Temperaturen der zwei Seiten von F für X und Y, so erhalten wir für $\frac{d}{\lambda} \geqq 0$:

$$K = K_1 + K_2 = \frac{p_2}{4} \cdot \frac{T_1 - Y}{T_2} + \frac{p_2}{4} \frac{X - T_2}{T_2}$$
$$= \frac{p_2}{4} \left\{ \frac{T_1 - T_2}{T_2} - \frac{Y - X}{T_2} \right\}.$$

Da wir laut der Experimente bei allen Drücken des Gases $Y = X$ setzen können, werden wir also für die Radiometerkraft in dem ganzen Gebiet, $0 \leqq \frac{d}{\lambda} \leqq \infty$, schreiben können:

$$\frac{K}{T_1 - T_2} = \frac{K_1 + K_2}{T_1 - T_2} = \frac{1}{2} \cdot \frac{p_2}{T_2} \cdot \frac{1}{\mu_1 + \beta_1 \left(\frac{d}{\lambda}\right) + \alpha_1 \left(\frac{d}{\lambda}\right)^2}$$

in Übereinstimmung mit dem absoluten Manometer, wo α_1 und β_1 bekannte Konstanten sind, während μ_1 eine bekannte Funktion von $\frac{d}{\lambda}$ ist.

Brüche und Littwin haben mit verschiedenen Gasen eine grosse Menge Messungen im ganzen Druckgebiet ausgeführt und besonders die Grösse, R_{max}, und die Lage, λ_{max}, des Maximums untersucht; sie haben die erhaltenen Resultate für alle Gase in der Radiometergleichung:

$$2 \cdot \frac{R_{max}}{R} = \frac{\lambda}{\lambda_{max}} + \frac{\lambda_{max}}{\lambda},$$

zusammengefasst.

Diese Gleichung kann auch geschrieben werden:

$$\frac{R}{R_{max}} = \frac{2}{\frac{\lambda}{\lambda_{max}} + \frac{\lambda_{max}}{\lambda}}.$$

Die Übereinstimmung mit meiner Formel (XII):

$$\frac{R}{R_{max}} = \frac{P'}{P'_{max}} = \frac{2 + \delta}{\frac{p}{p_{max}} + \frac{p_{max}}{p} + \delta}, \text{ worin } \delta = \frac{\beta_1}{\sqrt{\mu_1 \alpha_1}} = 1.983,$$

welche für das absolute Manometer abgeleitet ist, ist in diesem Falle einleuchtend; für $\delta = 0$ geht Gleichung (XII) in die von Littwin und Brüche gefundene Gleichung über. Leider haben B. & L. die Temperaturdifferenz zwischen den Platten K und W nicht direkt und während den Versuchen gemessen; dieses hat aber P. Schmudde[1] in seiner Arbeit

[1] P. Schmudde: Z. f. Ph., Bd. 53, 1929, p. 331.

gemacht, aber in dieser Untersuchung hat die Platte, F, ihre Lage geändert, weil die Radiometerkraft nicht kompensiert wurde.

Brüche und Littwin haben mit den folgenden Gasen: He, Ne, Ar, Kr, H_2, O_2, N_2, CO_2 und CH_4, gearbeitet, und die Lage, p_{max}, von der maximalen Radiometerkraft, R_{max}, experimentell bestimmt. Aus der Formel:

$$p_{max} \cdot \lambda_{max} = \sqrt{\frac{\pi}{2}} \cdot \frac{\eta_0}{\sqrt{{}_1\varrho_0}} \left(\frac{T}{273.1}\right)^{1+n} = {}_1\lambda$$

können die Werte von λ_{max} für die gefundenen Werte von p_{max} berechnet werden, und es stellte sich heraus:

Dass für alle Gase das Maximum des Radiometereffektes gerade dann auftritt, wenn die freie Weglänge die bestimmte Grösse, λ'_{max} = konstant, erreicht hat; dieses ist in Übereinstimmung damit, dass wir gefunden haben:

$$p_{max} = \frac{{}_1\lambda}{d} \sqrt{\frac{\mu_1}{\alpha_1}}; \text{ wo aber } p_{max} \cdot \lambda_{max} = {}_1\lambda,$$

erhalten wir für alle Gase mit $\mu_1 = 2.70$ und $\alpha_1 = 0.1309$:

$$\lambda_{max} = d \sqrt{\frac{\alpha_1}{\mu_1}} \quad \text{oder} \quad \frac{d}{\lambda_{max}} = \sqrt{\frac{\mu_1}{\alpha_1}} = 4.54,$$

unabhängig von den Eigenschaften des Gases.[1]

B. & L. fanden für den Abstand $WF = WK = d$ und für alle Gase:

1) $d' = 9.5$ mm, $\lambda'_{max} = 1.9$ mm (Platin blank)
2) $d' = 9.5$ mm, $\lambda'_{max} = 1.9$ mm (Platin schwarz)
3) $d'' = 2.0$ mm, $\lambda''_{max} = 0.5$ mm (Platin blank),

[1] Wenn man die Variation von μ_1 mit $\frac{d}{\lambda}$ in Betracht zieht, wird $\frac{d}{\lambda_{max}} =$ ca. 4.35.

woraus $\frac{d'}{\lambda'_{max}} = 5.0$ und $\frac{d''}{\lambda''_{max}} = 4.0$, oder im Mittel: $\frac{d}{\lambda_{max}} =$ $= \text{ca. } 4.5$, in befriedigender Übereinstimmung[1] mit unserem theoretischen Resultat.

Bei den meisten vorliegenden experimentellen Untersuchungen über das Flügelradiometer kann man aber nicht eine so befriedigende Übereinstimmung erwarten, weil diese Messungen durch die weniger gut definierten Verhältnisse der umgebenden und begrenzenden Oberflächen so beeinflüsst sind, dass die mathematische Behandlung von den bei grösserer Dichte entstehenden Strömungen nicht durchzuführen ist.

§ 11. In § 4 haben wir bei der Berechnung von dem Strömungszustande am Rande der Platte A angenommen, dass die entstehende thermische Gleitströmung nicht zwischen den Platten A und B durchdringt, weil der Temperaturunterschied, $T_1 - T_2$, nur am Rande der Platte A in dem absoluten Manometer liegt; in dem Falle der Knudsen'schen Konstruktion in der rationellen Ausführung wird dieses auch richtig sein, wenn der Abstand zwischen den Platten A und B hinreichend klein ist; experimentell könnte dieses durch gleichzeitige Messung von der Radiometerkraft, K, und von dem Abstand, d, zwischen den Platten untersucht werden, weil man dann die gemessene und berechnete Radiometerkraft mit einander vergleichen könnte.

[1] Vgl. auch Ernst Fredlund: Ann. d. Ph., Bd. 13, 1937, p. 808. Fredlund findet mit einem ähnlichen Radiometer in Wärmestrom für Wasserstoff:

$$\frac{\lambda_{max}}{L} = 0.13,$$

wo $L = 2d$;

also:

$$\frac{d}{\lambda_{max}} = \frac{L}{2\lambda_{max}} = \text{ca. } 4.$$

Für atm. Luft und CO_2 wurde $\frac{d}{\lambda_{max}} = \text{ca. } 2{,}8$ gefunden.

Leider sind die vorliegenden Messungen nicht hinreichend genau um dieses zu tun, und es ist darum nicht ohne Interesse ganz kurz zu überlegen, wie die Formel für die Radiometerkraft, K, sich gestalten würde, wenn der Temperaturunterschied $T_1 - T_2$ nicht am Rande liegt, sondern in der Platte A, z. B. dadurch, dass das Centrum, O, der Platte die Temperatur, T_1, hat, während die Temperatur am Rande, T_2, ist; in diesem Falle wird die Gleitströmung bei der Platte A vom Rande bis zum Centrum, O, durchdringen, während das einströmende Gas bei der Platte B in entgegengesetzter Richtung zurückströmen wird. Der Strömungszustand wird von dem Temperaturgradienten in der Platte A abhängig werden; einfachkeitshalber nehmen wir an, dass die Temperaturverteilung in der Platte A eine symmetrische, parabolische Temperaturverteilung wird (vgl. Fig. 9) und also geschrieben werden kann:

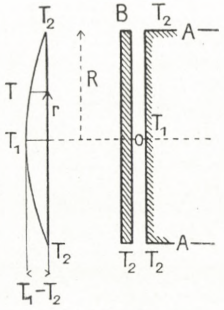

Fig. 9.

$$T = T_1 - \frac{r^2}{R^2}(T_1 - T_2), \quad \text{wo} \quad T_1 > T_2,$$

oder:

$$\frac{dT}{dr} = -2\frac{r}{R^2}(T_1 - T_2).$$

Um den Druckverlauf zwischen den Platten zu bestimmen, können wir wieder die Formel (VII), weil keiner Temperaturgradient in der Platte B anwesend ist, verwenden und erhalten also:

$$\frac{dp}{dr} = \frac{9}{2} \cdot k_1 \cdot \frac{\eta^2}{p \cdot {}_1\varrho \cdot d^2 \left(1 + 6k_2 \frac{\gamma_M}{d}\right)\left(1 + \frac{\lambda}{d}\right)} \cdot \frac{1}{T} \cdot \frac{dT}{dr}$$

$$= E \cdot \frac{1}{p} \cdot \frac{dT}{dr}.$$

Für kleine Temperaturunterschiede und also kleine Druckdifferenzen erhalten wir hieraus:

$$p - p_2 = E \cdot \frac{1}{\bar{p}} (T_1 - T_2) \left(1 - \frac{r^2}{R^2}\right); \quad \bar{p} = \frac{1}{2}(p + p_2)$$

und also für die totale Radiometerkraft der Platte A mit der Oberfläche, πR^2:

$$K_1' = \int_0^R (p - p_2)\, 2\pi r dr = \frac{E}{\bar{p}} (T_1 - T_2) \frac{1}{2} \cdot \pi R^2,$$

oder:

$$K_1' = \frac{9}{4} k_1 \frac{\eta^2}{{}_1\varrho \cdot \bar{p} \cdot d^2 \left(1 + 6 k_2 \cdot \frac{\gamma_M}{d}\right)\left(1 + \frac{\lambda}{d}\right)} \cdot \frac{\pi R^2}{T} (T_1 - T_2).^1$$

Vergleichen wir diese Formel für K_1' mit dem Ausdruck für $\frac{dp}{dr}$, bezw. K, in § 4 (Formel VII), dann sehen wir, dass:

$$K_1' = \frac{1}{2} K,$$

also genau die Hälfte von dem Werte, den wir gefunden haben, wenn der ganze Temperaturunterschied am Rande der Platte liegt; ob die wahre Temperaturverteilung in der Platte A nicht genau unserer parabolischen Formel folgt, wird wahrscheinlich keinen grossen Einfluss haben.

In diesem Falle wird die vollständige Formel für die Radiometerkraft per cm^2 und per Grad Celsius, K_1, sein:

$$K_1 = \frac{1}{\pi R^2} \cdot \frac{K_1'}{T_1 - T_2} = \frac{p_1 - p_2}{T_1 - T_2} = \frac{1}{4 T_2} \cdot \frac{1}{\alpha_1 \left(\frac{d}{{}_1\lambda}\right)^2 \cdot p + \beta_1 \left(\frac{d}{{}_1\lambda}\right) + \mu_1 \cdot \frac{1}{p}}$$

[1] Dieser Ausdruck ist in Übereinstimmung mit dem Ausdruck, den Fanselau in anderer Weise berechnet hat (G. Fanselau: Dissertation, Berlin, 1927, p. 21).

oder

$$K_1 = \frac{1}{2\,T_2} \cdot \frac{1}{2\,\alpha_1 \left(\frac{d}{{}_1\lambda}\right)^2 \cdot p + 2\,\beta_1 \left(\frac{d}{{}_1\lambda}\right) + 2\,\mu_1 \cdot \frac{1}{p}}.$$

Die Grösse und die Lage des Maximums sind also bestimmt durch:

$$p_{\max} = \frac{{}_1\lambda}{d}\sqrt{\frac{2\,\mu_1}{2\,\alpha_1}} \text{ und } P''_{\max} = 4\,T_2\left(\frac{p_1 - p_2}{T_1 - T_2}\right)_{\max} = \frac{{}_1\lambda}{d}\frac{1}{2\sqrt{\mu_1\,\alpha_1} + \beta_1}.$$

Würde man diese Formel verwenden für die vorliegenden Observationsreihen für Wasserstoff und Sauerstoff von Martin Knudsen, so würde man hieraus den Wert, $\mu_1 = 1.055$, finden, wodurch also $\delta = \frac{\beta_1}{\sqrt{\alpha_1 \mu_1}}$ etwas grösser sein würde.

Die Abstände zwischen den Platten d_{H_2} und d_{O_2} würden bezw. 0.026 und 0.052 werden, während die Relation: $\frac{d}{\lambda_{\max}} = \sqrt{\frac{\mu_1}{\alpha_1}} = 2.85$, wird; dieser Wert ist aber nicht in Übereinstimmung mit den Versuchen von Brüche und Littwin.

Wir ersehen hieraus, dass eine gleichzeitige Messung von der Radiometerkraft, K, und dem Abstand, d, bei bekannter Temperaturdifferenz, $T_1 - T_2$, und Druck p_2 nach Vergleichung mit dem berechneten Ausdruck für die Kraft, K, eventuell angeben könnte, in wiefern die entstandene thermische Gleitströmung zwischen den Platten durchdringen würde.

§ 12. G. Hettner[1] hat in einer interessanten Arbeit sein Zweiplattenradiometer beschrieben; dies ist in der Weise konstruiert, dass es ein einfaches, aber hochempfindliches

[1] G. Hettner: Z. f. Ph., Bd. 47, 1928, p. 499.

Messinstrument für Wärmestrahlung geworden ist; das Zweiplattenradiometer von Hettner ist im Grunde genommen dasselbe Instrument wie das absolute Manometer von Martin Knudsen, nur mit dem Unterschiede, dass der Temperaturgradient in der Hettner'schen Konstruktion in der beweglichen Platte B liegt; dieser Temperaturgradient wird erzeugt durch Strahlung, und umgekehrt kann also das Radiometer für Strahlungsmessung verwendet werden; weil der Temperaturgradient nicht am Rande der Platte liegt, sondern in der Platte, B, selbst, werden die theoretischen Betrachtungen in § 11 für diesen Fall gelten und die Grösse der Radiometerkraft, K, wird also, wenn $\frac{d}{\lambda} \rightarrow \infty$:

$$K_1 = \frac{9}{4} k_1 \cdot \frac{\eta^2}{\varrho T} \cdot \frac{\pi R^2}{d^2} \Delta T,$$

wo $\Delta T = T_1 - T_2$ ist.

Weil der Temperaturgradient aber in der beweglichen Platte, welche eine dünne, kreisförmige Scheibe mit Radius R war, liegt, wird zu der Kraft, K_1, ausserdem die gewöhnliche Radiometerkraft, K', für eine kreisförmige Scheibe o h n e Gegenplatte hinzukommen; diese Kraft ist für $\frac{d}{\lambda} \rightarrow \infty$ nach Epstein[1]:

$$K' = k_1 \cdot 3\pi \frac{\eta^2}{\varrho T} \Delta T,$$

so dass die totale Radiometerkraft wird:

$$K = K_1 + K' = \frac{9}{4} k_1 \cdot \frac{\eta^2}{\varrho T} \cdot \frac{\pi R^2}{d^2} \Delta T + k_1 \cdot 3\pi \cdot \frac{\eta^2}{\varrho T} \Delta T,$$

woraus:

[1] Paul S. Epstein: Z. f. Ph., Bd. 54, 1929, p. 537.

$$K = 3\pi k_1 \cdot \frac{\eta^2}{\varrho T}\left[\frac{3}{4}\frac{R^2}{d^2}+1\right]\cdot \Delta T,$$

oder genau die Formel, welche G. FANSELAU[1] abgeleitet hat.

Ist, d, gegenüber, R, klein, kann der Einfluss von dem Glied K' vernachlässigt werden; in diesem Falle ist die Änderung von K mit $\frac{d}{\lambda}$ durch die Berechnung in § 11 gegeben und wird also dieselbe wie für das absolute Manometer sein; die grösste Empfindlichkeit für das Zweiplattenradiometer wird man also erhalten, wenn:

$$\frac{d}{\lambda} = \sqrt{\frac{\mu_1}{\alpha_1}} = \text{ca. } 4.3.$$

HETTNER hat in seinen Versuchen, in welchen das verwendete Zweiplattenradiometer mit Atm. Luft gefüllt war, gefunden, dass die maximale Empfindlichkeit bei dem Druck, p_{max} = ca. 0.2 mm Hg, erreicht wurde.

Für Atm. Luft ist $p\lambda = 6.5$, und also für p = ca. 0.2 mm Hg = ca. 265 Bar, λ_{max} = ca. 0.024 cm; hieraus würde erfolgen, dass der Abstand, d, in dem HETTNER-schen Versuch war, $d = 4.3 \cdot 0.024$ cm = ca. 0.1 cm; dies ist in guter Übereinstimmung mit der Angabe von HETTNER, dass der Abstand, d, von der Grössenordnung 0.5 bis 1 mm war.

Aus der in § 11 abgeleiteten Formel für die Änderung von K mit $\frac{d}{\lambda}$ geht hervor, dass die maximale Empfindlichkeit, P''_{max}, des HETTNER'schen Messinstrument verdoppelt wird, wenn Wasserstofffüllung verwendet wird;

[1] G. FANSELAU, loc. cit., p. 21.

mit Heliumfüllung wird die maximale Empfindlichkeit für dasselbe Instrument dreimal so gross werden.

Der Direktion des Dänischen Carlsbergfonds bin ich für gewährte Stütze sehr zu Dank verpflichtet; in einer folgenden Abhandlung beabsichtige ich einige andere Typen von dem Radiometer und insbesondere die photophoretischen Erscheinungen näher zu untersuchen.

Færdig fra Trykkeriet den 30. Juni 1937.

Det Kgl. Danske Videnskabernes Selskab.
Mathematisk-fysiske Meddelelser. **XIV**, 14.

ÜBER DIE URSPRÜNGLICHE BAHN DES KOMETEN 1863 VI

VON

HANS Q. RASMUSEN

KØBENHAVN
LEVIN & MUNKSGAARD
EJNAR MUNKSGAARD
1937

Printed in Denmark.
Bianco Lunos Bogtrykkeri A/S.

Für diesen Kometen hat P. G. Rosén[1] mit Hilfe von 191 über 185 Tage verteilten Beobachtungen, unter Rücksicht auf die Störungen seitens Venus, Erde, Mars, Jupiter und Saturn, eine definitive Bahnrechnung ausgeführt. Seine Elemente lauten:

Oskulationsepoche 1863 Oktober 25.0 Berlin M. Z.

$T =$ 1863 Dezember 29.203772 Berlin M. Z.

$$\left.\begin{aligned} \omega &= 78^\circ\ 5'54''.77 \\ \Omega &= 105\ \ 1\ 23.60 \\ i &= 83\ 19\ 17.28 \end{aligned}\right\} 1863.0$$

$\log q =$ 0.1183045 $\pm$ 0.0000031

$e =$ 1.0006499 $\pm$ 0.0000650

Auf das Normaläquinoktium 1950.0 und auf M. Z. Greenwich bezogen lauten diese Elemente:

Oskulationsepoche 1863 Oktober 25.0 G. M. Z.

$T =$ 1863 Dezember 29.166562 G. M. Z.

$$\left.\begin{aligned} \omega &= 78^\circ\ 6'33''.13 \\ \Omega &= 106\ 14\ 11.52 \\ i &= 83\ 19\ \ 2.46 \end{aligned}\right\} 1950.0$$

$q =$ 1.313120 $\pm$ 0.000009

$e =$ 1.0006499 $\pm$ 0.0000650

$\frac{1}{a} =$ $-$ 0.0004949 $\pm$ 0.0000495

$$\left.\begin{aligned} P_x &= -0.1669438 & Q_x &= +0.2505822 \\ P_y &= -0.2344136 & Q_y &= -0.9495204 \\ P_z &= +0.9576952 & Q_z &= -0.1887315 \end{aligned}\right\} 1950.0$$

[1] Komet VI 1863. Upsala 1866 (Dissertation).

Mit diesen Elementen ergaben sich für das Oskulationsdatum 1863 Okt. 25.0 die folgenden Koordinaten und Geschwindigkeitskomponenten:

$$x = -0.4882349 \qquad 10\frac{dx}{dt} = +0.0290051$$

$$y = +0.9827145 \qquad 10\frac{dy}{dt} = -0.1824501$$

$$z = +1.1999962 \qquad 10\frac{dz}{dt} = +0.0477639$$

Ausgehend von diesen Koordinaten und Geschwindigkeitskomponenten habe ich durch numerische Integration die auf 1950.0 bezogenen heliozentrischen, rechtwinkligen Äquatorkoordinaten des Kometen, unter Rücksicht auf die Anziehung seitens Sonne, Merkur, Venus, Erde, Mars, Jupiter und Saturn, bis zu 1844 rückwärtsgerechnet. Diese Koordinaten sind in der folgenden Tafel gegeben:

G. M. Z.	x	y	z
1863 Nov. 10.5 ...	−0.435 573	+0.672 729	+1.266 306
Okt. 31.5 ...	0.468 657	0.862 705	1.229 223
— 21.5 ...	0.498 183	1.046 157	1.182 784
— 11.5 ...	0.524 462	1.222 810	1.128 618
— 1.5 ...	0.547 819	1.392 666	1.068 144
Sept. 21.5 ...	0.568 563	1.555 901	1.002 568
— 11.5 ...	0.586 987	1.712 798	0.932 891
— 1.5 ...	0.603 354	1.863 699	0.859 934
Aug. 22.5 ...	0.617 894	2.008 966	0.784 368
— 12.5 ...	0.630 812	2.148 968	0.706 737
— 2.5 ...	0.642 287	2.284 059	0.627 486
Juli 23.5 ...	0.652 474	2.414 576	0.546 972
— 13.5 ...	0.661 509	2.540 833	0.465 490
— 3.5 ...	0.669 510	2.663 123	0.383 277
Juni 23.5 ...	−0.676 579	+2.781 714	+0.300 530

G. M. Z.	x	y	z
1863 Juni 13.5 ...	−0.682 808	+2.896 851	+0.217 407
— 3.5 ...	0.688 275	3.008 762	0.134 041
Mai 24.5 ...	0.693 050	3.117 651	+0.050 538
— 14.5 ...	0.697 195	3.223 708	−0.033 011
— 4.5 ...	0.700 764	3.327 105	0.116 535
Apr. 24.5 ...	0.703 805	3.428 000	0.199 971
— 14.5 ...	0.706 362	3.526 540	0.283 271
— 4.5 ...	0.708 473	3.622 855	0.366 393
März 10.5 ...	0.712 017	3.854 697	0.573 211
Febr. 13.5 ...	0.713 431	4.075 047	0.778 334
Jan. 19.5 ...	0.713 067	4.285 274	0.981 537
1862 Dez. 25.5 ...	0.711 201	4.486 512	1.182 689
Nov. 30.5 ...	0.708 057	4.679 715	1.381 728
— 5.5 ...	0.703 813	4.865 685	1.578 638
Okt. 11.5 ...	0.698 617	5.045 110	1.773 426
Sept. 16.5 ...	0.692 592	5.218 579	1.966 124
Aug. 22.5 ...	0.685 839	5.386 601	2.156 773
Juli 28.5 ...	0.678 445	5.549 623	2.345 421
Juli 3.5 ...	0.670 483	5.708 033	2.532 123
Juni 8.5 ...	0.662 015	5.862 177	2.716 932
Apr. 19.5 ...	0.643 769	6.158 850	3.081 104
Febr. 28.5 ...	0.624 058	6.441 712	3.438 381
Jan. 9.5 ...	0.603 151	6.712 430	3.789 190
1861 Nov. 20.5 ...	0.581 255	6.972 373	4.133 928
Okt. 1.5 ...	0.558 536	7.222 678	4.472 964
Aug. 12.5 ...	0.535 125	7.464 300	4.806 632
Juni 23.5 ...	0.511 131	7.698 049	5.135 243
Mai 4.5 ...	0.486 641	7.924 620	5.459 079
März 15.5 ...	0.461 729	8.144 614	5.778 397
Jan. 24.5 ...	0.436 456	8.358 553	6.093 435
1860 Dez. 5.5 ...	0.410 873	8.566 897	6.404 410
Okt. 16.5 ...	0.385 024	8.770 049	6.711 522
Juli 8.5 ...	0.332 674	9.162 176	7.314 878
März 30.5 ...	−0.279 650	+9.537 367	−7.904 816

G. M. Z.	x	y	z
1859 Dez. 21.5 ...	−0.226 139	+9.897 594	−8.482 460
Sept. 12.5 ...	0.172 285	10.244 476	9.048 787
Juni 4.5 ...	0.118 204	10.579 361	9.604 647
Febr. 24.5 ...	0.063 992	10.903 390	10.150 786
1858 Nov. 16.5 ...	−0.009 725	11.217 535	10.687 861
Aug. 8.5 ...	+0.044 530	11.522 634	11.216 458
Apr. 30.5 ...	0.098 716	11.819 416	11.737 097
Jan. 20.5 ...	0.152 788	12.108 522	12.250 245
1857 Okt. 12.5 ...	0.206 703	12.390 517	12.756 320
Juli 4.5 ...	0.260 428	12.665 907	13.255 704
1856 Dez. 16.5 ...	0.367 204	13.198 633	14.235 732
Mai 30.5 ...	0.472 957	13.709 814	15.192 725
1855 Nov. 12.5 ...	0.577 615	14.202 016	16.128 689
Apr. 26.5 ...	0.681 176	14.677 376	17.045 331
1854 Okt. 8.5 ...	0.783 696	15.137 680	17.944 129
März 22.5 ...	0.885 266	15.584 423	18.826 372
1853 Sept. 3.5 ...	0.986 000	16.018 863	19.693 205
Febr. 15.5 ...	1.086 014	16.442 055	20.545 650
1852 Juli 30.5 ...	1.185 422	16.854 890	21.384 625
Jan. 12.5 ...	1.284 322	17.258 123	22.210 963
1851 Juni 26.5 ...	1.382 797	17.652 399	23.025 421
1850 Dez. 8.5 ...	1.480 910	18.038 269	23.828 688
Mai 22.5 ...	1.578 702	18.416 209	24.621 396
1849 Nov. 3.5 ...	1.676 194	18.786 631	25.404 125
Apr. 17.5 ...	1.773 382	19.149 899	26.177 405
1848 Sept. 29.5 ...	1.870 236	19.506 335	26.941 725
März 13.5 ...	1.966 704	19.856 237	27.697 531
1847 Aug. 26.5 ...	2.062 707	20.199 880	28.445 231
Febr. 7.5 ...	2.158 145	20.537 541	29.185 192
1846 Juli 22.5 ...	2.252 908	20.869 496	29.917 740
Jan. 3.5 ...	2.346 881	21.196 043	30.643 162
1845 Juni 17.5 ...	2.439 964	21.517 494	31.361 709
Nov. 29.5 ...	2.532 090	21.834 177	32.073 599
1844 Mai 13.5 ...	+2.623 232	+22.146 429	−32.779 022

Für 1845 Juni 17.5 wurden aus dieser Tafel die folgenden Koordinaten und Geschwindigkeitskomponenten $\left(x, y, z, \frac{dx}{dt}, \frac{dy}{dt}, \frac{dz}{dt}\right)$, ferner die Reduktionen auf den Schwerpunkt des Systems Sonne-Jupiter-Saturn $\left(\xi, \eta, \zeta, \frac{d\xi}{dt}, \frac{d\eta}{dt}, \frac{d\zeta}{dt}\right)$ und die reduzierten Koordinaten und Geschwindigkeitskomponenten $\left(\bar{x}, \bar{y}, \bar{z}, \frac{d\bar{x}}{dt}, \frac{d\bar{y}}{dt}, \frac{d\bar{z}}{dt}\right)$ berechnet (für die Bezeichnungen vgl. z. B. die Publikation des Kopenhagener Observatoriums Nr. 98: E. Strömgren und H. Q. Rasmusen, Über die ursprüngliche Bahn des Kometen 1907 I Giacobini):

$x = +2.439964$	$y = +21.517494$	$z = -31.361709$
$\xi = -\quad 6298$	$\eta = -\quad 76$	$\zeta = +\quad 130$
$\bar{x} = +2.433666$	$\bar{y} = +21.517418$	$\bar{z} = -31.361579$

$100\,\frac{dx}{dt} = -0.0463064$	$100\,\frac{dy}{dt} = -0.1595058$
$100\,\frac{d\xi}{dt} = +\quad 2101$	$100\,\frac{d\eta}{dt} = -\quad 7344$
$100\,\frac{d\bar{x}}{dt} = -0.0460963$	$100\,\frac{d\bar{y}}{dt} = -0.1602402$

$$100\,\frac{dz}{dt} = +0.3575922$$
$$100\,\frac{d\zeta}{dt} = -\quad 3167$$
$$100\,\frac{d\bar{z}}{dt} = +0.3572755$$

Mit diesen numerischen Werten wurden die Grösse $\bar{r} = \sqrt{\bar{x}^2 + \bar{y}^2 + \bar{z}^2}$ und das Quadrat der Geschwindigkeit $\bar{V}^2_{100} = \left(100\,\frac{d\bar{x}}{dt}\right)^2 + \left(100\,\frac{d\bar{y}}{dt}\right)^2 + \left(100\,\frac{d\bar{z}}{dt}\right)^2$ berechnet.

Das Integral der lebendigen Kraft lautet:

$$\bar{V}^2_w = w^2 k^2 (1 + \Sigma m)\left(\frac{2}{\bar{r}} - \frac{1}{\bar{a}}\right),$$

woraus:

$$\frac{1}{\bar{a}} = \frac{2}{\bar{r}} - \frac{\bar{V}_w^2}{w^2 k^2 (1 + \Sigma m)},$$

wo wir $w = 100$ und $1 + \Sigma m = 1.00124646$ (= der Gesamtmasse von Sonne, Merkur, Venus, Erde, Mars, Jupiter und Saturn) zu setzen haben.

Wir erhalten dann für 1845 Juni 17.5 den folgenden Wert des Bahnelementes $\frac{1}{a}$:

$$\frac{1}{\bar{a}} = +0.0000116.$$

Die ausgeprägt hyperbolische Bahn $\left(\frac{1}{a} = -0.0004949\right)$ ist also in eine schwach elliptische $\left(\frac{1}{\bar{a}} = +0.0000116\right)$ verwandelt worden. Die Hinzuziehung der Störungen seitens Uranus und Neptun hätte aller Wahrscheinlichkeit nach die Elliptizität noch etwas verstärkt. Der aus unserer Untersuchung hervorgegangene elliptische Wert des inversen Wertes der »ursprünglichen« grossen Halbachse der Bahn liegt dem parabolischen Wert sehr nahe, und er ist kleiner als der aus der definitiven Bahnrechnung hervorgegangene mittlere Fehler des in der Nähe der Perihelzeit oskulierenden $\frac{1}{a}$; das Resultat der Untersuchung ist jedoch, dass die Hyperbolizität auch in dem jetzt vorliegenden Fall sich als illusorisch erwiesen hat.

Für pekuniäre Unterstützung bin ich dem Carlsbergfond zu grossem Dank verpflichtet.

1936, November.

Hans Q. Rasmusen

Færdig fra Trykkeriet den 11. Juni 1937.

Det Kgl. Danske Videnskabernes Selskab.
Mathematisk-fysiske Meddelelser. **XIV**, 15.

ENZYMIC HYDROLYSIS OF GLUCOSIDES

II. HYDROLYSIS OF PROPYL- AND ISOPROPYL-β-d-GLUCOSIDES AND SOME CONSIDERATIONS ON THE MECHANISM OF THE ENZYMIC HYDROLYSIS OF β-GLUCOSIDES

BY

STIG VEIBEL AND FRANCISKA ERIKSEN

KØBENHAVN
LEVIN & MUNKSGAARD
EJNAR MUNKSGAARD
1937

Printed in Denmark.
Bianco Lunos Bogtrykkeri A/S.

In a previous paper (VEIBEL and ERIKSEN, 1936, 2) we examined the enzymic hydrolysis of methyl- and ethyl-β-d-glucosides. We determined the hydrolysis constants and the affinity constants at 30° and at 20° as well as the inhibiting effect of the products of hydrolysis.

In the present paper the hydrolysis of propyl- and isopropyl-β-d-glucosides is examined in the same way, and the corresponding constants are determined. Below we are presenting the experimental material calculated in the same way as we have used in the previous paper in order to allow a comparison of the hydrolysis of the four glucosides examined.

This comparison shows that both the affinity constants and the hydrolysis constants differ considerably for the four glucosides, but that no proportionality exists between affinity constant and hydrolysis constant, the latter having been referred to unity of emulsin in the solution.

As the affinity constants are not the same for the different glucosides it would perhaps be more correct to refer the hydrolysis constants not to the amount of emulsin present in the solution, but to the amount of emulsin bound to the glucoside. We have recalculated the hydrolysis constants on this assumption and have found that, for each glucoside, the hydrolysis constant is inversely proportional to the concentration of the glucoside, at all events at the beginning of the hydrolysis. As pointed out in the previous paper (l. c. p. 15) the decrease in the reaction constants towards the end of the reactions may be ascribed to the inhibiting

action of the products of hydrolysis, attached to part of the emulsin, thus diminishing the quantity bound to the glucoside. In order to take this fact into account we have recalculated all the hydrolysis constants, this time by calculating them "from point to point", and for each point we have calculated the amount of emulsin bound to the glucoside, considering the amount of inhibiting substances present. The product $k \cdot c$ should then be constant all through the hydrolysis. This is surely not the case, but the decrease of this product is not so great as the decrease of the hydrolysis constants, calculated as previously. We are therefore of opinion that the reaction which determines the velocity of hydrolysis, is the decomposition of the addition compound of glucoside and emulsin into glucose, alcohol, and emulsin.

Variation of the aglucone bound to the glucose molecule will therefore influence the velocity of hydrolysis in two ways:

a) The affinity constant, which determines the concentration of the addition-compound glucoside-emulsin, is, for a series of glucosides, dependent on the nature of the aglucone.
b) The value of k, the hydrolysis constant of the glucoside-emulsin-compound, may differ with the aglucone introduced in the glucose molecule.

If the assumptions made here are correct, it is possible to calculate the time necessary to produce any degree of hydrolysis for any concentration of the glucoside, when the following constants are known:

$\underline{k_m}$, $\underline{k_{m1}}$, and $\underline{k_{m2}}$, the dissociation constants for the compounds of emulsin with the glucoside and with the two products of hydrolysis,

$\underline{e}$ and $\underline{\text{sal. f.}}$, the weight of emulsin present in 50 ml. of the solution and the enzymic power of the emulsin preparation used,

k_{obs}, the hydrolysis constant determined for one concentration of the glucoside,

$k_{obs} \cdot c / x \cdot e \cdot (sal.\ f.)$ then being a constant for each glucoside, x being the amount of emulsin actually bound to the glucoside, when regard is paid to the products of hydrolysis. (x is expressed as a fraction of e).

Experimental.

1. Propyl-β-d-glucoside.

The preparation of propyl-β-d-glucoside used here had M. P. 102—03° and $[\alpha]_D^{20} = -39.5°$ (VEIBEL and ERIKSEN, 1936, 1).

a) Determination of the velocity constant at 30° and its temperature coefficient.

The experiments were carried out as described previously (l. c. 1936, 2). k is calculated with the minute as unit of time and logarithms to base 10.

Table I.

Hydrolysis at 30°.

$c_{emulsin}$ 0.2188 g in 50 ml. $\alpha_{emulsin} = -0.425°$. Sal. f. = 0.044.

$c_{glucoside}$ 0.0400 M. $\alpha_{beg.} = -0.600°$, $\alpha_{end} = +0.620°$.

Time min.	Samples kept h.	α	corr.	α corr.	x	c — x	k·10⁴
0	—	—1.025	—	—1.025	0.105	1.220	—
20	5.0	—0.920	—	—0.920	0.105	1.115	19.55
40	5.5	—0.810	—	—0.810	0.215	1.005	21.55
60	6.0	—0.710	0.005	—0.705	0.320	0.900	22.02
90	6.0	—0.570	0.005	—0.565	0.460	0.760	22.84
120	6.0	—0.470	0.005	—0.465	0.560	0.660	22.24
180	21.0	—0.310	0.015	—0.295	0.730	0.490	22.01
240	20.5	—0.180	0.020	—0.160	0.865	0.355	22.34
						mean value...	21.8

$k/e \cdot (sal.\ f.) = 22.6 \cdot 10^{-2}$.

Table II.

Hydrolysis at 20°.

$c_{emulsin}$ and $c_{glucoside}$ as in Table I.

Time min.	Samples kept h.	α	corr.	α corr.	x	c — x	$k \cdot 10^4$
0	—	— 1.025	—	— 1.025	—	1.220	—
20	4.5	— 0.960	—	— 0.960	0.065	1.155	11.89
40	5.0	— 0.905	—	— 0.905	0.120	1.100	11.24
60	5.0	— 0.855	—	— 0.855	0.170	1.050	10.86
90	5.5	— 0.785	—	— 0.785	0.240	0.980	10.57
120	5.5	— 0.700	—	— 0.700	0.325	0.895	10.98
180	20.5	— 0.605	0.010	— 0.595	0.430	0.790	10.49
240	20.0	— 0.490	0.010	— 0.480	0.545	0.675	10.71
300	19.5	— 0.420	0.015	— 0.405	0.620	0.600	10.27
						mean value...	10.9

$k/e \cdot (sal.\ f.) = 11.3 \cdot 10^{-2}$.

As k_{30} / k_{20} is 2.0, the heat of activation is 12200 cal.

The enzymic hydrolysis of propylglucoside not having been investigated previously, we have examined whether the rate of hydrolysis is proportional to the concentration of emulsin. Table III shows this to be the case.

Table III.

Proportionality between rate of hydrolysis and enzymic concentration.

$c_{emulsin}$	$c_{glucoside}$	$k \cdot 10^4$	$k/e \cdot (sal.\ f.)$
0.0665 g	0.0400 M	7.05	$24.1 \cdot 10^{-2}$
0.1330 g	0.0400 M	14.10	$24.1 \cdot 10^{-2}$
0.1995 g	0.0400 M	20.65	$23.5 \cdot 10^{-2}$

b. The affinity constant and its temperature coefficient.

The affinity constant has been determined at 30° and at 20°. Tables IV and V and fig. 1 show that at both temperatures the affinity constant is 6.3, so that the heat of formation for the glucoside-emulsin-compound is zero.

Table IV.

Affinity constant. 30°.

$c_{emulsin}$ = 0.2200 g in 50 ml. $\alpha_{emulsin}$ = −0.430° in all experiments.

Time min.	Samples kept h.	α	corr.	α corr.	x	1/v
I. 0.0200 M glucoside. 1/c = 50.						
0	3.0	−0.730	—	−0.730	—	—
20	3.0	−0.655	—	−0.655	0.075	13.35
40	4.0	−0.590	—	−0.590	0.140	7.14
60	4.5	−0.535	—	−0.535	0.195	5.12
80	5.5	−0.480	—	−0.480	0.250	4.00
II. 0.0400 M glucoside. 1/c. = 25.						
0	3.0	−1.030	—	−1.030	—	—
20	3.5	−0.925	—	−0.925	0.105	9.53
40	4.0	−0.805	—	−0.805	0.225	4.44
60	5.0	−0.695	—	−0.695	0.335	2.98
80	5.5	−0.610	—	−0.610	0.420	2.38
III. 0.0800 M glucoside. 1/c = 12.5.						
0	3.0	−1.630	—	−1.630	—	—
20	3.5	−1.455	—	−1.455	0.175	5.71
40	4.0	−1.290	—	−1.290	0.340	2.94
60	5.0	−1.125	0.005	−1.120	0.510	1.96
80	6.0	−0.970	0.005	−0.965	0.665	1.53
IV. 0.1600 M glucoside. 1/c = 6.25.						
0	3.5	−2.830	—	−2.830	—	—
20	3.5	−2.580	—	−2.580	0.250	4.00
40	4.5	−2.315	—	−2.315	0.515	1.94
60	5.0	−2.085	0.005	−2.080	0.750	1.33
80	6.0	−1.880	0.005	−1.875	0.955	1.05
V. 0.2400 M glucoside. 1/c = 4.17.						
0	3.5	−4.030	—	−4.030	—	—
20	4.0	−3.695	—	−3.695	0.335	2.98
40	4.5	−3.400	0.005	−3.395	0.635	1.58
60	5.5	−3.135	0.005	−3.130	0.900	1.11
80	6.0	−2.870	0.010	−2.860	1.170	0.85
VI. 0.3200 M glucoside. 1/c = 3.13.						
0	3.5	−5.230	—	−5.230	—	—
20	4.0	−4.840	—	−4.840	0.390	2.56
40	4.5	−4.520	0.005	−4.515	0.715	1.40
60	5.5	−4.210	0.005	−4.205	1.025	0.98
80	6.0	−3.905	0.010	−3.895	1.335	0.75

Table V.

Affinity constant. 20°.

$c_{emulsin}$ = 0.2000 g in 50 ml. $\alpha_{emulsin}$ = — 0.390° in all experiments.

Time min.	Samples kept h.	α	corr.	α corr.	x	1/v
I. 0.0200 M glucoside. 1/c = 50.0.						
0	3.0	— 0.690	—	— 0.690	—	—
20	3.5	— 0.660	—	— 0.660	0.030	33.33
40	5.0	— 0.625	—	— 0.625	0.065	15.40
60	5.5	— 0.595	—	— 0.595	0.095	10.52
80	6.5	— 0.565	—	— 0.565	0.125	8.00
II. 0.400 M glucoside. 1/c = 25.0.						
0	3.5	— 0.990	—	— 0.990	—	—
20	4.0	— 0.930	—	— 0.930	0.060	16.67
40	5.0	— 0.875	—	— 0.875	0.115	8.71
60	6.0	— 0.825	—	— 0.825	0.165	6.06
80	6.5	— 0.780	—	— 0.780	0.210	4.76
III. 0.0800 M glucoside. 1/c = 12.5.						
0	3.5	— 1.590	—	— 1.590	—	—
20	4.0	— 1.500	—	— 1.500	0.090	11.11
40	5.0	— 1.415	—	— 1.415	0.175	5.72
60	6.0	— 1.345	—	— 1.345	0.245	4.08
80	6.5	— 1.270	—	— 1.270	0.320	3.13
IV. 0.1600 M glucoside. 1/c = 6.25.						
0	3.5	— 2.790	—	— 2.790	—	—
20	4.0	— 2.655	—	— 2.655	0.135	7.41
40	5.5	— 2.525	—	— 2.525	0.265	3.77
60	6.0	— 2.405	0.005	— 2.400	0.390	2.56
80	7.0	— 2.295	0.005	— 2.290	0.500	2.00
V. 0.2400 M glucoside. 1/c = 4.17.						
0	4.0	— 3.990	—	— 3.990	—	—
20	4.5	— 3.820	—	— 3.820	0.170	5.89
40	5.5	— 3.655	—	— 3.655	0.335	2.98
60	6.5	— 3.495	0.005	— 3.490	0.500	2.00
80	7.0	— 3.350	0.005	— 3.345	0.645	1.55
VI. 0.3200 M glucoside. 1/c = 3.13.						
0	4.5	— 5.190	—	— 5.190	—	—
20	5.0	— 5.015	—	— 5.015	0.175	5.72
40	5.5	— 4.830	—	— 4.830	0.360	2.78
60	6.5	— 4.650	0.005	— 4.645	0.545	1.94
80	7.0	— 4.480	0.005	— 4.475	0.715	1.40

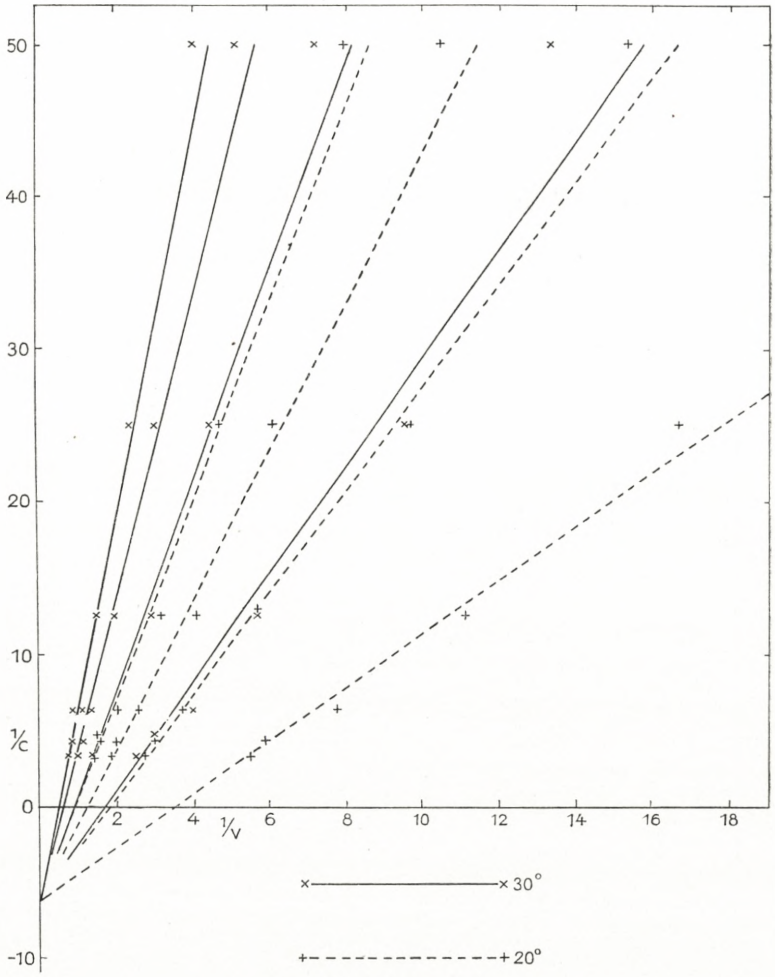

Fig. 1.

c. The influence of the products of hydrolysis.

As in the previous paper the influence of the products of hydrolysis was determined by hydrolysing solutions, which were 0.0400 M in glucoside and at the same time 0, 0.01, 0.02, 0.04, 0.08 or 0.12 M in glucose or in propyl alcohol. Tables VI and VII show the influence of glucose and propyl

alcohol respectively, tables VIII—XI are examples showing the variations within single experiments.

Table VI.

Influence of glucose.

$c_{emulsin}$ and $c_{glucoside}$ as in table VIII. 1 ml toluene added.

$c_{glucose}$	0.00	0.01	0.02	0.04	0.08	0.12 M
$k \cdot 10^4$	28.0	27.2	25.3	24.2	21.9	20.0

Table VII.

Influence of propyl alcohol.

$c_{emulsin}$ and $c_{glucoside}$ as in table X. No toluene added.

$c_{alcohol}$	0.00	0.01	0.02	0.04	0.08	0.12 M
$k \cdot 10^4$	24.9	22.6	21.3	19.8	18.5	16.7

Table VIII.

Influence of glucose. 1 ml toluene added.

$c_{emulsin}$ 0.2290 g in 50 ml. $\alpha_{emulsin} = -0.435°$. Sal.f. = 0.044. $c_{glucoside} = 0.0400$ M. $c_{glucose} = 0.0200$ M. $\alpha_{beg.} = -0.720°$, $\alpha_{end} = +0.500°$.

Time min.	Samples kept h.	α	corr.	α corr.	x	c — x	$k \cdot 10^4$
0	4.0	— 0.725	0.005	— 0.720	—	1.220	—
20	5.0	— 0.590	0.005	— 0.585	0.135	1.085	25.46
40	6.0	— 0.470	0.005	— 0.465	0.255	0.965	25.46
60	7.0	— 0.360	0.005	— 0.355	0.365	0.855	25.73
90	9.5	— 0.225	0.010	— 0.215	0.505	0.715	25.78
120	10.0	— 0.105	0.015	— 0.090	0.630	0.590	26.29
180	24.5	+ 0.030	0.035	+ 0.065	0.785	0.435	24.88
240	24.5	+ 0.145	0.040	+ 0.185	0.905	0.315	24.50
300	24.5	+ 0.230	0.040	+ 0.270	0.990	0.230	24.15
						mean value...	25.3

In this case both components of the glucoside are acting as inhibitors, the alcohol perhaps to a somewhat greater extent than the glucose. From tables XII and XIII it is seen that the affinity-constant for the emulsin-glucose-

Table IX.

Influence of glucose. 1 ml. toluene added.

$c_{emulsin}$ and $c_{glucoside}$ as in table VIII. $c_{glucose}$ 0.1200 M.

$\alpha_{beg.} = +0.820°$, $\alpha_{end} = +2.040°$.

Time min.	Samples kept h.	α	corr.	α corr.	x	c — x	k·10⁴
0	4.5	+ 0.800	0.020	+ 0.820	—	1.220	—
20	6.0	+ 0.895	0.025	+ 0.920	0.100	1.120	18.57
40	6.5	+ 1.000	0.025	+ 1.025	0.205	1.015	19.96
60	7.5	+ 1.085	0.030	+ 1.115	0.295	0.925	20.04
90	10.0	+ 1.205	0.045	+ 1.250	0.430	0.790	20.97
120	10.0	+ 1.310	0.045	+ 1.355	0.535	0.685	20.91
180	25.0	+ 1.395	0.115	+ 1.510	0.690	0.530	20.12
240	25.0	+ 1.515	0.120	+ 1.635	0.815	0.405	19.95
300	25.0	+ 1.600	0.120	+ 1.720	0.900	0.320	19.37
						mean value...	20.0

Table X.

Influence of propyl alcohol. No toluene added.

$c_{emulsin} = 0.2308$ g in 50 ml. $\alpha_{emulsin} = -0.450°$.

Sal. f. = 0.044. $c_{glucoside} = 0.0400$ M. $c_{alcohol} = 0.02$ M.

$\alpha_{beg.} = -1.050°$, $\alpha_{end} = +0.170°$.

Time min.	Samples kept h.	α	corr.	α corr.	x	c — x	k·10⁴
0	4.0	— 1.050	—	— 1.050	—	1.220	—
20	4.0	— 0.935	—	— 0.935	0.115	1.105	21.5
40	5.0	— 0.830	—	— 0.830	0.220	1.000	21.6
60	5.5	— 0.745	—	— 0.745	0.305	0.915	20.8
90	6.0	— 0.625	0.005	— 0.620	0.430	0.790	20.9
120	22.0	— 0.520	0.015	— 0.505	0.545	0.675	21.4
180	24.5	— 0.345	0.020	— 0.325	0.725	0.495	21.8
240	24.5	— 0.230	0.020	— 0.210	0.840	0.380	21.1
300	24.5	— 0.140	0.025	— 0.115	0.935	0.285	21.1
						mean value...	21.3

compound is $K_{m1} = 0.21$; $K_{M1} = 4.8$, the affinity constant for the propylalcohol-emulsin-compound is $K_{m2} = 0.18$; $K_{M2} = 5.6$.

Table XI.

Influence of propyl alcohol. No toluene added.

$c_{emulsin}$ and $c_{glucoside}$ as in table X. $c_{alcohol} = 0.1200$ M.

$\alpha_{beg.} = -1.050°$, $\alpha_{end} = +0.170°$.

Time min.	Samples kept h.	α	corr.	α corr.	x	c — x	$k \cdot 10^4$
0	5.0	— 1.050	—	— 1.050	—	1.220	—
20	5.0	— 0.970	—	— 0.970	0.080	1.140	14.7
40	5.5	— 0.880	—	— 0.880	0.170	1.050	15.9
60	6.0	— 0.790	—	— 0.790	0.260	0.960	17.4
90	6.5	— 0.680	0.005	— 0.675	0.375	0.845	17.8
120	22.0	— 0.600	0.010	— 0 590	0.460	0.760	17.1
180	24.5	— 0.430	0.015	— 0.415	0.635	0.585	17.7
240	24.5	— 0.335	0.020	— 0.315	0.735	0.485	16.7
300	24.5	— 0.245	0.020	— 0.225	0.825	0.395	16.3
						mean value...	16.7

The accuracy of these determinations is not very great, but it is seen that the value found here for glucose within the limits of the experiment is the same as found previously (l. c. 1936 2, p. 24).

Table XII.

Affinity constant for the compound emulsin-glucose.

$K_m = 0.16$, S = 0.04, G = 0.01 — 0.12.

G..	0.00	0.01		0.02		0.04		0.08		0.12	
t	v_o	v	v_o/v	v	v_o/v	v	v_o/v	v	v_o/v	v	v_o/v
20	0.155	0.150	1.035	0.135	1.150	0.130	1.192	0.120	1.293	0.100	1.550
40	0.285	0.275	1.038	0.255	1.119	0.250	1.142	0.225	1.268	0.205	1.392
60	0.405	0.385	1.053	0.365	1.112	0.360	1.128	0.310	1.306	0.295	1.374
90	0.555	0.545	1.019	0.505	1.100	0.485	1.144	0.455	1.221	0.430	1.290
mean value...			1.036		1.120		1.152		1.272		1.402
K_{m_1}			0.222		0.133		0.211		0.237		0.239

mean value... $K_{m1} = 0.21$, $K_{M1} = 4.8$

Table XIII.

Affinity constant for the compound alcohol-emulsin.

$K_m = 0.16$, S = 0.04, G = 0.01 — 0.12.

G..	0.00	0.01		0.02		0.04		0.08		0.12	
t	v_o	v	v_o/v	v	v_o/v	v	v_o/v	v	v_o/v		v_o/v
20	0.125	0.120	1.041	0.115	1.086	0.105	1.190	0.100	1.250	0.080	1.568
40	0.250	0.230	1.086	0.220	1.135	0.205	1.220	0.185	1.352	0.170	1.472
60	0.350	0.320	1.094	0.305	1.150	0.285	1.230	0.280	1.250	0.260	1.350
90	0.475	0.450	1.055	0.430	1.104	0.420	1.131	0.395	1.204	0.375	1.266
mean value...			1.069		1.119		1.193		1.264		1.414
K_{m_2}			0.116		0.135		0.166		0.242		0.232

mean value... $K_{m2} = 0.18$, $K_{M2} = 5.6$

2. Isopropyl-β-d-glucoside.

The preparation of isopropylglucoside used here had M. P. 128—29° and $[\alpha]_D^{20} = -40.9°$ (Veibel and Eriksen, 1936, 1).

Table XIV.

Hydrolysis at 30°.

$c_{emulsin} = 0.1845$ g in 50 ml. $\alpha_{emulsin} = -0.360°$,
Sal. f. = 0.044. $c_{glucoside} = 0.0400$ M. $\alpha_{beg.} = -0.625°$.
$\alpha_{end} = +0.620°$.

Time min.	Samples kept h.	α	corr.	α corr.	x	c — x	$k \cdot 10^4$
0	4.0	— 0.985	—	— 0.985	—	1.245	—
30	4.5	— 0.860	—	— 0.860	0.125	1.120	15.32
60	4.5	— 0.770	—	— 0.770	0.215	1.030	13.72
90	5.0	— 0.680	—	— 0.680	0.305	0.940	13.56
120	4.5	— 0.600	—	— 0.600	0.385	0.860	13.39
180	4.0	— 0.485	—	— 0.485	0.500	0.745	12.39
240	3.5	— 0.395	—	— 0.395	0.590	0.655	(11.62)
300	20.0	— 0.320	0.015	— 0.305	0.680	0.565	(11.44)
360	19.5	— 0.260	0.015	— 0.245	0.740	0.505	(10.88)
						mean value...	13.7

$k/e \cdot (sal.\ f.) = 16.9 \cdot 10^{-2}$.

Table XV.

Hydrolysis at 20°.

$c_{emulsin}$ and $c_{glucoside}$ as in table XIV.

Time min.	Samples kept h.	α	corr.	α corr.	x	c — x	$k \cdot 10^4$
0	4.0	— 0.985	—	— 0.985	—	1.245	—
30	4.5	— 0.925	—	— 0.925	0.060	1.185	7.15
60	5.0	— 0.875	—	— 0.875	0.110	1.135	6.70
90	5.0	— 0.820	—	— 0.820	0.165	1.080	6.86
120	5.0	— 0.780	—	— 0.780	0.205	1.040	6.51
180	4.0	— 0.715	—	— 0.715	0.270	0.975	5.90
240	3.5	— 0.645	—	— 0.645	0.340	0.905	5.77
300	20.5	— 0.600	0.010	— 0.590	0.395	0.850	5.89
360	20.0	— 0.550	0.010	— 0.540	0.445	0.800	(5.34)
					mean value...		6.4

$$k/e \cdot (\text{sal. f.}) = 7.9 \cdot 10^{-2}.$$

a. Determination of the velocity constant at 30° and its temperature coefficient.

Tables XIV and XV give the results of hydrolysis experiments at 30° and at 20°.

It is seen that $k_{30} / k_{20} = 2.15$, and consequently the heat of activation is 13500 cal.

As in the case of propyl-glucoside we have examined whether proportionality exists between concentration of emulsin and rate of hydrolysis. Table XVI shows that this is the case.

Table XVI.

Proportionality between rate of hydrolysis and concentration of emulsin.

$c_{emulsin}$	$c_{glucoside}$	$k \cdot 10^4$	$k/e \cdot (\text{sal. f.})$
0.0845 g	0.0400 M	5.9	$15.9 \cdot 10^{-2}$
0.1690 g	0.0400 M	11.9	$16.0 \cdot 10^{-2}$
0.2535 g	0.0400 M	17.6	$15.8 \cdot 10^{-2}$

Scheiber (1935) has examined the hydrolysis of isopropyl-glucoside, but his results are not directly comparable with

Table XVII.

Affinity constant. 30°.

$c_{emulsin}$ = 0.2260 g in 50 ml. $\alpha_{emulsin}$ = — 0.440° in all experiments.

Time min.	Samples kept h.	α	corr.	α corr.	x	1/v
I. 0.200 M glucoside. 1/c = 50.0.						
0	3.5	— 0.755	—	— 0.755	—	—
30	3.5	— 0.675	—	— 0.675	0.080	12.50
60	4.0	— 0.610	—	— 0.610	0.145	6.90
90	5.0	— 0.560	—	— 0.560	0.195	5.13
120	6.0	— 0.510	—	— 0.510	0.245	4.08
II. 0.0400 M glucoside. 1/c = 25.0.						
0	3.5	— 1.060	—	— 1.060	—	—
30	4.0	— 0.920	—	— 0.920	0.140	7.14
60	4.5	— 0.805	—	— 0.805	0.255	3.92
90	5.5	— 0.705	—	— 0.705	0.355	2.82
120	6.0	— 0.620	0.005	— 0.615	0.445	2.25
III. 0.0800 M glucoside. 1/c = 12.5.						
0	3.5	— 1.690	—	— 1.690	—	—
30	4.0	— 1.480	—	— 1.480	0.210	4.76
60	4.5	— 1.250	—	— 1.250	0.440	2.27
90	5.5	— 1.050	0.005	— 1.045	0.645	1.55
120	6.0	— 0.880	0.005	— 0.875	0.815	1.23
IV. 0.1600 M glucoside. 1/c = 6.25.						
0	3.5	— 2.940	—	— 2.940	—	—
30	4.0	— 2.535	—	— 2.535	0.405	2.47
60	4.5	— 2.150	0.005	— 2.145	0.795	1.26
90	5.5	— 1.825	0.005	— 1.820	1.120	0.89
120	6.0	— 1.525	0.010	— 1.515	1.425	0.70
V. 0.2400 M glucoside. 1/c = 4.17.						
0	3.5	— 4.190	—	— 4.190	—	—
30	4.0	— 3.660	—	— 3.660	0.530	1.89
60	5.5	— 3.150	0.005	— 3.145	1.045	0.96
90	6.0	— 2.700	0.010	— 2.690	1.500	0.67
120	6.0	— 2.320	0.010	— 2.310	1.880	0.53
VI. 0.3200 M glucoside. 1/c = 3.13.						
0	4.0	— 5.440	—	— 5.440	—	—
30	4.5	— 4.780	0.005	— 4.775	0.665	1.50
60	5.5	— 4.165	0.005	— 4.160	1.280	0.78
90	6.0	— 3.620	0.010	— 3.610	1.830	0.55
120	6.5	— 3.125	0.015	— 3.110	2.330	0.43

Table XVIII.

Affinity constant. 20°.

$c_{emulsin} = 0.2520$ g in 50 ml. $\alpha_{emulsin} = -0.495°$ in all experiments.

Time min.	Samples kept h.	α	corr.	α corr.	x	1/c
I. 0.0200 M glucoside. 1/c = 50.0.						
0	4.0	−0.810	—	−0.810	—	—
30	4.5	−0.765	—	−0.765	0.045	22.22
60	6.0	−0.730	—	−0.730	0.080	12.50
90	7.0	−0.695	—	−0.695	0.115	8.70
120	9.5	−0.660	—	−0.660	0.150	6.67
II. 0.0400 M glucoside. 1/c = 25.0.						
0	4.0	−1.120	—	−1.120	—	—
30	4.5	−1.050	—	−1.050	0.070	14.30
60	6.5	−0.975	—	−0.975	0.145	6.90
90	7.0	−0.920	—	−0.920	0.200	5.00
120	9.5	−0.870	0.005	−0.865	0.255	3.92
III. 0.0800 M glucoside. 1/c = 12.5.						
0	4.0	−1.745	—	−1.745	—	—
30	5.5	−1.605	—	−1.605	0.140	7.14
60	6.5	−1.460	—	−1.460	0.285	3.51
90	7.0	−1.360	0.005	−1.355	0.390	2.56
120	10.0	−1.270	0.005	−1.265	0.480	2.08
IV. Glucoside 0.1600 M. 1/c = 6.25.						
0	4.5	−2.995	—	−2.995	—	—
30	6.0	−2.765	—	−2.765	0.230	4.35
60	6.5	−2.560	0.005	−2.555	0.440	2.27
90	7.0	−2.375	0.005	−2.370	0.625	1.60
120	10.0	−2.185	0.010	−2.175	0.820	1.22
V. 0.2400 M glucoside. 1/c = 4.17.						
0	4.5	−4.245	—	−4.245	—	—
30	6.0	−3.955	—	−3.955	0.290	3.45
60	7.0	−3.630	0.005	−3.625	0.620	1.61
90	7.5	−3.370	0.005	−3.365	0.880	1.14
120	10.0	−3.130	0.010	−3.120	1.125	0.89
VI. 0.3200 M glucoside. 1/c = 3.13.						
0	4.5	−5.495	—	−5.495	—	—
30	6.5	−5.135	0.005	−5.130	0.365	2.74
60	7.0	−4.765	0.005	−4.760	0.735	1.36
90	7.5	−4.410	0.010	−4.400	1.095	0.91
120	10.5	−4.120	0.015	−4.105	1.390	0.72

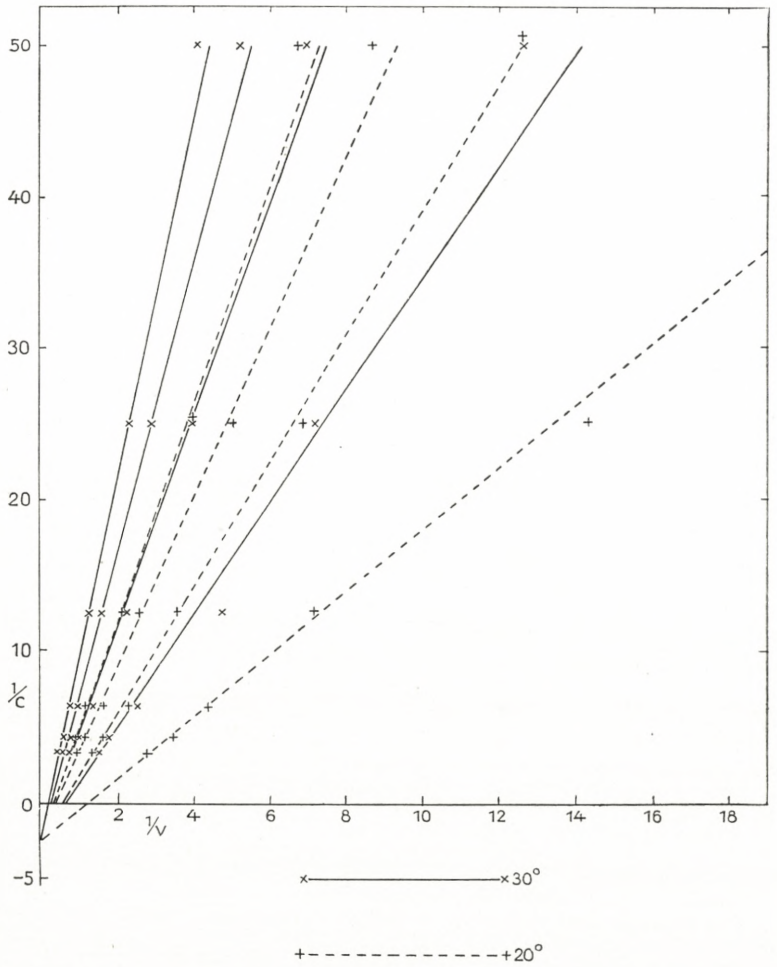

Fig. 2.

ours, his experiments having been carried out at p_H 5, whereas we are working at p_H 4.4. Nevertheless we have calculated the results reported by SCHEIBER in our way. The value of k/e·(sal. f.) for a 0.052 M solution is $11.7 \cdot 10^{-2}$, and we think that this value agrees tolerably with the value $15.9 \cdot 10^{-2}$ found by us for a 0.0400 M solution.

Table XIX.

Influence of glucose.

$c_{emulsin}$ and $c_{glucoside}$ as in table XXI. 1 ml toluene added.

$c_{glucose}$	0.00	0.01	0.02	0.04	0.08	0.12
$k \cdot 10^4$	18.3	17.5	15.7	14.3	11.2	9.5

Table XX.

Influence of isopropylalcohol.

$c_{emulsin}$ and $c_{glucoside}$ as in table XXIII. No toluene added.

$c_{alcohol}$	0.00	0.01	0.02	0.04	0.08	0.12
$k \cdot 10^4$	15.3	14.7	14.3	13.9	13.2	12.4

Table XXI.

Influence of glucose. 1 ml toluene added.

$c_{emulsin}$ 0.2182 g in 50 ml. $\alpha_{emulsin} = -0.430°$. sal. f. = 0.044

$c_{glucoside}$ 0.0400 M. $c_{glucose}$ 0.0200 M. $\alpha_{beg.} -0.740°$, $\alpha_{end} +0.505°$.

Time min.	Samples kept h.	α	corr.	α corr.	x	c — x	$k \cdot 10^4$
0	4.5	— 0.745	0.005	— 0.740	—	1.245	—
30	5.0	— 0.590	0.005	— 0.585	0.155	1.095	18.59
60	6.0	— 0.485	0.005	— 0.480	0.260	0.985	16.96
90	6.0	— 0.380	0.005	— 0.375	0.365	0.880	16.74
120	6.5	— 0.315	0.005	— 0.310	0.430	0.815	15.33
180	22.0	— 0.190	0.025	— 0.165	0.575	0.670	14.95
240	21.5	— 0.075	0.030	— 0.045	0.695	0.550	14.78
300	21.0	+ 0.015	0.030	+ 0.045	0.785	0.460	14.41
360	21.5	+ 0.080	0.035	+ 0.115	0.855	0.390	14.00
						mean value...	15.7

b. The affinity constant and its temperature coefficient.

The affinity constant has been determined at 30° and at 20°. Tables XVII and XVIII and fig. 2 show that at both temperatures the affinity constant is 2.5, so that the heat of formation of the glucoside-emulsin-compound is zero.

Table XXII.

Influence of glucose. 1 ml toluene added.

$c_{emulsin}$ and $c_{glucoside}$ as in table XXI. $c_{glucose}$ 0.1200 M.

$\alpha_{beg} = +0.800°$. $\alpha_{end} = +2.045°$.

Time min.	Samples kept h.	α	corr.	α corr.	x	c — x	x · 10^4
0	4.5	+ 0.780	0.020	+ 0.800	—	1.245	—
30	6.0	+ 0.855	0.025	+ 0.880	0.080	1.165	9.61
60	6.0	+ 0.940	0.025	+ 0.965	0.165	1.080	10.29
90	6.5	+ 1.020	0.030	+ 1.050	0.250	0.995	10.82
120	6.5	+ 1.075	0.030	+ 1.105	0.305	0.940	10.17
180	22.0	+ 1.095	0.095	+ 1.190	0.390	0.855	9.07
240	22.0	+ 1.180	0.095	+ 1.275	0.475	0.770	8.70
300	22.0	+ 1.255	0.100	+ 1.355	0.555	0.690	8.54
380	22.0	+ 1.350	0.100	+ 1.450	0.650	0.595	8.91
						mean value...	9.5

Table XXIII.

Influence of isopropylalcohol. No toluene added.

$c_{emulsin}$ = 0,2250 g in 50 ml. $\alpha_{emulsin} = -0.440°$. Sal.f. = 0.044.

$c_{glucoside}$ = 0.0400 M. $c_{alcohol}$ = 0.02 M. $\alpha_{beg} = -1.065°$,

$\alpha_{end} = +0.180°$.

Time min.	Samples kept h.	α	corr.	α corr.	x	c — x	k · 10^4
0	4.5	— 1.065	—	— 1.065	—	1.245	—
30	5.0	— 0.940	—	— 0.940	0.125	1.120	15.32
60	6.0	— 0.825	—	— 0.825	0.240	1.005	15.57
90	6.5	— 0.740	—	— 0.740	0.325	0.920	14.60
120	6.5	— 0.660	0.005	— 0.655	0.410	0.835	14.46
180	22.5	— 0.525	0.015	— 0.510	0.555	0.690	14.24
240	22.0	— 0.420	0.015	— 0.405	0.660	0.585	13.67
300	23.0	— 0.335	0.020	— 0.315	0.750	0.495	13.35
360	22.5	— 0.265	0.020	— 0.245	0.820	0.425	12.97
						mean value...	14.3

c. The influence of the products of hydrolysis.

As usual the hydrolysis of solutions being 0.04 M in glucoside and besides 0.00, 0.01, 0.02, 0.04, 0.08 or 0.12 M in glucose or in alcohol was examined. Tables XIX and XX

Table XXIV.

Influence of isopropylalcohol. No toluene added.

$c_{emulsin}$ and $c_{glucoside}$ as in table XXIII. $c_{alcohol}$ 0.1200 M.

Time min.	Samples kept h.	α	corr.	α corr.	x	c — x	$k \cdot 10^4$
0	4.5	— 1.065	—	— 1.065	—	1.245	—
30	6.0	— 0.965	—	— 0.965	0.100	1.145	12.12
60	6.0	— 0.865	—	— 0.865	0.200	1.045	12.68
90	6.5	— 0.770	—	— 0.770	0.295	0.950	13.05
120	6.5	— 0.690	0.005	— 0.685	0.380	0.865	13.18
180	22.5	— 0.560	0.010	— 0.550	0.515	0.730	12.88
240	22.5	— 0.470	0.015	— 0.455	0.610	0.635	12.18
300	23.0	— 0.380	0.015	— 0.365	0.700	0.545	11.96
360	22.5	— 0.320	0.015	— 0.305	0.760	0.485	11.37
						mean value...	12.4

Table XXV.

Affinity constant for the compound emulsin-glucose.

$K_m = 0.40$, $S = 0.04$, $G = 0.01 - 0.12$.

G	0.00	0.01		0.02		0.04		0.08		0.12	
t	v_o	v	v_o/v	v	v_o/v	v	v_o/v	v	v_o/v	v	v_o/v
30	0.170	0.160	1.062	0.155	1.096	0.135	1.259	0.100	1.700	0.080	2.130
60	0.305	0.295	1.033	0.260	1.172	0.245	1.243	0.185	1.650	0.165	1.850
90	0.425	0.415	1.026	0.365	1.165	0.340	1.250	0.265	1.605	0.250	1.702
120	0.500	0.485	1.032	0.430	1.162	0.405	1.237	0.325	1.540	0.305	1.640
mean value			1.038		1.149		1.247		1.624		1.831
K_{m1}			0.240		0.122		0.147		0.117		0.131

mean value $K_{m1} = 0.15$; $K_{M1} = 6.6$

show respectively the influence of glucose and isopropylalcohol, Tables XXI—XXIV are examples showing the variations within single experiments.

Here also both components act as inhibitors. By comparison with propylglucoside it is seen that isopropylalcohol does not inhibit as much as does propylalcohol. Tables XXV and XXVI give material for the calculation of the

Table XXVI.

Affinity constant for the compound emulsin-isopropylalcohol.

$K_m = 0.40$, S = 0.04, G = 0.01—0.12.

G	0.00	0.01		0.02		0.04		0.08		0.12	
t	v_o	v	v_o/v	v	v_o/v	v	v_o/v	v	v_o/v	v	v_o/v
30	0.135	0.130	1.035	0.125	1.070	0.120	1.125	0.115	1.175	0.100	1.350
60	0.250	0.245	1.022	0.240	1.045	0.235	1.065	0.225	1.115	0.200	1.250
90	0.345	0.335	1.030	0.325	1.062	0.320	1.080	0.305	1.135	0.295	1.170
120	0.435	0.420	1.038	0.410	1.062	0.405	1.078	0.395	1.105	0.380	1.150
mean value			1.03		1.06		1.09		1.13		1.23
K_{m1}			0.30		0.30		0.40		0.58		0.47

mean value $K_{m1} = 0.41$; $K_{M1} = 2.5$

affinity constants of glucose and isopropylalcohol. The values found for glucose are $K_{m1} = 0.15$; $K_{M1} = 6.6$ (i. e. within the limits of the experiment the same value as found previously), for isopropylalcohol $K_{m2} = 0.41$; $K_{M2} = 2.5$.

Discussion.

We have now established the following constants for methyl-, ethyl-, propyl- and isopropyl-β-d-glucoside:

Table XXVII.

M = 0.0400	Methyl	Ethyl	Propyl	Isopropyl
$10^2 \cdot k_{30}/e \cdot$(sal. f.)	2.7	5.3	22.6	16.9
K_m	0.62	0.25	0.16	0.40
K_{m1}	0.21	0.17	0.21	0.15
K_{m2}	—	—	0.18	0.41

The mean value for K_{m1} (glucose) is 0.18. The K_{m2}-values for methyl- and ethylalcohol are so small that we have not been able to determine them with the experimental technique used here.

Josephson (1925, p. 145) has found that for some of the glucosides examined by him the equation $K_m = K_{m1} \cdot K_{m2}$ holds good. We have not been able to determine the K_{m2}-

values for methyl- and ethylalcohol, and consequently we cannot determine the product $K_{m1} \cdot K_{m2}$ for these two glucosides. For propyl- and isopropyl-glucoside Josephson's equation surely does not hold good, as will be seen from the following figures:

$$\text{Propyl: } K_m = 0.16;\ K_{m1} = 0.18;\ K_{m2} = 0.18;$$
$$K_{m1} \cdot K_{m2} = 0.032$$
$$\text{Isopropyl: } K_m = 0.40;\ K_{m1} = 0.18;\ K_{m2} = 0.41;$$
$$K_{m1} \cdot K_{m2} = 0.074.$$

It must, however, be kept in mind that Josephson divides the inhibiting action of the alcohols into two parts, one, which is independent of the affinity between the glucosidase and the alcohol, and another, which is due to this affinity, and it is only this part of the inhibiting effect which is to be taken into account in the calculation of the K_{m2}-values used in the Josephson-expression. Our experiments do not afford material for the determination of the two different effects of the alcohols, but the non-competitive part of the inhibiting action of the alcohols must be very great to obtain agreement between the observed and the calculated K_m-values, the latter being only some 20 % of the observed values.

Both the fact that glucose and at least two of the four alcohols examined have an inhibiting effect on the hydrolysis of the β-glucosides with emulsin, and that it has been possible to determine the dissociation constants for the emulsin-inhibitor-compounds as well as for the emulsin-glucoside-compounds, made us try to refer the hydrolysis-constants not to the amount of emulsin present in the solution, as we have done till now, but to the amount of emulsin really bound to the glucoside. As the molarity

of the emulsin-solution is not known, we have calculated how many per cent. of the emulsin have combined with the glucoside, and as we have previously referred the hydrolysis-constants to the unity of emulsin present in the solution, it is not difficult to recalculate the constants, referring them to unity of emulsin combined.

From the mass-action expression

$$K_m = \frac{(E - ES)(S - ES)}{ES}$$

or, as S is always very great compared with ES,

$$K_m = \frac{(E - ES)S}{ES},$$

it is seen that $\frac{ES}{E} = \frac{S}{(K_m + S)}$.

For all four glucosides examined we have used solutions 0.0400 M in glucoside. In Table XXVIII is indicated the amount of emulsin combined with the four glucosides and the hydrolysis constants referred to unity of emulsin combined.

Table XXVIII.

Rate of hydrolysis referred to unity of emulsin combined.

	$10^2 \cdot k/(e \cdot sal.\ f.)$	K_m	% Emulsin combined	$10^2 \cdot k/(e_{comb} \cdot sal.\ f.)$
Methyl	2.7	0.62	6.1	44
Ethyl	5.3	0.25	13.8	39
Propyl	22.6	0.16	20.0	113
Isopropyl	16.9	0.40	9.1	186

It is seen that calculated in this way the order of the velocity of hydrolysis differs from the one found, when the velocity constants are referred to unity of emulsin dissolved.

It is well known that when the velocity constants of hydrolysis are determined for different substrate concentrations, no proportionality exists between k and c. If the

Table XXIX.

Constancy of the expression $k/(K_m + c)$.

c	K_m	% emulsin combined	k/(e·sal.f.)	k/e_{comb}	$c \cdot k/e_{comb} = k(K_m + c)$
			Methylglucoside		
0.0204	0.62	3.1	$2.8 \cdot 10^{-2}$	$90.5 \cdot 10^{-2}$	$1.80 \cdot 10^{-2}$
0.0409	0.62	6.1	2.8	45.9	1.85
0.0826	0.62	11.7	2.6	22.2	1.82
0.1672	0.62	21.3	2.4	11.2	1.87
0.3334	0.62	35.0	2.0	5.7	1.90
0.6689	0.62	51.8	1.4	2.7	1.81
					1.84
			Ethylglucoside		
0.0200	0.25	7.4	$5.4 \cdot 10^{-2}$	$73.0 \cdot 10^{-2}$	$1.46 \cdot 10^{-2}$
0.0400	0.25	13.8	5.8	42.0	1.68
0.0800	0.25	24.3	5.1	21.0	1.68
0.1600	0.25	39.0	4.1	10.5	1.68
0.3200	0.25	56.2	2.9	5.2	1.66
0.6400	0.25	71.9	1.7	2.4	1.54
					1.62
			Propylglucoside		
0.0200	0.16	11.2	$29.2 \cdot 10^{-2}$	$260 \cdot 10^{-2}$	$5.20 \cdot 10^{-2}$
0.0400	0.16	20.0	22.7	114	4.56
0.0800	0.16	33.3	17.2	51.6	4.13
0.1600	0.16	50.0	12.4	24.8	3.97
0.2400	0.16	60.0	10.0	16.7	4.00
0.3200	0.16	66.7	8.5	12.8	4.10
					4.33
			Isopropylglucoside		
0.0200	0.40	4.8	$18.9 \cdot 10^{-2}$	$394 \cdot 10^{-2}$	$7.88 \cdot 10^{-2}$
0.0400	0.40	9.1	16.6	183	7.32
0.0800	0.40	16.7	14.5	86.8	6.94
0.1600	0.40	28.6	12.4	42.4	6.79
0.2400	0.40	37.5	11.1	29.6	7.10
0.3200	0.40	44.5	10.0	22.5	7.20
					7.21

velocity constants are referred to the emulsin combined, the constants reduced in this way are inversely proportional to the concentration of the substrate, as the measured reac-

tion seems to be the hydrolysis of the compound emulsin-substrate into emulsin, glucose and alcohol. This means that the product $k(K_m + c)$ has a constant value (k being the directly observed velocity constant).

The determination of the affinity constant of the glucosides affords material for the determination of the hydrolysis constants at 6 different glucoside concentrations. In Table XXIX we have calculated the velocity constants referred to unity of the applied emulsin and we have also indicated the amount of the emulsin, which has combined with the substrate, as well as the velocity constants referred to the emulsin combined and the product $k \cdot (K_m + c)$. It is seen that the concordance is as good as may be expected.

We have then examined whether the inhibiting effect of the products of hydrolysis may be explained by the affinity of emulsin to the products of hydrolysis, that is, whether the inhibition is competitive or not. The velocity constants being proportional to the concentration of emulsin, this may be examined, competitive inhibition meaning that the velocity constants of hydrolysis decrease exactly as much as the percentage of emulsin combined with glucoside decreases by the addition of glucose or alcohol.

When the affinity constants of the compounds emulsin-glucoside and emulsin-glucose are known, it is possible to calculate, how much the amount of emulsin combined with each component decreases, both components being found together. If it is calculated for a solution, containing glucoside and glucose, that the fraction $\underline{a}$ of the emulsin will combine with glucoside, glucose not being present, and the fraction $\underline{b}$ will combine with glucose, glucoside not being present, then the fractions $\underline{x}$ and $\underline{y}$, which will combine

with each component, when both are present, may be calculated from the equations:

$$x = (1 - y)\,a; \qquad y = (1 - x)\,b$$

or

$$x = a \cdot \frac{1 - b}{1 - ab}.$$

If the inbibition is competitive, $\frac{k}{x}$ has to be constant for all experiments with the same glucoside concentration.

In Table XXX we have made this calculation for the action of glucose on the hydrolysis of all four glucosides

Table XXX.

Elimination of the effect of inhibitors.

$c_{inhibitor}$	$k \cdot 10^4$	$k \cdot 10^4/a$	b %	x %	$k \cdot 10/x$
1. Methylglucoside. Inhibitor glucose. $c_{glucoside} = 0.0400$ M. a = 6.1 %.					
0.00	3.5	57.4	0.0	6.1	57.4
0.01	3.2	52.5	5.3	5.8	55.2
0.02	3.0	49.2	10.0	5.5	54.3
0.04	2.6	42.6	18.2	5.0	51.5
0.08	2.4	39.3	30.8	4.3	55.8
0.12	2.2	36.1	40.0	3.8	58.6
2. Ethylglucoside. Inhibitor glucose. $c_{glucoside} = 0.0400$ M. a = 13.8 %					
0.00	8.5	61.6	0.0	13.8	61.6
0.01	8.0	58.0	5.3	13.1	60.9
0.02	7.7	55.8	10.0	12.6	61.2
0.04	7.0	50.7	18.2	11.6	60.5
0.08	5.9	42.8	30.8	10.0	59.2
0.12	5.7	41.3	40.0	8.8	65.0
3. Propylglucoside. Inhibitor glucose. $c_{glucoside} = 0.0400$ M. a = 20.0 %.					
0.00	28.0	140.0	0.0	20.0	140.0
0.01	27.7	138.5	5.3	19.1	145.0
0.02	25.3	126.5	10.0	18.4	137.7
0.04	24.2	121.0	18.2	17.0	142.6
0.08	21.9	109.5	30.8	14.8	148.5
0.12	20.0	100.0	40.0	13.0	153.3

Table XXX

(continued).

Elimation of the effect of inhibitors.

$c_{inhibitor}$	$k \cdot 10^4$	$k \cdot 10^4/a$	b %	x %	$k \cdot 10^4/x$
4. Propylglucoside. Inhibitor propylalc. $c_{glucoside}$ = 0.0400 M. a = 20.0 %.					
0.00	24.9	124.5	0.0	20.0	124.5
0.01	22.6	113.6	5.3	19.1	118.3
0.02	21.3	106.5	10.0	18.4	116.0
0.04	19.8	99.0	18.2	17.0	116.6
0.08	18.5	92.5	30.8	14.8	125.5
0.12	16.7	83.5	40.0	13.0	128.0
5. Isopropylglucoside. Inhibitor glucose. $c_{glucoside}$ = 0.0400 M. a = 9.1 %.					
0.00	18.3	201.1	0.0	9.1	201.1
0.01	17.5	192.3	5.2	8.6	202.5
0.02	15.7	172.5	10.0	8.3	189.9
0.04	14.3	157.1	18.2	7.6	189.0
0.08	11.2	123.0	30.8	6.5	173.0
0.12	9.5	104.4	40.0	5.7	167.6
6. Isopropylglucoside. Inhibitor isopropylalc. $c_{glucoside}$ = 0.0400 M. a = 9.1 %.					
0.00	15.3	168.1	0.0	9.1	168.1
0.01	14.7	161.6	2.4	8.9	165.1
0.02	14.3	157.1	4.7	8.7	164.2
0.04	13.9	152.8	8.9	8.4	166.3
0.08	13.2	145.1	16.2	7.7	170.6
0.12	12.4	136.2	22.6	7.2	172.4

and for the action of propyl- and isopropyl-alcohol on the hydrolysis of propyl- and isopropylglucoside respectively.

The table, although the constancy of $\frac{k}{x}$ is not excellent, shows that the figures give no evidence of a non-competitive inhibition as assumed by JOSEPHSON (1925). It is, however, to be observed that JOSEPHSON used much higher alcohol concentrations than those used in these experiments.

A consequence of the observations discussed above is that the method of calculating the hydrolysis constant used

in this and the previous papers is not the correct one. We have till now calculated the hydrolysis constants with the same c_0-value for all samples withdrawn within a single experiment. As the amount of emulsin bound to the glucoside varies within the experiment, both on account of the decrease of the glucoside concentration and on account of the increase of the concentration of glucose and alcohol (both substances being able to act as inhibitors), it seems to be more correct to calculate the velocity constants "from point to point" and to find for each point the amount of emulsin really bound to the glucoside, taking the actually existing concentrations of glucose and alcohol into consideration.

In order to get constants which are comparable, it is therefore necessarry to calculate the value of $\frac{k \cdot c}{x \cdot e \cdot (sal.f.)}$, where

k is the velocity constant for the hydrolysis from c_n to c_{n+1}.

c is the glucoside concentration c_n.

x is the fraction of the emulsin present, which is bound to the glucoside at the concentration $\frac{(c_n + c_{n+1})}{2}$, considering the presence of inhibiting substances.

e the amount of emulsin present in 50 ml of the solution.

sal. f. the enzymic power of the emulsin preparation, determined by its action on salicin.

The calculation of the value of x is somewhat more complicated when two inhibiting substances are present than when only one such substance is present.

When a, b and c are the fractions of the emulsin, which are bound to the glucoside and the two inhibiting substances,

these substances being the only ones in the solutions, and $\underline{x}$, $\underline{y}$ and $\underline{z}$ being the fractions of the emulsin bound to each substance, when they are all together in the solution, then

$$x = a(1 - y - z)$$
$$y = b(1 - x - z)$$
$$z = c(1 - x - y)$$

or

$$x = a \cdot \frac{(1-b)(1-c)}{1 - ab - ac - bc + 2abc}$$

and the corresponding expressions for y and z.

In Tables XXXI—XXXIV we have recalculated all experiments mentioned in this and the previous paper. It is seen that for each temperature the value of $\frac{k \cdot c}{x \cdot e \cdot (\text{sal. f.})}$ is really constant within the limit of the experiment. As always it is not allowable to compare experiments where toluene has been added with experiments without the addition of toluene.

In a recent paper MOELWYN-HUGHES (1936; comp. CHRISTIANSEN (1924)) has pointed out that in a reaction

$$A + B \underset{k_1}{\overset{k_2}{\rightleftarrows}} AB; \qquad AB \xrightarrow{k_3} C + D$$

the observed velocity-constant is

$$k_{obs} = \frac{k_3 \cdot k_2}{k_1 + k_3}.$$

If $k_1 >> k_3$ (the BRØNSTED condition)

$$k_{obs} = k_3 \cdot \frac{k_2}{k_1} = k_3 \cdot \frac{[AB]}{[A][B]}$$

which is identical with the expression

$$\frac{k \cdot c}{x \cdot e\,(\text{sal. f.})} = \text{const.},$$

Table XXXI.

Methylglucoside.

$c_{glucoside}$	$c_{glucose}$	$c_{alcohol}$	k_{o-t}	$k_{t_1-t_2}$	$k \cdot c/x \cdot e$(sal.f.)
30° without toluene.					
0.0400	0.00	0.00	$2.56 \cdot 10^{-4}$	$2.46 \cdot 10^{-4}$	$1.86 \cdot 10^{-2}$
0.0204	0.00	0.00	2.39	2.58	2.06
0.0409	0.00	0.00	2.40	2.28	1.86
0.0826	0.00	0.00	2.20	2.15	1.90
0.1672	0.00	0.00	1.97	1.93	1.93
0.3334	0.00	0.00	1.65	1.59	1.95
0.6689	0.00	0.00	1.17	1.15	1.92
0.0400	0.00	0.00	2.67	2.54	1.92
0.0400	0.00	0.01	2.64	2.49	1.87
0.0400	0.00	0.02	2.59	2.45	1.84
0.0400	0.00	0.04	2.61	2.45	1.84
0.0400	0.00	0.08	2.58	2.42	1.82
0.0400	0.00	0.12	2.54	2.41	1.81
			mean value...		1.89
30° with addition of toluene.					
0.0400	0.00	0.00	$3.46 \cdot 10^{-4}$	$3.48 \cdot 10^{-4}$	$3.15 \cdot 10^{-2}$
0.0400	0.01	0.00	3.22	3.20	2.96
0.0400	0.02	0.00	2.98	2.81	2.75
0.0400	0.04	0.00	2.81	2.72	2.85
0.0400	0.08	0.00	2.36	2.33	2.82
0.0400	0.12	0.00	2.25	2.19	3.02
			mean value...		2.93
20° without toluene.					
0.0400	0.00	0.00	$1.39 \cdot 10^{-4}$	$1.19 \cdot 10^{-4}$	$0.87 \cdot 10^{-2}$
0.0189	0.00	0.00	1.66	1.38	1.01
0.0333	0.00	0.00	1.43	1.36	1.04
0.0769	0.00	0.00	1.26	1.10	0.89
0.1540	0.00	0.00	1.13	1.02	0.94
0.3030	0.00	0.00	0.99	0.79	0.88
0.5958	0.00	0.00	0.86	0.64	0.95
			mean value...		0.94

$k_{30}/k_{20} = 1.89/0.94 = 2.0$

Effect of toluene: $2.93/1.89 = 1.55$.

k being k_{obs} and const. $= k_3$, $c = [A]$, $x \cdot e\,(\text{sal. f.}) = \frac{[AB]}{[B]}$.

From the constancy of $\frac{k \cdot c}{x \cdot e(\text{sal. f.})}$ it may be concluded that

Table XXXII.

Ethylglucoside.

$c_{glucoside}$	$c_{glucose}$	$c_{alcohol}$	k_{o-t}	$k_{t_1-t_2}$	$k \cdot c/x \cdot e$ (sal. f.)
30° without toluene.					
0.0400	0.00	0.00	$5.95 \cdot 10^{-4}$	$5.49 \cdot 10^{-4}$	$1.48 \cdot 10^{-2}$
0.0200	0.00	0.00	5.02	5.10	1.44
0.0400	0.00	0.00	5.42	5.35	1.72
0.0800	0.00	0.00	4.83	4.73	1.65
0.1600	0.00	0.00	3.77	3.80	1.64
0.3200	0.00	0.00	2.69	2.67	1.58
0.6400	0.00	0.00	1.59	1.68	1.53
0.0400	0.00	0.00	4.65	4.41	1.59
0.0400	0.00	0.01	4.70	4.47	1.61
0.0400	0.00	0.02	4.68	4.43	1.59
0.0400	0.00	0.04	4.76	4.44	1.60
0.0400	0.00	0.08	4.57	4.34	1.56
0.0400	0.00	0.12	4.56	4.36	1.56
			mean value...		1.58
30° with addition of toluene.					
0.0400	0.00	0.00	$8.16 \cdot 10^{-4}$	$7.62 \cdot 10^{-4}$	$2.27 \cdot 10^{-2}$
0.0400	0.01	0.00	7.86	7.34	2.29
0.0400	0.02	0.00	7.32	7.03	2.29
0.0400	0.04	0.00	6.87	6.36	2.25
0.0400	0.08	0.00	5.82	5.49	2.22
0.0400	0.12	0.00	5.67	5.19	2.38
			mean value...		2.28
20° without toluene.					
0.0400	0.00	0.00	$2.56 \cdot 10^{-4}$	$2.30 \cdot 10^{-4}$	$0.59 \cdot 10^{-2}$
0.0200	0.00	0.00	2.52	2.46	0.75
0.0400	0.00	0.00	2.62	2.47	0.81
0.0800	0.00	0.00	2.27	2.17	0.81
0.1600	0.00	0.00	1.77	1.70	0.80
0.3200	0.00	0.00	1.28	1.25	0.80
0.6400	0.00	0.00	0.76	0.80	0.81
			mean value...		0.77

$k_{30}/k_{20} = 1.58/0.77 = 2.05$

Effect of toluene: $2.28/1.58 = 1.44$.

the formation of the emulsin-glucoside-compound has a velocity constant which is much greater than the hydrolysis constant for its decomposition into emulsin, glucose and alcohol.

Table XXXIII.

Propylglucoside.

$c_{glucoside}$	$c_{glucose}$	$c_{alcohol}$	k_{o-t}	$k_{t_1-t_2}$	$k \cdot c/x \cdot e$ (sal.f.)
30° without toluene.					
0.0400	0.00	0.00	$21.7 \cdot 10^{-4}$	$22.3 \cdot 10^{-4}$	$5.27 \cdot 10^{-2}$
0.0200	0.00	0.00	28.4	28.6	5.78
0.0400	0.00	0.00	21.9	22.9	5.13
0.0800	0.00	0.00	16.7	17.3	4.62
0.1600	0.00	0.00	11.9	11.8	4.18
0.2400	0.00	0.00	9.8	9.5	4.14
0.3200	0.00	0.00	8.3	8.0	4.18
0.0400	0.00	0.00	24.9	24.9	5.69
0.0400	0.00	0.01	22.6	22.6	5.40
0.0400	0.00	0.02	21.3	21.1	5.20
0.0400	0.00	0.04	19.8	20.1	5.33
0.0400	0.00	0.08	18.6	18.4	5.50
0.0400	0.00	0.12	16.7	16.7	5.56
			mean value...		5.08
30° with addition of toluene.					
0.0400	0.00	0.00	$28.7 \cdot 10^{-4}$	$27.3 \cdot 10^{-4}$	$6.42 \cdot 10^{-2}$
0.0400	0.01	0.00	27.2	26.8	6.53
0.0400	0.02	0.00	25.3	24.9	6.26
0.0400	0.04	0.00	24.2	23.3	6.28
0.0400	0.08	0.00	21.9	21.4	6.53
0.0400	0.12	0.00	20.0	19.9	6.77
			mean value...		6.47
20° without toluene.					
0.0400	0.00	0.00	$10.9 \cdot 10^{-4}$	$10.7 \cdot 10^{-4}$	$2.27 \cdot 10^{-2}$
0.0200	0.00	0.00	12.0	12.5	2.65
0.0400	0.00	0.00	10.7	10.3	2.42
0.0800	0.00	0.00	7.9	7.6	2.16
0.1600	0.00	0.00	6.0	5.9	2.21
0.2400	0.00	0.00	5.1	5.0	2.35
0.3200	0.00	0.00	4.1	4.1	2.32
			mean value...		2.34

$k_{30}/k_{20} = 5.08/2.34 = 2.2$

Effect of toluene: $6.47/5.08 = 1.27$.

It is known that emulsin has not only a hydrolysing effect, but that it is also able to katalyse the synthesis of glucosides. Veibel (1936) has determined the equilibrium

Tabel XXXIV.

Isopropylglucoside.

30°. Without toluene.

$c_{glucoside}$	$c_{glucose}$	$c_{alkohol}$	k_{0-t}	$k_{t_1-t_2}$	$k \cdot c/x \cdot e$(sal.f.)
0.0400	0.00	0.00	12.8	11.5	6.96
0.0200	0.00	0.00	18.8	17.9	8.26
0.0400	0.00	0.00	16.5	16.0	7.76
0.0800	0.00	0.00	14.0	14.4	7.72
0.1600	0.00	0.00	12.4	12.2	7.84
0.2400	0.00	0,00	11.0	10.6	7.82
0.3200	0.00	0.00	9.9	9.7	8.02
0.0400	0.00	0.00	15.3	14.4	7.32
0.0400	0.00	0.01	14.7	13.8	7.12
0.0400	0.00	0.02	14.3	13.4	7.01
0.0400	0.00	0.04	13.9	13.0	6.99
0.0400	0.00	0 08	13.2	12.4	7.27
0.0400	0.00	0.12	12.5	12.0	7.50
			mean value...		7.51

30°. With addition of toluene.

0.0400	0.00	0.00	18.4	16.5	8.79
0.0400	0.01	0.00	17.5	16.1	8.94
0.0400	0.02	0.00	15.7	14.3	8.23
0.0400	0.04	0.00	14.3	13.1	8.08
0.0400	0.08	0.00	11.2	10.6	7.44
0.0400	0.12	0.00	9.5	9.2	7.32
			mean value...		8.13

20°. Without toluene.

0.0400	0.00	0.00	6.5	5.6	3.24
0.0200	0.00	0.00	10.1	9.9	3.94
0.0400	0.00	0.00	8.52	8.25	3.43
0.0800	0.00	0.00	8.29	7.95	3.57
0.1600	0.00	0.00	6.63	6.51	3.54
0.2400	0.00	0.00	5.99	5.92	3.78
0.3200	0.00	0.00	5.50	5.44	3.85
			mean value...		3.62

$k_{30}/k_{20} = 7.51/3.62 = 2.1$

Effect of toluene: $8.13/7.51 = 1.08$

constant for mixtures of glucoside, glucose and alcohol for a series of alcohols and has found that methyl glu-

Table XXXV.

Glucoside	K_m	K_{m_1}	K_{m_2}	$k \cdot c/x \cdot e$ (sal. f.)	k_{30}/k_{20}	Effect of toluene
Methyl ...	0.62	0.18	..	$1.89 \cdot 10^{-2}$	2.0	1.55
Ethyl	0.25	0.18	..	$1.58 \cdot 10^{-2}$	2.0_5	1.44
Propyl....	0.16	0.18	0.18	$5.08 \cdot 10^{-2}$	2.1_5	1.27
Isopropyl.	0.40	0.18	0.14	$7.51 \cdot 10^{-2}$	2.1	1.08

coside is the one which has the highest equilibrium concentration, the equilibrium constant being 0.311 for a glucose-methylalcohol-water-acetone mixture with the concentrations $c_{glucose}$ 0.150 M, $c_{alcohol}$ 3.000 M, c_{water} 15.00 M at the beginning. Presuming the equilibrium constant to be the same for 0.04 M glucoside solutions in water (which is probably not quite correct), the equilibrium concentration of methyl glucoside is calculated to be 0.0002 M, i. e. only $^1/_2$ % will not be hydrolysed. In the calculation of the velocity constants it is therefore unnecessary to consider the reversibility of the process.

Tables XXXVI—XLIII are examples showing the variations within single experiments, the constants being calculated from point to point. For each glucoside is given the experiment showing the best constancy of the constants as well as the experiment showing the greatest deviations. It is quite clear, that the constancy is not as good here as when calculating the constants from the starting point to the time t, the variations in rotation being in many cases only 0.050° and the polarimeter does not allow a greater accuracy of the readings than 0.005°. Table XLV is a recalculation of table XXXIX, the only difference being that some of the readings have been substituted by readings 0.005° (in two cases 0.010°) greater or smaller than the original ones. This table shows that the deviations from the constant value do not surpass the limits of the experiments.

It is therefore to be assumed that the mean values of the constants are correct.

In the tables the meaning of the columns is:

1 = time from the beginning
2 = α_t
3 = velocity constant calculated from t = 0 to t = t
4 = velocity constant calculated from t = n to t = n + 1
5 = $c_{glucoside}$ at time t
6 = % emulsin bound to glucoside at time t if no glucose and alcohol present
7 = % emulsin bound to glucose at time t if no glucoside and alcohol present
8 = % emulsin bound to alcohol at time t if no glucoside and glucose present
9 = % emulsin actually bound to glucoside at time t
10 = value of x
11 = $\frac{k}{x}$
12 = $\frac{k \cdot c}{x}$

Table XXXVI.

Methylglucoside 0.0400 M. Hydrolysis 30°. e = 0.2233 g in 50 ml. sal. f. = 0.043.

1	2	3	4	5	6	7	9	10	11	12
0	1.075	—	3.16	0.0400	6.06	0.00	6.06	5.78	54.7	2.19
120	0.985	3.16	2.47	0.0367	5.58	1.80	5.49	5.29	46.7	1.71
240	0.920	2.82	2.02	0.0342	5.24	3.12	5.08	4.93	41.0	1.40
360	0.870	2.55	2.33	0.0324	4.96	4.05	4.77	4.53	51.4	1.66
540	0.790	2.48	2.58	0.0294	4.53	5.56	4.29	3.98	64.9	1.91
780	0.685	2.51	2.27	0.0255	3.95	7.45	3.66	3.10	73.3	1.87
1440	0.485	2.40	2.18	0.0181	2.83	10.84	2.53	2.22	98.0	1.77
1980	0.370	2.34	1.99	0.0138	2.17	12.71	1.90	1.57	126.7	1.75
2880	0.245	2.23	..	0.0091	1.45	14.65	1.24	..	..	..
mean value		2.56	2.38							1.78

$k \cdot c/x \cdot e(sal.\ f.) = 1.86 \cdot 10^{-2}$

Tabel XXXVII.

Methylglucoside 0.0400 M. Hydrolysis 30°. e = 0.2259 g in 50 ml. sal. f. = 0.043.

1	2	3	4	5	6	7	9	10	11	12
0	1.075	—	2.80	0.0400	6.06	0.00	6.06	5.81	51.6	2.07
120	0.995	2.80	2.84	0.0370	5.64	1.64	5.55	5.32	53.3	1.98
240	0.920	2.82	2.65	0.0342	5.23	3.12	5.08	4.88	54.3	1.86
360	0.855	2.76	2.41	0.0318	4.88	4.36	4.68	4.52	53.3	1.70
480	0.800	2.67	2.46	0.0298	4.58	5.36	4.35	3.98	61.8	1.84
780	0.675	2.59	2.10	0.0251	3.89	7.65	3.61	3.09	68.2	1.71
1440	0.490	2.37	..	0.0182	2.86	10.80	2.56	..	..	..
mean value		2.67	2.54							1.86

$k \cdot c/x \cdot e \cdot (\text{sal. f.}) = 1.92 \cdot 10^{-2}$

Table XXXVIII.

Ethylglucoside 0.0400 M. Hydrolysis 30°. e = 0.2818 g in 50 ml. sal. f. = 0.044.

1	2	3	4	5	6	7	8	9	10	11	12
0	1.175	—	7.12	0.0400	13.79	0.00	—	13.79	13.12	54.3	2.18
60	1.065	7.12	6.39	0.0363	12.66	2.02	—	12.44	11.50	53.7	1.95
120	0.975	6.75	5.61	0.0332	11.72	3.64	—	11.35	10.50	53.5	1.78
240	0.835	6.18	6.95	0.0284	10.21	6.08	—	9.65	8.29	83.8	2.38
360	0.690	6.42	4.29	0.0235	8.59	8.40	—	7.92	7.37	58.2	1.37
510	0.595	5.80	5.39	0.0203	7.50	9.86	—	6.81	5.65	95.4	1.93
840	0.395	5.64	4.93	0.0134	5.11	12.88	—	4.48	3.37	146.2	1.97
1440	0.200	5.34	3.23	0.0068	2.65	15.58	—	2.25	2.02	160.0	1.09
1740	0.160	4.98	..	0.0054	2.13	16.13	—	1.79	..	..	..
mean value		6.03	5.49								1.83

$k \cdot c/x \cdot e \,(\text{sal. f.}) = 1.48 \cdot 10^{-2}$

Tables XXXI—XXXIV show that there is no evidence of a non-competitive inhibition and that all experiments agree with the assumption that the process determining the velocity of the reaction is the hydrolysis of the addition-compound of glucoside and emulsin into glucose, alcohol and emulsin, the concentration of this addition compound being determined by the values of the dissociation constants of

Table XXXIX.

Ethylglucoside. Inhibition by ethyl alcohol.

Glucoside 0.0400 M. Alcohol 0.08 M. e = 0.2008 g in 50 ml. sal. f. = 0.043.

1	2	3	4	5	6	7	8	9	10	11	12
0	1.175	—	5.11	0.0400	13.79	0.00	—	13.79	13.30	38.4	1.54
60	1.095	5.11	4.43	0.0373	12.97	1.48	—	12.81	12.41	35.7	1.33
120	1.030	4.77	4.29	0.0351	12.30	2.65	—	12.01	11.31	37.9	1.33
240	0.915	4.54	4.41	0.0311	11.08	4.71	—	10.61	9.98	44.2	1.38
360	0.810	4.49	3.87	0.0276	9.93	6.45	—	9.35	8.64	44.8	1.24
540	0.690	4.28	3.93	0.0235	8.59	8.40	—	7.92	7.31	53.7	1.26
720	0.585	4.21	..	0.0199	7.38	10.04	—	6.69	..	..	..
mean value		4.57	4.34								1.35

$k \cdot c/x \cdot e\,(\text{sal. f.}) = 1.56 \cdot 10^{-2}$

Table XL.

Propylglucoside 0.0400 M. Hydrolysis 30°. e = 0.2188 g in 50 ml. sal. f. = 0.044.

1	2	3	4	5	6	7	8	9	10	11	12
0	1.220	—	19.55	0.0400	20.00	0.00	0.00	20.00	19.00	102.9	4.12
20	1.115	19.55	22.55	0.0366	18.60	1.90	1.90	18.00	17.05	132.3	4.84
40	1.005	21.55	23.97	0.0329	17.10	3.80	3.80	16.10	15.15	158.2	5.21
60	0.900	22.02	24.48	0.0295	15.60	5.50	5.50	14.20	12.95	189.0	5.57
90	0.760	22.84	20.42	0.0249	13.40	7.70	7.70	11.70	10.90	187.3	4.66
120	0.660	22.21	21.57	0.0216	11.90	9.30	9.30	10.10	8.80	245.1	5.29
180	0.490	22.01	23.33	0.0160	9.10	11.70	11.70	7.50	6.40	364.5	5.83
240	0.355	22.34	..	0.0117	6.84	13.58	13.58	5.30	..	..	..
mean value		21.8	22.3								5.07

$k \cdot c/x \cdot e\,(\text{sal. f.}) = 5.27$

the addition-compounds emulsin-glucoside, emulsin-glucose and emulsin-alcohol.

The temperature coefficient seems to be the same in all cases, the deviations not being greater than may be expected from the inexactness of the measurements. That is to say that the critical increment is the same in all

Table XLI.

Propylglucoside 0.0400 M. Hydrolysis 30°. e = 0.2308 g in 50 ml. sal. f. = 0.044.

1	2	3	4	5	6	7	8	9	10	11	12
0	1.220	—	23.5	0.0400	20.00	0.00	0.00	20.00	18.84	124.6	4.99
20	1.095	23.5	26.3	0.0359	18.32	2.23	2.23	17.67	16.55	159.1	5.71
40	0.970	24.9	23.6	0.0318	16.59	4.36	4.36	15.42	14.54	162.5	5.17
60	0.870	24.6	22.5	0.0285	15.13	6.01	6.01	13.65	12.59	178.3	5.09
90	0.745	23.8	23.1	0.0244	13.25	7.97	7.97	11.52	10.61	218.0	5.33
120	0.635	23.6	29.1	0.0208	11.52	9.64	9.64	9.69	8.01	362.9	7.56
180	0.425	25.4	24.0	0.0139	8.01	12.66	12.66	6.33	5.41	443.9	6.19
240	0.305	25.1	23.6	0.0100	5.88	14.29	14.29	4.48	3.84	615.9	6.16
300	0.220	24.8	..	0.0072	4.31	15.41	15.41	3.20	..	..	..
mean value		24.9	24.9								5.78

$k \cdot c/x \cdot e\,(\text{sal. f.}) = 5.69 \cdot 10^{-2}$

Table XLII.

Isopropylglucoside. 0.0400 M. Hydrolysis 30°. e = 0.1845 g in 50 ml. sal. f. = 0.044.

1	2	3	4	5	6	7	8	9	10	11	12
0	1.245	—	15.3	0.0400	9.09	0.00	0.00	9.09	8.56	178.9	7.16
30	1.120	15.3	12.1	0.0360	8.25	2.17	0.97	8.02	7.65	158.5	5.70
60	1.030	13.7	13.2	0.0331	7.64	3.69	1.66	7.27	6.91	191.6	6.34
90	0.940	13.6	12.9	0.0302	7.02	5.18	2.33	6.54	6.23	206.7	6.24
120	0.860	13.4	10.4	0.0276	6.46	6.45	2.94	5.91	5.48	189.5	5.24
180	0.745	12.4	9.3	0.0239	5.65	8.21	3.78	5.04	4.71	197.9	4.74
240	0.655	11.6	10.7	0.0210	5.00	9.55	4.43	4.37	4.03	265.4	5.59
300	0.565	11.4	8.1	0.0182	4.34	10.80	5.05	3.69	3.50	232.1	4.22
360	0.505	10.9	..	0.0162	3.89	11.68	5.49	3.30	..	..	..
mean value		12.8	11.5								5.65

$k \cdot c/x \cdot e\,(\text{sal. f.}) = 6.96 \cdot 10^{-2}$

cases, but that the "constant of action" differs from glucoside to glucoside. This constant may be calculated from the expression

$$\ln k = \frac{-Q}{R \cdot T_1} + \ln \alpha$$

Table XLIII.

Isopropylglucoside. 0.0400 M. Hydrolysis 30°. e = 0.2252 g in 50 ml. sal. f. = 0.044.

1	2	3	4	5	6	7	8	9	10	11	12
0	1.245	—	16.6	0.0400	9.09	0.00	0.00	9.09	8.51	195.5	7.82
30	1.110	16.6	15.8	0.0357	8.49	2.33	1.04	7.93	7.46	212.3	7.57
60	0.995	16.2	14.5	0.0320	7.40	4.26	1.91	6.99	6.61	219.8	7.03
90	0.900	15.7	15.3	0.0289	6.74	5.81	2.64	6.22	5.88	259.4	7.50
120	0.810	15.6	14.8	0.0260	6.11	7.22	3.30	5.53	4.97	298.2	7.76
180	0.660	15.3	12.5	0.0212	5.03	9.46	4.38	4.41	4.03	311.2	6.60
240	0.555	14.6	12.8	0.0178	4.27	10.98	5.14	3.65	3.34	383.4	6.84
300	0.465	14.3	12.7	0.0149	3.60	12.18	5.77	3.02	2.76	461.3	6.89
360	0.390	14.0	..	0.0125	3.04	13.26	6.29	2.50	..	..	..
mean value		15.3	14.4								7.25

$k \cdot c/x \cdot e(\text{sal.f.}) = 7.32 \cdot 10^{-2}$

Table XLIV.

Recalculation of table XXXVIII.

1	2 old	2 new	4	5	6	7	9	10	11	12 old	12 new
0	1.175	1.175	6.78	0.0400	13.79	—	13.79	13.14	51.6	2.18	2.06
60	1.065	1.070	6.73	0.0364	12.72	1.96	12.49	11.92	56.5	1.95	2.06
120	0.975	0.975	6.05	0.0332	11.72	3.64	11.35	10.44	57.9	1.78	1.92
240	0.835	0.825	6.21	0.0281	10.00	6.20	9.54	8.76	70.9	2.38	1.99
360	0.690	0.695	4.99	0.0237	8.64	8.30	7.98	7.33	68.0	1.37	1.61
510	0.595	0.585	5.00	0.0199	7.38	10.04	6.69	5.64	88.7	1.93	1.77
840	0.395	0.400	4.84	0.0136	5.22	12.79	4.59	3.45	140.2	1.97	1.91
1440	0.200	0.205	4.51	0.0070	2.72	15.49	2.30	1.99	226.7	1.09	1.58
1740	0.160	0.150	..	0.0051	2.00	16.24	1.68	..	..	..	..
										1.83	1.86

where the integration constant is the constant of action and Q the critical increment determined by the expression

$$Q = R \cdot \frac{T_1 \cdot T_2}{T_1 - T_2}.$$

In the expression determining α, k has to be calculated with natural logarithms, whereas the k-values in this paper are calculated with logarithms to base 10.

The mean value of $\frac{k_{30}}{k_{20}}$ is 2.1. From this value is calculated the following values of α:

	Methyl	Ethyl	Propyl	Isopropyl
$\alpha \cdot 10^{-10}$	1.21	1.01	3.16	4.79
K_m	0.62	0.25	0.16	0.40

As the molar concentration of emulsin is not known, the values of α are not the correct ones, but differ from the correct values by a factor which is the same for all glucosides.

An influence of the structure of the aglucone is to be expected on the value of K_m, the dissociation constant of the compound emulsin-glucoside, and of α, the action constant. It is to be seen that the influence on both series of constants is of the same order of magnitude, but that they are not influenced in the same direction.

The examination is continued with glucosides of butyl- and amyl-alcohols.

Summary.

1. The enzymic hydrolysis of propyl- and of isopropyl-β-d-glucoside has been examined. Table XLV gives the values of the velocity-constants, calculated in the usual way (minutes as unit of time, logarithms to base 10), of the affinity constants K_m for the two glucosides, K_{m1} for glucose and K_{m2} for the two alcohols, and of the critical increment Q.

Table XLV.

	Propylglucoside	Isopropylglucoside
$10^2 \cdot k/e \cdot$(sal. f.) 30°	22.6	16.9
» 20°	11.3	7.9
K_m 30° and 20°	0.16	0.40
K_{m1} 30°	0.21	0.15
K_{m2} 30°	0.18	0.41
Q	12200	13500

2. The fraction of emulsin, bound to the glucoside, is $\frac{S}{(K_m + S)}$, S being the glucoside concentration. It has been shown that for the glucosides examined till now, i. e. methyl-, ethyl-, propyl- and isopropyl-glucoside, the product $k(K_m + S)$ is independent of the glucoside concentration and has, for the 4 glucosides, the following values:

	Methyl	Ethyl	Propyl	Isopropyl
$10^2 \cdot k \cdot (K_m + S)/e \cdot (sal.f.)$	1.84	1.62	4.33	7.21

3. The fraction of emulsin bound to glucoside, if inhibitors are present, may be calculated when all affinity constants are known.

This fraction x is

$$x = a \cdot \frac{(1-b)\cdot(1-c)}{1-ab-ac-bc+2abc}.$$

$\underline{a}$, $\underline{b}$ and $\underline{c}$ being the fractions of emulsin bound to glucoside, glucose and alcohol respectively, if these substances alone were present in the solution.

4. All experiments have been recalculated, the velocity constants being calculated "from point to point". It has been shown that the value of $\frac{k \cdot c}{x \cdot e\,(sal.f.)}$, which is identical with k_3 in an equation given by MOELWYN-HUGHES (1936): $k_{obs} = k_3 \cdot \frac{[AB]}{[A][B]}$, is constant for all concentrations of glucose and emulsin.

		Methyl	Ethyl	Propyl	Isopropyl
$k_3 = 10^2 \cdot k \cdot c/x \cdot e(sal.f.)$	30°	1.89	1.58	5.08	7.51
»	20°	0.94	0.77	2.34	3.62

This means that when for a glucoside the values of k_3, K_m, K_{m1} and K_{m2} and the enzymic power of the emulsin preparation are known, the total description of the hydro-

lysis at any concentration of emulsin, glucoside, glucose and the alcohol in question is possible.

5. The average value of $\frac{k_{30}}{k_{20}}$, when the constants are calculated in this way, is 2.1. The critical increment is, therefore, 13100 cal.

6. The action constant, α in the expression $\ln k = \frac{-Q}{RT} + \ln \alpha$, for the four glucosides has the following values:

	Methyl	Ethyl	Propyl	Isopropyl
$\alpha \cdot 10^{-10}$	1.21	1.01	3.16	4.79

7. The effect of toluene has been examined in all four cases. The values of $\frac{k_{toluene}}{k}$ are

	Methyl	Ethyl	Propyl	Isopropyl
$k_{toluene}/k$	1.55	1.44	1.27	1.08

using emulsin preparations with sal. f.-values about 0.04.

Thanks are due to the Carlsberg Foundation for a grant which enabled one of us (F. E.) to take part in this work.

(From the Chemical Laboratory, University of Copenhagen).

REFERENCES

CHRISTIANSEN (1924). Z. phys. Chem. 113, 35.
JOSEPHSON (1925). Z. physiol. Chem. 147, 1.
MOELWYN-HUGHES (1936). Transact. Farad. Soc. 32, 1723.
SCHEIBER (1935). Dissertation, Leipzig.
VEIBEL (1936). Enzymologia 1, 124.
VEIBEL and ERIKSEN (1936 1). Bull. soc. chim. [5] 3, 277.
— (1936 2). Kgl. d. Vid. Selsk. math.-fys. Medd. XIII, nr. 17.

Færdig fra Trykkeriet den 25. September 1937.